A Crystallographic and Spectroscopic Investigation of Some Organo-chalcogen Complexes of Ruthenium

---

A thesis presented for the degree of
Doctor of Philosophy in Chemistry
at the University of Canterbury
Christchurch, New Zealand.

by

C. T. Page

University of Canterbury
1978

DEDICATION

This thesis is dedicated to my parents, Mrs V.M. and Mr A.T. Page and to my wife Lois.

ACKNOWLEDGEMENTS

I would like to sincerely thank Dr J. E. Fergusson and Dr Ward T. Robinson for their advice and encouragement throughout this work.

The assistance given by fellow students, especially Tony Greenaway and Grant Holloway, is gratefully acknowledged.

I acknowledge the award of a U.G.C. Scholarship.

CONTENTS

LIST OF FIGURES

LIST OF TABLES

ABBREVIATIONS

Me	methyl
Et	ethyl
Pr	n-propyl
Bu	n-butyl
Ph	phenyl
Bz	benzyl
DMSO	dimethyl sulphoxide
bte	cis-bis(1,2-benzylthio)ethylene
dbtx	αα'-dibenzylthio-o-xylene
BzSH	benzyl mercaptan.

In tables of infrared data

s	strong
m	medium
w	weak
sh	shoulder
br	broad

ABSTRACT

The work described in this thesis is concerned principally with the study, by crystallographic and spectroscopic methods, of a series of divalent ruthenium complexes $[RuX_3(NO)L_2]$ (X = Cl, Br or I, and the ligands L are dialkyl and phenyl alkyl sulphides or selenides). A small number of Pt, Pd, Rh and Ru complexes containing the chelating ligands cis-bis(1,2-benzylthio)ethylene and αα'-dibenzylthio-o-xylene have also been prepared.

The spectroscopic methods employed were infrared and ultraviolet-visible absorption and ^1H and ^{13}C nuclear magnetic resonance. The results have been related, where possible, to the nature of the metal-ligand bond.

A detailed investigation of the variable temperature ^1H n.m.r. spectra of the $[RuX_3(NO)L_2]$ complexes, employing computer simulation techniques, has resulted in the determination of the rate of inversion of configuration about the sulphur (or selenium) atom (of the chalcogen ligand). Variations in the rate of inversion have been correlated with the halogen ligand X and the chalcogen ligand.

An oxidation reaction involving the complex $[RuBr_3(NO)(Et_2S)_2]$ is stimulated by the energy of visible radiation when the complex is dissolved in chloroform. The study of the reaction using crystallographic and spectroscopic techniques has lead to the isolation of an intermediate product $[RuBr_3(NO)(Et_2SO)(Et_2S)]$ and an end product $[RuBr_3(NO)(Et_2SO)]_2$.

The crystal and molecular structures of $[RuBr_3(NO)(Et_2SO)]_2$ and $[RuBr_3(NO)(Et_2SO)(Et_2S)]$ have been determined using three-dimensional X-ray diffractometer data. In both crystal structures the octahedrally coordinated ruthenium atoms have a diethyl sulphoxide ligand bonded through the oxygen atom. A linearly coordinated nitrosyl group occupies the position trans to the sulphoxide group. The crystal and molecular structure of $[RuBr_3(NO)(PhSEt)_2]$ contains two crystallographically independent molecules (they are mirror images) in the asymmetric unit. The ruthenium atom is octahedrally coordinated to trans sulphur atoms and a meridional arrangement of bromine atoms.

CHAPTER 1

INTRODUCTION

The work to be described in this thesis covers the preparations and the spectroscopic and structural properties of Ru, Rh, Ir, Os, Pd and Pt complexes with ligands containing the donor atoms O, S and Se.

Most of the complexes studied also contained the '$RuX_3(NO)$' moiety where X = halogen. Octahedral complexes of the type $[RuX_3(NO)L_2]$ where L is an organic chalcogen ligand have been isolated and investigated, in order to obtain information on the nature of the metal-ligand bonds and factors that influence them. Single crystal X-ray structural determinations of three of the complexes prepared in this work have been carried out.

1.1 A SUMMARY OF THE PRESENT WORK

A series of new thioether and organo-sulphoxide complexes of stoichiometry $[RuX_3(NO)L_2]$ have been prepared. These complexes together with a related series of thioether complexes prepared previously,[1] have been investigated spectroscopically. The spectroscopic techniques used were infra-red (both low and high frequency), ^1H n.m.r., ^{13}C n.m.r. and ultraviolet-visible absorption spectroscopy. These techniques enabled the stereochemistry of the $[RuX_3(NO)L_2]$ complexes to be determined and yielded information about the nature of the bonding within the complexes.

The nuclear magnetic resonance measurements were also carried out over a range of temperatures. As a result, thermodynamic data relating to a fluxional process involving an inversion of configuration about the sulphur atom of the ligand were obtained.

Visible radiation was found to induce a photochemical oxidation of the sulphide ligand in a number of the $[RuX_3(NO)L_2]$ complexes. A study of this reaction involved crystallographic studies as well as the usual spectroscopic techniques. The nature of an intermediate and a final product of the photochemical reaction was elucidated by single crystal X-ray analysis. The thioether ligand was oxidised to a sulphoxide which then coordinates to the ruthenium through the oxygen atom.

An attempt was made to complete previous crystallographic work[2,3] on some arsenic sulphide complexes of cobalt and zinc. However, previous difficulties encountered with this system were not resolved satisfactorily.

In chapter 2 the preparative and spectroscopic studies of the various complexes are presented. The work deals mainly with the investigation of the $[RuX_3(NO)L_2]$ complexes. In chapter 3 the variable temperature n.m.r. results for a number of thioether complexes of the type $[RuX_3(NO)L_2]$ are reported. The investigation of the photochemical oxidation of diethyl sulphide in the complex $[RuBr_3(NO)(Et_2S)_2]$ is presented in chapter 4. In chapters 5, 6 and 7 details on the three crystallographic determinations of $[RuBr_3(NO)(Et_2SO)]_2$, $[RuBr_3(NO)(Et_2SO)(Et_2S)]$ and $[RuBr_3(NO)(EtSPh)_2]$

respectively are reported. The crystallographic investigations of the cobalt and zinc arsenic sulphide system are presented as an appendix.

Most of the chapters contain a brief review of previous work relevant to the material being discussed, as well as the experimental data.

CHAPTER 2

PREPARATIVE AND SPECTROSCOPIC STUDIES ON A SERIES OF RUTHENIUM COMPLEXES WITH ORGANIC CHALCOGEN LIGANDS

A preparative and spectroscopic study of a series of ruthenium nitrosyl halogeno complexes with dialkyl or phenyl-alkyl chalcogen ligands has been undertaken. Attempts were also made to prepare similar complexes with rhodium, rhenium and osmium. Complexes of platinum, palladium, ruthenium and rhodium with chelating organic sulphide ligands have also been prepared.

2.1 INTRODUCTION

The work to be described extends a previous brief spectroscopic study[1] of a series of $[RuX_3(NO)L_2]$ complexes where X = Cl, Br, I and L = Et_2S, PhSEt, n-Pr_2S, n-PrSPh, Et_2Se or PhSeEt, with the isolation of complexes containing Me_2S, MeSPh, Bz_2S or DMSO ligands. A more detailed spectroscopic study (infrared, ^1H n.m.r., ^{13}C n.m.r. and ultraviolet visible) of the whole range of complexes has been undertaken in the present work in order to study:

a) the stereochemistry of the complexes,

and b) the influence of different ligands on the metal-ligand bond.

The six coordinate $[RuX_3(NO)L_2]$ complexes have three possible configurations as shown in Figure 2.1. The isomeric forms were investigated using principally nuclear magnetic resonance spectra. The low frequency infrared spectra did not distinguish between the isomers.

FIGURE 2.1

Possible Configurations of the $[RuX_3(NO)L_2]$ Complexes.[a]

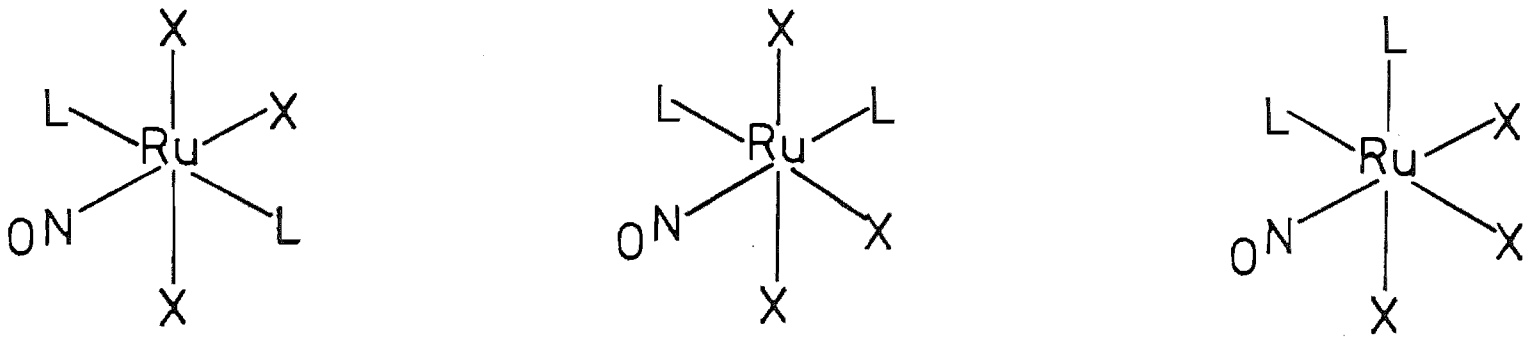

trans-meridional cis-meridional cis-facial

[a] cis and trans refer to the arrangement of the L ligands, meridional and facial to those of the X ligands.

2.1.1 A Brief Survey of Previous Studies of Thioether Complexes

(a) $[MX_3(NO)L_2]$ complexes

(i) Trans-meridional configuration

The only thioether complexes reported[4] which are similar to those above are $[RuCl_3(NO)(PhSMe)_2]$ and $[RuCl_3(NO)(n\text{-}BuSEt)_2]$. On the other hand a number of tertiary phosphine complexes of the type $[RuX_3(NO)L_2]$ have been reported.[4-12] Two crystal structure determinations[9,10] of these latter complexes indicate that they generally adopt the trans-meridional configuration (see Figure 2.1). Similar complexes of Rh,[14] Ir,[15] Os,[8,16] and Re[17,18] have been studied, and in general have the trans-meridional configuration, which was confirmed by a single crystal structure analysis of $[ReCl_3(NO)(MePPh_2)_2]$.[19]

Analogous organic phosphine oxide or arsine oxide complexes of ruthenium[20] or molybdenum[21] have also been reported. The trans-meridional configuration also dominates when the nitrosyl ligand is replaced with a carbonyl group (i.e. $[MX_3(CO)L_2]$) and L is a tertiary phosphine.[14,22-26] A series of complexes of the type $[RuX_3YL_2]$ where Y = PPh_3 and L = Et_2S, Me_2S[27] or Y = MeOH and L = i-PrSPh[28] have been isolated, and the sulphide donor properties were investigated.

(ii) Cis-meridional and cis-facial configuration

Some evidence for the cis-facial configuration has been presented[7] for the tertiary phosphine complexes of

the type $[RuX_3(NO)L_2]$. When L_2 is a bidentate tertiary phosphine (or arsine) ligand the phosphorus atoms must occupy cis coordination sites, and therefore the cis-meridional configuration is also a possibility.[12]

(b) $[MX_3L_3]$ and $[MX_2L_2]$ complexes

Second and third row transition metal (Pt, Ir, Rh and Au) complexes with thioethers (Et_2S, Me_2S and Bz_2S) were first obtained during 1930-1940.[29-32] More recently the Pt and Pd halogeno complexes with dialkyl sulphides (or selenides and tellurides) have been the subject of a number of studies.[33-41] The low frequency infrared spectra in particular have been studied in order to investigate the nature of the M-X and M-S(Se) bonding. The stereochemical arrangement of the ligands in these $[MX_2L_2]$ complexes have been identified.

Spectroscopic studies of complexes of the type $[MX_3L_3]$, (M = Ru, Os, Rh, Ir; X = Cl, Br, I and L = dialkyl (or phenylalkyl) sulphide), have been carried out.[40-43] Also the isomeric forms and variations in composition (e.g. $[Rh(R_2S)_4Cl_2]Cl$) of the rhodium and iridium dialkyl sulphide complexes have been investigated.[44,45] The infrared and nuclear magnetic resonance spectra of several mercury dialkyl sulphide complexes have been studied.[33,41,46]

2.1.2 A Review of the Modes of Coordination of Nitrosyl Ligands

Ruthenium has a strong affinity for nitric oxide, forming numerous nitrosyl complexes. Over the past 20 years

the bonding within the Metal-N-O unit has been extensively studied. As late as 1968 it was shown[55] conclusively that the M-N-O bond system was not always linear but could be bent with the M-N-O angle ranging from 120° to 180°. Aspects of nitrosyl complexes have been reviewed such as bonding,[56,57] stereochemistry,[58] synthetic methods,[59] spectral studies[60] and structural characteristics.[61]

Nitric oxide is an odd electron molecule with one electron residing in a σ or π antibonding orbital. If this unpaired electron is transferred to the metal atom on coordination then the nitrosyl formally bonds as NO^+ in a linear manner. Hence with the additional donation of a σ pair the nitrosyl becomes a three electron donor ligand. The nitrosyl group can also accept π electrons back from full metal d orbitals into an unoccupied antibonding π orbital, as shown below. This back bonding strengthens the

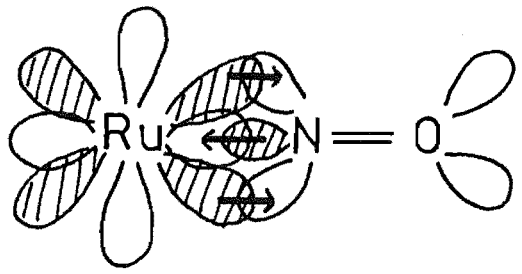

metal-nitrogen bond, and gives it multiple bond character. This bonding description is confirmed from the observed short M-N bond distances of ca. 1.71 Å[61] for linearly coordinated nitrosyls compared with a formal Ru-N single bond length of 2.15 Å obtained for the $[Ru(NH_3)_5(DMSO)]^{2+}$ complex.[62]

However, when the M-N-O bond system is bent (~120°) the metal atom is considered to have donated an electron to the nitrosyl giving formally NO^-. The sp hybridised nitrogen atom in the linear NO^+ situation now becomes sp^2 hybridised for NO^- and the nitrosyl ligand donates only one electron to the M-N bond.

linear bent

Lewis dot structures

Also the back donation of electrons from the metal orbitals is not possible hence the M-N bond is generally longer (ca. 1.89 Å) compared with the linearly coordinated NO.

Linear coordination of NO leads to a reduction in the formal oxidation state of the metal, while bent coordination results in an increase in the formal oxidation state. A range of intermediate M-N-O angles between the extremes of 120° and 180° have been observed.[57,60] It is reported[63] that the nitrosyl ligand can interchange between the two bonding modes and therefore may act as both an electron pair sink and pump. This occurs when the 5 coordinate cationic complexes of the type $[M(NO)L_2Y_2]^{2+}$, where M = Ir, Rh; L = PPh_3, Y = MeCN, react with a bidentate bipyridine species. The configuration changes from square pyramidal to trigonal bipyramidal and the resulting interconversion of the NO bonding mode from bent to linear results

in a reduction of the metal's oxidation state.

The large variation in the M-N-O bond angle is reflected in the wide range observed for the ν(N-O) stretching frequency in the infrared, i.e. 1400-2000 cm^{-1}. The nitrosyl ligands generally exhibit ν(N-O) absorptions at the lower frequency when coordination is bent and at the higher frequency for linear coordination. When the bond angles are intermediate, assignment of the mode of coordination using infrared data is not reliable because other factors within the complexes will also have an effect (e.g. bond strength) on the stretching frequency of the N-O bond. Ibers and Haymore[10] have proposed a set of empirical rules to allow for these other factors. Values are either added to or subtracted from the observed ν(N-O) value depending on the overall charge associated with the complex, the ligand type, the periodic row and column number. By following this procedure they found that the adjusted stretching frequencies fell into two distinct groups above and below 1610-1620 cm^{-1}. With this approach the ν(N-O) position may be used to suggest the mode of coordination of the nitrosyl ligand.

2.2 RESULTS AND DISCUSSION

A series of $[RuX_3(NO)L_2]$ complexes, where X = Cl, Br, I and L = Me_2S, MeSPh, Et_2S, PhSEt, Pr_2S, PhSPr, Bz_2S, Et_2Se, PhSeEt and DMSO, were prepared by adding the chalcogens, in small excess, to an ethanolic solution of the '$RuX_3(NO)$' entity. The solution was heated under reflux then on partial removal of the solvent in vacuo the complexes precipitate out. The complexes formed were air stable.

2.2.1 High Frequency Infrared Spectra (4000-400cm^{-1})

The high frequency infrared spectra of the $[RuX_3(NO)L_2]$ complexes are characterised by an intense absorption in the 1800-1900cm^{-1} region attributable to the ν(N-O) stretching frequency. A distinctive feature of the sulphoxide complexes is a band in region 900-1200cm^{-1} which is associated with the ν(S-O) stretching vibration. The results are listed in Tables 2.1, 2.2 and 2.3. Even without using the Ibers and Haymore adjustment[10] of subtracting 30cm^{-1} (the correction necessary for these Ru(II) compounds) the ν(N-O) values of 1825-1878cm^{-1}, lie well above 1610-1620cm^{-1}. Therefore the nitrosyl ligand is expected to be coordinated in a linear manner. Unfortunately the crystal structure analysis of $[RuBr_3(NO)(PhSEt)_2]$ (see Chapter 7) was not of sufficient accuracy to resolve whether the nitrosyl was coordinated either linearly or bent. However, for the $[RuBr_3(NO)(Et_2SO)(Et_2S)]$ complex the crystal structure determination (see Chapter 6) clearly showed that the nitrosyl was bonded in a linear fashion. The diamagnetism of the complexes suggests a spin paired d^6 Ru(II) configuration which is further support for a linear Ru-N-O linkage.

Some trends in the ν(N-O) stretching frequency are apparent from the data in Tables 2.1 and 2.2. The observed differences are often very small (i.e. 0-25cm^{-1}), reducing the significance of the trends but in general the following trends in ν(N-O) are observed:

(i) R_2S complexes > PhSR complexes for the chloro species,

(ii) R_2S complexes < PhSR complexes for the bromo species,

TABLE 2.1

Infra-red spectra of the $[RuCl_3(NO)L_2]$ complexes, (cm^{-1})

Assignment	L = Me_2S	MeSPh	Et_2S[a]	PhSEt[a]	Pr_2S[a]	PhSPr[a]	Et_2Se[a]	PhSeEt[a]	Bz_2S
ν(N-O)	1886sh			1864sh				1857sh	
	1872	1876	1868	1845	1870	1867	1867	1835	1874
	1856sh								
ν(Ru-Cl) trans to NO	348s	352m	356sh	347s	342s	350sh	336s	340s	335s
ν(Ru-Cl) trans to Cl	332s	343sh	342s	335s	331sh	335sh	325sh	331sh	328sh
	316m	332s	334s	327sh	319sh	327s	304sh	320sh	324sh
ν(Ru-S(Se))	290m	301m	289m	296m	292m	295m	226m	233m	291m
	271m		282m					205s(?)	
δ(Ru-S(Se)-C)	224m	218m		211s	222w	220m	146w	146w	206m
Other bands								302m	
							292m	295m	
								277w	268m
			252w	252w					253w
					210w				236w
	163m		179w	171w		165w			172m
	121w	128w	162w		135m	145w			
						108w			

[a] Initially determined in reference 1.

TABLE 2.2

Infra-red spectra of the $[RuBr_3(NO)L_2]$ complexes, (cm^{-1}).

Assignment	L=Me_2S	MeSPh	Et_2S[a]	PhSEt[a]	Pr_2S[a]	PhSPr	Et_2Se[a]	PhSeEt[a]	Bz_2S
ν(N-O)	1872	1873	1857	1870	1849	1867	1850	1862	1868
ν(Ru-Br)	275s	264s	249s	268s	270s	264s	263s	260s	270s
				250m					259m
ν(Ru-S(Se))	315s(?)	307m	280sh		322m(?)		228s	221w	
	293w	298m						209m	
		293m							
δ(Ru-S(Se)-C)	236m					235m			
	208s	235s	229s	230s	228s	220m	112w	110m	223s
Other bands			353w					303w	
		212m	212w	213m		183w			
	180w		162m		132-	145w			
	124s	121w	122m	117w	125m(br)	125w			

[a] Initially determined in reference 1.

TABLE 2.3

Infra-red spectra of some ruthenium sulphoxide complexes, (cm^{-1})

Assignment	$RuCl_3(NO)(Me_2SO)_2$	$RuBr_3(NO)(Me_2SO)_2$	$RuBr_3(NO)(Et_2SO)(Et_2S)$	$[RuBr_3(NO)(Et_2SO)]_2$
ν(N-O)	1890	1894	1866	1878
		1874		
ν(S-O)	910	1122	924	921
		916		
ν(Ru-O)	515	504	515	519
	505			
ν(Ru-X)	350s	277s	263s	280-250s (br)
	345s	270s	245m	
	339s			
Other bands		367m		350m
		339m	284m ν(Ru-S)	323w
		307w		228s
	253w	247sh		
	187w	201w	214w	162w
	154w	183w	112m	115w

(iii) Cl > Br > I for the same R_2S ligand,

(iv) Cl < Br < I for the same PhSR ligand,

(v) sulphide complexes > selenide complexes

(this parallels tertiary phosphine and arsine complexes[7] where the ν(NO) decreases in the order P > As).

It would appear that different effects dominate for the different series of complexes and it is not possible to single out any particular factor. Electronic effects which may influence the ν(N-O) stretching frequency are:

(i) the halogen ligands can act as π electron acceptors in the order I > Br > Cl,

(ii) the greater electron withdrawing ability of a phenyl group with respect to an alkyl group will cause the sulphur atom to be slightly more electropositive in the PhSR complexes, which would assist in a drift of electron density towards the Ru-S bond,

(iii) the greater electronegativity of the chloride ligand compared with the bromide.

The ν(N-O) absorption for the $[RuCl_3(NO)L_2]$ complexes where L = Me_2S, PhSEt or PhSeEt is split into two or three bands, but in solution only a single ν(N-O) absorption is observed. Such an effect has been noted previously[7,11,12] and is assigned to solid state effects. A weak absorption observed in the region 590-600cm^{-1} has been assigned previously[64] to the ν(Ru-N) and/or δ(Ru-N-O) absorptions.

(a) High frequency infrared results for ruthenium sulphoxide complexes

The infrared spectrum of the complex $[RuCl_3(NO)(DMSO)_2]$ contains an absorption at 910cm^{-1} associated with the ν(S-O)

stretching frequency when the sulphoxide ligand is bonded to the ruthenium through the oxygen atom. The corresponding bromo complex has two absorptions, at 916 and 1122cm^{-1}, suggesting both a sulphur and oxygen bonded sulphoxide ligand. The complex $[RuCl_3(NO)(DMSO)_2]$ has been reported previously[65] but the mode of coordination of the sulphoxide ligand was not investigated. Table 2.4 lists the sulphoxide complexes of ruthenium and the mode of coordination of the sulphoxide ligand. It appears from the information available that the sulphoxide ligand generally bonds to Ru(II) through sulphur, unless steric interactions make oxygen coordination more favourable. The two sulphoxide complexes whose structures were determined in this work (see Chapters 6 and 7), $[RuBr_3(NO)(Et_2SO)]_2$ and $[RuBr_3(NO)(Et_2SO)(Et_2S)]$, have the sulphoxides bonded through oxygen, the infrared data is in agreement with this. In both compounds it appears that steric factors are the reason for oxygen coordination (see p152 and Table 2.4).

An absorption at ca. 500cm^{-1} for oxygen bonded sulphoxide complexes has been assigned[66] previously to the ν(Ru-O) stretching vibration. A similar assignment is given in Table 2.3.

2.2.2 Low Frequency Infrared Spectra (400-40cm^{-1})

The low frequency infrared spectra of the $[RuX_3(NO)L_2]$ complexes have been recorded and assignments made for the ruthenium-halogen and ruthenium-sulphur (or selenium) vibrations. The results are given in Tables 2.1 and 2.2 with the appropriate assignments. Some typical low frequency

TABLE 2.4

Mode of Coordination of the Sulphoxide Ligand to Ruthenium

	S coordinated	O coordinated	Reference
$RuCl_3(NO)(DMSO)_2$		✓	This work
$RuBr_3(NO)(DMSO)_2$	✓	✓	This work
$RuCl_3(PR_3)_2(DMSO)$	✓		27
$[Ru(NH_3)_5(DMSO)]^{2+}$	✓		62
$RuBr_3(NO)(Et_2SO)(Et_2S)$		✓	This work
$[RuBr_3(NO)(Et_2SO)]_2$		✓	This work
$[RuCl_3(DMSO)_3]^-$	✓		66
$RuCl_2(DMSO)_4$	3✓	✓	67

infrared spectra obtained for a number of the $[RuX_3(NO)L_2]$ complexes are given in Figure 2.2.

Since numerous studies[28,33-35,37-40,43,46] of the low frequency infrared spectra of transition metal halogen complexes with dialkyl sulphide ligands have been carried out, the assignment of the ruthenium-halogen and ruthenium-chalcogen stretching vibrations are readily made by comparison with previous results. Comparison of the spectra of chloro complexes with those of bromo complexes also aids in the assignments.

(a) Assignment of absorption bands

The ν(Ru-Cl) absorptions occur as three intense bands in the 304-356cm^{-1} region. As observed previously[40,43] the ν(Ru-Br) mode often yields less peaks than expected from symmetry considerations. Therefore only one or two strong absorptions in the 235-275cm^{-1} region were observed and assigned to the ν(Ru-Br) stretching vibrations. Absorptions of medium to weak intensity around 280-300cm^{-1} have been assigned to the ν(Ru-S) stretching frequency, and ca. 220cm^{-1} to the ν(Ru-Se) stretching frequency. This is in accord with previous reports.[34,38-40,43,46] The less intense ν(Ru-S) stretching mode may sometimes be masked by the broad ν(Ru-Cl) stretching absorption.[40]

The point group symmetry of the trans-meridional $[RuX_3(NO)L_2]$ complex is C_{2v}, and three normal modes $(2a_1 + b_1)$ for the Ru-X stretching vibrations are expected, all of which are infrared active.[68]

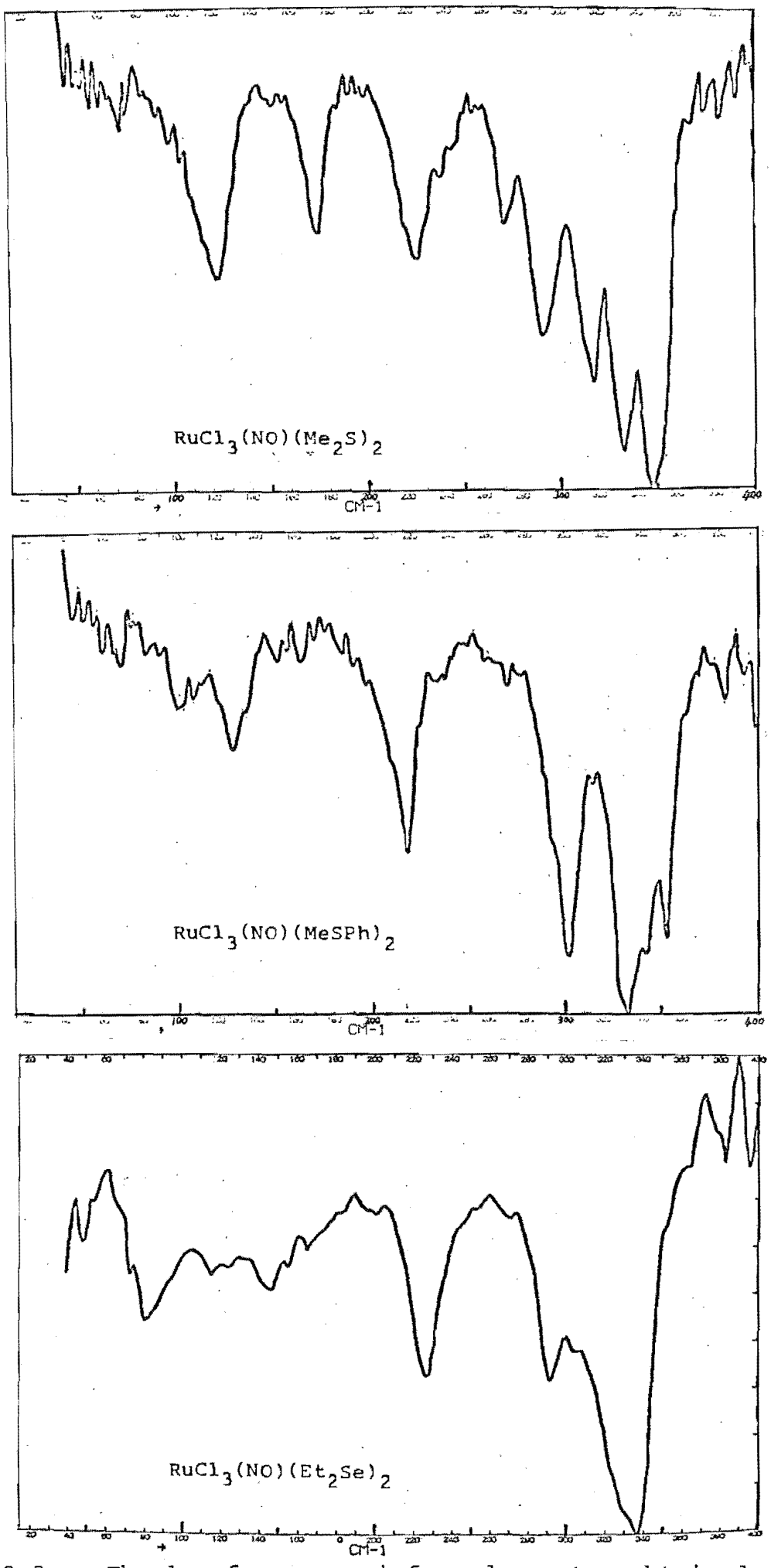

FIGURE 2.2. The low frequency infrared spectra obtained for some of the $[RuX_3(NO)L_2]$ complexes

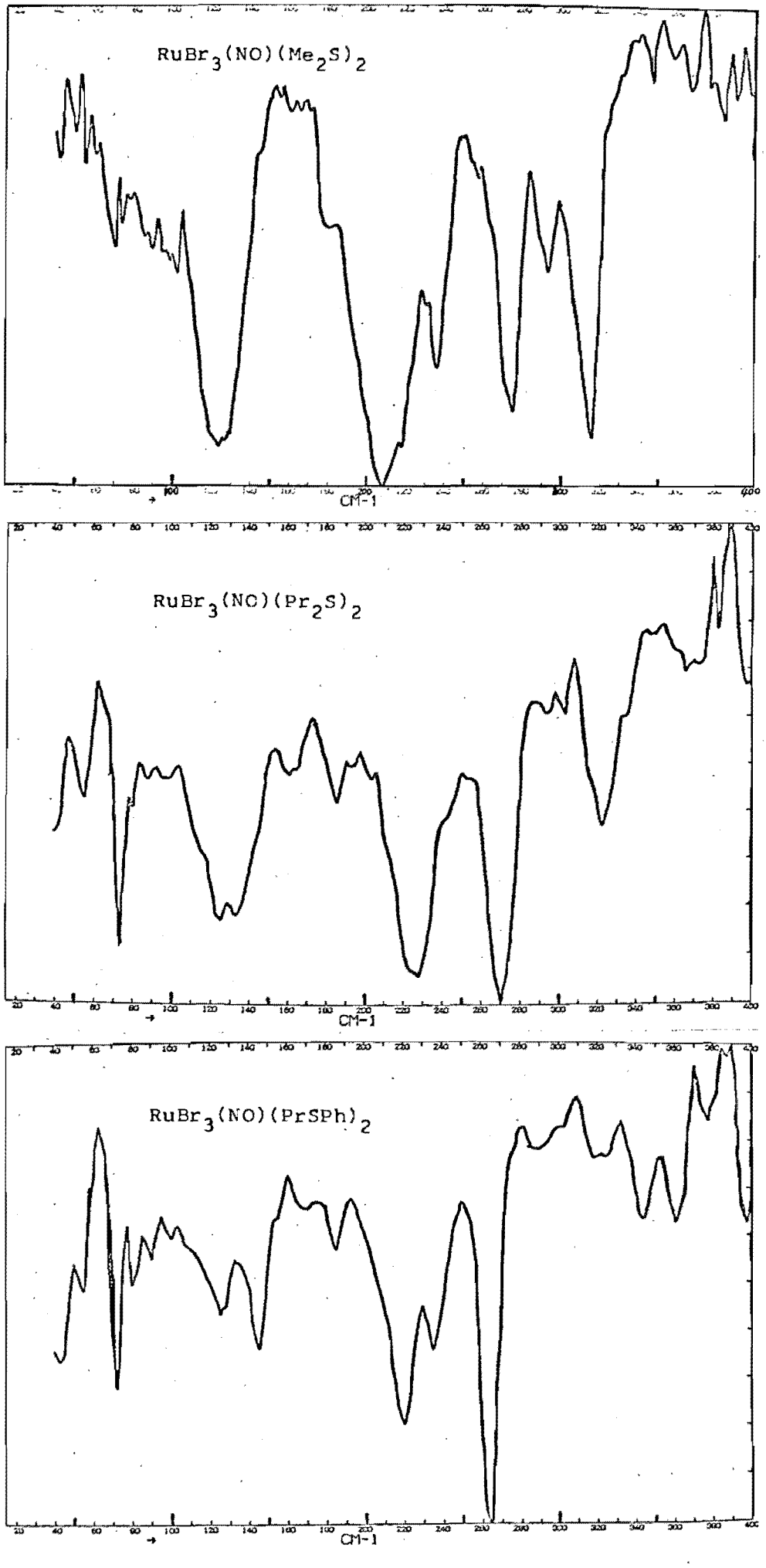

FIGURE 2.2 continued.

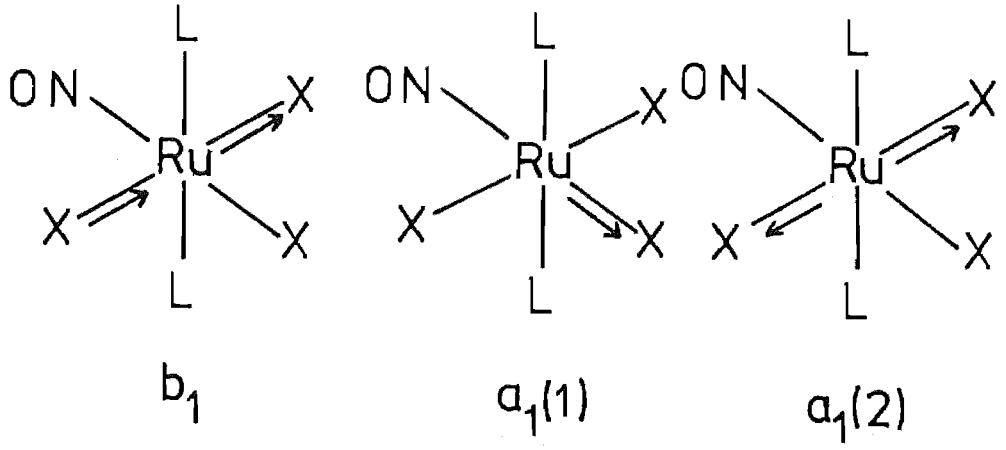

The three Ru-X stretching modes (illustrated above), should appear as three intense absorptions as the rate of change of dipole moment with bond length is large for the Ru-X bonds. Of the three the $a_1(2)$ mode which involves the symmetrical vibration of the trans halogen ligands may be the weakest because the dipole moment changes will be the least.

The crystal structures of the phosphine complexes $[RuCl_3(NO)(PPh_3)_2]$[10] and $[RuCl_3(NO)(PMePh_2)_2]$[9] indicate that the Ru-Cl bond for the Cl ligand <u>trans</u> to the NO group is significantly shorter than the other Ru-Cl bonds, i.e. 2.353 Å compared with 2.394 Å, and 2.357 Å compared with 2.405 and 2.391 Å respectively. The Re-Cl bond <u>trans</u> to the NO group in $[ReCl_3(NO)(PMePh_2)_2]$[19] is 2.326 Å while the other Re-Cl bonds are 2.354 Å. The structure of $[RuBr_3(NO)(PhSEt)_2]$, (see Chapter 7) although less accurately determined, shows a similar tendency, i.e. the average Ru-Br bond length <u>trans</u> to the NO group is 2.51 Å while the mean of the other Ru-Br bond distances is 2.52 Å. On this evidence the highest energy ν(Ru-X) stretching mode is assigned to the Ru-X bond <u>trans</u> to the NO group, i.e. the $a_1(1)$ mode.

The highest energy ν(Ru-Cl) absorption for $[RuCl_3(NO)(R_2S)_2]$ occurs in the 336-356cm^{-1} region, which is approximately 20cm^{-1} higher than the observed ν(Ru-Cl) absorption for the $[RuCl_3(R_2S)_3]$ complexes.[28,40] This is not expected on the basis of the different oxidation state of ruthenium in the two types of complexes, and emphasises the influence of the nitrosyl ligand on the trans Ru-Cl bond. Presumably the electron acceptor properties of NO confers a greater electropositive character on the metal than by an increase in oxidation state. The three ν(Ru-Cl) absorptions also occur at a higher frequency than for the analogous tertiary phosphine complexes,[7] i.e. ca. 347, 335 and 327cm^{-1} compared with 327, 318 and 288cm^{-1}. This has been commented on previously.[40,43]

A strong absorption around 220cm^{-1} is observed in most of the thioether complexes and is assigned to the δ(Ru-S-C) bending mode. The assignment is made on the basis of similar reported assignments.[13,33,38,39]

Other bands in the low frequency spectra are usually weak and specific assignments have not been attempted.

(b) Determination of configuration

The trans-meridional and cis-meridional configurations (Figure 2.1) have a meridional arrangement of halogen ligands and three infrared active ν(Ru-X) stretching modes are expected. The cis-facial configuration has a point symmetry for the molecule of C_s. Hence the e mode (in C_{3v} symmetry for facial $[MX_3L_3]$)[68] becomes non degenerate and with the a_1 mode, three infrared active absorptions are expected.

Therefore each of the three isomers should exhibit up to three Ru-X stretching vibrations and cannot be distinguished without a detailed analysis. For most of the chloro complexes three absorptions were observed and one or two for the bromo complexes.

2.2.3 ^{1}H N.M.R. spectra

The ^{1}H n.m.r. spectra of the $[RuX_3(NO)L_2]$ complexes which were recorded in deuterochloroform are reported in this work. The observed ^{1}H n.m.r. resonances and assignments based on a first order spectral analysis of the free and coordinated (in a $RuX_3(NO)L_2$ complex) organic chalcogen ligands are listed in Table 2.5, and illustrated in Figure 2.3. Three regions of absorption are observed (depending on the nature of the organic group bonded to the chalcogen atom), i.e. resonances due to the methyl group, methylene group and phenyl group. Relative to tetramethyl silane at zero ppm, these resonances usually appear in the 1-1.5, 2-4 and 7-8 ppm regions respectively. The chemical shift values were obtained by taking the mid-point of each resonance multiplet peak. Some typical ^{1}H n.m.r. spectra are reproduced in Figure 2.4.

(a) The effect of coordination on the chemical shift position

Coordination of the organic chalcogen ligand to ruthenium, means donation of a lone electron pair from the sulphur (or selenium) atom into a vacant ruthenium orbital. The sulphur atom then becomes more electropositive and there will be a drift of electron density from the organic

TABLE 2.5

^{1}H n.m.r. spectra

Chemical shift δ(ppm) from Me_4Si. Coupling constants for the alkyl protons are 7-8 Hz and 2-3 Hz for phenyl protons.

Compound	α	β	γ	Phenyl[a]
Me_2S	2.12(s)			
$RuCl_3(NO)(Me_2S)_2$	2.66(s)			
$RuBr_3(NO)(Me_2S)_2$	2.76(s)			
MeSPh	2.25(s)			7.11
$RuCl_3(NO)(MeSPh)_2$	2.97(s)			7.35(p+m), 7.70(o)
$RuBr_3(NO)(MeSPh)_2$	3.12(s)			7.35(p+m), 7.75(o)
Et_2S	2.53(q)	1.23(t)		
$RuCl_3(NO)(Et_2S)_2$[b]	3.19(q)	1.46(t)		
$RuBr_3(NO)(Et_2S)_2$[b]	3.28(q)	1.47(t)		
EtSPh	2.87(q)	1.23(t)		7.21

TABLE 2.5 continued.

$RuCl_3(NO)(EtSPh)_2$[b]	3.70(q)	1.30(t)		7.41(p+m), 7.76(o)
$RuBr_3(NO)(EtSPh)_2$[b]	3.79(q)	1.27(t)		7.38(p+m), 7.77(o)
$n\text{-}Pr_2S$	2.48(t)	1.61(sx)	0.97(t)	
$RuCl_3(NO)(Pr_2S)_2$[b]	3.13(t)	1.84(sx)	1.07(t)	
$RuBr_3(NO)(Pr_2S)_2$[b]	3.18(t)	1.84(sx)	1.08(t)	
n-PrSPh	2.82(t)	1.61(sx)	0.96(t)	7.20
$RuCl_3(NO)(PrSPh)_2$[b]	3.60(t)	1.65(sx)	1.00(t)	7.36(p+m), 7.72(o)
$RuBr_3(NO)(PrSPh)_2$[b]	3.71(t)	ca. 1.6	ca. 1.0	7.37(p+m), 7.77(o)
Et_2Se	2.58(q)	1.39(t)		
$RuCl_3(NO)(Et_2Se)_2$[b]	3.38, 3.08[c]	1.55(t)		
$RuBr_3(NO)(Et_2Se)_2$[b]	3.42, 3.13[c]	1.54(t)		
$RuI_3(NO)(Et_2Se)_2$[b]	3.38(q)	1.55(t)		
EtSePh	2.83(q)	1.35(t)		7.14, 7.20, 7.45
$RuCl_3(NO)(EtSePh)_2$[b]	3.67(q)	1.44(t)		7.36(p), 7.44(m), 7.78(o)
$RuBr_3(NO)(EtSePh)_2$[b]	3.75(q)	1.42(t)		7.39(p+m), 7.78(o)

TABLE 2.5 continued.

Bz_2S	3.58(s)	7.26
$RuCl_3(NO)(Bz_2S)_2$	4.42(s)	7.27
$RuBr_3(NO)(Bz_2S)_2$	4.58(s)	7.25

s = singlet, t = triplet, q = quartet, sx = sextet

[a] For the phenyl resonances; p = para, m = meta, o = ortho.

[b] Initially determined in reference 1.

[c] Overlapping quartet resonances of equal intensity.

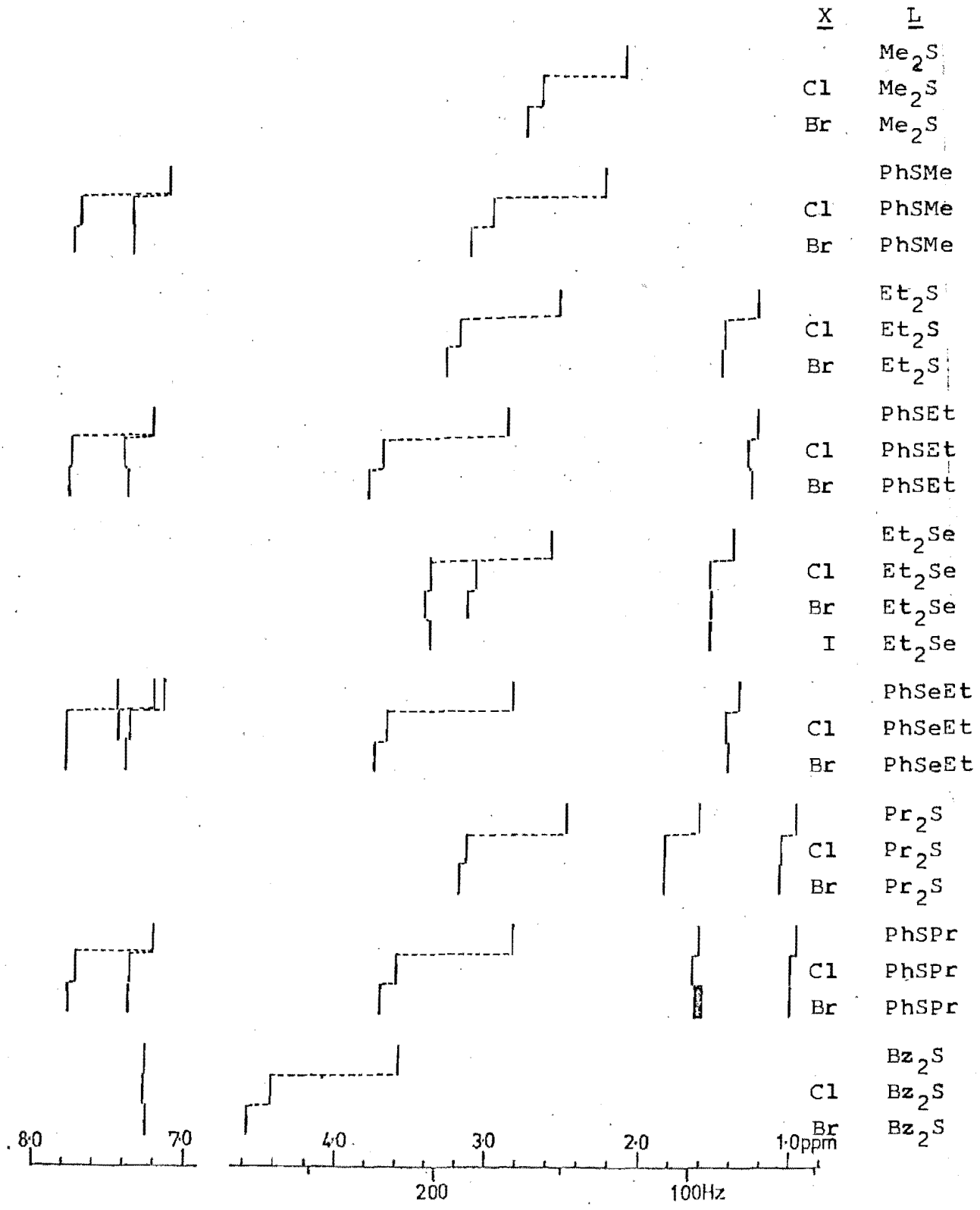

FIGURE 2.3

The relative positions of the ^{1}H n.m.r. absorptions for the free thioether ligands, $[RuCl_3(NO)L_2]$ and $[RuBr_3(NO)L_2]$ complexes.

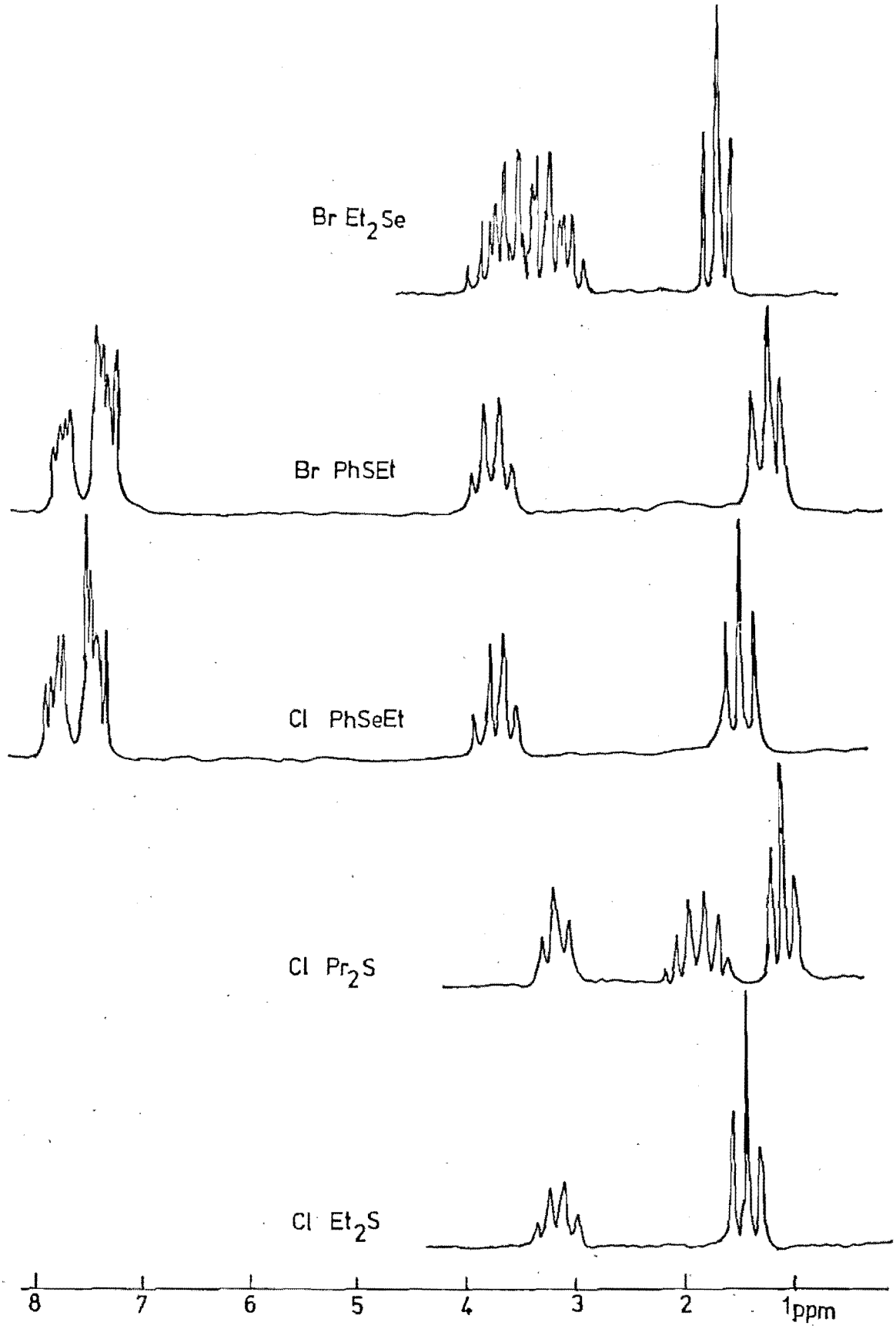

FIGURE 2.4

The ^1H n.m.r. spectra observed for some of the $[RuX_3(NO)L_2]$ complexes.

groups to the sulphur. The reduction of electron density on the protons results in a deshielding of the nucleus, which is observed as a downfield shift of the resonances. The greatest deshielding occurs for the protons on the carbon atom bonded to sulphur (or selenium) atom, i.e. the α carbon. The magnitude of the downfield shift of the α protons on coordination, is observed to be 32-42 Hz for the dialkyl chalcogen ligands and 42-55 Hz for the phenylalkyl chalcogen ligands. While delocalisation of the electron density from sulphur towards the phenyl group would account for the larger downfield shift of the free phenylalkyl ligands when compared with free dialkyl ligands, the difference observed on coordination is difficult to explain. The smaller shift for the β protons follows an opposite trend, i.e. 9-15 Hz for R_2S complexes but 2-5 Hz for PhSR complexes. Perhaps the β protons are in such a position that they become involved in the shielding cone of the phenyl group.[33]

Both the $[RuCl_3(NO)(Et_2Se)_2]$ and $[RuBr_3(NO)(Et_2Se)_2]$ complexes exhibit further splitting from the expected first order spectrum, which is related to the ability of the ligands to undergo an inversion of configuration about the three coordinate sulphur or selenium atom. This aspect will be considered in more detail in Chapter 3.

The phenyl proton resonances for the PhSR compounds usually appear as a single absorption (~7.2 ppm), but on coordination two groups of resonance multiplets occur with an integrated intensity ratio of 2:3. The peak of smaller area which has shifted ~30 Hz downfield on coordination is assigned to the resonance of the ortho protons, while the second (shifted 9-14 Hz downfield) corresponds to the resonance

of the meta and para protons. The ortho protons being nearer the chalcogen atom are expected to be deshielded the greatest.

(b) The effect of change in halogen ligand

The position of the methylene multiplet is probably the most sensitive to changes in the electron distribution within the $[RuX_3(NO)L_2]$ complexes. For analogous compounds the methylene resonances in the bromo complexes are 3-9 Hz further downfield than for the chloro complexes. Other resonances show only a small shift with halogen, if any at all.

The possible explanations for increased deshielding of order Cl < Br are:

(i) metal to halogen $M_{d_\pi} \rightarrow X_{d_\pi}$ bonding is expected to be greater for the bromo complexes compared with the chloro complexes,

(ii) the increasing size of the halogen ligand in the order Cl < Br, may cause more intramolecular non-bonded interactions,

(iii) the polarisability of the halogen ligands is considered to increase in the order Cl < Br. However, it appears from a previous study[11] that the most likely explanation is (i). The greater deshielding of the α carbon protons in the bromo complexes is therefore in terms of the modification of electron density within the complexes through metal to halogen $M_{d_\pi} \rightarrow X_{d_\pi}$ bonding. A greater $Ru_{d_\pi} \rightarrow Br_{d_\pi}$ interaction (compared with the chloro situation), will decrease the electron density on the ruthenium, and assist in an electron drift from the sulphide (or selenide) ligand to the metal and consequently further deshield the α protons.

The deshielding of the methylene protons in the $[RuX_3(NO)L_2]$ complexes is greater than observed[33,40] for the square planar platinum and palladium complexes of the MX_2L_2 type, (where X = halogen and L = organic sulphide ligands). For example, a downfield shift of 20-30 Hz occurs for the MX_2L_2 complexes while 40-50 Hz is observed for the $[RuX_3(NO)L_2]$ complexes. The difference is probably associated with the nitrosyl ligand and its ability to accept π electrons from the ruthenium atom. As a consequence an additional deshielding is observed for the $[RuX_3(NO)L_2]$ complexes.

(c) Determination of stereochemistry

^1H n.m.r. results have been used previously[6,7,13] to determine which isomeric form of the complexes $[RuX_3(NO)L_2]$ exist. When L is a tertiary phosphine ligand, there is the possibility of 'virtual coupling'[6,7,13] occurring if the phosphine ligands are in mutually trans positions. However, this does not occur for dialkyl sulphide complexes.

In the cis-meridional isomer (see Figure 2.1) the sulphide ligands are in different chemical environments and two separate resonances for each proton type should be observed. The results obtained rule this out as only one chemical environment is observed in the n.m.r. spectra.

For the cis-facial isomer free rotation about the Ru-S bond will be restricted because of close interactions (as observed from molecular models) between the organic groups bonded to the sulphur atom. When the sulphide ligand is of the type R_2S, the ligand arrangement involving

least steric interaction would place the alkyl groups on the same sulphur atom in different magnetic environments. This would also be observed as two separate resonances for each proton type in the alkyl group. This situation has been reported[7] for a tertiary phosphine complex having the cis-facial stereochemistry.

For the trans-meridional isomer free rotation about the Ru-S bond would be unimpeded and as a result the magnetic influence of the nitrosyl in the 'RuX_3NO' moiety will be averaged over all the R groups. The spectrum expected in this case agrees with what is observed.

Hence, from the ^1H n.m.r. results it appears that the most likely arrangement is the trans-meridional isomer. This was confirmed (see Chapter 7) by a single crystal X-ray analysis of $[RuBr_3(NO)(PhSEt)_2]$ where the halogen ligands are in a meridional position and the sulphide ligands were mutually trans.

2.2.4 ^{13}C N.M.R. Spectra

The ^{13}C n.m.r. spectra of the $[RuX_3(NO)L_2]$ complexes have been obtained in deuterochloroform. The spectra are relatively simple with single sharp resonance peaks for each type of carbon atom environment, as coupling between the carbon atoms is not observed due to the low abundance of the carbon-13 isotope (1.11%). Also decoupling between the ^1H and ^{13}C nuclei removes any further resonances arising from ^1H-^{13}C coupling.

The results are listed in Table 2.6 and some of the spectra are portrayed in Figure 2.5.

TABLE 2.6

^{13}C n.m.r. spectra

In ppm downfield from Me_4Si

Compound	α	β	γ	Phenyl		
				p	m	o
$RuCl_3(NO)(Me_2S)_2$	22.66					
$RuCl_3(NO)(MeSPh)_2$	20.84			129.33	129.63	130.91
$RuCl_3(NO)(Et_2S)_2$	30.72	13.17				
$RuCl_3(NO)(EtSPh)_2$	32.00	12.23		129.68	130.66	131.05
$RuCl_3(NO)(Pr_2S)_2$	39.26	21.74	13.17			
$RuCl_3(NO)(PrSPh)_2$	39.74	20.69	13.08	129.68	130.58	130.96
$RuCl_3(NO)(Et_2Se)_2$	26.38	13.69				
$RuCl_3(NO)(EtSePh)_2$	29.45 29.12	12.78		129.89	130.70	131.31
$RuCl_3(NO)(Bz_2S)_2$	41.94			128.39	128.91	130.07
$RuBr_3(NO)(Me_2S)_2$	25.18					
$RuBr_3(NO)(MeSPh)_2$	23.71			129.48	129.68	130.95
$RuBr_3(NO)(Et_2S)_2$	32.76	13.61				
$RuBr_3(NO)(EtSPh)_2$	35.15	12.89		129.68	130.64	131.04
$RuBr_3(NO)(Pr_2S)_2$	41.30	22.06	13.09			
$RuBr_3(NO)(Et_2Se)_2$	27.93	13.97				
$RuBr_3(NO)(EtSePh)_2$	31.55 30.96	13.28		129.88	130.66	131.25
$RuBr_3(NO)(Bz_2S)_2$	44.44			128.34	128.82	129.92

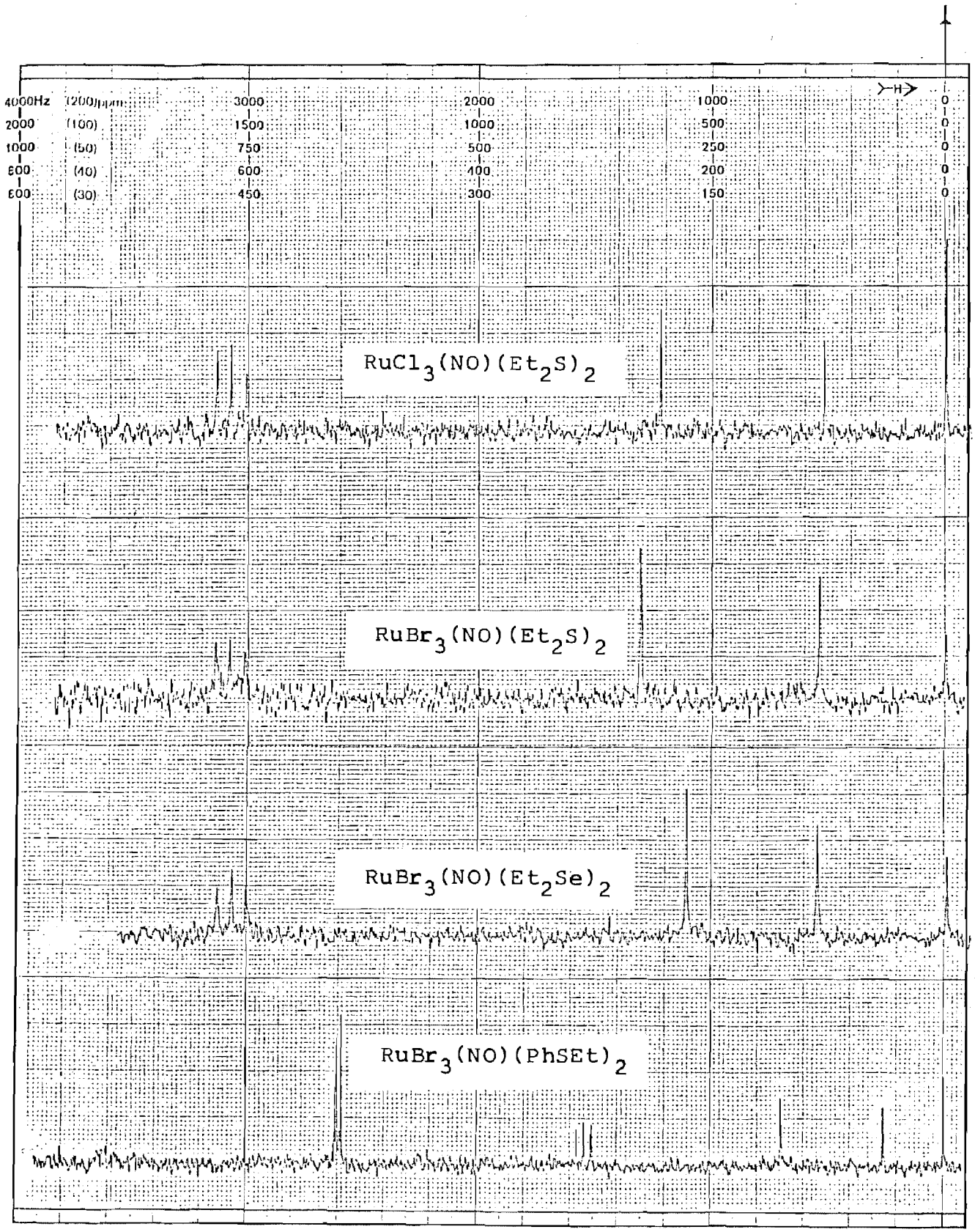

FIGURE 2.5

The ^{13}C n.m.r. spectra observed for some of the $[RuX_3(NO)L_2]$ complexes.

(a) The effect of change in halogen ligand

Analogous to the ^{1}H n.m.r. spectra, the ^{13}C resonance shifts further downfield (40-60 Hz) when the chloro ligands are changed to bromo ligands (see Figure 2.6). A similar explanation to that given above for the shift in the ^{1}H n.m.r. spectra may be used (see section 2.2.3(b)) to interpret the trends observed.

The phenyl carbon resonances occur as three separate signals corresponding to the ortho, meta and para carbon atoms in the phenyl group. As for the ^{1}H n.m.r. spectra, the resonance furthest downfield is assigned to the ortho carbon atoms, and the next lowest resonance to the meta carbon atoms.

(b) Determination of stereochemistry

The ^{13}C n.m.r. results lend support to the trans-meridional isomer being the most likely structure for the $[RuX_3(NO)L_2]$ complexes. However, for the $[RuX_3(NO)(PhSeEt)_2]$ complexes the ^{13}C n.m.r. spectrum has a doublet rather than a singlet for the methylene carbon atoms. The ^{13}C n.m.r. spectrum showed no shift in position of the resonances as the temperature was varied. This suggests that a mechanism involving a rapid interchange between two environments is unlikely to be the cause of the splitting. The variable temperature ^{1}H n.m.r. spectra of the PhSeEt complexes indicate that the methylene protons on each of the PhSeEt ligands are in equivalent environments. The X-ray powder photographs of the $[RuBr_3(NO)(PhSEt)_2]$ and $[RuBr_3(NO)(PhSeEt)_2]$ complexes indicate that they are isomorphous. Therefore since the single crystal X-ray structure of the sulphide

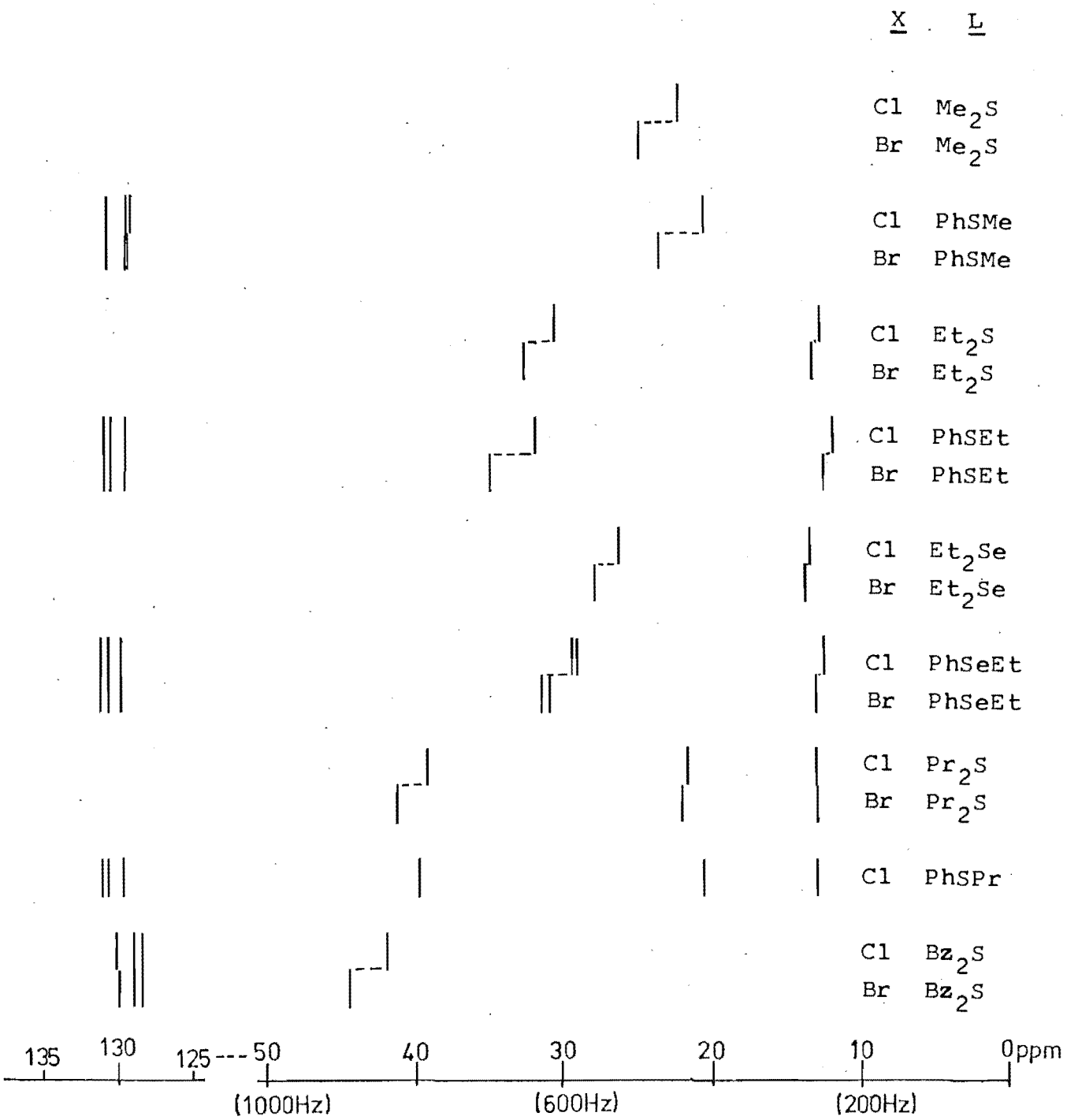

FIGURE 2.6

Relative shifts in the ^{13}C n.m.r. positions for the $[RuX_3(NO)L_2]$ complexes

complex (see Chapter 7) show it to be the trans-meridional isomer, this suggests that the splitting of the methylene resonance in the ^{13}C n.m.r. spectra for the selenide complexes is unlikely to be due to a different structure. However, the X-ray results refer to the solid state while the n.m.r. spectra are obtained of solutions. It is possible that a stronger $Ru_{d_\pi} \rightarrow Se_{d_\pi}$ interaction slows the Ru-Se bond rotation so the ethyl groups may be constrained in slightly different environments.

2.2.5 U.V. - Visible Spectra

The observed U.V. and visible absorptions for the $[RuX_3(NO)L_2]$ complexes in the range 250-800nm, measured in chloroform, are listed in Table 2.7. Some typical spectra are illustrated in Figure 2.7.

Two intense bands are recorded in the U.V. region (extinction coefficients 7000-25000) and one weak band in the visible region (extinction coefficient ~200). The intense bands are probably charge transfer or intraligand transitions and the weak band a ligand field transition.

The ligand field absorption (in the 430-500nm region) is assigned to the spin allowed $^1A_1 \rightarrow {}^1T_1$ transition for a d^6 spin paired transition metal octahedral complex. The band maxima are at lower energy for the bromo complexes compared with the chloro complexes (see Figure 2.8) in accord with the ligand field strength of the halogens. Similarly this transition was observed at lower energies for the selenide complexes compared with the sulphides. Evidence of further ligand field bands was probably masked by the intense charge transfer bands.

TABLE 2.7

Electronic Spectra, (nm)

Molar extinction coefficient in parentheses

Compound	$^1A_1 \rightarrow {}^1T_1$	S(Se) → M	Intraligand or X → M
$RuCl_3(NO)(Me_2S)_2$	426	276	253
	(100)	(15,000)	(14,000)
$RuCl_3(NO)(MeSPh)_2$	461	326	266
	(250)	(21,000)	(13,000)
$RuCl_3(NO)(Et_2S)_2$[a]	441	287	256
	(150)	(14,000)	(13,000)
$RuCl_3(NO)(EtSPh)_2$[a]	459	325	267
	(200)	(16,000)	(11,000)
$RuCl_3(NO)(Pr_2S)_2$[a]	439	291	260
	(200)	(18,000)	(14,000)
$RuCl_3(NO)(PrSPh)_2$[a]	465	326	268
	(250)	(25,000)	(16,000)
$RuCl_3(NO)(Et_2Se)_2$[a]	468	310	270
	(150)	(7,000)	(13,000)
$RuCl_3(NO)(EtSePh)_2$[a]	469	338	277
	(200)	(22,000)	(12,000)
$RuCl_3(NO)(Bz_2S)_2$	442	306	259
	(200)	(19,000)	(16,000)
$RuBr_3(NO)(Me_2S)_2$	481	300	
	(200)	(13,000)	
$RuBr_3(NO)(MeSPh)_2$	481	334	
	(200)	(18,000)	

TABLE 2.7 continued.

$RuBr_3(NO)(Et_2S)_2$[a]	476	301	
	(200)	(11,000)	
$RuBr_3(NO)(EtSPh)_2$[a]	485	329	
	(200)	(15,000)	
$RuBr_3(NO)(Pr_2S)_2$[a]	476	304	
	(200)	(10,000)	
$RuBr_3(NO)(PrSPh)_2$	482	331	
	(100)	(9,000)	
$RuBr_3(NO)(Et_2Se)_2$[a]	483	327	282
	(200)	(14,000)	(15,000)
$RuBr_3(NO)(EtSePh)_2$[a]	490	342	288
	(200)	(15,000)	(12,000)
$RuBr_3(NO)(Bz_2S)_2$	478	316	283
	(300)	(21,000)	(21,000)
$RuI_3(NO)(Et_2Se)_2$		386	272
		(2,000)	(10,000)

[a] Initially determined in reference 1.

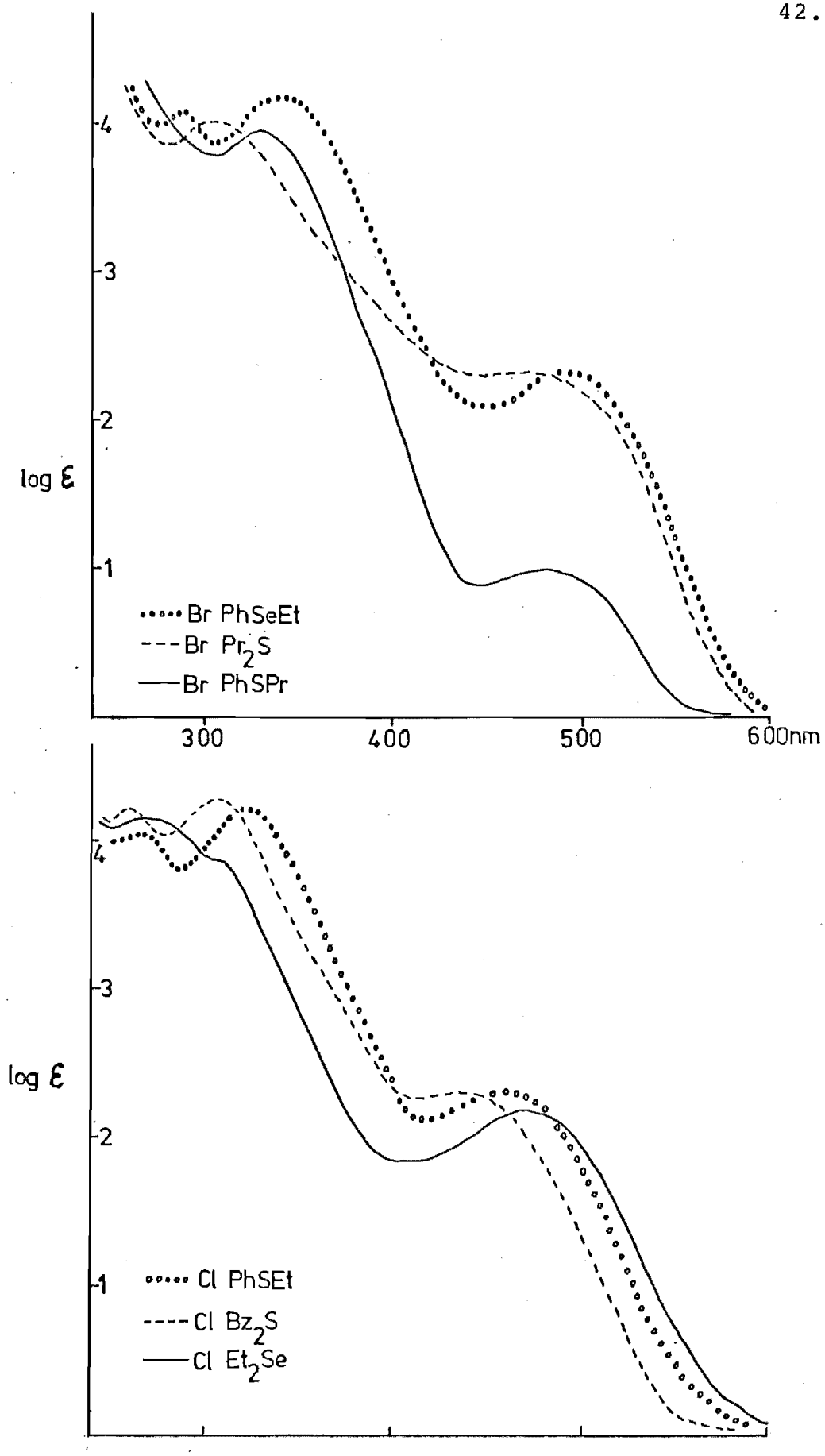

FIGURE 2.7

U.v.-visible spectra observed for some of the $[RuX_3(NO)L_2]$ complexes.

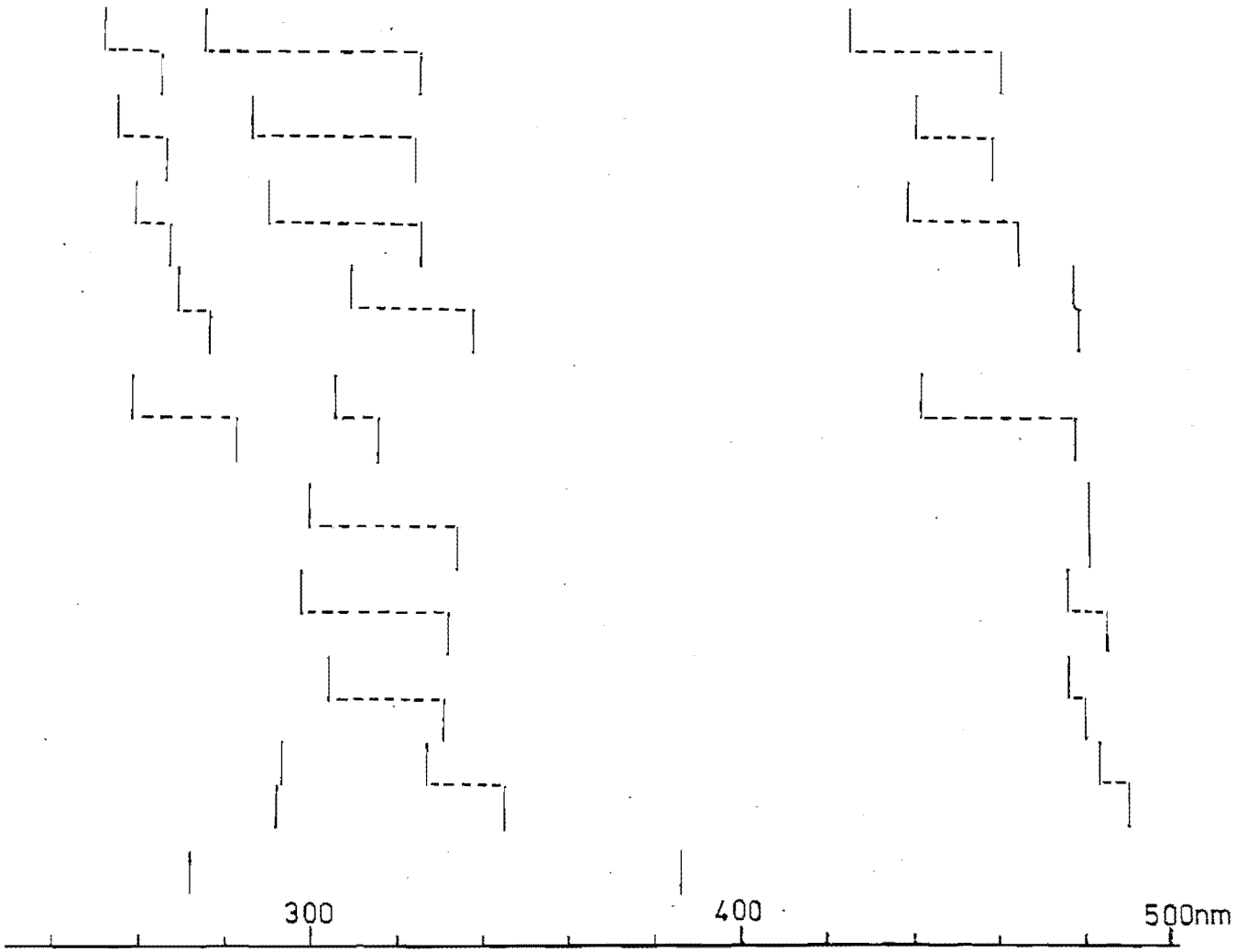

X	L
Cl	Me_2S
Cl	PhSMe
Cl	Et_2S
Cl	PhSEt
Cl	Pr_2S
Cl	PhSPr
Cl	Et_2Se
Cl	PhSeEt
Cl	Bz_2S
Br	Bz_2S
Br	Me_2S
Br	PhSMe
Br	Et_2S
Br	PhSEt
Br	Pr_2S
Br	PhSPr
Br	Et_2Se
Br	PhSeEt
I	Et_2Se

FIGURE 2.8

Relative shifts in the u.v.-visible absorptions for the $[RuX_3(NO)L_2]$ complexes.

The position of the intense band of lower energy (in the 275-345nm range) varied by up to 50nm when the dialkyl sulphide ligand was changed to a phenylalkyl sulphide ligand. The same trend was observed when changing from sulphide to selenide ligands. A change of the halogen ligands had little affect on the band position (often less than 10nm). Hence the band is assigned as S (or Se) → Ru charge transfer transition, as reported previously.[33,40,43]

The U.V. spectra of the free phenylalkyl sulphide has an intense absorption (ε~10,000) around 255nm.[28] Hence the strong band observed in the region 250-280nm may be assigned (for the phenylalkyl sulphide complexes) to an intraligand transition of the ligand. However, for the free dialkyl sulphide ligands the intraligand absorption occurs at ca. 202nm (ε~2,000)[69] so the 250-280nm band in complexes of these ligands probably has another origin.

The majority of the bromo complexes do not exhibit this high energy band, and where it is observed (e.g. the selenide complexes) it was around 20nm lower in energy than for the chloro complexes. Therefore the absorption may arise from a X → M charge transfer transition.

2.2.6 X-ray Studies

Both X-ray powder photographs and some preliminary single crystal X-ray photographic studies were carried out on a number of complexes, the results of the preliminary structural studies are given in Table 2.8.

X-ray powder photographs indicated the following pairs of complexes are isomorphous:

TABLE 2.8

Results of Preliminary X-ray Structural Studies

Compound	Crystal System	Space group	a	b	c	α	β	γ
$RuBr_3(NO)(Me_2S)_2$	Orthorhombic		12.3 Å	18.0 Å	10.6 Å	90°	90°	90°
$RuBr_3(NO)(Et_2S)_2$	Orthorhombic		15.0	29.5	7.9	90	90	90
$RuCl_3(NO)(PhSEt)_2$	Monoclinic	$P2_1/c$	10.7	10.9	36.4	90	96.7	90
$RuBr_3(NO)(PhSEt)_2$ [a]	Monoclinic	$P2_1$	15.352	16.712	8.584	90	90.36	90
$RuBr_3(NO)(Et_2SO)(Et_2S)$ [a]	Monoclinic	$P2_1/c$	13.633	8.514	16.340	90	106.56	90
$[RuBr_3(NO)(Et_2SO)]_2$ [a]	Triclinic	$P\bar{1}$	8.042	11.020	7.324	104.83	102.31	88.54

[a] See chapters 5, 6, 7 for full details of crystal structures.

(i) $[RuBr_3(NO)(PhSEt)_2]$ and $[RuBr_3(NO)(PhSeEt)_2]$,

(ii) $[RuBr_3(NO)(Et_2S)_2]$ and $[RuCl_3(NO)(Et_2S)_2]$.

Several other compounds had a pattern of diffraction lines with similarities but not exactly the same, e.g. $[RuCl_3(NO)(PhSEt)_2]$ and $[RuCl_3(NO)(PhSeEt)_2]$ as well as $[RuCl_3(NO)(PhSMe)_2]$ and $[RuBr_3(NO)(PhSMe)_2]$.

2.3 OTHER TRANSITION METAL COMPLEXES WITH ORGANIC SULPHIDE LIGANDS

Attempts were made to prepare complexes of osmium, rhodium and rhenium of the type $[MCl_3(NO)(Et_2S)_2]$. In addition organic sulphide chelating ligands (cis-bis(1,2-benzylthio)ethylene and αα'-dibenzylthio-o-xylene) and benzyl mercaptan (BzSH) were used as ligands in order to increase the range of complexes studied, particularly in relation to the variable temperature n.m.r. studies (see Chapter 3). Attempts were made to prepare ruthenium, rhodium, platinum and palladium complexes incorporating the chelating ligands mentioned above. Generally these complexes form products of low solubility and appear in some cases to be polymeric species.

(a) Diethyl sulphide complexes with osmium, rhodium and rhenium

Attempts were made to prepare the $[MCl_3(NO)(Et_2S)_2]$ complexes by following the various methods reported for the preparation of the corresponding $[MCl_3(NO)(PR_3)_2]$ complexes, (where M = Os, Rh, Re and Ru). However, none of the products obtained had a ν(N-O) absorption in the infrared

spectra, and only in the rhodium case was the product characterised (as $[RhCl_3(Et_2S)_3]$), see experimental section for details.

(b) Cis-bis(1,2 benzylthio)ethylene complexes

The chelating ligand cis-bis(1,2 benzylthio)ethylene, (bte),

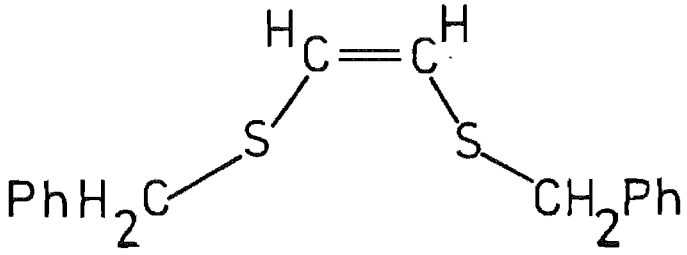

has been reported[70] as forming the two palladium complexes, $[PdCl_2(bte)]$ and $[PdBr_2(bte)]$. In this work the hydrated halides $RuCl_3$, $RuBr_3$ and $RhCl_3$ were treated with an alcohol solution of bte. The insoluble products formed had carbon and hydrogen analyses consistent with the empirical formula $[MX_3(bte)]_n$.

Palladium and platinum complexes with the chelating bte ligand were prepared according to a reported method. The complexes isolated were of the form $[PdCl_2(bte)]$. Since the products obtained with the bte ligand did not prove to be readily soluble in common organic solvents for n.m.r. studies no further work with these complexes was undertaken.

(c) αα' dibenzylthio-o-xylene complexes

The ligand αα' dibenzylthio-o-xylene, dbtx,

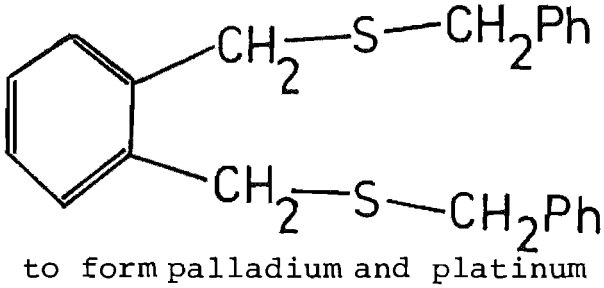

was reported[71] to form palladium and platinum complexes of the

type $[MBr_2(dbtx)]$. In this study, using the same method the chloro complex, $[PdCl_2(dbtx)]$ was prepared. However, the product was not sufficiently soluble in common solvents so no further study of this complex was undertaken.

(d) Benzyl mercaptan complexes

Alcoholic solutions of benzyl mercaptan, BzSH, and the '$RuCl_3(NO)$' and '$RuBr_3(NO)$' entities, readily yielded precipitates that gave carbon and hydrogen analyses consistent with the formulation $[RuX(NO)(BzS)_3]_2$. The thiols are known to coordinate more strongly by loss of the proton,[72] while the infrared spectra confirmed the presence of the NO group and a halogen ligand.

A further product of the preparation of the bromo complex was a good yield of clear crystals, which had ^1H n.m.r. and ^{13}C n.m.r. spectra, melting point and carbon and hydrogen analyses consistent with the product being dibenzyl disulphide,

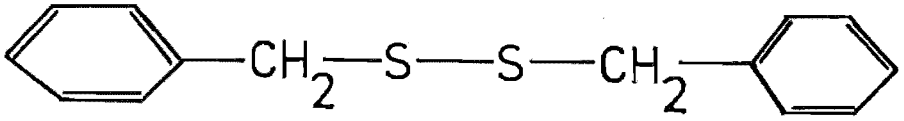

Details of the preparations and analyses are given in the experimental section.

2.4 EXPERIMENTAL

The carbon and hydrogen analytical data are listed in Table 2.9. The physical methods used are outlined in appendix B.

TABLE 2.9

Analytical data

Compound	Melting Point (°C)	Calculated (%) C	Calculated (%) H	Found (%) C	Found (%) H
$RuCl_3(NO)(Me_2S)_2$	161[a]	13.3	3.34	13.9	3.65
$RuCl_3(NO)(MeSPh)_2$	170-5	34.6	3.32	34.7	3.58
$RuCl_3(NO)(Et_2S)_2$	79-83	23.0	4.83	21.4	4.68
$RuCl_3(NO)(EtSPh)_2$	150	37.4	3.92	37.0	3.93
$RuCl_3(NO)(Pr_2S)_2$	51	30.4	5.95	30.0	6.01
$RuCl_3(NO)(PrSPh)_2$	141	39.9	4.46	38.9	4.56
$RuCl_3(NO)(Et_2Se)_2$	83	18.8	3.94	18.4	4.01
$RuCl_3(NO)(EtSePh)_2$	142	31.6	3.32	31.6	3.27
$RuCl_3(NO)(Bz_2S)_2$	199	50.5	4.24	50.2	4.59
$RuCl_3(NO)(Me_2SO)_2$	222[a]	12.2	3.07	12.5	2.97
$RuBr_3(NO)(Me_2S)_2$	125[a]	9.7	2.44	9.9	2.47
$RuBr_3(NO)(MeSPh)_2$	187	27.2	2.60	26.6	2.93
$RuBr_3(NO)(Et_2S)_2$	133	17.4	3.66	17.6	3.60
$RuBr_3(NO)(EtSPh)_2$	163	29.7	3.11	29.9	3.24
$RuBr_3(NO)(Pr_2S)_2$	72	23.7	4.65	24.4	4.77
$RuBr_3(NO)(Et_2Se)_2$	98	14.9	3.13	15.2	3.15
$RuBr_3(NO)(EtSePh)_2$	152	25.9	2.72	26.7	2.82
$RuBr_3(NO)(Bz_2S)_2$	166	42.1	3.53	42.2	3.65
$RuBr_3(NO)(Me_2SO)_2$	183[a]	9.1	2.30	10.3	2.54
$RuI_3(NO)(Et_2Se)_2$		12.2	2.56	12.6	2.82

[a] Decomposed.

2.4.1 Starting Materials

(a) Organic chalcogen ligands

The ligands BzSH, DMSO, Et_2S and Et_2Se were obtained commercially and used without further purification. Most of the other organic sulphide and selenide compounds that were used were prepared as described previously,[33,40] by heating under reflux sodium sulphide (or thiophenol in the case of the PhSR compounds) with the corresponding alkyl bromide in ethanol. Dibenzyl sulphide was prepared[41] by refluxing benzyl chloride and sodium sulphide in ethanol. Dimethyl sulphide was synthesised by heating under reflux sodium sulphide and methyl iodide in a methanol water solution. The reaction products were distilled, followed by the addition of ice cold water which enabled the dimethyl sulphide to be isolated as the organic phase.[73,74]

The cis-bis(1,2 benzylthio)ethylene, bte, used was a commercial product, which had a ^1H n.m.r. spectrum with $\delta_{CH} = 6.02$, $\delta_{CH_2} = 3.88$, $\delta_{C_6H_5} = 7.30$ ppm and a melting point of 60°C. The αα'-dibenzylthio-o-xylene, dbtx, was prepared[71] by treating an ethanolic solution of sodium with equimolar amounts of benzyl mercaptan and dibromo-o-xylene. The dbtx product precipitated when water was added to the solution. The ^1H n.m.r. spectrum of the dbtx species yielded $\delta_{C_6H_4} = 7.15$, $\delta_{C_6H_5} = 7.25$ and $\delta_{CH_2} = 3.57$ and 3.65 ppm.

(b) Metal halide or halogeno compounds

The compounds K_2PtCl_4, hydrated $RuCl_3$ and $RhCl_3$ were commercially available, while K_2PdCl_4 was prepared by dissolving $PdCl_2$ in a 0.2M hydrochloric acid solution and

adding KCl. Orange-brown crystals of K_2PdCl_4 were obtained by slowly evaporating the solution in a stream of air. The K_2OsCl_6 was prepared in earlier work.[1]

The entity '$RuCl_3(NO)$' was obtained by adding freshly prepared nitric oxide gas[73] to an ethanol solution of $RuCl_3.xH_2O$ (1.0 g per 100 ml ethanol) for a period of a few hours.[7]

The hydrated $RuBr_3$ was prepared by adding HBr to $RuCl_3.xH_2O$ and evaporating the solution to dryness three times. The '$RuBr_3(NO)$' entity was then prepared by reacting the hydrated $RuBr_3$ with nitric oxide as for the chloro compound.

2.4.2 Preparations of Trihalogenonitrosylbis(organo chalcogen)ruthenium Complexes

(a) General method

The organic sulphide (or selenide) ligand (0.5 ml) was added to 30 ml of the ethanol solution of '$RuCl_3(NO)$' or '$RuBr_3(NO)$' (prepared from 1.0 g $RuCl_3.xH_2O$ per 100 ml ethanol) and heated under reflux for one hour. In the case of the Me_2S compounds a condenser containing a dry ice/isopropyl alcohol cooling agent was used, since the boiling point of dimethyl sulphide is 37°C.

The volume of the mother liquor was then reduced by up to 50% under vacuo until the $[RuX_3(NO)L_2]$ complex crystallised out. The complex was filtered and washed with ice cold petroleum ether (50-70°). If any difficulty was experienced in obtaining a crystalline compound (e.g. Pr_2S and PhSPr complexes) the partially evaporated solution was cooled in an ice bath for a period or left

to stand for 3-4 weeks at room temperature.

Where recrystallisation was necessary ethanol was used as the solvent. Yields of between 60-80% were normally achieved. To obtain single crystals of sufficient size for X-ray studies, concentrated solutions of the $[RuX_3(NO)L_2]$ complexes in ethanol were allowed to stand in a cold room over a period of several weeks.

The bromo and iodo derivatives could also be prepared from the chloro complexes by metathetical reactions with NaBr or NaI. An ethanol solution of the chloro complex was heated under reflux with NaX for two hours and then cooled on ice to allow the $[RuX_3(NO)L_2]$ product to crystallise.

2.4.3 Attempted Preparations of $[MCl_3(NO)(Et_2S)_2]$ Type Complexes

(a) Osmium complex

The reagents N-methyl-N-nitroso-p-toluenesulfonamide, (nmts), (0.25 g) or phenyl nitrite[8] were added to a 2-methoxyethanol solution (25 ml) of K_2OsCl_6 (0.1 g) and Et_2S (0.5 ml). The solution was heated under reflux for one hour then cooled. On reduction of the volume in vacuo a precipitate was obtained but the infrared spectrum revealed no ν(N-O) absorption.

(b) Rhodium complexes

Using the nmts reagent (0.5 g) and hydrated $RhCl_3$ (0.1 g) the same method as in 2.4.3(a) was followed, but again no evidence of a nitrosyl group was found.

Further attempts using a different procedure[14] by first preparing '$RhCl_3(NO)$' were tried. The diethyl sulphide ligand (0.5 ml) was added to the '$RhCl_3(NO)$' solution (0.1 g of hydrated $RhCl_3$ per 10 ml ethanol) and heated under reflux for one hour. A precipitate formed on cooling and was characterised as $[RhCl_3(Et_2S)_3]$ from its X-ray powder photograph and infrared spectrum.

(c) Rhenium complexes

The oxoethoxo complex of rhenium(V), $[ReO(OEt)Cl_2(PPh_3)_2]$, was prepared[76] and from this was obtained $(Me_4N)_2[ReCl_5(NO)]$[77] by bubbling nitric oxide through an ethanolic solution also containing tetra methyl ammonium chloride. This pentachloronitrosyl complex was used in attempts to prepare $[ReCl_3(NO)(Et_2S)]$. Diethyl sulphide (1.0 ml) was added to an ethanolic solution (40 ml) of $(Me_4N)[ReCl_5(NO)]$ (0.3 g) and heated under reflux for approximately twelve hours. The solvent was removed in vacuo and the infrared spectra of the residue indicated that there was a weak $\nu(NO)$ absorption at 1750 cm^{-1}. However, the product was very sensitive to moisture and a carbon and hydrogen analysis was not consistent with the residue being $[ReCl_3(NO)(Et_2S)_2]$.

2.4.4 Preparations using cis-bis(1,2 benzylthio)ethylene

(a) Ruthenium and rhodium complexes

The bte ligand (0.2 g) was added to an ethanolic solution (at 50°C) of hydrated $RuBr_3$ (0.1 g). On cooling a black precipitate formed, was filtered and dried in air. The product obtained was only slightly soluble in common solvents.

When 2-methoxyethanol as the solvent and hydrated $RuCl_3$ (0.1 g) were used, a dark brown product was obtained. The infrared spectra of the chloro and bromo species formed were similar. The analysis of the chloro species yielded C = 39.6% and H = 3.6%. These results are consistent with the empirical formula $[RuCl_3(bte)]_n$, where calculated for $C_{16}H_{16}Cl_3S_2Ru$, C = 40.0% and H = 3.4%.

A similar preparation using hydrated $RhCl_3$ (0.1 g) was tried using methanol as the solvent. The insoluble brown product obtained had an infrared spectrum similar to that recorded for the ruthenium species.

(b) Palladium complex

The preparation was carried out[70] by treating a warm solution of K_2PdCl_4 (0.25 g) in water (10 ml) with a warm methanol solution (15 ml) of bte (0.23 g). A yellow precipitate immediately formed and was filtered off, washed with methanol and dried. The product was recrystallised from methanol. Analysis: found C = 38.0% and H = 3.4%; calculated for $[PdCl_2(bte)]$, $C_{16}H_{16}Cl_2S_2Pd$, C = 42.7% and H = 3.6%. The ^1H n.m.r. spectrum indicated the product was contaminated with some free ligand. Even though it was not very soluble in deutero-chloroform the n.m.r. spectrum obtained yielded $\delta_{C_6H_5}$ = 7.42, δ_{CH} = 6.28 and $\delta_{CH_2} \approx$ 4.2 ppm.

(c) Platinum complexes

The bidentate ligand, bte, (0.15 g) was added to a solution of K_2PtCl_4 (0.23 g) dissolved in water (20 ml) and was heated under reflux for five hours. An orange-brown product

was obtained when the solution was cooled on ice. The product separated into two forms by washing with chloroform. The analysis for the chloroform insoluble portion was C = 31.1% and H = 2.7%, and the chloroform soluble portion was C = 21.2% and H = 1.7%. Neither of these analyses is consistent with a $[PtCl_2(bte)]$ formula.

2.4.5 Preparations with αα'-dibenzylthio-o-xylene

The reported method[71] for the preparation of the bromo complexes of palladium and platinum was followed. The yellow palladium chloro product, $[PdCl_2(dbtx)]$, precipitated readily but was only slightly soluble in deuterochloroform. The ^1H n.m.r. spectrum recorded gave δ_{CH_2} = 3.51 and 4.20 ppm, $\delta_{C_6H_5}$ and $\delta_{C_6H_4}$ ≈ 7-7.6 ppm (a broad multiplet). One of the methylene resonances has been shifted downfield by 34 Hz on coordination of the dbtx species, while the other has stayed essentially unchanged.

2.4.6 Preparations with Benzyl Mercaptan

(a) Chloronitrosyltris(benzyl sulphide)ruthenium complex

A '$RuCl_3(NO)$' solution in ethanol (prepared from 0.25 g of hydrated $RuCl_3$ per 25 ml) to which benzyl mercaptan (1 ml) was added, and gave a brown precipitate immediately, the solution was then heated to near boiling. The analysis of the product yielded C = 44.3%, H = 3.8% and Cl = 6.6%. On the basis of these results the precipitate may be of the type $[RuCl(NO)(BzS)_3]_2$, (for $C_{21}H_{21}ClNOS_3Ru$, C = 47.1%, H = 4.0% and Cl = 6.6%).

(b) Bromonitrosyltris(benzyl sulphide)ruthenium complex

The same method as described for the chloro species in 2.4.6(a) was used to prepare the bromo complex. Analysis: found C = 41.2%, H = 3.6% and Br = 12.8%; calculated for $C_{21}H_{21}BrNOS_3Ru$ C = 43.5%, H = 3.7% and Br = 13.8%.

After three weeks a clear crystalline material appeared in the solution left to stand. This product was found to be dibenzyl disulphide. Analysis: found C = 68.2% and H = 5.8%; calculated for $C_{14}H_{14}S_2$ C = 68.3% and H = 5.7%.

CHAPTER 3

DYNAMIC NUCLEAR MAGNETIC RESONANCE STUDY OF SOME RUTHENIUM NITROSYL CHALCOGEN COMPLEXES

3.1 INTRODUCTION

In solution, a number of inorganic and organometallic complexes are known to undergo rapid intramolecular rearrangement (e.g. pyramidal inversion of the lone electron pairs on nitrogen and phosphorus), as well as intermolecular processes (e.g. dissociation and then association). In order to investigate the dynamic process occurring, a frequency spectrum with a timescale comparable with the lifetime of the stereochemically non-rigid molecules is required, see Table 3.1. The nuclear magnetic resonance method extends over a wide timescale and covers a region which is not accessible to the other techniques listed in Table 3.1.

TABLE 3.1

Characteristic times of some physical methods.[78]

Method	Time, (s)
Electron diffraction	10^{-20}
X-ray diffraction	10^{-18}
Electronic spectra	10^{-14}-10^{-15}
Vibrational spectra	10^{-11}-10^{-13}
Electron spin resonance	10^{-4}-10^{-8}
Nuclear magnetic resonance	10^{0}-10^{-7}
Visual methods (separation of isomers)	10^{2}

3.1.1 Use of the Dynamic Nuclear Magnetic Resonance Technique

(a) General

The timescale for the nuclear magnetic resonance (n.m.r.) technique is such that fluxional processes with lifetimes in the range 10^{0} to 10^{-5} sec (and therefore rates of interchange of 10^{0} to 10^{5} sec^{-1}) may conveniently be studied. Alteration of the temperature of the sample (in solution) will influence the rate of conversion from one configuration to another in the stereochemically non-rigid molecule. In the case of the n.m.r. technique the change of rate with temperature is observed as an alteration in both the n.m.r. signal position and shape, see Figure 3.1. Hence measurement of the spectral changes enables the rate of interchange of configurations to be determined. Knowledge of the rate at various temperatures allows a kinetic analysis of the fluxional process to be undertaken.

When the rate of the fluxional process is slow with respect to the n.m.r. timescale (see Figure 3.1), i.e. lifetimes of 10^{0}-10^{-2} sec, the individual forms of the stereochemically non-rigid molecule may be observed as separate resonance signals in the n.m.r. spectrum. That is, the spectrum consists of a superposition of the spectra of the individual species. To achieve a sufficiently slow rate of interchange between configurations often requires the temperature of the sample to be lowered. When the separate forms are observed and then the temperature is raised, so as to increase the rate of interchange, part or all of the spectrum is observed

	Relative Sample Temperature	Relative Rate of Fluxional Process	Spectrum Observed
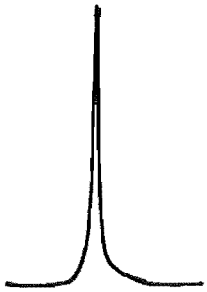	high	fast	sharp, averaged signal
	intermediate	intermediate	coalescence of signal into a broad peak
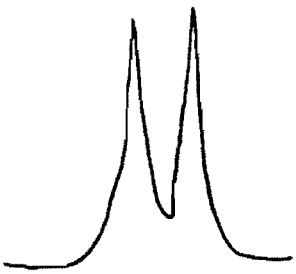	low	slow	separate signals due to each form of the 2 configurations

FIGURE 3.1

Variation of line-shape of a n.m.r. spectrum with temperature for a simple fluxional process between two configurations

as a broad peak with no fine structure (i.e. coalescence occurs). Further warming increases the rate of the fluxional process so it becomes fast with respect to the n.m.r. time-scale. Hence a given nucleus will only experience an average of the different magnetic environments of the individual states of the fluxional molecule, and a single, averaged spectrum of the interconversion process is recorded, (Figure 3.1).

The n.m.r. technique has proved to be a useful method for obtaining information on fluxional processes which occur in transition metal compounds. A number of extensive review articles have been published[78-82] discussing the dynamic nuclear magnetic resonance method.

(b) Computer simulation technique

Systems which are at equilibrium (that is where no net chemical change is taking place) will be considered, as opposed to situations where the chemical change may be observed by the progressive disappearance (or appearance) of, for example, a spectral line over a period of time. At equilibrium, the interchange of configurations of a fluxional molecule is reversible between two (or more) forms. The simple A ⇌ B

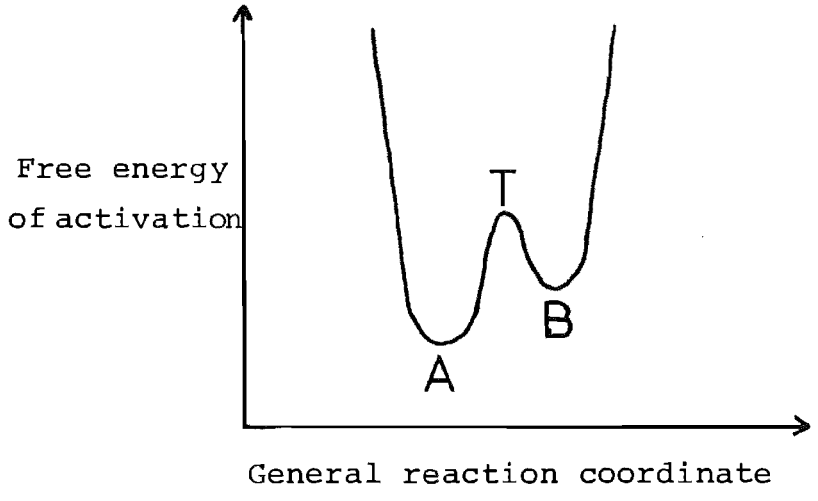

interchange is represented by the diagram[78] above, showing a potential energy surface of the exchange between the energy states A and B, achieved through a transition state T. For the less complex nuclear spin systems where intramolecular exchange occurs, it is possible to simulate a complete n.m.r. spectrum using documented computer programs.[80,83,84]

In order that a computer simulation can be carried out the static parameters, such as chemical shifts, spin coupling constants and sometimes population ratios of the species must be known. However, when the equilibrium is between energetically equivalent conformations (i.e. the energy A equals the energy B in the diagram above), the population parameters for the forms A and B are equal. This is the situation for the compounds studied in this work. The other information required is obtained from the experimental spectra recorded at low temperatures where the exchange process is "frozen", that is, when only a small fraction of the molecules can overcome the energy barrier in unit time. The data obtained are fitted to an equation (usually linear) which incorporates the temperature, and this is extrapolated to cover the temperature region where the exchange broadened spectra occur so that the static parameters for that region are able to be calculated.

One further static parameter required before a computer line shape analysis can proceed is the effective transverse relaxation time T_2^*, which is given by the equation,[80]

$$T_2^* = \frac{1}{\pi w}$$

where w is the width (in Hz) at half height of a peak not

broadened by interchange of configurations.

Insertion of the static parameters in the computer program allows the shape of the n.m.r. spectrum to be calculated for a given rate value. Hence by altering the rate value, the shape of the calculated spectrum is changed until it coincides with that observed experimentally.

3.1.2 Intramolecular Rate Processes of Transition Metal Complexes with Chalcogen Donor Atom Ligands

(a) General system

In metal complexes of chalcogen donor atom ligands the configuration around the three coordinate chalcogen atom is pyramidal, (i.e. a distorted tetrahedron with the lone pair of electrons occupying the fourth position). This has been established from X-ray crystal structure analyses [47,49-51,85] (see Chapters 6 and 7) of dialkyl and aryl alkyl sulphide and dialkyl selenide complexes of transition metals. The transition metal complexes in which the monodentate organosulphide ligand is three coordinate have the capability of undergoing a pyramidal inversion of configuration[86] about the sulphur atom as follows:

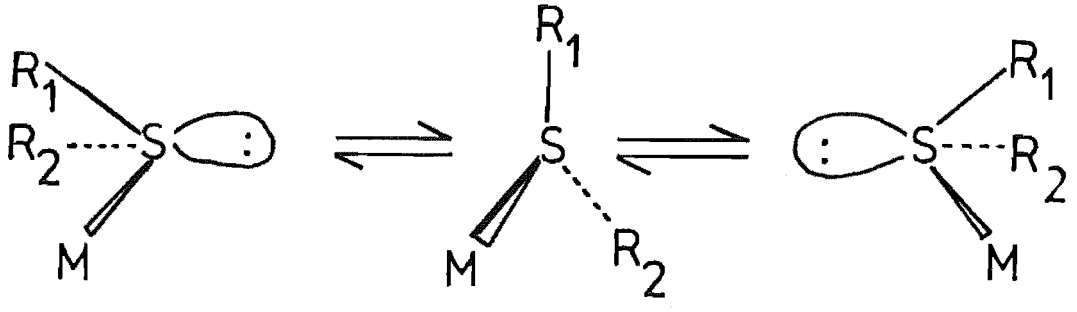

(b) Systems that display inversion of configuration at the chalcogen atom

One of the earliest reports of the inversion process occurring at a chalcogen atom was in 1961,[87] where a complex multiplet was observed in the methylene region of the ^1H n.m.r. spectrum of the compound $[Et_2S.BH_3]$. However, no evidence was found for the non-equivalence of the methylene protons of the ethyl group for $[Et_2S.BF_3]$. To explain this difference it was suggested that an averaging process involving exchange of BF_3 between the two lone pair positions of the sulphur atom occurred. A more recent study[88] of the BH_3, BCl_3 and BF_3 complexes with Et_2S and Et_2O revealed that a hindered inversion about the pyramidal oxygen or sulphur atom was required in order to explain the ^1H n.m.r. spectra.

In 1966 a variable temperature ^1H n.m.r. study of the two complexes, $[MCl_2(MeSCH_2CH_2SMe)]$ where M = Pt and Pd,[89] revealed peaks coalescing and then reforming as the temperature was increased. It was proposed that the interchange due to inversion about the sulphur atom occurred as shown below.

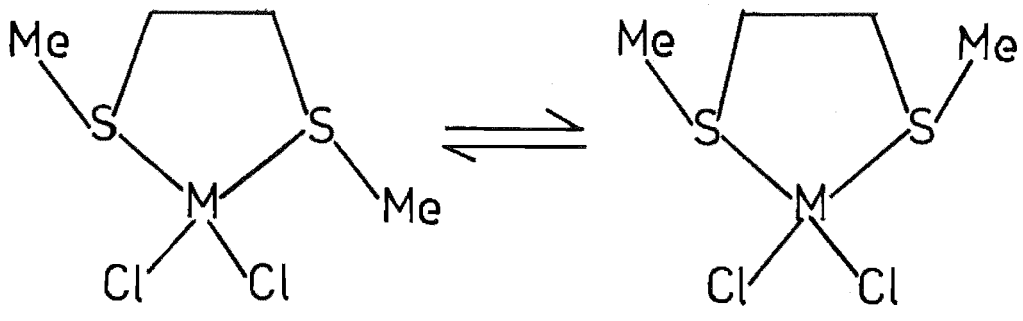

Extensive investigations followed into the variable temperature ^1H n.m.r. spectra of cis- and trans- complexes of $[PtCl_2(Bz_2S)_2]$, $[PtCl_2(Et_2S)_2]$ and $[PtCl_2(BzSMe)_2]$.[90,91] In these complexes where the sulphur atom is in a pyramidal configuration the two methylene protons of the ethyl (or benzyl) group are magnetically non-equivalent (i.e. they are diastereotopic, see section 3.2.2 for a more detailed explanation). The AB pattern (see p. 59) due to the non-equivalent methylene protons, observed in the ^1H n.m.r. spectrum of $[PtCl_2(Bz_2S)_2]$, collapsed as the temperature increased, giving at higher temperatures an A_2 pattern due to the two now equivalent methylene protons. This result was explained in terms of an inversion process at the sulphur atom. At low temperatures the n.m.r. spectrum of the ethyl groups in the $[PtCl_2(Et_2S)_2]$ complex was accounted for by a ABM_3 spin system, if second order splitting due to the 33% abundance of the ^{195}Pt isotope was ignored. The ABM_3 pattern became an A_2M_3 system above the coalescence temperature due to the apparent equivalence of the methylene protons when inversion of configuration about the sulphur atom is rapid. Rate constants at the coalescence temperature were determined for the complexes studied and the free energies of activation reported.[90,91]

Cross et al. have examined[92] a series of bidentate organic sulphide complexes of platinum and palladium of the type $[MX_2(RSCH_2CH_2SR)]$, (M = Pt, Pd; X = Cl, Br, I and R = Me, Et, n-Pr, i-Pr, n-Bu). The coalescence temperatures of the methylene bridging protons were reported and it was found that in agreement with Haake and Turley's results,[90,91] the

process could be explained by inversion about the sulphur atom. The same explanation was given for the changes observed in the variable temperature spectra of $[Au^{III}Cl_3(Bz_2S)]$ and $[Au^{I}Cl(Bz_2S)]$[93] and $[(Me)_2Au(MeSCH_2CH_2SMe)]NO_3$.[94]

Since these preliminary reports of inversion of configuration about the sulphur atom, related systems have been the subject of an increasing number of studies. The coalescence phenomenon was reported[33] for a series of $[PdX_2(RLR')_2]$ complexes, where X = Cl, Br, I, NO_2; RR' = Et_2, PhEt, n-Pr_2, i-Bu_2, i-BuPh and L = S or Se. Trends emerging from these studies indicate that the coalescence temperature for bromo complexes is less than for chloro complexes. Also the coalescence temperature was lower for the sulphide complexes than for the selenide complexes, and lower for palladium complexes than for platinum complexes. No change was observed in the spectra of mercury dialkyl sulphide complexes[33] within the temperature range studied. This may be a consequence of the tetrahedral stereochemistry of the mercury complexes.

Recent work[95,96] by Cross et al. on complexes of the type $[MX_2(LEt_2)_2]$, where M = Pt, Pd; X = Cl, Br, I and L = S, Se, Te, extends the range of studies on chalcogen atom inversion processes. They also studied[97] the influence of additional free ligand on the n.m.r. spectra of the $[MX_2(LEt_2)_2]$ complexes. This confirmed that the dominant process being observed in these variable temperature studies was actually inversion about the pyramidal chalcogen atom. In most cases two separate coalescences of the methylene signal were observed. The first was the coalescence previously reported[95,96] which is

independent of the presence of free ligand, while a second coalescence of the methylene signal occurred, some 50-100 degrees above the first coalescence temperature which was dependent on the presence of free ligand. At this higher temperature, the ^{195}Pt-^{1}H coupling in the Pt complexes (see section 3.1.3(c)) was not present above the second coalescence temperature. The disappearance of coupling is consistent with exchange taking place between the free and coordinated chalcogen ligands.[91,96,99] Also the coalescence temperature was dependent on the concentration of the metal complex involved, as expected for an interchange of ligands. A similar temperature difference between the two coalescence temperatures for palladium complexes suggests that the coalescence at the lower temperature is due to the pyramidal inversion processes. In the case of the palladium complexes the diagnostic advantage of metal-proton coupling, as observed in the Pt complexes, is not available to distinguish the different processes involved in the two coalescences.

Detailed studies have recently been reported[98-100] on the barriers to inversion about the sulphur atom for Rh, Ir, Pt and Pd complexes with $SR(CH_2SiMe_3)$ ligands, where R = Me, Ph or CH_2SiMe_3. Abel et al. also studied[99] the possible existence of chemically distinct structures with the sulphur atom lone pair of electrons either in a mutually cis- or trans- configuration across the S-M-S bond system as shown below:

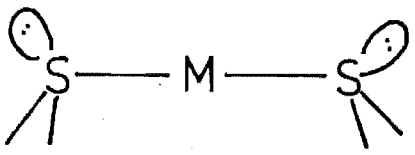

cis

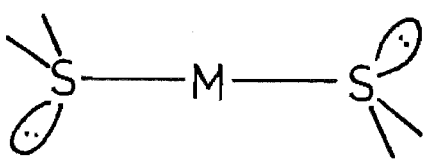

trans

They found no evidence for the existence of two separate structures. This would suggest that the M-S or M-Se bond rotation is reasonably rapid. This situation will be examined more closely in section 3.2.4(b).

The probability that the inversion process occurred simultaneously about both the sulphur atoms in the bis-sulphide complexes was also studied by Abel et al.[100] Their results indicated that the dominant process was the single site inversion.

(c) Mechanism of the inversion of configuration process

The first mechanism proposed[91] considered that the inversion about the sulphur atom was achieved by the formation of an intermediate where both of the sulphur atom lone pairs of the R_2S ligand interact with the metal atom, i.e.

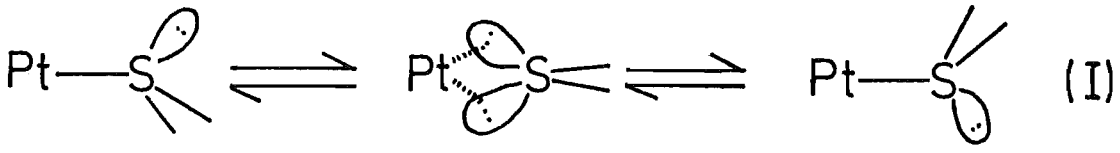

(I)

This mechanism (I) was proposed in order to explain the fast inversion process about the sulphur atom for the transition metal organosulphide compounds compared with the much slower inversion about the sulphur atom in organic sulphoxides (ca. 10^{20} times slower), where the inversion is said to involve a planar transition state, i.e.

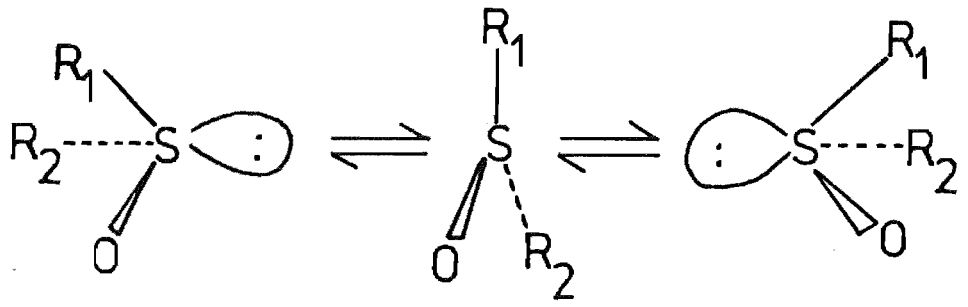

(II)

The 'umbrella' type inversion mechanism (II) has a planar transition state where the M-S bond is represented as a σ bond in which the sulphur atom uses a sp^2 type hybrid and the lone pair is in a p orbital. Mechanism (I) also has a planar transition state and therefore Abel et al. proposed[99] that in real terms mechanisms (I) and (II) are the same, and that the large rate difference between inversions of organic sulphoxides and transition metal complexes is probably due to the stabilisation of the metal complex transition state by $S_{p\pi} \rightarrow M_{d\pi}$ orbital overlap. Retention of M-S bonding throughout the inversion process is confirmed from the observation that the ^{195}Pt-^{1}H coupling is retained above the inversion coalescence temperature, where the spectrum represents an average of the overall process. If the M-S bond was broken and then reformed the ^{195}Pt-^{1}H coupling would not be observed.[90,96,99]

A dissociation-recombination mechanism cannot be completely ruled out for Au[93] and Pd[33,95-97] complexes with chalcogen donor atom ligands, as neither metal atom has a suitable magnetic isotope which can couple with the protons which enables the two mechanisms to be distinguishable. However, the close similarity of the results obtained[93,97]

for the Au and Pd complexes with those of Pt, as well as the success of computer simulation of the experimental spectra,[93] does suggest for compounds other than those of Pt that the inversion mechanism retains some degree of M-S bonding.

Cross et al.[96] modified the description of the sulphur atom inversion mechanism by introducing a rotation step in order to show how the environments of the H_A and H_B methylene protons are interchanged.

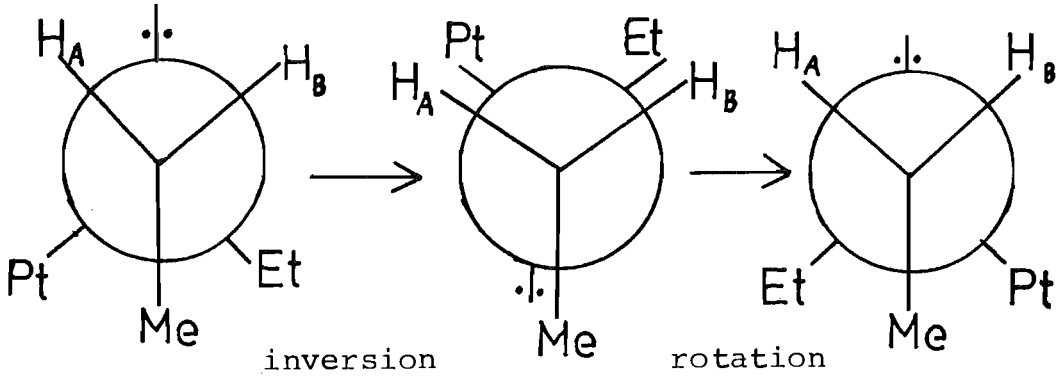

After inversion a second step of rotation about the S-CH_2 bond of the ethyl group places the H_B proton in the environment initially occupied by H_A. The free energy barrier to this rotation is reported[101] to be approximately 7 kJ mol^{-1}. Hence compared with the free energies of activation of the inversion process which is calculated to be 50-70 kJ mol^{-1}, the slow step in the above process is inversion. Therefore the activation parameter determined will effectively indicate the energy barrier to inversion about the sulphur atom.

(d) Thermodynamic parameters for the inversion process

Comparison of computer simulated spectra with those obtained experimentally allows the rate of inversion of configuration at a certain temperature to be readily determined. The simulation is compared with experimentally observed spectra close to the coalescence temperature, as it is in this region that the change of line-shape of the experimental spectrum is most sensitive to changes in temperature. This means that the rate constants obtained from data in this region will be the most accurate. By making use of normal thermodynamic equations (see details in section 3.2.5) the activation energy and other thermodynamic parameters can be quantitatively determined from the inversion rate data at a certain temperature.

The most precise thermodynamic parameters are obtained using a range of inversion rate values at various temperatures. In early work[90,91,96] approximate methods[78] were used to calculate rate constants, as the activation parameters were usually based on rate data at one temperature, and therefore have an estimated[78] error of around 10%. The free energies of activation, $\Delta G^{\ddagger}$, determined for $[PtX_2(SEt_2)_2]$, $[PtX_2(SeEt_2)_2]$ and $[PdX_2(SeEt_2)_2]$ complexes are listed in Table 3.2. The first report[93] of a computer simulated line-shape analysis of the experimental data (on a gold sulphide complex (Table 3.2)) led to a $\Delta G^{\ddagger}$ value at 298.15K of 72.2 kJ mol^{-1}, which compared favourably with the less precisely estimated $\Delta G^{\ddagger}$ values.

Computer simulation of the spectra obtained in a variable temperature ^1H n.m.r. study of Rh, Ir, Pd, Pt halide complexes with the $LR(CH_2SiMe_3)$ ligand, (R = Me, Ph, CH_2SiMe_3 and L = S, Se), has recently been reported.[98-100] The ligands were chosen so that the methylene protons undergo a simple AB $\rightleftharpoons$ BA exchange during the inversion process about the sulphur atom. This spin system is able to be simulated relatively easily using band shape fitting computer programs. The results are listed in Table 3.2. From the data in the table it may be seen that an increase in $\Delta G^{\ddagger}$ of between 15 to 20 kJ mol^{-1} is observed when the sulphur atom is changed to a selenium atom. A small decrease of 1-2 kJ mol^{-1} occurs when the R group is changed from Me to Ph. However, the reverse trend occurs for the activation energy, E_a, with an increase of 5-6 kJ mol^{-1}. There appears to be no significant correlation between the activation parameters and the nature of the halogen bonded to the transition metal, whereas a correlation does exist[33,96] with the coalescence temperature.

Hunter et al. have also recently[102-105] used the band shape fitting programs to simulate the ^1H n.m.r. spectra observed for sulphide and selenide chelating ligands of the type $RLCH_2CH_2LR$, where R = i-Pr, L = Se and R = Bz, L = S. Complexes with Pd halides and with Cr, Mo and W carbonyls were studied and the trend in $\Delta G^{\ddagger}$ values for the transition metals was in the order:

$$Pd > W > Cr > Mo.$$

Due to the good fit of the simulated spectra to the experimental spectra, the authors modified their earlier explanation that the coalescence was due to a ring-inversion

TABLE 3.2

Activation Parameters for the Barrier to Inversion about a Chalcogen Atom

Complex[a]	$\Delta G^{\ddagger}_{298}$ kJ mol^{-1}	E_a kJ mol^{-1}	$\Delta S^{\ddagger}$ J K^{-1} mol^{-1}	Reference
$AuCl(Bz_2S)$	72.2		39.8	93
$PtCl_2(Et_2S)_2$	58.2[c]			91
$PtBr_2(Et_2S)_2$	56.9[c]			96
$PtCl_2(Et_2Se)_2$	76.2[c]			96
$PtBr_2(Et_2Se)_2$	76.2[c]			96
$PdCl_2(Et_2Se)_2$	67.8[c]			96
$PdBr_2(Et_2Se)_2$	66.9[c]			96
$RhCl_3(SL_2)_3$[b]	68.6 (28)[d]	73.0 (14)	7 (14)	98
$IrCl_3(SL_2)_3$	66.6 (9)	66.5 (5)	-9 (5)	98
$PdCl_2(SL_2)_2$	54.6 (6)	51.2 (3)	-20 (4)	99
$PtCl_2(SL_2)_2$	61.3 (25)	56.3 (13)	-25 (13)	99
$PdCl_2(SeL_2)_2$	69.3 (11)	60.7 (6)	-37 (6)	99
$PtCl_2(SeL_2)_2$	77.9 (14)	65.8 (8)	-49 (8)	99
$PdCl_2(MeSL)_2$	54.5 (11)	51.0 (5)	-20 (5)	100
$PdCl_2(PhSL)_2$	53.2 (8)	56.2 (4)	2 (4)	100
$PtCl_2(MeSL)_2$	61.3 (9)	55.9 (5)	-20 (5)	100
$PtCl_2(PhSL)_2$	59.3 (8)	62.5 (4)	2 (4)	100
$PtBr_2(MeSL)_2$	60.9 (24)	59.2 (12)	-14 (12)	100
$PtBr_2(PhSL)_2$	59.0 (11)	54.5 (6)	-23 (6)	100
$PdCl_2(PhSeL)_2$	68.7 (14)	71.1 (7)	0 (7)	100
$PtBr_2(PhSeL)_2$	80.3 (18)	83.8 (10)	3 (9)	100

[a] Parameters are those for *trans*-chalcogen complexes or values for *trans*-chalcogen ligands.

[b] L = (CH_2SiMe_3).

[c] $\Delta G^{\ddagger}$ values at coalescence temperature.

[d] Figures in parentheses represent error in the least significant figure shown.

(i.e. an exchange between possible skew conformations of the

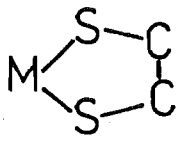

ring), to a process involving inversion about the chalcogen atom.

The present work to be described below, consists of calculations of the energy barrier to inversion using computer line-shape methods for some ruthenium nitrosyl halide complexes containing dialkyl and aryl-alkyl chalcogen ligands.

3.2 RESULTS, CALCULATIONS AND DISCUSSION

3.2.1 Ruthenium Nitrosyl Chalcogen complexes

A dynamic nuclear magnetic resonance study of a series of complexes of the type $[RuX_3(NO)L_2]$, where X = Cl, Br and L = Me_2S, MeSPh, Et_2S, PhSEt, n-Pr_2S, Bz_2S, Et_2Se and PhSeEt, was undertaken to determine the thermodynamic parameters relating to the energy barrier to inversion about the chalcogen atom. Variable temperature ^1H n.m.r. spectra of the complexes were recorded over a temperature range of 200-375K. At the normal operating temperature of the n.m.r. spectrometer (ca. 310K), the ^1H n.m.r. spectrum of the Et_2S and PhSEt complexes consisted of a quartet resonance in the methylene region. As the temperature of the sample was lowered the quartet was observed to change into a broad featureless peak which then reformed into a series of

overlapping quartets, (around 250K), of varying intensities. The spectral changes were reversible, and the temperature range over which the coalescence phenomena occurred was found to be little affected by altering the concentration of the sample. These results obtained for the $[RuCl_3(NO)L_2]$ and $[RuBr_3(NO)L_2]$ complexes (where L = Et_2S and PhSEt), may be explained in terms of inversion of configuration about the sulphur atom while retaining some Ru-S interaction. The possibility of the inversion mechanism being achieved by dissociation of the sulphide ligand and then recombination using the other lone pair of electrons cannot be ruled out, since Ru-^{1}H coupling is not observed as no suitable magnetic isotope of ruthenium exists. However, the lack of dependence of the temperature of coalescence on the sample concentration, and the close similarity of the coalescence temperatures and spectral changes of the ruthenium diethyl sulphide complexes to those of the platinum complexes,[91,95,96] supports an inversion process during which Ru-S interaction is maintained. Ligand-exchange processes involving dissociation-recombination mechanisms may occur at higher temperatures as was shown by Cross et al.,[97] but the spectrum of $[RuBr_3(NO)(Et_2S)_2] + Et_2S$ up to 370K showed no evidence of an exchange between free and coordinated ligands. Hence the inversion process can be interpreted on the basis of a purely intramolecular inversion of configuration process.

The possibility of quantum mechanical tunnelling through the barrier to sulphur inversion, is not expected to be a likely mechanism[86,91] in the ruthenium complexes studied here.

3.2.2 Interpretation of the Variable Temperature ^{1}H n.m.r. Spectra

The methylene protons of the thioether ligands such as Et_2S, PhSEt, Pr_2S and Bz_2S in transition metal complexes (i.e. protons on the carbon atom bonded to the sulphur atom), are magnetically non-equivalent and therefore will have different chemical shifts. The explanation for the different methylene proton environments is as follows. The carbon atom to which the two methylene protons are attached is called a prochiral centre when two of the groups bonded to it are identical.

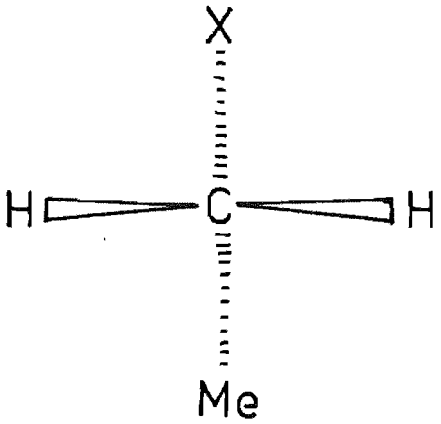

In the system studied here X is a sulphur atom which itself is either a chiral or prochiral centre depending on whether the R groups bonded to it are the same or different, (i.e. whether $R_1 = R_2$ below).

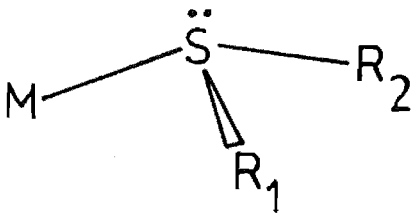

As a consequence of the two adjacent prochiral centres there is no plane of symmetry which bisects the H-C-H angle. This means that the two methylene protons are non-equivalent and thus are called diastereotopic.[81,106] It is clear from the Newman projection diagram, viewing down the S-C bond,

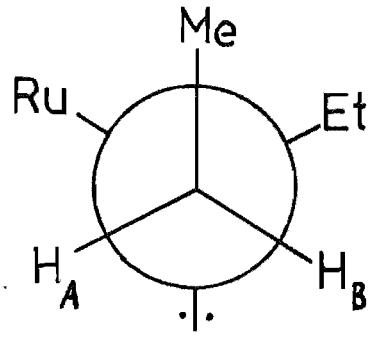

for the diethyl sulphide complex that the environments of the two methylene protons, H_A and H_B, are non-equivalent.

Supporting evidence for the above comes from a study of the complexes formed by the two ligands, Me_2S and MeSPh. The complexes $[RuX_3(NO)L_2]$ (where L = Me_2S and PhSMe) cannot be used in establishing the rate of inversion about the sulphur atom because of the absence of diastereotopic protons. This was confirmed by the absence of any change in their variable temperature ^1H n.m.r. spectra. This effect has been observed previously[94,107] for other transition metal thioether compounds.

Since the methylene protons are non-equivalent, the ethyl group in the $[RuX_3(NO)L_2]$ complexes where L = Et_2S, Et_2Se, PhSEt and PhSeEt, can be described in terms of an ABX_3 nuclear spin type. The A and B represent the non-equivalent H_A and H_B protons (as shown above), and the X_3 corresponds to the three equivalent methyl protons. In the

case of the sulphide complexes at room temperature (ca. 300K), the two methylene protons are observed as being equivalent, due to the rapid exchange of their environments, and therefore can now be described in terms of an A_2X_3 spin type.

As there is no coupling between the methylene groups on different ethyl groups in the ruthenium complexes, and as the ethyl groups in any one complex have equivalent chemical shifts, the only structure observed in the signal in the methylene region that is not expected from first-order splitting, arises from the non-equivalence of the two protons, H_A and H_B.

3.2.3 Determination of the Static Parameters for the ABX_3 System

The static parameters required from the experimental spectra in order to be able to simulate the ABX_3 type exchange broadened spectra are as follows:

(a) ν_A, ν_B, ν_X - the true chemical shift positions of the A, B and X multiplets,

(b) J_{AB}, J_{AX}, J_{BX} - the spin coupling constants between the A, B and X multiplets,

and (c) T_2^* - the effective transverse relaxation time.

As shown in Figure 3.2 the AB region of the n.m.r. spectrum consists of four overlapping quartets.

The following method, which was adapted from the AB situation described previously (p 60),[108] was used to determine the parameters using the labels given in Figure 3.2.

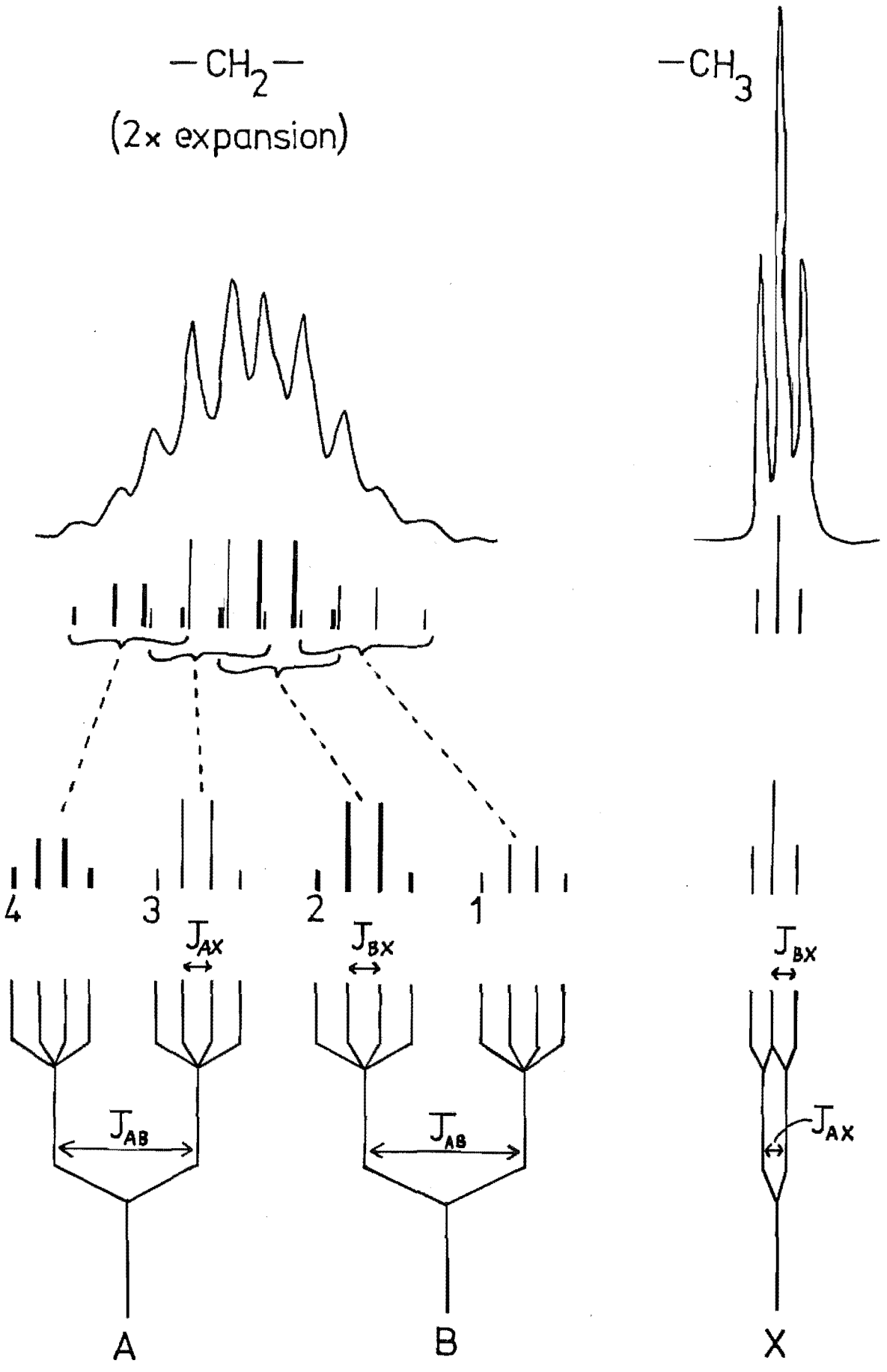

FIGURE 3.2

Interpretation of the methylene and methyl regions of the ^{1}H n.m.r. spectrum of $[RuCl_3(NO)(Et_2S)_2]$ at 261K.

If ν_1, ν_2, ν_3 and ν_4 are the centres of their respective quartets then

$$\nu_A - \nu_B = \sqrt{(\nu_4 - \nu_1)(\nu_3 - \nu_2)}$$
$$= y.$$

And the central point of the whole AB multiplet

$$\tfrac{1}{2}(\nu_3 + \nu_2) = z.$$

Hence the positions of the true chemical shift for the A and B protons are

$$\nu_A = z + \tfrac{1}{2}y$$

and $$\nu_B = z - \tfrac{1}{2}y.$$

The other values T_2^* (see section 3.1.1(b)), J_{AB}, J_{AX} and J_{BX} can be measured directly from the spectra. The chemical shift difference, $\nu_A - \nu_B$, for the AB multiplet can be determined from the experimental spectra, using the above equations, only when inversion about the sulphur atom is sufficiently slow to allow the fine structure to be analysed, (i.e. at temperatures below ca. 260K for the sulphide complexes).

In order to determine the parameters in the region around coalescence, where no fine structure is observed, a series of ^1H n.m.r. spectra for each $[RuX_3(NO)L_2]$ complex was obtained at temperatures well below the coalescence temperature (e.g. from 200-250K for the sulphide complexes and 300-340K for the selenide complex). The chemical shifts, ν_A and ν_B, of the diastereotopic methylene protons were observed to change with temperature and hence the chemical

shifts in the coalescence region were obtained by extrapolating from the data obtained below the coalescence temperature. The chemical shift difference, $\nu_A - \nu_B$, was usually found to be linearly dependent on temperature and a least-squares analysis yielded the results shown in Figure 3.3. The static parameters for each ruthenium compound studied are listed in Table 3.3.

The X multiplet appears as a triplet over the entire temperature range studied because in this case the value of J_{AX} is very close to that of J_{BX}. Also throughout the temperature range the spin coupling constants J_{AB}, J_{AX} and J_{BX} were found to be essentially invariant for each complex. This was also the case for T_2^*, which was determined from the linewidth of the methyl signal since this signal was not broadened by the exchange process.

The $[RuX_3(NO)(Bz_2S)_2]$ complexes, where X = Cl and Br, belong to the AB spin system and the static parameters were determined in a similar manner to that described for the ABX_3 system, except there is only one spin coupling constant, J_{AB}. A value for T_2^* was obtained using the linewidth of the single sharp absorption of the phenyl group protons.

The static parameters obtained were used in the total line shape analysis carried out using a locally adapted version of the computer program DNMR3.[83,84] The good simulation of the observed spectra that was obtained confirms that the methods of determining the static parameters were satisfactory.

3.2.4 Simulation of Experimental ^1H n.m.r. spectra

(a) Mechanism of inversion to be simulated

The mechanism of the intramolecular inversion process

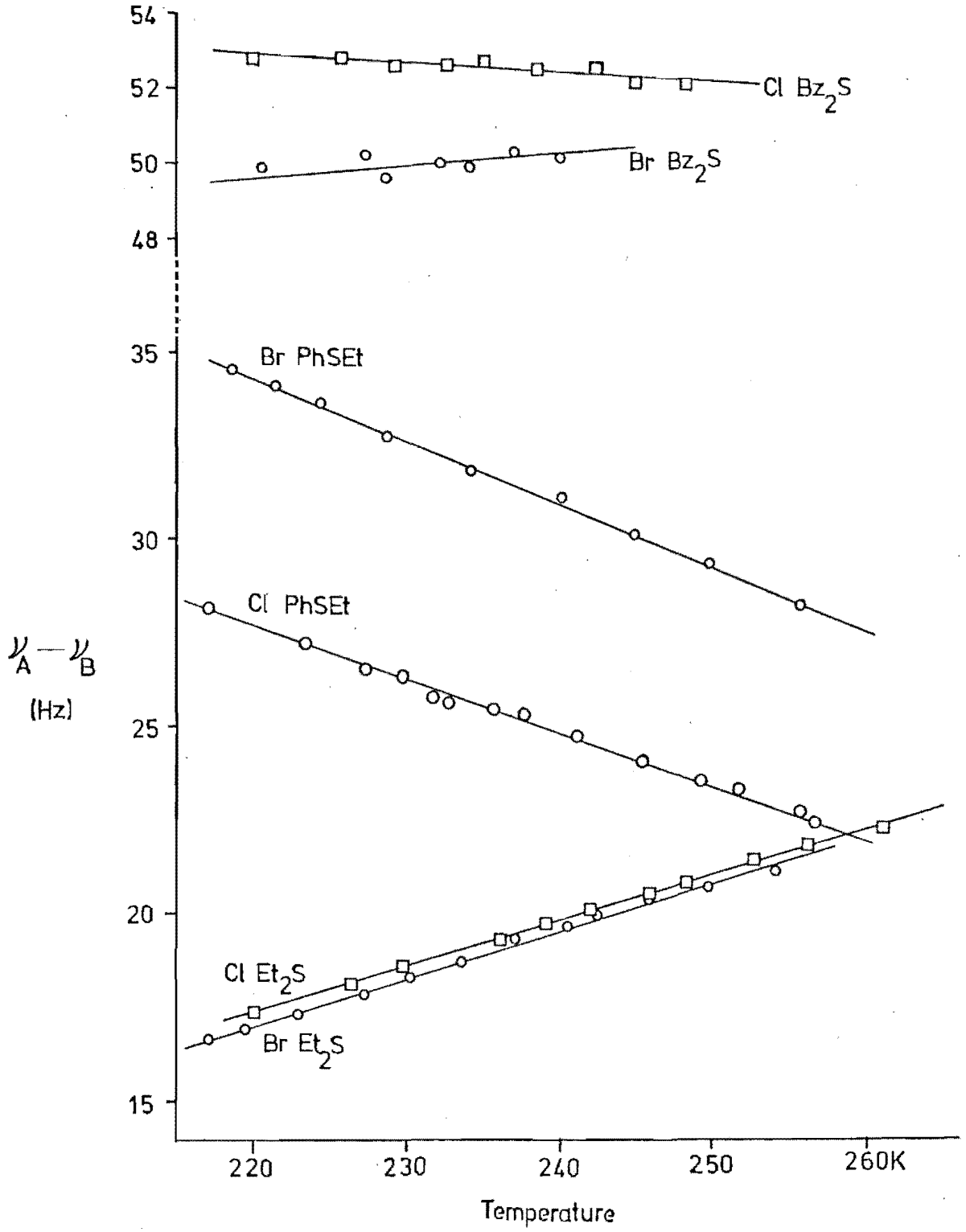

FIGURE 3.3

The chemical shift difference, $\nu_A - \nu_B$, as a function of the temperature for the $[RuX_3(NO)L_2]$ complexes

TABLE 3.3

Spectral Parameters for $[RuX_3(NO)L_2]$ Complexes

Complex	$\nu_A-\nu_B$ [a,b,c]	J_{AB} [c]	J_{AX} [c]	J_{BX} [c]	T_2^* [d]
$RuCl_3(NO)(Et_2S)_2$	-9.3(3)+0.121(1).T	-13.5	7.4	7.0	0.16
$RuBr_3(NO)(Et_2S)_2$	-10.8(6)+0.126(3).T	-13.8	7.6	7.1	0.16
$RuCl_3(NO)(PhSEt)_2$	59.2(8)-0.144(3).T	-13.8	7.2	7.3	0.13
$RuBr_3(NO)(PhSEt)_2$	71.49(7)-0.169(3).T	-14.0	7.2	7.3	0.12
$RuCl_3(NO)(Bz_2S)_2$	58.9(11)-0.027(5).T	-13.5	-	-	0.09
$RuBr_3(NO)(Bz_2S)_2$	41(4)+0.04(2).T	-13.4	-	-	0.09
$RuCl_3(NO)(Et_2Se)_2$	36.8	-11.0	7.0	7.0	0.25

[a] T is the temperature in K.

[b] Figures in brackets are the estimated standard deviations in the least significant figure, from a least squares analysis.

[c] Results in Hz.

[d] Relaxation time, $T_2^* = 1/\pi.w$, where w is the natural linewidth at half height in Hz.

that takes place about the sulphur atom is likely to be the same as that proposed by Abel et al.,[99] (see details in section 3.1.3(c)). If the S-C and Ru-S bond rotations are relatively fast with respect to the inversion process, as is postulated in other transition metal thioether complexes,[96,99] then the diastereotopic methylene protons (H_A and H_B), undergo a mutual exchange of environments involving one of the following types:

$$ABX_3 \rightleftharpoons BAX_3$$

$$AB \rightleftharpoons BA .$$

Figure 3.4 shows the ABX_3 interchange process for the diethyl sulphide complex (the other ligands around the ruthenium atom have been omitted for clarity).

(b) An alternative mechanism

Evidence for the rapid rotation about the S-C bond[101] has been presented in section 3.1.2(c), but there is also the possibility of slow rotation about the Ru-S bond. Such a rotation by itself, will not interchange the environments of the separate methylene protons. In order to check if slow rotation about the Ru-S bond is the reason for the observed spectral changes in the variable temperature ^1H n.m.r. spectra, a study of a possible sulphur atom lone pair cis ⇌ trans interchange mechanism was investigated.

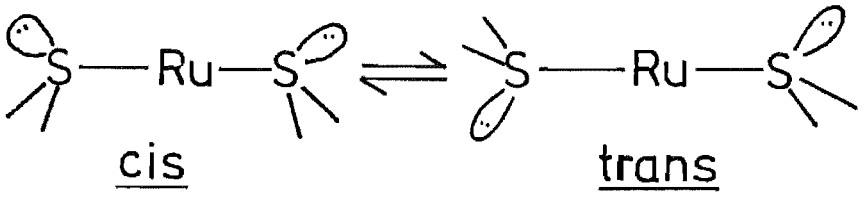

cis trans

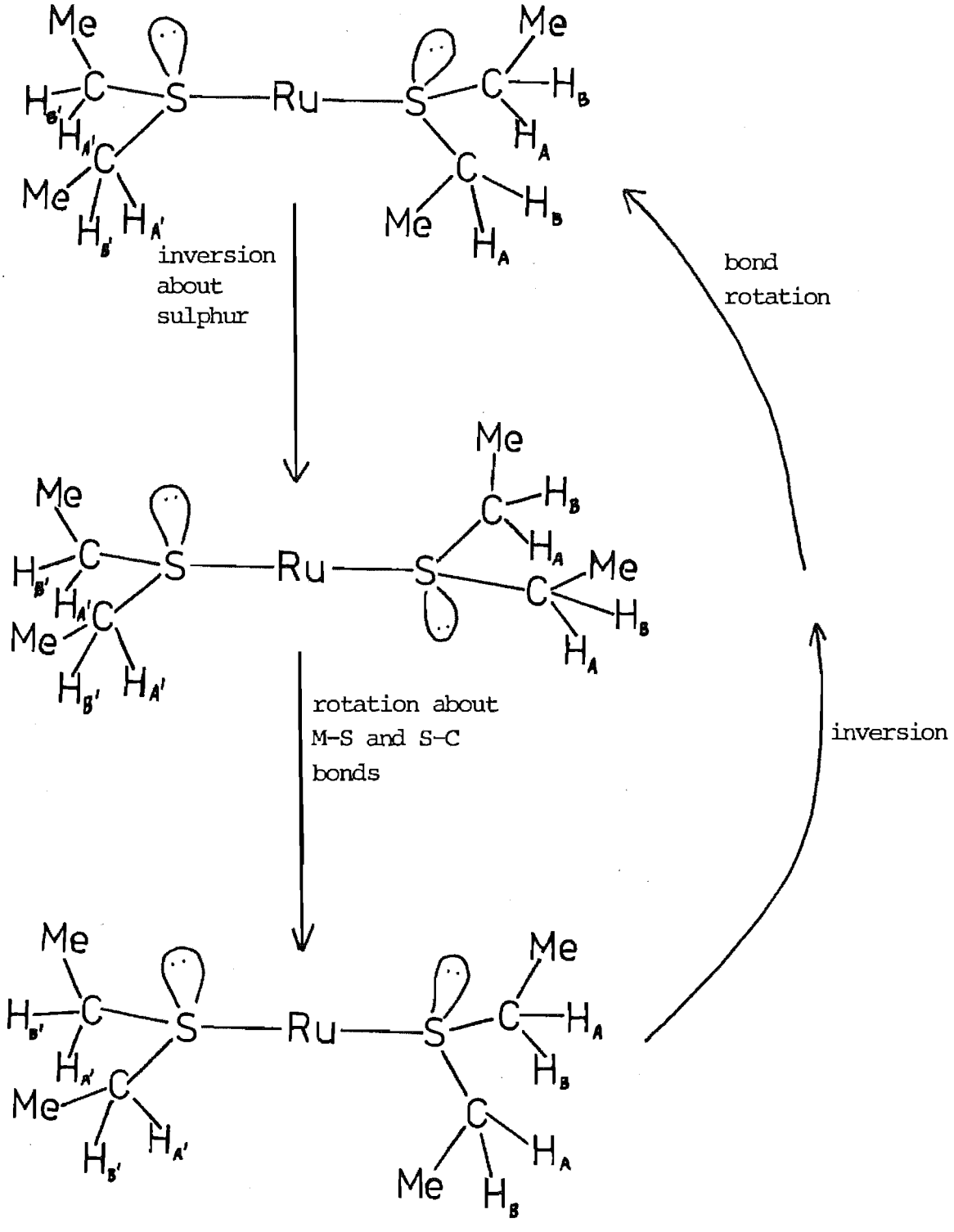

FIGURE 3.4

Conformations of complexes during the inversion process.

This type of mechanism would give rise to at least two distinctly different structures which should be distinguishable in the ^{1}H n.m.r. spectrum. However, no broadening or splitting of the methyl resonance signal was observed. Hence the methyl protons are all chemical shift equivalent. If the methylene protons on each structure above were equivalent, the geminal coupling between the A and B protons would be nil, (i.e. an A_2X_3 spin system would exist). Hence the cis-trans interchange ($A_2X_3 \rightleftharpoons B_2X_3$), would give rise to a methylene signal of just two overlapping quartets. This system has been used previously[88] but was unable to simulate the experimental spectra successfully.

In this study, simulation using the A_2X_3 system gave reasonable agreement with the more intense absorptions in the experimental spectra but failed in fitting the weaker absorptions. Also when compared with the almost exact fit obtained using an ABX_3 type system, it is clear that interpretation in terms of an A_2X_3 system is not satisfactory. Figure 3.5 shows a comparison between the two systems.

Further support for the use of an ABX_3 spin system comes from the ^{13}C n.m.r. spectrum of $[RuBr_3(NO)(Et_2S)_2]$ over the temperature range 203 to 305K. This showed no evidence for the ethyl carbon atoms being in different environments as would be required if an $A_2X_3 \rightleftharpoons B_2X_3$ interchanging system was observed.

(c) Simulation of the AB and ABX_3 systems

In order to obtain accurate data on the inversion process the experimental spectra must show significant changes

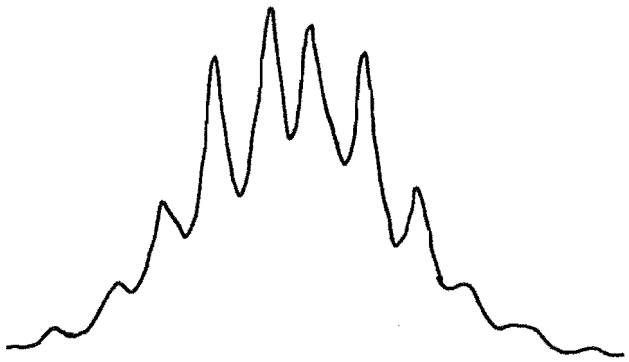

Experimentally observed spectra of the methylene region

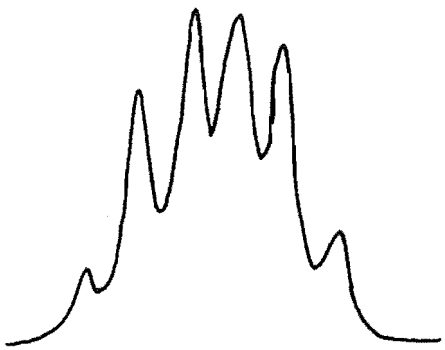

Simulated using A_2X_3 system

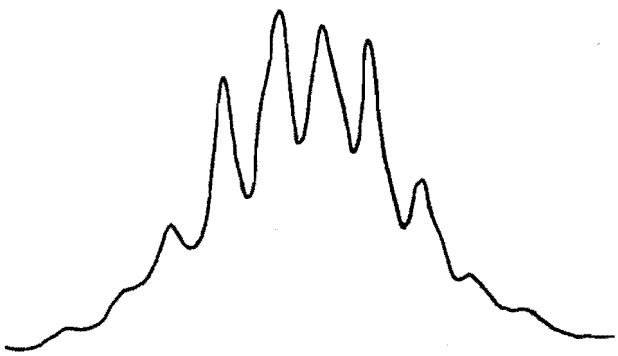

Simulated using ABX_3 system

FIGURE 3.5

Comparison between 2 different spin systems and the experimentally observed spectrum of $[RuCl_3(NO)(Et_2S)_2]$ at 261K

in shape with a small change in temperature. This occurs in the region around the coalescence temperature. Sensitivity to temperature change is also increased by choosing a reasonably complex spin system on which to carry out a simulation analysis.[110] The ABX_3 system of the Et_2S and PhSEt ligand complexes satisfies the above criteria, and reasonably precise results were consequently obtained. The simulation of the $[RuCl_3(NO)(Et_2Se)_2]$ n.m.r. spectra was limited by the maximum temperature obtainable with the n.m.r. spectrometer (i.e. 373K). At this temperature the selenide complexes were approaching or had just reached their coalescence temperature.

The AB system of the Bz_2S ligand complexes was a less complex system to simulate. Hence the sensitivity of the experimental spectra to small temperature changes only occurs close to the coalescence temperature.

A temperature range of around 20 degrees on either side of the coalescence temperature of the complexes was studied to generate the simulation. The range could have been extended but would have had little influence on the numerical values obtained. By systematically varying the rate of inversion, the line shape of the computer simulated spectra is altered until it best fits the experimentally observed spectra at a certain temperature.

Typical examples of the variable temperature ^1H n.m.r. spectra in the methylene region for the seven $[RuX_3(NO)L_2]$ complexes studied in detail are shown in Figures 3.6(a) - (g). The simulated spectra with the rate value k, which gave the best agreement with the experimental spectra are also shown.

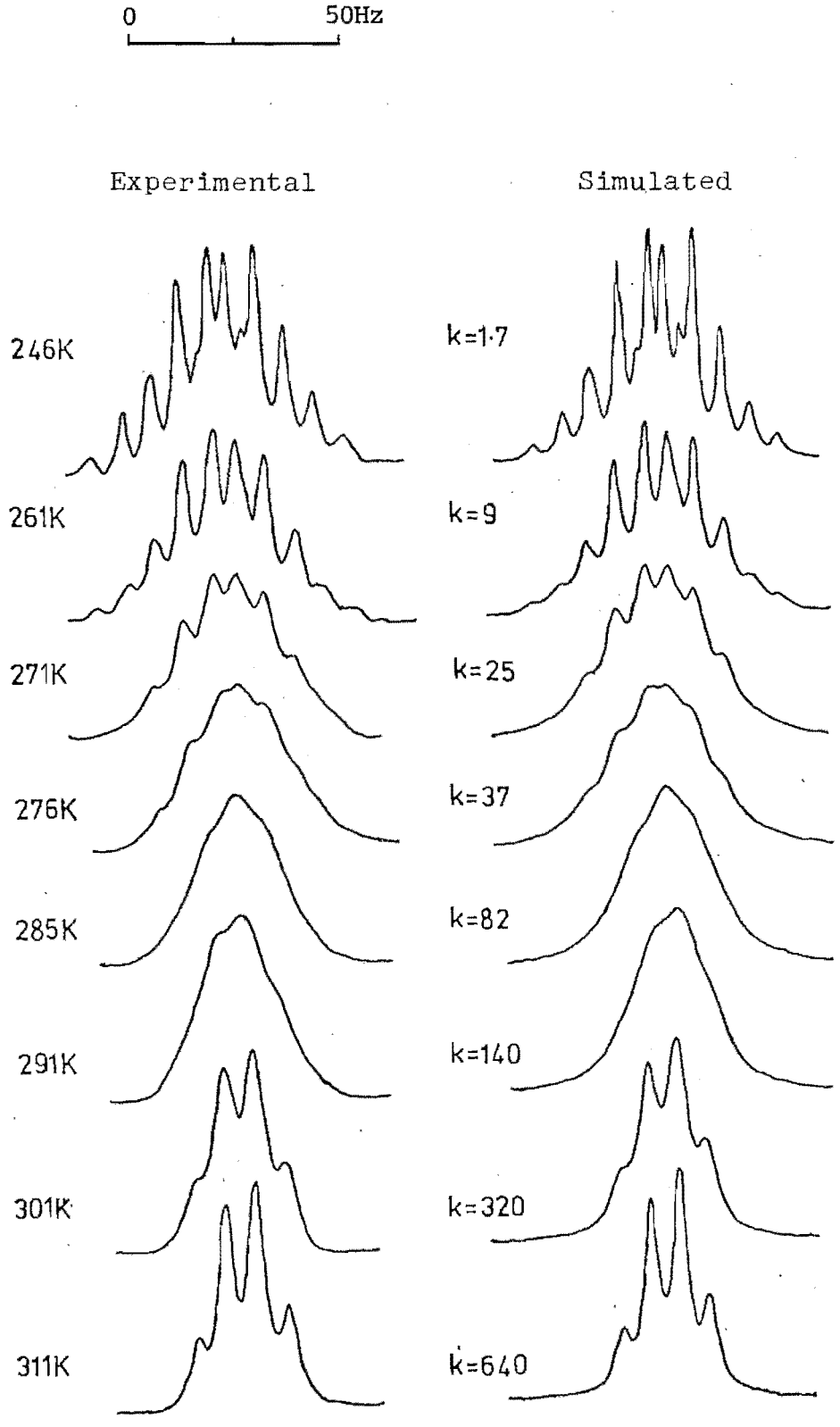

FIGURE 3.6

Comparison between the experimentally observed ^{1}H n.m.r. spectra at various temperatures and computer simulated spectra for: (a) $[RuCl_3(NO)(Et_2S)_2]$

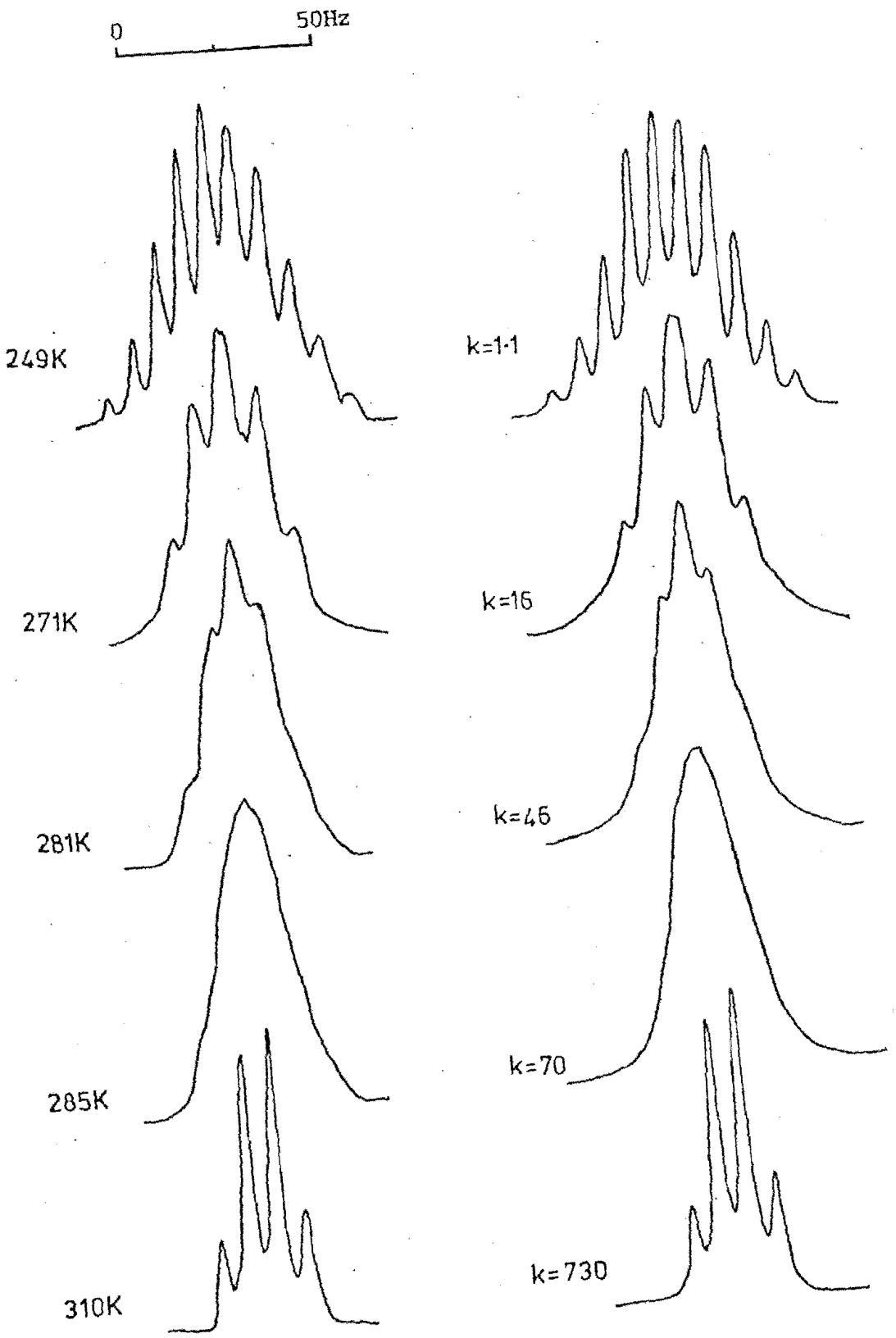

FIGURE 3.6 continued.

(b) $[RuCl_3(NO)(PhSEt)_2]$

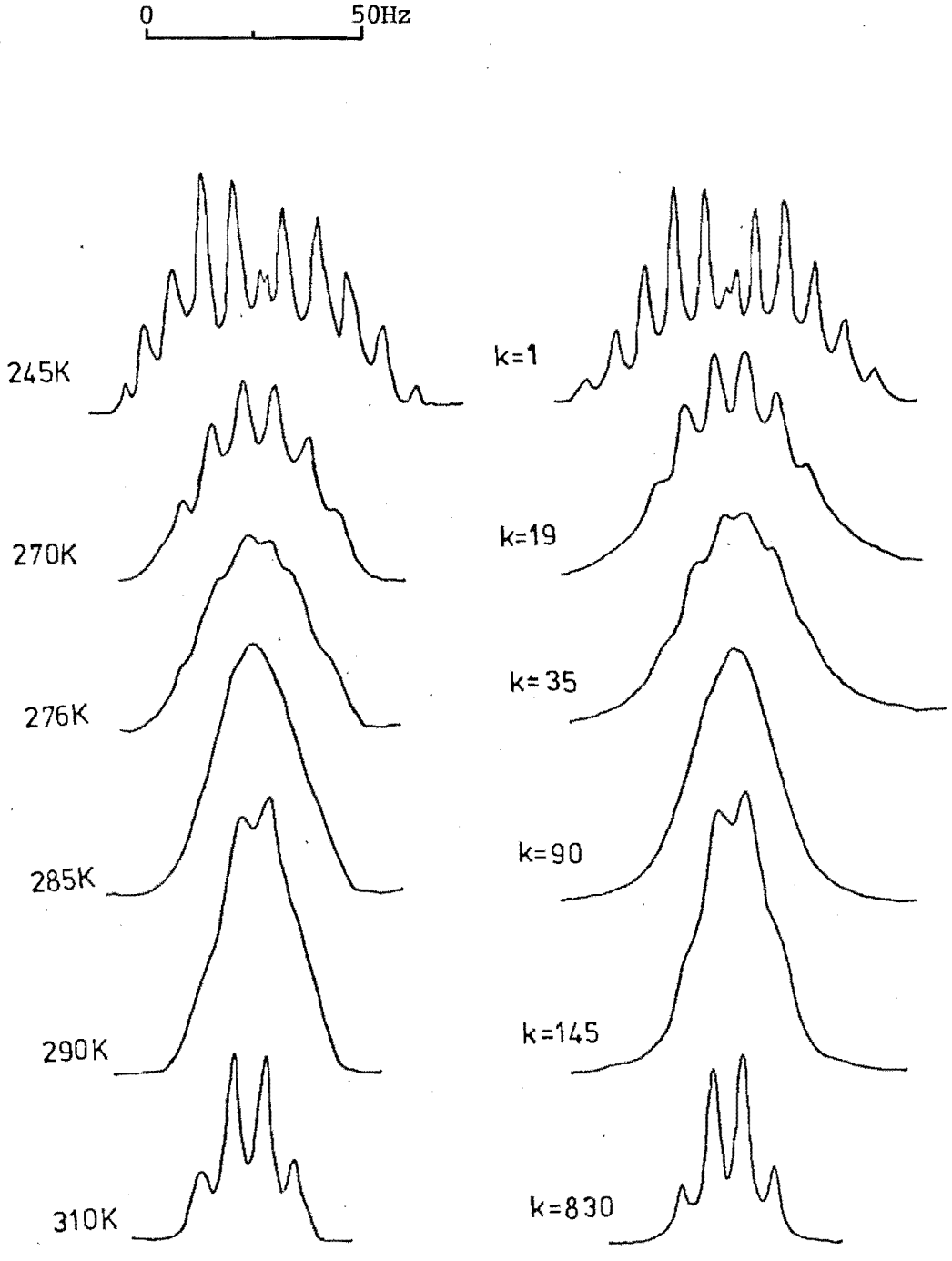

FIGURE 3.6 continued.

(c) $[RuBr_3(NO)(PhSEt)_2]$

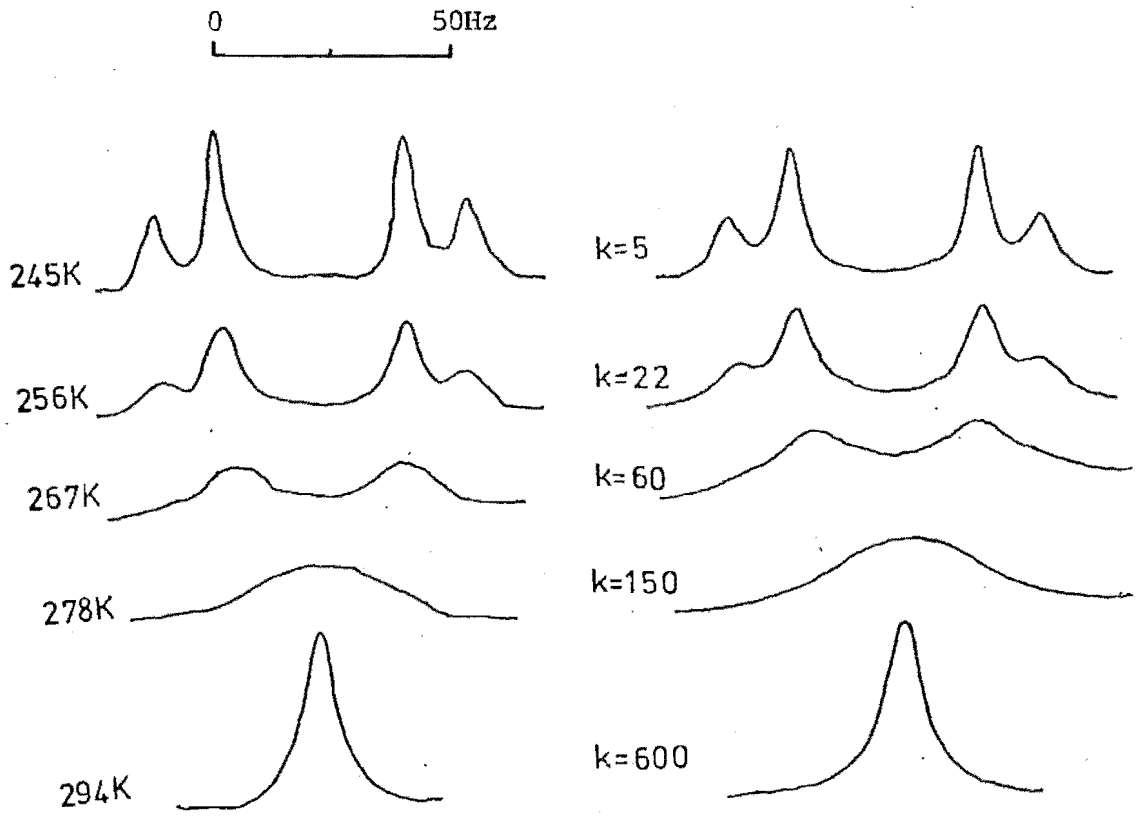

FIGURE 3.6 continued

(d) $[RuCl_3(NO)(Bz_2S)_2]$

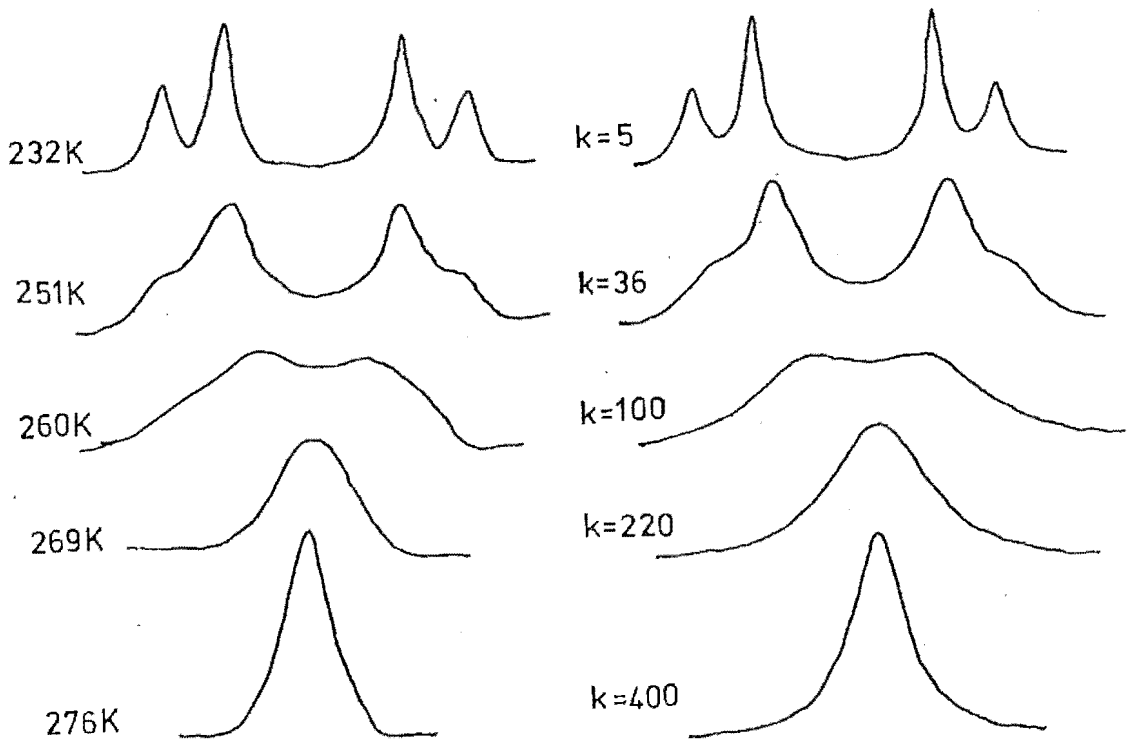

FIGURE 3.6 continued

(e) $[RuBr_3(NO)(Bz_2S)_2]$

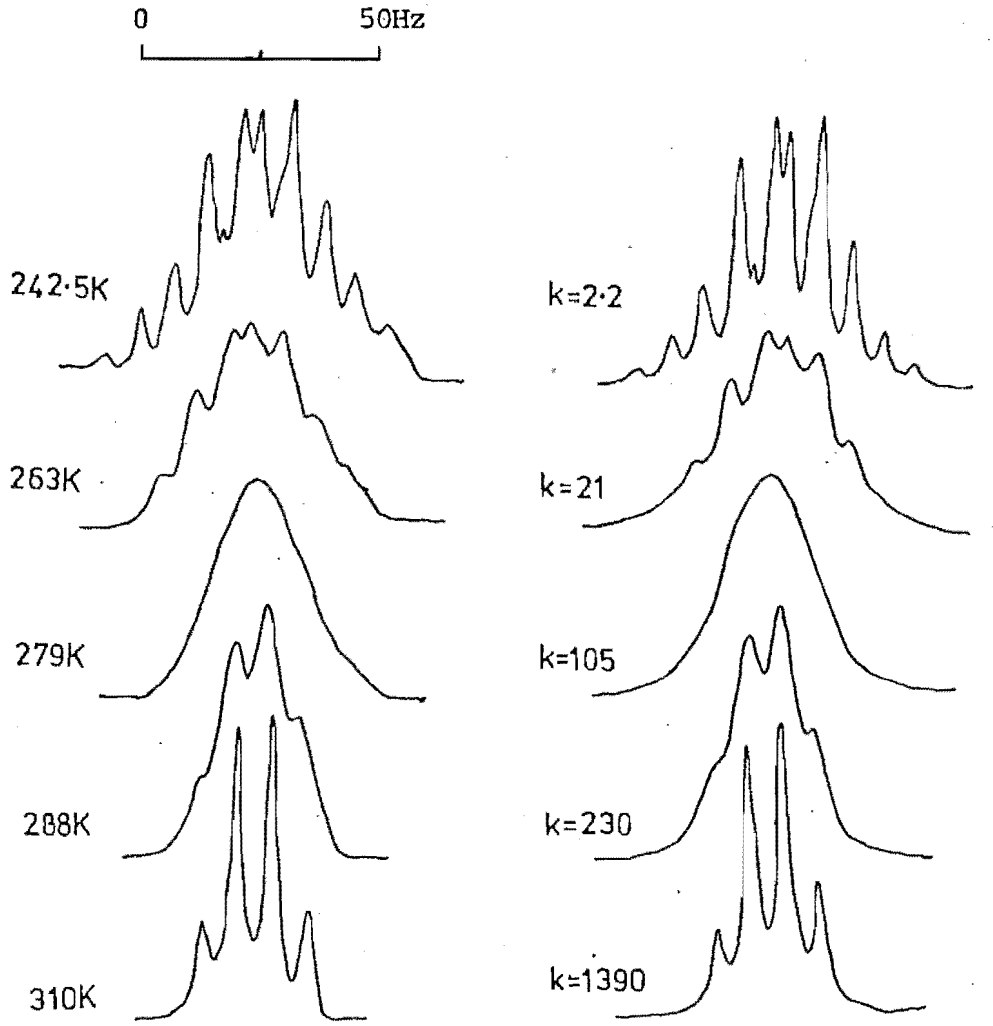

FIGURE 3.6 continued

(f) $[RuBr_3(NO)(Et_2S)_2]$

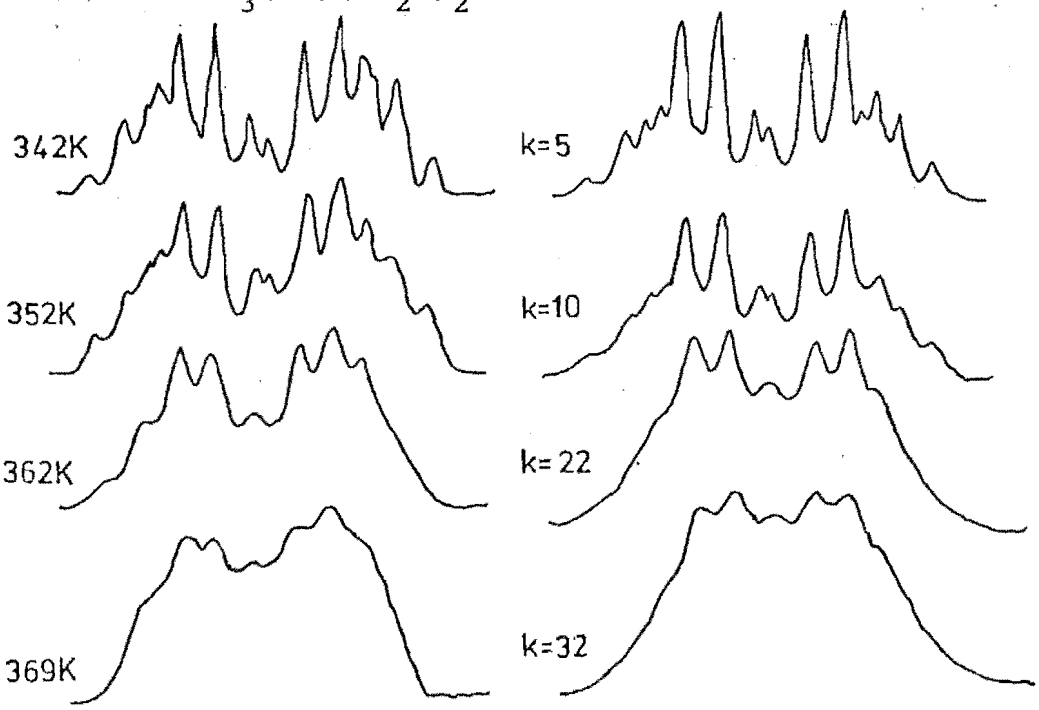

FIGURE 3.6 continued

(g) $[RuCl_3(NO)(Et_2Se)_2]$

The spectra obtained at the normal operating temperature (ca. 305K) of the ^{1}H n.m.r. spectrometer (i.e. in the fast exchange region for the sulphide complexes) and also spectra obtained in the slow exchange region (ca. 245K) are included in the figures.

The coalescence temperatures T_c, (the region of collapse of the methylene signal where it shows no fine structure), the rate (k) at 298.15K and at the coalescence temperature are listed in Table 3.4. The values for the rate at 298.15K are obtained from extrapolation of a linear plot of ln k against $^{1}/_{T}$, where T is the sample temperature. Some coalescence temperatures for the ruthenium complexes studied here have been reported,[111] but they were estimated from a small number of experimental spectra obtained over a wide temperature range and are not precise.

3.2.5 Calculation of Thermodynamic Parameters

Since the slow step in the mechanism for the mutual exchange of the methylene proton positions is considered to be the inversion of configuration about the sulphur atom the values obtained for the rate constant k (at various temperatures) were taken to be the rate constants for the inversion process. Hence the energy barrier to inversion about the sulphur atom, that occurs in solutions of the complexes, may be determined.

From the Arrhenius equation

$$\ln k = -E_a/RT + \ln A,$$

a plot of ln k against -1/RT for the rate constant data was

TABLE 3.4

Coalescence Temperatures and Exchange Rates

Complex	T_c [a] / K	k_{Tc} [b] / sec^{-1}	$k_{298.15}$ [b] / sec^{-1}	Solvent
$RuCl_3(NO)(Et_2S)_2$	288	112	249	$CDCl_3$
$RuBr_3(NO)(Et_2S)_2$	279	104	542	$CDCl_3$
$RuCl_3(NO)(PhSEt)_2$	285	73	255	$CDCl_3$
$RuBr_3(NO)(PhSEt)_2$	286	97	299	$CDCl_3$
$RuCl_3(NO)(n\text{-}Pr_2S)_2$	280	-	-	$CDCl_3$
$RuBr_3(NO)(n\text{-}Pr_2S)_2$	275	-	-	$CDCl_3$
$RuCl_3(NO)(Bz_2S)_2$	278	156	766	$CDCl_3$
$RuBr_3(NO)(Bz_2S)_2$	263	128	2192	$CDCl_3$
$RuCl_3(NO)(Et_2Se)_2$	ca. 380	ca. 70	ca. 0.1	PhCl
$RuBr_3(NO)(Et_2Se)_2$	370	-	-	PhCl
$RuCl_3(NO)(PhSeEt)_2$	368	-	-	PhCl

[a] Temperature estimated from a series of variable temperature spectra, error ±1 degree.

[b] Error ±4 sec^{-1}.

found to be linear for the $[RuX_3(NO)L_2]$ complexes (X = Cl, Br and L = Et_2S, Et_2Se, PhSEt and Bz_2S). The slope of the Arrhenius plot yields the activation energy E_a, and the frequency factor, log A, may be obtained from the intercept. Between eight and fourteen data points were used in the least-squares analysis to obtain the activation parameters.

The free energy of activation of the transition state $\Delta G^{\ddagger}$ was obtained using the Eyring equation

$$k = K(k_B T/h)\exp(-\Delta G^{\ddagger}/T),$$

where K is the transmission coefficient and is taken to be unity,[80] k_B is the Boltzmann constant, h is the Planck constant, R the gas constant and T the absolute temperature of the sample. Replacing $\Delta G^{\ddagger}$ by

$$\Delta H^{\ddagger} - T.\Delta S^{\ddagger}$$

in the Eyring equation, gives

$$k = K(k_B T/h)\exp(-\Delta H^{\ddagger}/RT)\exp(\Delta S^{\ddagger}/R).$$

Therefore $\Delta H^{\ddagger}$ and $\Delta S^{\ddagger}$, the enthalpy and entropy respectively of the transition state for the inversion process, can be obtained from a least-squares plot of

$$-R \ln(hk/k_B T K) \text{ against } 1000/T,$$

the slope of which is $\Delta H^{\ddagger}$ and the intercept of which is $-\Delta S^{\ddagger}$, (see Figure 3.7).

The results are collected in Table 3.5, the values in parentheses are the estimated standard deviations of the measurement in the least significant figure. The

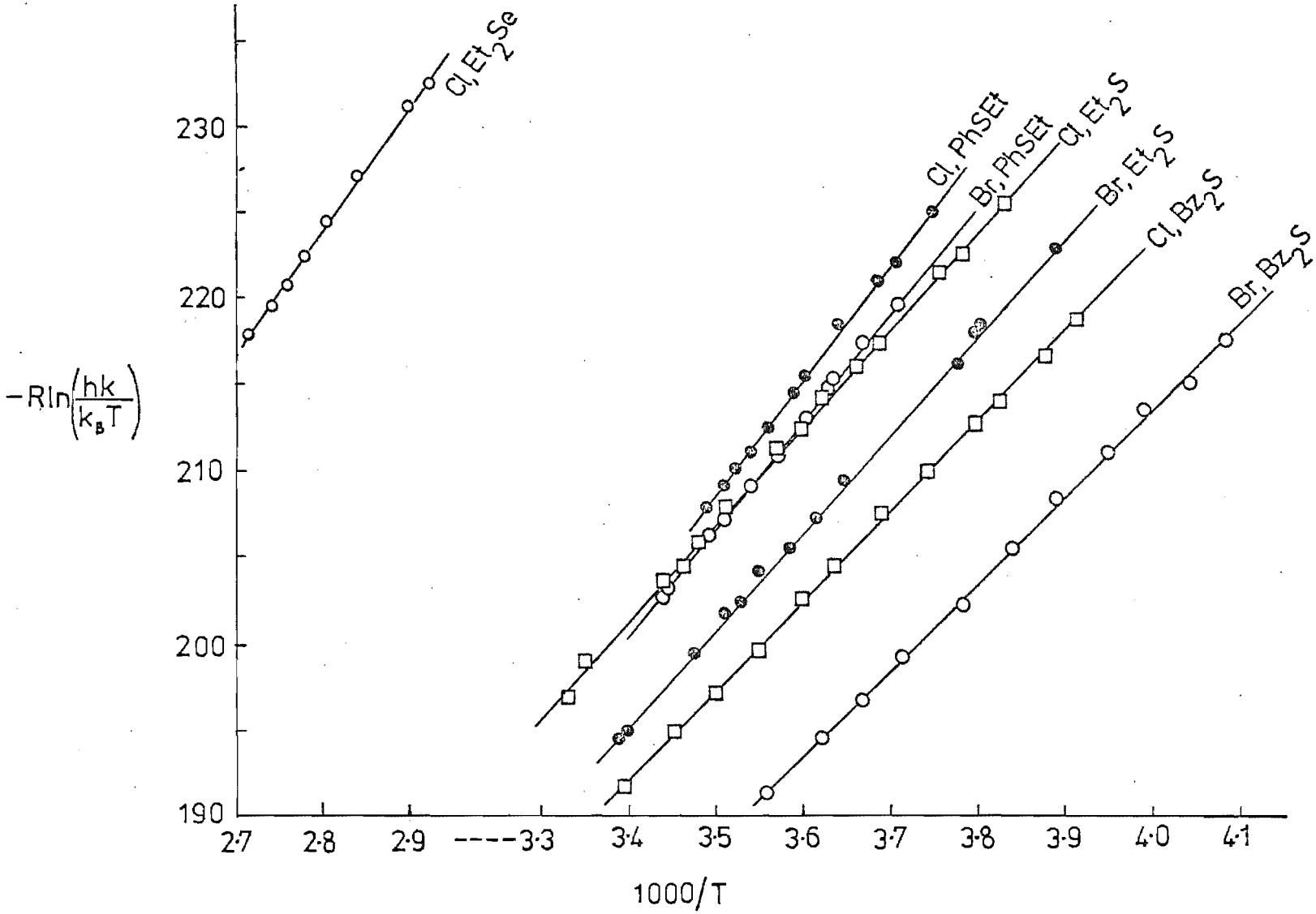

FIGURE 3.7

Correlation of $-R\ell n(hk/k_B T)$ with 1000/T for the $[RuX_3(NO)L_2]$ complexes

statistical errors given are considered to be a reasonable estimate of the experimental error.[110] The transmission coefficient K is normally taken to be 1.0, but because the inversion process involves the formation of a transition state which may then have a potential energy well in either direction, there is some support for using a value of 0.5. However, this only alters the entropy value by a small amount, e.g. $\Delta S^{\ddagger}$ increases by 5.8 J K^{-1} mol^{-1} for each complex, so the usual value for K of 1.0 was used throughout.

3.2.6 Analysis of the Thermodynamic Results

The values of the energy barrier to inversion about the sulphur atom, E_a, of 53 to 69 kJ mol^{-1} are comparable with values reported for other monodentate organosulphide transition metal compounds.[98-100] Earlier reports[91,96] of the inversion process estimated the free energy of activation $\Delta G^{\ddagger}$ using approximate methods.[78,90] The values reported in the present work also compare reasonably well with the earlier reported values which are listed in Table 3.2. The selenide complexes are reported[96,99,100] to have an energy of activation of between 10 to 20 kJ mol^{-1} greater than the corresponding sulphide complexes, which correlates with the higher coalescence temperature observed for the selenide complexes. The present work confirms these observations with the $RuCl_3(NO)(Et_2Se)_2$ energy of activation being 17 kJ mol^{-1} greater than that obtained for $RuCl_3(NO)(Et_2S)_2$. The selenide complexes reach coalescence approximately 100 degrees above the corresponding sulphide

TABLE 3.5

Activation Parameters

Complex	E_a kJ mol^{-1}	log A	$\Delta G^{\ddagger a}$ kJ mol^{-1}	$\Delta H^{\ddagger}$ kJ mol^{-1}	$\Delta S^{\ddagger}$ J K^{-1} mol^{-1}
$RuCl_3(NO)(Et_2S)_2$	57.9(4)	12.53(7)	59.4(8)	55.5(4)	-12.8(14)[b]
$RuBr_3(NO)(Et_2S)_2$	59.7(4)	13.19(7)	57.4(7)	57.4(3)	0.0(12)
$RuCl_3(NO)(PhSEt)_2$	69.2(8)	14.5(2)	59.3(16)	66.9(8)	25.5(28)
$RuBr_3(NO)(PhSEt)_2$	64.8(4)	13.84(7)	58.9(8)	62.5(4)	12.2(13)
$RuCl_3(NO)(Bz_2S)_2$	54.4(5)	12.41(9)	56.6(10)	52.1(5)	-15.0(17)
$RuBr_3(NO)(Bz_2S)_2$	52.7(7)	12.6(1)	53.9(14)	50.5(7)	-11.6(26)
$RuCl_3(NO)(Et_2Se)_2$	75.2(18)	12.2(3)	78.7(33)	72.3(18)	-21.6(51)

[a] $\Delta G^{\ddagger}$ at T = 298.15K.

[b] The standard deviations in the two least significant figures are given.

complexes. This same higher energy barrier to inversion for the heavier elements of a periodic group has also been reported[82,112] for group V, e.g. $AsR_3 > PR_3 > NR_3$.

The magnitude of the energy of activation of the transition state may reflect the degree of stabilisation of the transition state from π-overlap. This occurs between the filled (lone pair) p orbital with a partially empty transition metal atom d orbital. A partial vacancy of the ruthenium atom 4 d t_{2g} orbitals is achieved by delocalisation of electron density from the full t_{2g} orbitals onto the other ligands, especially the nitrosyl, (see section 2.1.2).

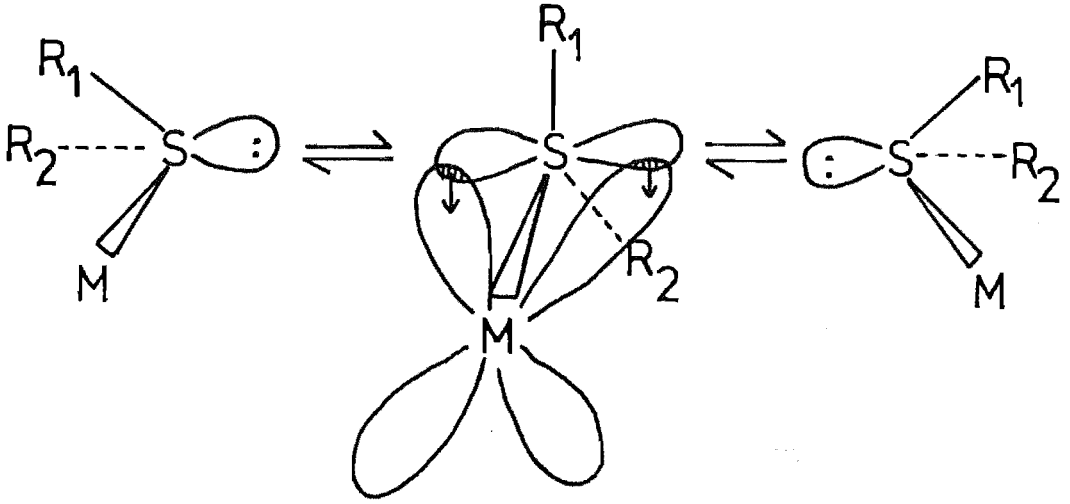

The proposed transition state for the inversion mechanism is shown above. One could expect that the better the $^{S}p_{\pi} \rightarrow {}^{M}d_{\pi}$ orbital overlap the smaller the activation energy required to form the transition state. The activation energies of the diethyl sulphide complexes are 5-10 kJ mol^{-1} lower than for the phenyl ethyl sulphide complexes. This could possibly arise from the electron withdrawing effect of

the phenyl group (with respect to the alkyl group) bonded to the sulphur atom, which would reduce somewhat the electron donation from the S_{p_π} orbital to the Ru_{d_π} orbital, hence leading to a slight increase in the energy of the transition state. The trend in E_a of Et_2S < PhSEt is in agreement with that observed[100] for the $[MCl_2(RS(CH_2SiMe_3))_2]$ complexes, M = Pd, Pt, when R is changed from a methyl group to a phenyl group. Hence, tentatively it can be said that by changing the R group attached to the sulphur atom from alkyl to aryl will lead to a small but significant increase in the activation energy of the sulphur atom inversion process.

No consistent trends in the activation parameters are obvious when comparing chloro and bromo complexes. Although there is a distinct difference between the chloro and bromo complexes as regards the rate of inversion (see Table 3.4), namely the bromo complexes have a faster rate of inversion than the chloro complexes at room temperature (298K). A possible $Ru_{d_\pi} \rightarrow Br_{d_\pi}$ overlap could increase the electronegativity of the ruthenium ion (relative to the situation in the chloro complex) allowing increased electron donation from the sulphur atom.

The enthalpies of the transition state, $\Delta H^{\ddagger}$, follow the same trends as the activation energies. The entropy values $\Delta S^{\ddagger}$ obtained for the transition state will depend on contributions from translational, rotational and vibrational components. For instance a more symmetrical and rigidly defined transition state compared with the ground state would be indicated by a large negative $\Delta S^{\ddagger}$ value. The dibenzyl sulphide complexes which have negative $\Delta S^{\ddagger}$ values may undergo

the inversion process forming a more symmetrical transition state. But a transition state involving the formation of a weaker Ru-S bond could result in a less ordered situation and hence a large positive $\Delta S^{\ddagger}$ value. The more positive $\Delta S^{\ddagger}$ values of the PhSEt complexes (compared with the Et_2S complexes), may indicate that the reduced $S_{p_\pi} \rightarrow Ru_{d_\pi}$ overlap (described above) occurs in the transition state. However, the $\Delta S^{\ddagger}$ values listed in Table 3.5 are all reasonably small and do not contribute strongly to the overall free energy of the system.

It is found[82] that for the pyramidal inversion of configuration processes where some M-L bonding is retained in the transition state, the $\Delta S^{\ddagger}$ and log A values are close to 0 and 13 respectively. In this study the results listed in Table 3.5 are in general agreement with this observation.

3.2.7 Variable Temperature ^1H n.m.r. study on other complexes

Some of the other organic sulphide and selenide complexes prepared were also studied by the variable temperature ^1H n.m.r. technique. The spectra of the $[RuX_3(NO)(Me_2S)_2]$ and $[RuX_3(NO)(MeSPh)_2]$ complexes where X = Cl, Br (as explained in section 3.2.2) showed no change when the temperature was varied due to a lack of diastereotopic protons. The $[RuX_3(NO)(Pr_2S)_2]$ complexes exhibited the coalescence phenomena but because the ABM_2X_3 spin system was too complex for the available simulation program (DNMR3), no line shape analysis was carried out.

The ^1H n.m.r. spectra of the $[RuX_3(NO)(Et_2Se)_2]$ complexes consisted of a series of quartet signals in the

methylene region due to the diastereotopic methylene protons undergoing a slow exchange of environments. At high temperatures (360-380K) the selenide complexes exhibited the same type of coalescence of the absorption signals in the methylene region as observed for the sulphide complexes. The $[RuCl_3(NO)(Et_2Se)_2]$ compound was the only selenide complex able to be simulated using the line-shape fitting program, because in the case of the bromo complex the static parameters J_{AB}, J_{AX}, J_{BX} and $\Delta\nu_{AB}$ were not able to be determined in the slow exchange region. Similarly the $[RuX_3(NO)(PhSeEt)_2]$ complexes were unable to be simulated. The coalescence temperatures of these complexes (except for $[RuBr_3(NO)(PhSeEt)_2]$) were obtained and are listed in Table 3.4.

The variable temperature ^1H n.m.r. spectra for the $[RuX_3(NO)(PhSeEt)_2]$ complexes were difficult to interpret. The normal probe temperature spectrum (305K) has a single methylene quartet and methyl triplet. The methylene quartet is then observed to split into a multiplet on cooling. A preliminary study at five temperatures carried out at approximately 20 degree intervals from 310K down, indicated that a possible coalescence may occur around 248K.[111] However, a more detailed variable temperature study has revealed that the coalescence occurs around 370K. The difficulties in interpretation of the spectra arise because in the methylene region the chemical shift difference between the quartet absorptions (from the diastereotopic methylene protons) varies as the temperature changes. Since only a single methylene quartet is observed at the normal probe temperature the chemical shifts of the H_A and H_B methylene

protons must be accidentally degenerate, i.e. $\nu_A - \nu_B = 0$. The change in chemical shift with temperature is shown in Figure 3.8(a). Another way of changing the chemical shift difference is to alter the solvent,[90] in this case chlorobenzene was used instead of deuterochloroform. The $\nu_A - \nu_B$ value is now greater than the coupling and the interpretation is simplified, see Figure 3.8(b). However, for $[RuBr_3(NO)(PhSeEt)_2]$ even the change in solvent still left $\nu_A - \nu_B < J$, which did not allow a coalescence temperature to be observed. For the $RuX_3(NO)(PhSeEt)_2$ complexes the ^{13}C n.m.r. spectra indicate that the methylene carbon atoms do not appear to be all equivalent, although the methyl carbon atoms are. No change was observed over the temperature range 253-328K. A possible explanation of this observed inequivalence has been given in section 2.2.4(b).

3.3 EXPERIMENTAL

^1H nuclear magnetic resonance measurements were obtained on a Varian T-60 NMR spectrometer, equipped with a variable temperature probe. The solvent used was deuterochloroform for low temperature measurements and Me_4Si was used as an internal standard. At high temperatures chlorobenzene was the solvent used. All the 60 MHz variable temperature ^1H n.m.r. spectra were obtained using an internal field frequency lock on either the intense Me_4Si or PhCl signal. The observed signal was filtered as little as possible so that satisfactory signal to noise ratios were obtained without distortion. The field homogeneity was continuously

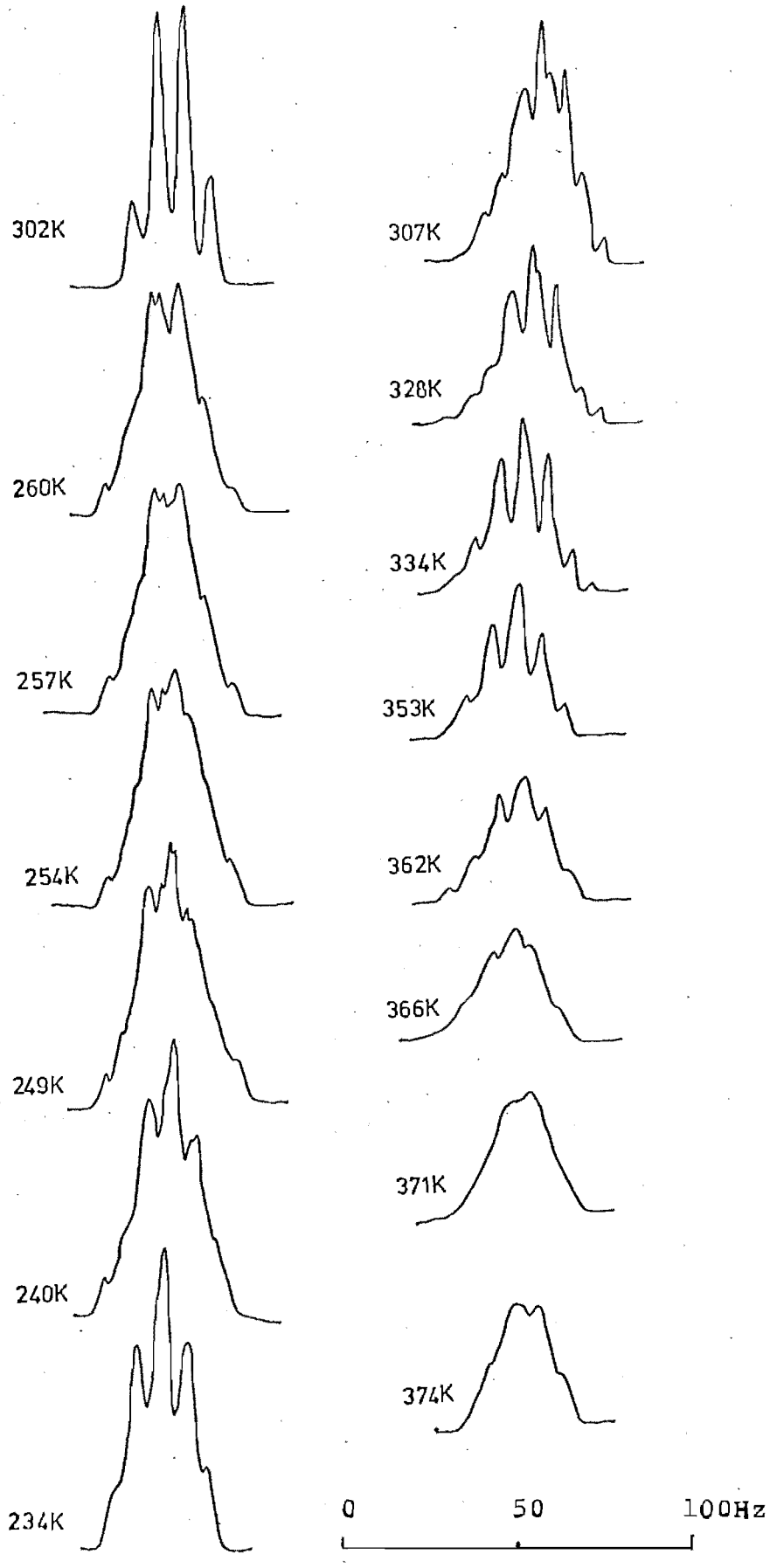

FIGURE 3.8

Change in the ^1H n.m.r. spectrum of $[RuCl_3(NO)(PhSeEt)_2]$, with temperature, using two different solvents.

monitored and corrected for any drift that occurred. Temperatures were measured by a thermocouple mounted in the probe, which was calibrated with methanol.[113] The temperature values are estimated to be accurate to within one degree.

The DNMR3 computer program[83,84] was used to calculate the exchange-broadened n.m.r. spectra. All calculations were carried out on the University of Canterbury Burroughs B6718 computer. The simulated spectra obtained from the DNMR3 program were plotted with a Calcomp plotter to the same size as the experimentally obtained spectra. The chemical shift and spin coupling constant values required for the simulation program, were measured from a two times expansion of the methylene region of the experimental spectra. A visual comparison between the experimental spectrum and a series of calculated spectra was used to determine the best fitting simulated spectrum.

The thermodynamic parameters were obtained from least-squares plots and the errors were obtained from the estimated standard deviations of these plots.

CHAPTER 4

PHOTOCHEMICAL REACTIONS OF RUTHENIUM NITROSYL THIOETHER COMPLEXES

4.1 INTRODUCTION

It was observed previously, and reported briefly[1] that when a dilute solution of $[RuBr_3(NO)(Et_2S)_2]$ in chloroform was exposed to sunlight, the solution rapidly changed colour. In order to characterise both the photochemical reaction and products, two crystalline materials were obtained which corresponded to an intermediate and an end product of the reaction. Single crystal X-ray crystallographic analyses were undertaken on the two materials in order to determine their molecular structure. The crystallographic results, reported in full in Chapters 5 and 6, show that the intermediate product isolated contained both a sulphide and sulphoxide ligand, $[RuBr_3(NO)(Et_2SO)(Et_2S)]$, while the end product was a dimeric sulphoxide complex, $[RuBr_3(NO)(Et_2SO)]_2$.

The photochemical reaction appeared to consist of photo-oxidation of the diethyl sulphide to diethyl sulphoxide while retaining some bonding interaction with the ruthenium atom. The intermediate product then undergoes a rearrangement to form a dimeric end product. Some of the results of this work have been published.[114,115]

4.1.1 Photo-oxidation Reactions of Ligands Coordinated to Transition Metals

Photochemical reactions of transition metal coordination

compounds are well established and several recent reviews have been published.[116,117,118] Such reactions which involve oxidation of ligands are not new. Vaska in 1963 reported[119] that a dioxygen adduct of iridium which, while stable in the dark, in light and in the presence of oxygen irreversibly changed to a dark coloured product (both the crystals and the solution). The triphenylphosphine in the complex $[O_2.IrCl(CO)(PPh_3)_2]$ had been converted to triphenylphosphine oxide through a peroxo intermediate.

Recently it was observed[120] that the solutions of the $[RuCl_2(PPh_3)_3]$ complex, rapidly absorbed oxygen, forming a polymeric material $[Ru(OPPh_3)Cl_2]_n$. In this case no evidence was found for a peroxo intermediate.

The rapid photo-induced oxidation of triphenylphosphine and carbon monoxide in <u>trans</u> $[RhCl(CO)(PPh_3)_2]$,[121] was said to proceed via a dioxygen intermediate, though no such product was isolated. An excess of triphenylphosphine inhibited the photochemical reaction, suggesting that dissociation of triphenylphosphine from the rhodium complex was a likely first step in the reaction. Also no change occurred when the solution was first degassed and then exposed to light. Several other analogous tertiary phosphine complexes were also found to be photosensitive in a similar manner.

Uncoordinated tertiary phosphines, containing at least one aryl group, have been reported[122] as being readily photo-oxidised. For example, exposure of oxygen saturated dichloromethane solutions of phosphines to an ordinary fluorescent room light was sufficient to cause photo-oxidation. Therefore in the case of tertiary phosphines, free or

coordinated to transition metals, there is good evidence that they can be readily photochemically oxidised.

There are no previous reports of similar photochemical oxidations occurring for thioethers coordinated to transition metals. But in the case of the free organic sulphides the corresponding sulphoxide may be formed by heating the sulphide in the presence of oxygen,[123] especially when free radical catalysts are available. For example, ultraviolet light will initiate the oxidation of the normally inert sulphides, such as dibenzyl sulphide. It appears that a free radical chain mechanism operates, as it does for phosphine, a simplified example of a possible mechanism[123] is as follows:

$$R_2S \xrightarrow{h\nu} R_2S^* \qquad \text{chain initiation}$$

$$R_2S^* + O_2 \longrightarrow R_2S.O_2^* \qquad \left.\begin{array}{l}\\ \text{chain}\\ \text{propagation}\end{array}\right\}$$

$$R_2S.O_2^* + R_2S \longrightarrow R_2S.O_2 + R_2S^* \qquad \left.\begin{array}{l}\\ \\ \end{array}\right\}$$

$$R_2S.O_2 + R_2S \longrightarrow R_2S.O + R_2S.O \qquad \left.\begin{array}{l}\\ \text{chain}\\ \text{termination}\end{array}\right\}$$

$$R_2S.O_2 + R_2S.O \longrightarrow \text{secondary decomposition products} \qquad \left.\begin{array}{l}\\ \\ \end{array}\right\}$$

Visible light has been reported as being necessary for a number of isomerisations of transition metal complexes.[124-126] For example, the cis-$[RuI_2(CO)_2(PPh_3)_2]$ complex isomerises to the trans form on exposure to daylight, and the $[IrCl_3(CO)L_2]$ complex (where the phosphines, L, are cis or trans to each other and the chloro ligands are meridional), undergoes isomerisation to a facial arrangement of chloro ligands over a period in visible light. When the photo-isomerisation process is inhibited by the

presence of free ligand a dissociative process is postulated[127] and when the free ligand has no effect an intramolecular twisting mechanism has been proposed.[128] In the system studied here a trans to cis isomerisation of the dialkyl sulphide ligands occurs in the first step of the reaction.

4.2 LIGHT INDUCED PHOTOCHEMICAL REACTION OF $[RuBr_3(NO)(Et_2S)_2]$

4.2.1 Initial Observations

Following a preliminary observation[1] that a dilute solution (10^{-3} - 10^{-4}M) of the $[RuBr_3(NO)(Et_2S)_2]$ complex in chloroform, undergoes a marked colour change in light, a more detailed analysis of the reaction system was undertaken. The colour of the solution changed from pale yellow-brown to a dark red over a period of a few minutes when exposed directly to sunlight. In indirect sunlight (e.g. on a laboratory bench), a number of days was necessary for the colour change to occur, while a sample kept in the dark was stable indefinitely (at least up to two years). Solid samples of $[RuBr_3(NO)(Et_2S)_2]$ remained unchanged even in daylight.

The rate of colour change was accelerated by the addition of diethyl sulphide, but appeared to be reduced by increasing the concentration of the solution.

The progress of the reaction was followed by recording the ^1H n.m.r. spectra after different intervals of exposure to sunlight. The visible absorption spectra of the solutions were also recorded at similar intervals. The results of these measurements are discussed below (sections 4.2.3(b) and 4.2.3(d)).

The infrared spectra of the solid product obtained differed in one main detail from the infrared spectrum of $[RuBr_3(NO)(Et_2S)_2]$, viz. the appearance of a strong absorption at 920 cm^{-1}. This absorption lies in the region expected for a ν(S-O) stretching mode when the oxygen atom (of a sulphoxide ligand) is bonded to a transition metal.

The wavelength of light necessary to bring about the colour change was determined by exposing samples to sunlight after passing through Ilford Bright Spectrum filters. Radiation within the wavelength range 380-480 nm was effective. U.V. radiation is not necessary as it is in fact absorbed by the glass through which the sunlight passed in all the reactions carried out. Attempts to define the wavelength range more exactly by the use of spectrophotometers were unsuccessful due to the low intensity of the light source.

4.2.2 The Source of the Oxygen Required for the Photo-oxidation Process

A series of experiments in which solutions of $[RuBr_3(NO)(Et_2S)_2]$ were exposed to direct sunlight under varying conditions were carried out in order to determine the source of the oxygen atom required when the sulphide ligand is oxidised to a sulphoxide. There are two possible sources, either atmospheric oxygen dissolved in the chloroform, (up to 0.22 ml/ml at 16°C),[129] or the ethanol present in chloroform (ca. 1-2%) to stabilize it. The conditions used and results obtained are listed in Table 4.1.

The NO group is another possible source of oxygen, however, it was considered unlikely because the infrared

TABLE 4.1

Conditions and Results of Exposing Chloroform Solutions of $RuBr_3(NO)(Et_2S)_2$ to Sunlight

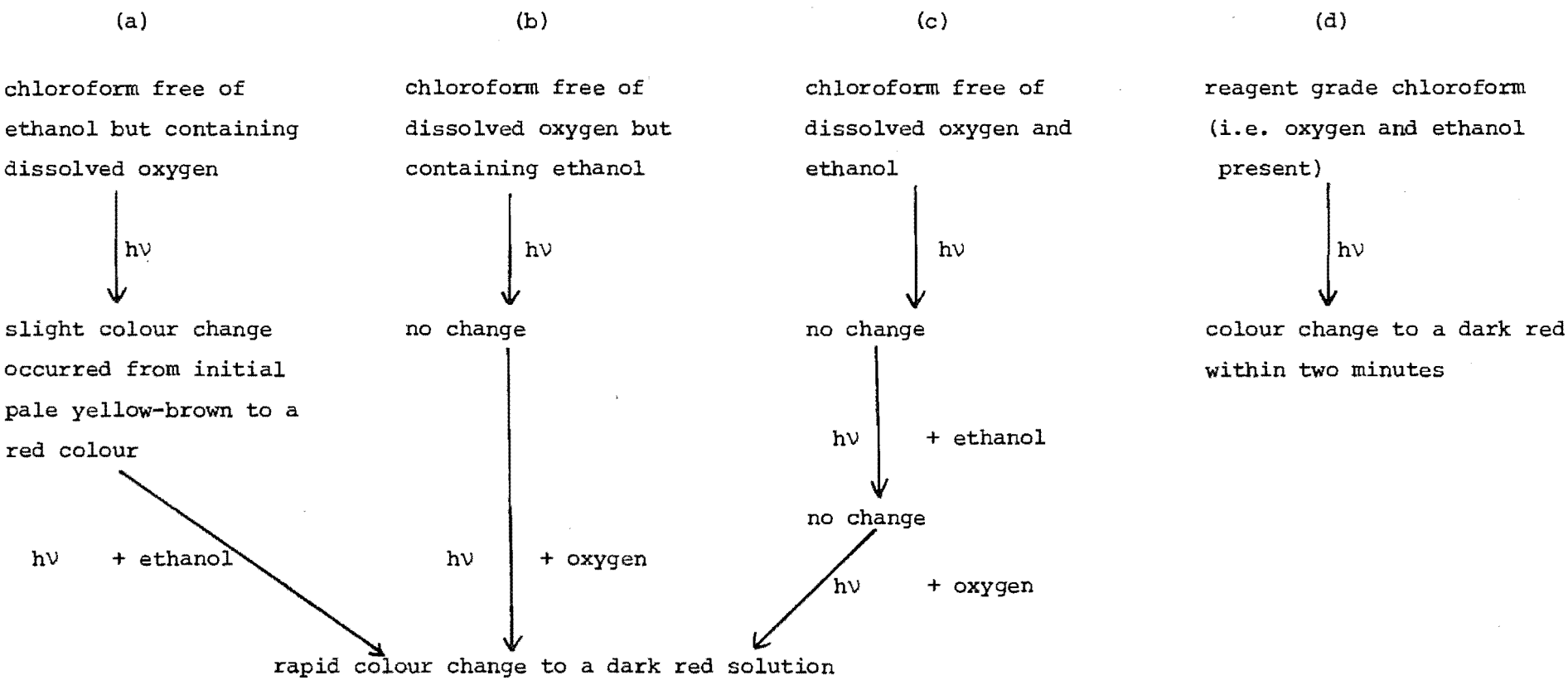

Details of the preparation of the above solutions are given in section 4.4.1

spectra indicated the presence of the ν(N-O) absorption, in the 1860-1880 cm^{-1} region, throughout the photo-oxidation reaction. The results show that rapid colour change only occurs when both ethanol and dissolved oxygen are present in the reaction. However, a slight colour change takes place when dissolved oxygen, but no ethanol, is present. This was confirmed from the ^{1}H n.m.r. samples (which contained no ethanol) where the colour change occurred slowly. Shaking the sample tube was observed to assist the rate of change, presumably due to oxygenation of the solution.

Therefore the results indicate that the presence of molecular oxygen in the chloroform and visible radiation were required before the photo-oxidation reaction could proceed. The role of the ethanol would appear to be catalytic. The same rapid colour change was observed if acetic acid or acetaldehyde were used in place of ethanol.

Since the ease of oxidation of the organic sulphides is known to be assisted by hydrogen bonding,[123] it is possible that ethanol assists in the photo-oxidation process in this manner.

The colour change also occurred when an ethanolic solution of $[RuBr_3(NO)(Et_2S)_2]$ was exposed to sunlight, but the rate was slower than in a chloroform solution. It was from this solution in ethanol that the intermediate product $[RuBr_3(NO)(Et_2SO)(Et_2S)]$, formed during the photo-oxidation step, was isolated (see section 4.2.3(c)).

The rate at which the reaction occurred, as demonstrated by changes in the ^{1}H n.m.r. spectrum, depended on the concentration of the sample. The more dilute the sample the more

rapid was the change. This may possibly be due to the limited amount of oxygen dissolved in the chloroform.

Sulphoxide ligands were produced when the complexes $[HgCl_2(SR_2)]$, (R = Me, Et, Pr, Bu, Ph), were treated with H_2O_2 giving the sulphoxide complexes of the type $[R_2SO.HgCl_2]$.[130] However, treatment of the complex $[RuBr_3(NO)(Et_2S)_2]$ with H_2O_2 caused a vigorous reaction to occur, and the infrared spectra of a solid product indicated that considerable chemical change had occurred, as there was no evidence for the presence of nitrosyl or sulphoxide ligands.

4.2.3 Identification of the Reaction Products

(a) ^1H n.m.r. results:

The photo-oxidation reaction of $[RuBr_3(NO)(Et_2S)_2]$ was followed by recording at regular intervals the n.m.r. spectrum of solutions that had been exposed to sunlight (note no ethanol in the solution). The initial spectrum was consistent with that expected for $[RuBr_3(NO)(Et_2S)_2]$ with a methylene quartet and a methyl triplet at δ = 3.28 and δ = 1.47 ppm, respectively. After irradiation of the sample with sunlight over a period of about two weeks, the absorption signals in the n.m.r. spectrum associated with $[RuBr_3(NO)(Et_2S)_2]$ had gradually disappeared and two new quartet resonances (δ = 3.20 and 3.03 ppm) and two new triplet resonances (δ = 1.44 and 1.39 ppm) appeared. After 14 to 28 days resonances due to the starting material had completely disappeared.

Crystals appeared in the n.m.r. tube after 1-2 months and new quartet and triplet signals appeared in the spectrum

at δ = 2.70 and 1.33 ppm respectively. After lengthy exposure to sunlight, further resonances appeared at δ = 3.00 and 1.40 ppm in the n.m.r. spectrum. These spectral changes with time are shown in Figure 4.1 and listed in Table 4.2 with suggested interpretations.

(b) Interpretation of the ^{1}H n.m.r. results

(i) Initially.

The 3.28 and 1.47 ppm resonance signals observed are due to the $[RuBr_3(NO)(Et_2S)_2]$ starting material.

(ii) After 20 days exposure.

In order to analyse the origin of the 3.20, 3.03, 1.44 and 1.39 ppm resonance signals an attempt was made to prepare the end product, $[RuBr_3(NO)(Et_2SO)]_2$, by an independent route starting with '$RuBr_3(NO)$' and Et_2SO. A complex was isolated whose infrared spectrum indicated the presence of an oxygen bonded sulphoxide ligand and the ^{1}H n.m.r. spectrum suggested two chemically distinct ethyl groups, with methylene resonances at 3.19 and 3.02 ppm and methyl resonances at 1.42 and 1.37 ppm. These latter results compare favourably with the ^{1}H n.m.r. spectrum observed for the solution of $[RuBr_3(NO)(Et_2S)_2]$ after approximately 2-4 weeks exposure to sunlight (see Table 4.2).

Crystals of this sulphoxide product were subsequently grown and a single crystal X-ray analysis was carried out to determine the exact molecular structure. The compound was shown to be $[RuBr_3(NO)(Et_2SO)(Et_2S)]$ with the structure below, (see Chapter 6 for details of the structure determination).

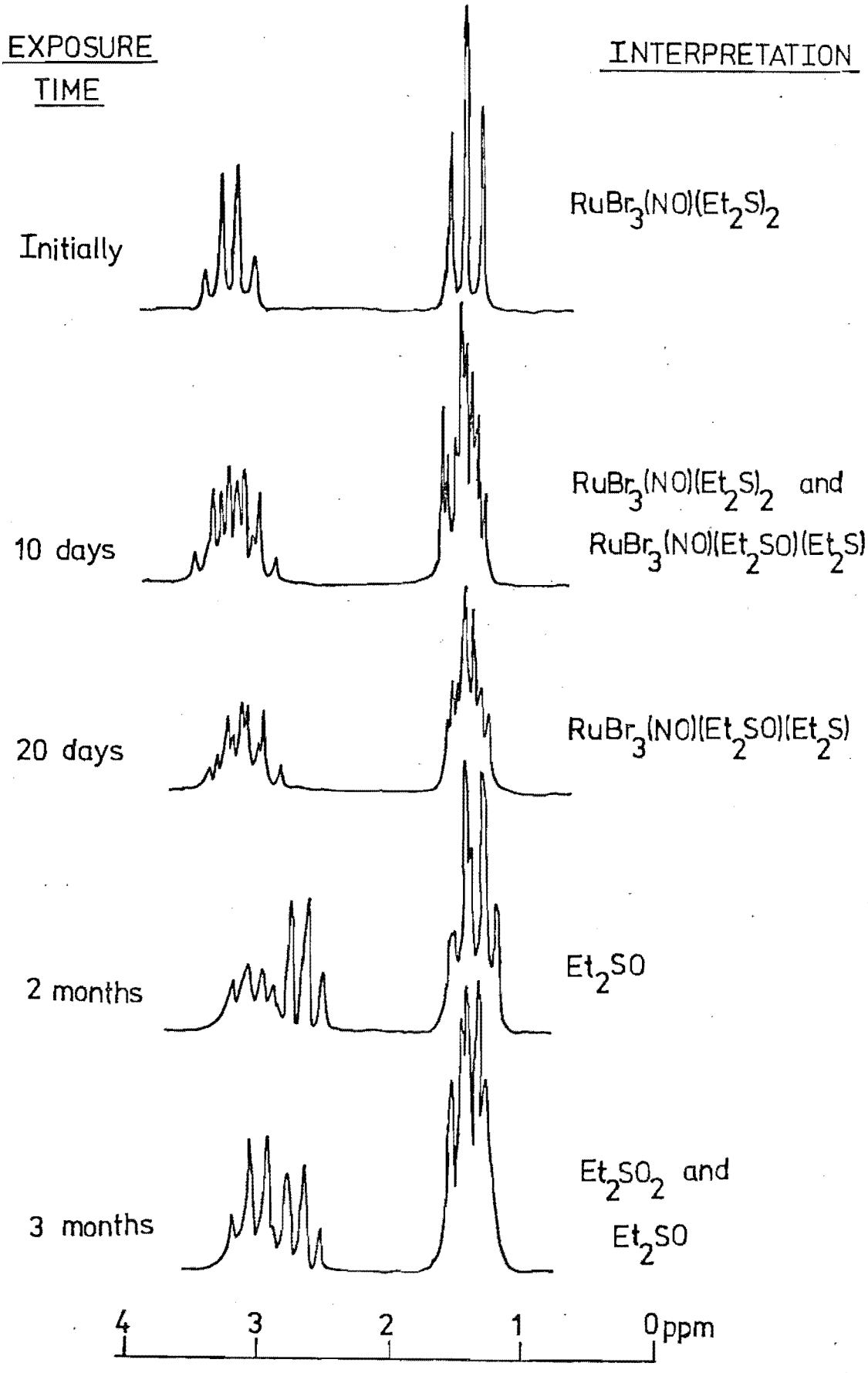

FIGURE 4.1

Changes observed in the ^{1}H n.m.r. spectrum when the $[RuBr_3(NO)(Et_2S)_2]$ solution is exposed to sunlight.

TABLE 4.2

Change in ^{1}H n.m.r. spectrum of $[RuBr_3(NO)(Et_2S)_2]$ with exposure to sunlight.[a]

Exposure Time	Resonance Signals Observed δ in ppm								Interpretation
Initially	3.28				1.47				$[RuBr_3(NO)(Et_2S)_2]$
10 days	3.28	3.20	3.03		1.47	1.44	1.39		Mixture of $[RuBr_3(NO)(Et_2S)_2]$ and $[RuBr_3(NO)(Et_2SO)(Et_2S)]$.
20 days		3.20	3.03			1.44	1.39		$[RuBr_3(NO)(Et_2SO)(Et_2S)]$
2 months[b]				2.70				1.33	Et_2SO
3 months			3.00	2.70			1.40	1.33	Et_2SO_2 and Et_2SO

[a] In conjunction with Figure 4.1.

[b] Crystals of $[RuBr_3(NO)(Et_2SO)]_2$ are forming by this time.

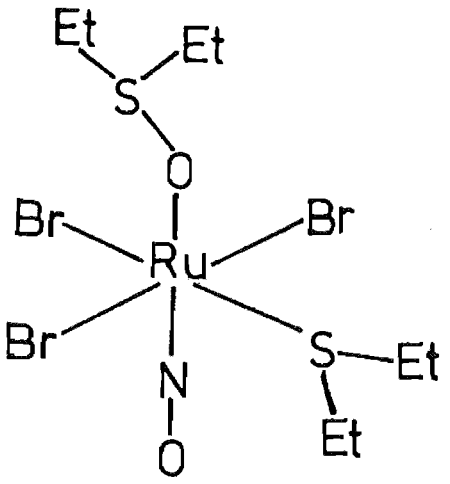

The diethyl sulphide ligand obtained in the complex probably arises from contamination of the diethyl sulphoxide with some diethyl sulphide. The sulphoxide is often contaminated with sulphide and/or sulphone.[131,132]

The same compound, $[RuBr_3(NO)(Et_2SO)(Et_2S)]$, was also isolated from the photo-oxidation of $[RuBr_3(NO)(Et_2S)_2]$ carried out in ethanol (see section 4.2.3(c)), confirming that the product is in fact produced during the photochemical reaction. Therefore it would appear reasonable (see section 4.2.3(c)) to assign the two sets of resonances 3.20, 1.44 ppm and 3.03, 1.39 ppm to the Et_2S and Et_2SO respectively in the complex $[RuBr_3(NO)(Et_2SO)(Et_2S)]$, and to postulate that this complex is an intermediate in the photo-oxidation reaction.

(iii) After 2 months exposure.

No evidence was found in the ^1H n.m.r. spectra for the presence of free diethyl sulphide. Although after 1-2 months a new set of ethyl resonances were observed in the ^1H n.m.r. spectrum (see Table 4.2). The positions of the new signals agreed with those reported[133-135] for

diethyl sulphoxide. This suggests that the diethyl sulphide liberated during the reaction is oxidised to diethyl sulphoxide.

No ^{1}H n.m.r. resonances were observed for the dimeric product $[RuBr_3(NO)(Et_2SO)]_2$ as it is insoluble in chloroform. However, it appeared after 2 months as crystals in the solution, i.e. at the same time as the diethyl sulphoxide signal appeared.

(iv) After 3 months exposure.

The new resonances at 3.00 and 1.40 ppm, which appeared in the n.m.r. spectrum after three months exposure of the $[RuBr_3(NO)(Et_2S)]$ solution to sunlight, correspond with those expected[136] for diethyl sulphone. It has been reported[137] that sulphoxides in the presence of light and oxygen can form sulphones.

(c) Isolation of $[RuBr_3(NO)(Et_2SO)(Et_2S)]$ from the photo-oxidation reaction

An ethanolic solution of $[RuBr_3(NO)(Et_2S)_2]$ which was allowed to evaporate slowly over a period of six weeks in the presence of daylight, produced a residue which on recrystallisation from ethanol gave a red crystalline product. The ^{1}H n.m.r. spectrum of this product contained three quartet absorptions in the methylene region at 3.28, 3.20 and 3.03 ppm and three triplet absorptions in the methyl region at 1.47, 1.43 and 1.39 ppm, (Table 4.3).

In case the product was a mixture of more than one compound a thin layer chromatogram was run and separation into two species was achieved. On a larger scale, using an activated alumina column, a good separation of the two

ruthenium complexes was obtained using benzene followed by chloroform as eluting agents. The first sample obtained from the column was identified as $[RuBr_3(NO)(Et_2S)_2]$ from its ^1H n.m.r., infrared spectrum (see Figure 4.2) and its X-ray powder photograph. The second product from the column was identified in a similar manner as $[RuBr_3(NO)(Et_2SO)(Et_2S)]$. The ^{13}C n.m.r. spectra of the various products are listed in Table 4.4 and confirm the identifications made.

The n.m.r. spectral results indicate that the 3.19 and 1.42 ppm ^1H n.m.r. and the 30.68 and 13.07 ppm ^{13}C n.m.r. absorptions correspond to the Et_2S group in $[RuBr_3(NO)(Et_2SO)(Et_2S)]$ (see Table 4.3 and 4.4), due to the similarity of the chemical shift values with those observed for $[RuBr_3(NO)(Et_2S)_2]$. The remaining absorptions can therefore be assigned to the Et_2SO group which is bonded to ruthenium through the oxygen atom.

(d) Ultra-violet visible absorption spectra of the photo-oxidation reaction

The changes in the ultraviolet visible absorption spectrum of $[RuBr_3(NO)(Et_2S)_2]$ during exposure of a chloroform solution to sunlight, have been previously reported[1] and the changes observed are shown in Figure 4.3 and absorption maxima are given in Table 4.5. The corresponding changes in the spectra of a sample of $[RuBr_3(NO)(Et_2S)_2]$ and Et_2S are presented in Figure 4.4 and Table 4.6.

4.2.4 Proposed Mechanism for the Photo-oxidation Reaction

It appears that the first step of the photo-oxidation of $[RuBr_3(NO)(Et_2S)_2]$ is the oxidation of one of the diethyl

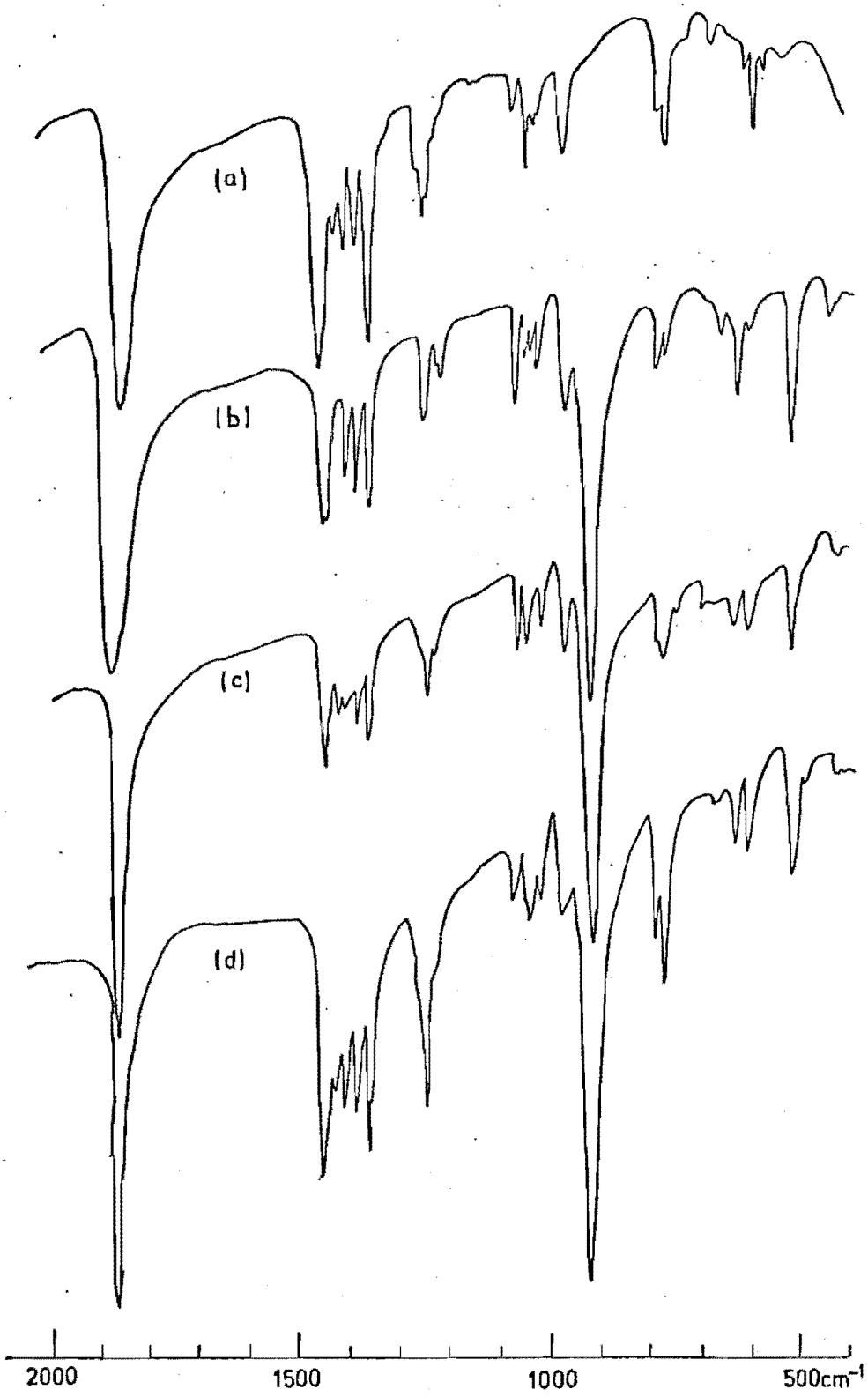

FIGURE 4.2

High frequency infrared spectra observed for (a) $[RuBr_3(NO)(Et_2S)_2]$, (b) $[RuBr_3(NO)(Et_2SO)]_2$, (c) $[RuBr_3(NO)(Et_2SO)(Et_2S)]$ using sulphoxide method and (d) $[RuBr_3(NO)(Et_2SO)(Et_2S)]$ from photo-oxidation reaction.

TABLE 4.3

^1H n.m.r. spectra

Chemical Shift δ(ppm) from Me_4Si, (±0.02ppm)

Compound	α			β		
Mixed product	3.28	3.20	3.03	1.47	1.43	1.39
1st sample from column	3.28			1.47		
2nd sample from column		3.22	3.06		1.45	1.39
$RuBr_3(NO)(Et_2S)_2$	3.28			1.47		
$RuBr_3(NO)(Et_2SO)(Et_2S)$		3.19	3.02		1.42	1.37
Photo-oxidation reaction (after 10-20 days)		3.20	3.03		1.44	1.39

TABLE 4.4

^{13}C n.m.r. spectra

In ppm downfield from Me_4Si, (±0.05ppm)

Compound	α			β		
Mixed product	42.37	32.72	30.66	13.57	13.07	6.64
1st sample from column		32.61		13.61		
2nd sample from column	42.27		30.64		12.98	6.63
$RuBr_3(NO)(Et_2S)_2$		32.76		13.61		
$RuBr_3(NO)(Et_2SO)(Et_2S)$	42.37		30.68		13.07	6.66

TABLE 4.5

Electronic Spectra of $[RuBr_3(NO)(Et_2S)_2]$

(in chloroform) Exposed to Sunlight

Exposure time			
Initially		475 (200)	300 (12,000)
1 hour	538 (1,300)		300-320 (sh) (7000)
1 day	530 (sh) (1,000)	440 (sh) (1,000)	
2 days	540 (sh) (800)	442 (1,000)	385 (sh) (1,200)
4 days	530 (sh) (800)	440 (1,200)	384 (1,500)
9 days		438 (1,300)	381 (1,800)
14 days		430 (1,600)	380 (2,200)
22 days		424 (1,900)	379 (2,400)
57 days		425 (5,000)	382 (5,000)

Values in parentheses relate the observed peak heights to the molar extinction coefficients of the initial sample.

TABLE 4.6

Electronic Spectra of $[RuBr_3(NO)(Et_2S)_2] + Et_2S$

(in chloroform) Exposed to Sunlight

Exposure time				
Initially		474 (150)		297 (12,000)
1 minute	554 (500)	501 (600)		293 (12,000)
10 minutes	551 (1,800)	504 (2,000)		284 (15,000)
1 hour	551 (2,000)	504 (2,300)	390(sh) (1,000)	282 (15,000)
2 days	546 (1,800)	499 (2,000)	399(sh) (1,000)	278 (16,000)
4 days		480(sh) (1,000)	377 (1,600)	274 (12,000)
10 days		470(sh) (1,000)	374 (2,500)	271 (12,000)
47 days		450(sh) (1,000)	373 (2,500)	272 (12,000)

Values in parentheses relate the observed peak heights to the molar extinction coefficients of the initial sample.

FIGURE 4.3 Position of u.v.-visible absorptions of $RuBr_3(NO)(Et_2S)_2$ after exposure to sunlight.

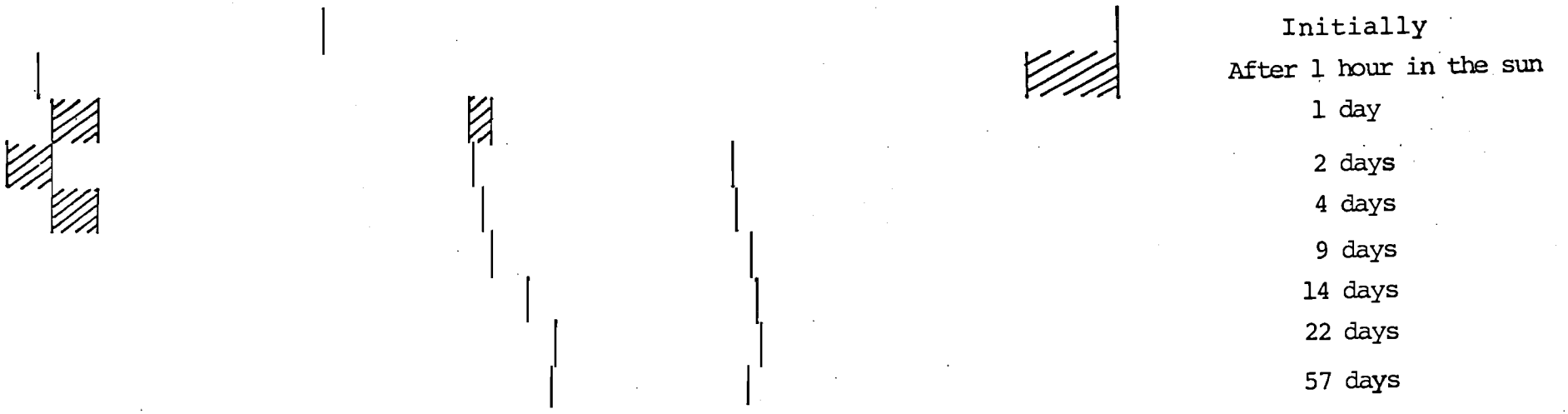

FIGURE 4.4 Position of u.v.-visible absorptions of $RuBr_3(NO)(Et_2S)_2 + Et_2S$ after exposure to sunlight.

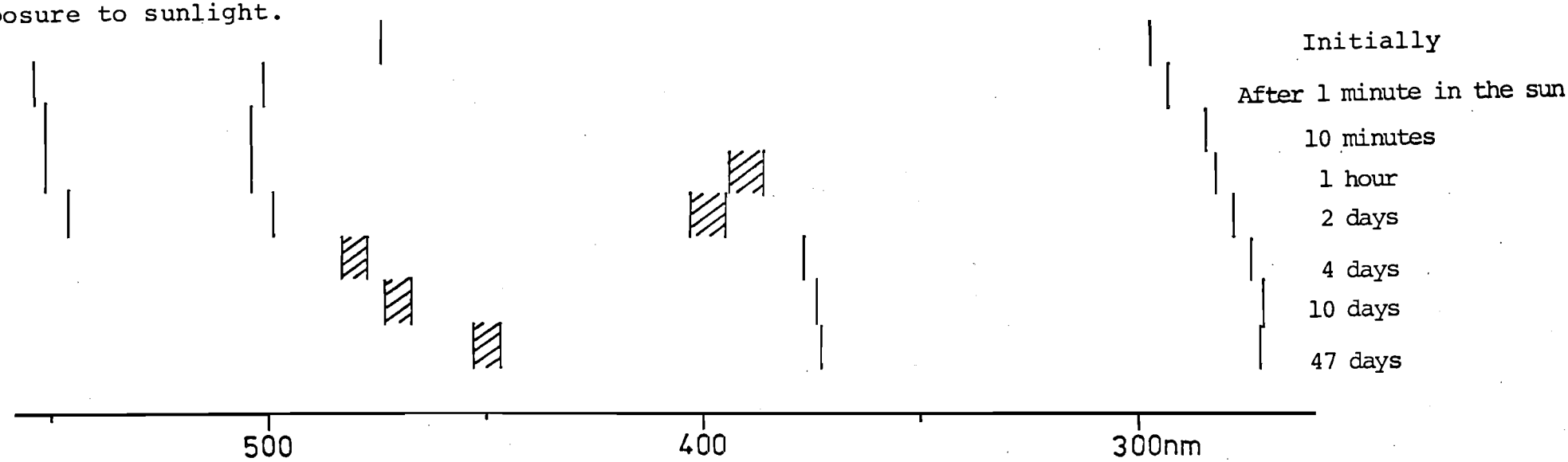

sulphide molecules leading to an intermediate complex $[RuBr_3(NO)(Et_2SO)(Et_2S)]$ which can be isolated. However, if not isolated this complex disappears from solution and the dimer $[RuBr_3(NO)(Et_2SO)]_2$ is produced. The steps are illustrated in Figure 4.5.

(a) Photo-oxidation and rearrangement step

The oxidation of the sulphide by molecular oxygen takes place with no spectroscopic evidence for an accumulation of free thioether in solution. This is confirmed by the fact that the photo-oxidation process is accelerated by the addition of Et_2S to the $[RuBr_3(NO)(Et_2S)_2]$ solution. Hence the dissociation of the sulphide ligand, if it occurs, is not likely to be the slow step in the reaction.

If the oxidation step does not proceed through a dissociation mechanism then the diethyl sulphide complex may form an activated complex by absorbing the visible radiation. This complex then undergoes oxidation through a free radical chain mechanism of the following type (showing only the involvement of the sulphur containing groups) where the sulphide ligand would retain some bonding interaction with the ruthenium atom until the chain termination steps:

$$R_2S \xrightarrow{h\nu} R_2S^* \qquad \text{chain initiation}$$

$$R_2S^* + O_2 \longrightarrow R_2S.O_2^* \qquad \left.\begin{array}{l}\\ \text{chain}\\ \text{propagation}\end{array}\right\}$$

$$R_2S.O_2^* + R_2S \longrightarrow R_2S.O_2 + R_2S^*$$

$$R_2S.O_2 + R_2S \longrightarrow R_2S.O + R_2S.O \qquad \left.\begin{array}{l}\\ \text{chain}\\ \text{termination}\end{array}\right\}$$

$$R_2S.O_2 + R_2S.O \longrightarrow \text{secondary decomposition products}$$

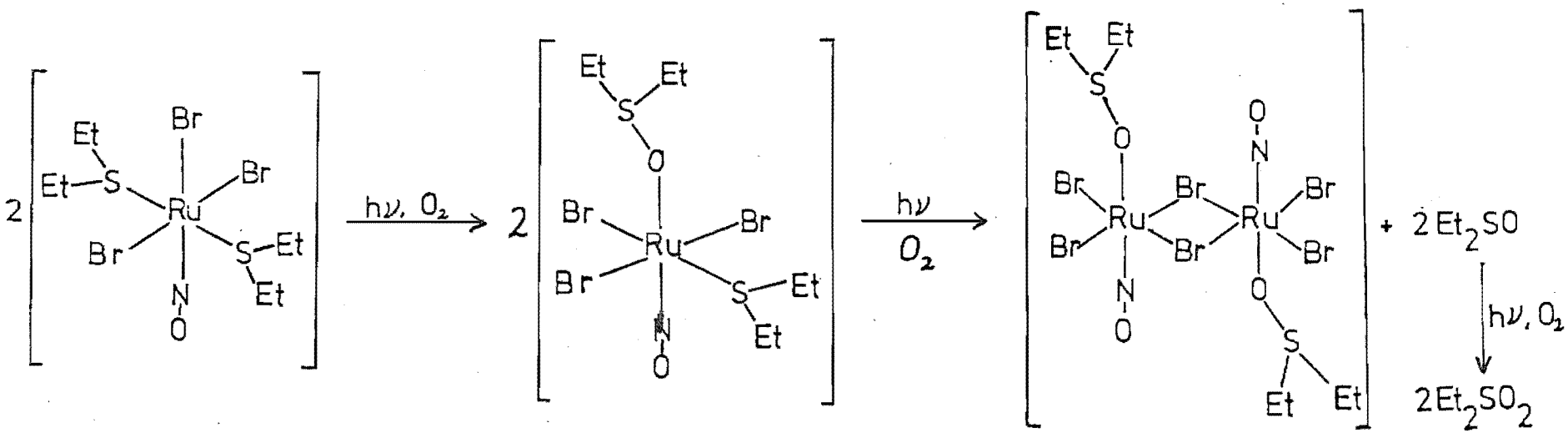

FIGURE 4.5

Proposed photo-oxidation reaction scheme.

With the above mechanism, the addition of diethyl sulphide to the reaction system would assist both the chain propagation and termination steps.

A possible step where the ethanol also participates (through hydrogen bonding) could be in the first chain termination step, as illustrated below.

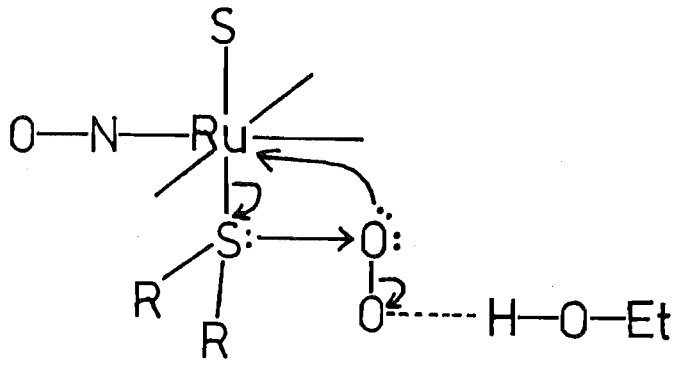

The reactive oxygen species that remains would then be available to oxidise another sulphide group. This step would be accelerated by the availability of diethyl sulphide, as was observed.

However, the formation of the $[RuBr_3(NO)(Et_2SO)(Et_2S)]$ intermediate of the photo-oxidation reaction also involves a rearrangement of the sulphur containing ligands about the ruthenium atom from <u>trans</u> to <u>cis</u>. This type of photo-isomerisation process of transition metal complexes is reported to occur in other systems.[124-127] If such a step, as is illustrated above, occurred then both the rearrangement around the ruthenium atom and the oxidation of the bonded sulphide ligand may proceed at the same time.

The solid state and solution infrared spectra measured of samples throughout the photo-oxidation process indicated that there was no change in the position of the ν(N-O) absorption. Therefore it seems unlikely that the nitrosyl ligand is involved directly in the oxidation step.

Attempts to isolate a possible dioxygen complex of ruthenium to investigate if the ruthenium atom was directly involved in promoting the oxidation of the sulphide ligand, as occurred with $[O_2.IrCl(CO)(PPh_3)_2]$,[119] were not successful.

(b) Dimerisation step

The final step in the reaction scheme (Figure 4.5) probably involves the loss of the unoxidised sulphide ligand from $[RuBr_3(NO)(Et_2SO)(Et_2S)]$ giving a five coordinate intermediate which undergoes dimerisation through bridging bromine atoms to form $[RuBr_3(NO)(Et_2SO)]_2$. The sulphide ligand is either oxidised to a sulphoxide while in solution or oxidised before dissociation from the ruthenium complex.

4.3 PHOTOCHEMICAL REACTIONS OF OTHER RUTHENIUM CHALCOGEN COMPLEXES

The colour change which accompanied the photo-oxidation of the diethyl sulphide ligand of $[RuBr_3(NO)(Et_2S)_2]$, was also observed to occur for other ruthenium complexes containing the ligands Me_2S, MeSPh, Pr_2S, EtSPh, Bz_2S, Et_2Se and EtSePh. Solutions of the bromo complexes undergo a pale yellow-brown to dark red colour change when irradiated with sunlight, while solutions of the chloro complexes changed

to a brown colour. The infrared spectra of the residues obtained when the solutions were allowed to evaporate under a stream of air, contain an absorption in the 900-1100 cm^{-1} region typical of ν(S-O) for a sulphoxide bonded through oxygen to a metal ion.

In the case of the dimethyl sulphide complex $[RuBr_3(NO)(Me_2S)_2]$ the product obtained after 2-3 months irradiation was a monomeric bis sulphoxide complex in which one sulphoxide ligand was bonded to the ruthenium through the sulphur atom and in the other through the oxygen atom. The evidence for this comes from the infrared spectrum which had two ν(S-O) absorptions, one at 1120 cm^{-1} (sulphur bonded) and one at 917 cm^{-1} (oxygen bonded). This spectrum (Figure 4.6) was similar to that obtained for the $[RuBr_3(NO)(Me_2SO)_2]$ complex discussed in Chapter 2. Some smaller crystals were also produced in the reaction and these had an infrared spectrum with only one ν(S-O) absorption, at 920 cm^{-1} (Figure 4.6). It could be that this is a dimeric dimethyl sulphoxide complex.

The ^1H n.m.r. spectra of the solutions of $[RuBr_3(NO)(Me_2S)_2]$ exposed to sunlight indicate that the methyl resonance at δ = 2.78 ppm loses intensity as the sample is irradiated, and two new signals at δ = 2.61 and 2.89 ppm appear. These (as in the same way for the diethyl sulphide system) presumably correspond to the formation of an intermediate $[RuBr_3(NO)(Me_2SO)(Me_2S)]$.

4.4 EXPERIMENTAL

4.4.1 Photo-oxidation Reaction

Ethanol free chloroform was prepared by washing

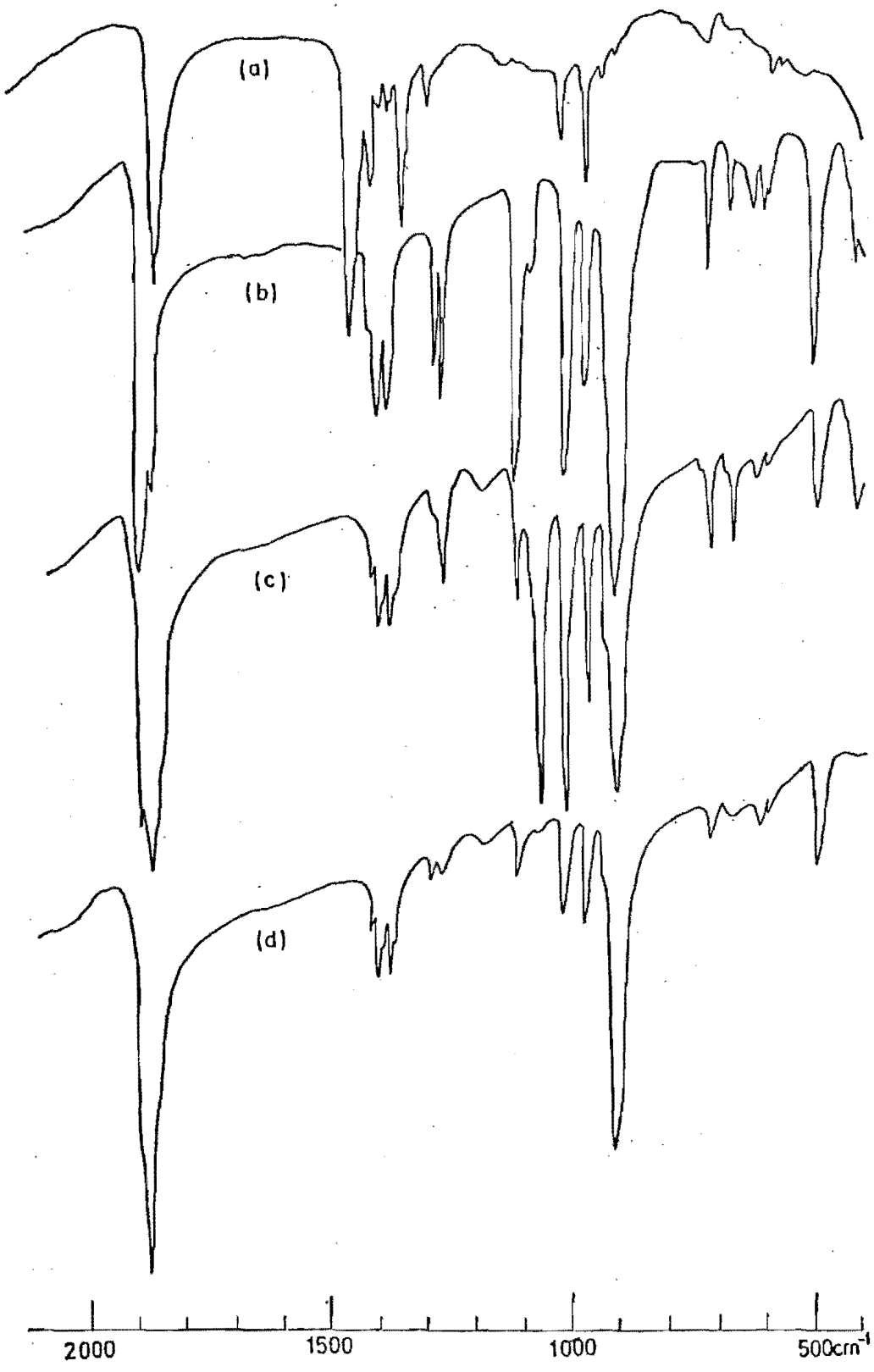

FIGURE 4.6

High frequency infrared spectra observed for
(a) $[RuBr_3(NO)(Me_2S)_2]$, (b) $[RuBr_3(NO)(Me_2SO)_2]$,
(c) $[RuBr_3(NO)(Me_2SO)_2]$ (+$[RuBr_3(NO)(Me_2SO)(Me_2S)]$?)
from photo-oxidation reaction and (d) $[RuBr_3(NO)(Me_2SO)]_2$?

AnalaR chloroform with concentrated H_2SO_4, then washing repeatedly with water. The chloroform was then dried over calcium chloride. Oxygen free chloroform was prepared by distilling the chloroform over phosphorus pentoxide under a nitrogen atmosphere and storing the solvent under nitrogen.

The solution of $[RuBr_3(NO)(Et_2S)_2]$ in oxygen free chloroform was prepared in a dry box under nitrogen, the sample was then exposed in a sealed glass container to sunlight passing through a window.

4.4.2 Preparations

(a) Diethyl sulphoxide and diethyl sulphone

Diethyl sulphoxide may be prepared by oxidising diethyl sulphide with a variety of oxidising agents, however, the sulphoxide readily undergoes further oxidation to diethyl sulphone, Et_2SO_2.

Diethyl sulphide (10 ml) was oxidised with periodate[138] to give diethyl sulphoxide (yield approximately 5 ml). The sulphoxide (1 ml) was added to 5-10 ml an ethanolic '$RuBr_3(NO)$' solution (in an attempt to prepare a diethyl sulphoxide complex of ruthenium) and heated under reflux for $^3/_4$ hour. The solvent was evaporated in a stream of air and the residue recrystallised from ethanol. The resulting light brown crystalline product analysed as slightly impure diethyl sulphone, (Found C = 36.4%, H = 7.6%; Calculated for $C_4H_{10}SO_2$ C = 39.4%, H = 8.2%). The melting point (71-72°C compared with 73°C reported[139]) and ^1H n.m.r. spectrum agreed with those for diethyl sulphone.[136]

Oxidation of diethyl sulphide (0.2 mole) with n-bromo-succinimide (0.2 mole) gave 5 ml of diethyl sulphoxide.[131]

(b) Tribromo(diethyl sulphoxide)(diethyl sulphide) nitrosylruthenium, $[RuBr_3(NO)(Et_2SO)(Et_2S)]$

When diethyl sulphoxide (1 ml, from the second preparative method above) was heated under reflux with '$RuBr_3(NO)$' (prepared using 1.0 g of hydrated $RuBr_3$ per 100 ml ethanol) gave a precipitate after removal of some of the solvent *in vacuo*. The product was a mixed sulphide, sulphoxide complex of ruthenium, as determined from an X-ray crystal structure analysis. The C and H analyses were not sufficiently accurate to enable the product to be identified as either a bis sulphoxide complex or a sulphide - sulphoxide complex; found C = 17.5%, H = 3.6%, compared with calculated for $C_8H_{20}Br_3NO_3S_2Ru$ C = 16.5%, H = 3.5% and calculated for $C_8H_{20}Br_3NO_2S_2Ru$ C = 16.9%, H = 3.6%, respectively.

(c) Separation of the mixed $[RuBr_3(NO)(Et_2S)_2]$, $[RuBr_3(NO)(Et_2SO)(Et_2S)]$ product obtained from the photo-oxidation reaction

A $[RuBr_3(NO)(Et_2S)_2]$ solution (initially approximately 0.05M) was allowed to evaporate slowly, exposed to daylight, over a period of six weeks. The residue obtained was recrystallised from ethanol and a product obtained that was identified by various spectroscopic techniques as a mixture of $[RuBr_3(NO)(Et_2S)_2]$ and $[RuBr_3(NO)(Et_2SO)(Et_2S)]$.

These two complexes were separated using an activated alumina (Fluka type H) column. Eluting with benzene initially caused the complexes to separate into two bands. Chloroform was then used to elute the two layers from the column. The solvents used were of reagent grade.

X-ray powder photographs as well as n.m.r. and infrared spectra confirmed the first sample from the column was $[RuBr_3(NO)(Et_2S)_2]$ and the second was $[RuBr_3(NO)(Et_2SO)(Et_2S)]$.

(d) Di-μ-bromo-bis[dibromo(diethyl sulphoxide)-nitrosylruthenium(II)]

A chloroform solution of $[RuBr_3(NO)(Et_2S)_2]$ (10^{-1} - 10^{-2}M) was exposed to sunlight passing through a window, over a period of one to two months. The mother liquor was poured off and dark red-brown crystals of $[RuBr_3(NO)(Et_2SO)]_2$ were obtained. The product was fully identified by a single crystal X-ray analysis (see Chapter 5).

(e) Attempts to prepare a ruthenium dioxygen complex

Solutions of $[RuBr_3(NO)(Et_2S)_2]$ were oxygenated with oxygen gas while being exposed to sunlight and also while in the dark. In neither case did the infrared spectrum indicate the formation of a ruthenium dioxygen species.

CHAPTER 5

THE CRYSTAL AND MOLECULAR STRUCTURE OF DI-μ-BROMO-BIS[DIBROMO(DIETHYL SULPHOXIDE)-NITROSYLRUTHENIUM(II)]

This chapter gives the details of the single crystal X-ray structural analysis of the dimeric complex $[RuBr_3(NO)(Et_2SO)]_2$. The analysis was one of two undertaken to elucidate the nature of the ruthenium complexes formed in a photochemical reaction. This dimeric species is a final product of the photochemical reaction.

The experimental procedures will be covered in detail in this chapter and referred to in the two further structural analyses reported in Chapters 6 and 7.

5.1 EXPERIMENTAL DETAILS

5.1.1 Preparation

A chloroform solution of $[RuBr_3(NO)(Et_2S)_2]$ was exposed to sunlight and a crystalline product was deposited after one to two months, as outlined in section 4.4.2(d). The mother liquor was poured off and the crystals dried in vacuo. Dark red-brown crystals, of empirical formula $RuBr_3(NO)(Et_2SO)$ were obtained.

5.1.2 Crystal Data

The cell parameters and crystallographic space group of the crystals were determined on the basis of precession photography using CuKα X-radiation. The lack

of systematic absences and symmetry axes in these photographs is consistent with the crystals belonging to the triclinic system. The success of this analysis has confirmed that the correct space group is $P\bar{1}$. Approximate values for the unit cell constants were measured from the precession photographs.

The density of the ruthenium complex (2.56(±0.03) g. cm^{-3}), obtained by the flotation method using an aqueous zinc bromide solution, is in good agreement with the calculated density (2.59 g. cm^{-3}) for two empirical formula units in the unit cell. Thus the one dimeric molecule found has a crystallographic centre of symmetry imposed on it in space group $P\bar{1}$.

A single crystal was mounted in a random orientation on a glass fibre attached to a goniometer head. After indexing two reflections on precession photographs the crystal was transferred to the Hilger and Watts computer controlled four-circle diffractometer and these indexed reflections were located.

The unit cell dimensions listed in Table 5.1 were obtained from a least-squares refinement of the setting angles of twelve reflections accurately centred in the 5 mm diameter circular receiving aperture of a diffracted beam collimator set 230 mm from the crystal. The parameters were considered to be sufficiently accurately determined when the observed and calculated values for the setting angles of the twelve reflections agreed to within 0.03^{o}. The radiation used was zirconium filtered molybdenum X-radiation with a mean wavelength of 0.7107 Å.

By convention[140] the triclinic unit cell is chosen such that the angles α, β and γ are all greater than 90°. However, the unconventional setting as listed in Table 5.1 was used in this data collection, and can be related to the conventional reduced cell of the dimensions shown in Table 5.1, by the matrix

$$\begin{matrix} 1 & 0 & 0 \\ 0 & -1 & 0 \\ 0 & 1 & 1. \end{matrix}$$

5.1.3 Collection of Intensity Data

The crystal selected for data collection was a rectangular prism, of dimensions 0.13 x 0.33 x 0.09 mm^3. Its suitability for intensity measurement was examined by means of open-counter ω-scans at a take off angle of 3°. Under these conditions a peak width at half height not exceeding 0.25°, for strong, low angle reflections, was judged to be very good.[141] For this crystal, symmetric peak profiles with typical scan widths of 0.12° were observed.

The θ-2θ scan technique was used to collect the intensities of all the independent reflections in that positive h hemisphere of reciprocal space for which $0 < 2\theta < 50^{\circ}$. A symmetric scan range of 1.20° in 2θ, centred on the calculated peak position, was composed of 60 steps each of one second duration. Stationary-crystal, stationary-counter background counts of 15 seconds were measured at each end of the scan range. Calibrated attenuators were necessary to bring nine strong reflections within the linear response range of the scintillation counter

TABLE 5.1

Crystal Data

	Value for the unit cell used	Dimensions of the reduced cell
Compound	$[RuBr_3(NO)(Et_2SO)]_2$	
Formula weight	476.98	
a/Å	8.042 (1)	8.04
b/Å	11.020 (2)	11.02
c/Å	7.324 (1)	11.57
α/deg	104.83 (1)	142.26
β/deg	102.31 (1)	96.36
γ/deg	88.54 (1)	91.46
V/Å^3	612.75	
d_{measd}/g. cm^{-3}	2.56	
d_{calcd}/g. cm^{-3}	2.59	

when rates exceeded 8000 counts/second. The intensities of three strong reflections were monitored at intervals of every 50 reflections and by the end of the data collection had dropped to 83% of their original values. These observations were used to place all the intensities on the same relative scale.

5.1.4 Reduction of Intensity Data

The integrated intensity measured for a reflection was given[142] by

$$I = c - 0.5(t_c/t_b)(B_1+B_2)$$

where c is the scan count obtained in time t_c; B_1 and B_2 are the background counts, each obtained in time t_b. The standard deviation for each measured intensity was

$$\sigma(I) = [c + 0.25(t_c/t_b)^2(B_1+B_2)+(pI)^2]^{\frac{1}{2}}$$

and p was initially given the value of 0.05 (this was changed to 0.065 to render $\Sigma w|F_o-F_c|^2$ independent of $|F_o|$ and $(\sin\theta)/\lambda$ at the end of the structure refinement). The p factor is included to avoid overweighting the more intense reflections.[143] Lorentz and polarisation corrections[140] were applied to I and $\sigma(I)$ to obtain values of F_o^2 and $\sigma(F_o^2)$, where F_o is the observed structure factor.

The data set consisted of 2165 unique reflections of which 1337 had $F_o^2 \geqslant 3\sigma(F_o^2)$. Since the linear absorption coefficient for MoKα X-radiation was significant at 117.49 cm^{-1}, absorption corrections were applied using a Gaussian integration (with 4^3 grid points) technique.[144] The transmission factors ranged from 0.18 to 0.40.

5.2 STRUCTURE SOLUTION AND REFINEMENT [145]

A three-dimensional Patterson synthesis was carefully analysed since the exact composition of the compound was not known. The Patterson function shows maxima at positions u v w corresponding to interatomic vectors between atoms in the unit cell at x_1,y_1,z_1 and x_2,y_2,z_2 such that

$$u = x_1 - x_2$$

$$v = y_1 - y_2$$

$$w = z_1 - z_2$$

Although, from the Patterson method, the intramolecular vectors for the heavy atoms (i.e. Ru and Br) were able to be identified, the absolute location of these atoms within the unit cell was not obvious.

Analysis using the vector superposition technique,[140] where the origin of one Patterson map is translated to a vector position in the other map, was used in order to determine the atomic positions. The dominant Patterson peak at 0.26, 0.28, 0.07 (in hindsight, the 2x, 2y, 2z peak for Ru) was the vector position chosen to coincide with the origin of the second duplicate map. As a result of this superposition process one should be able in principle, to obtain the structure, or at least part of it, by selecting only those peaks which superimpose on the two maps. The true origin for the superimposing maps was taken to be the midpoint of the translation vector. Figure 5.1 is a simple illustration of this process taken from Stout and Jensen.[140]

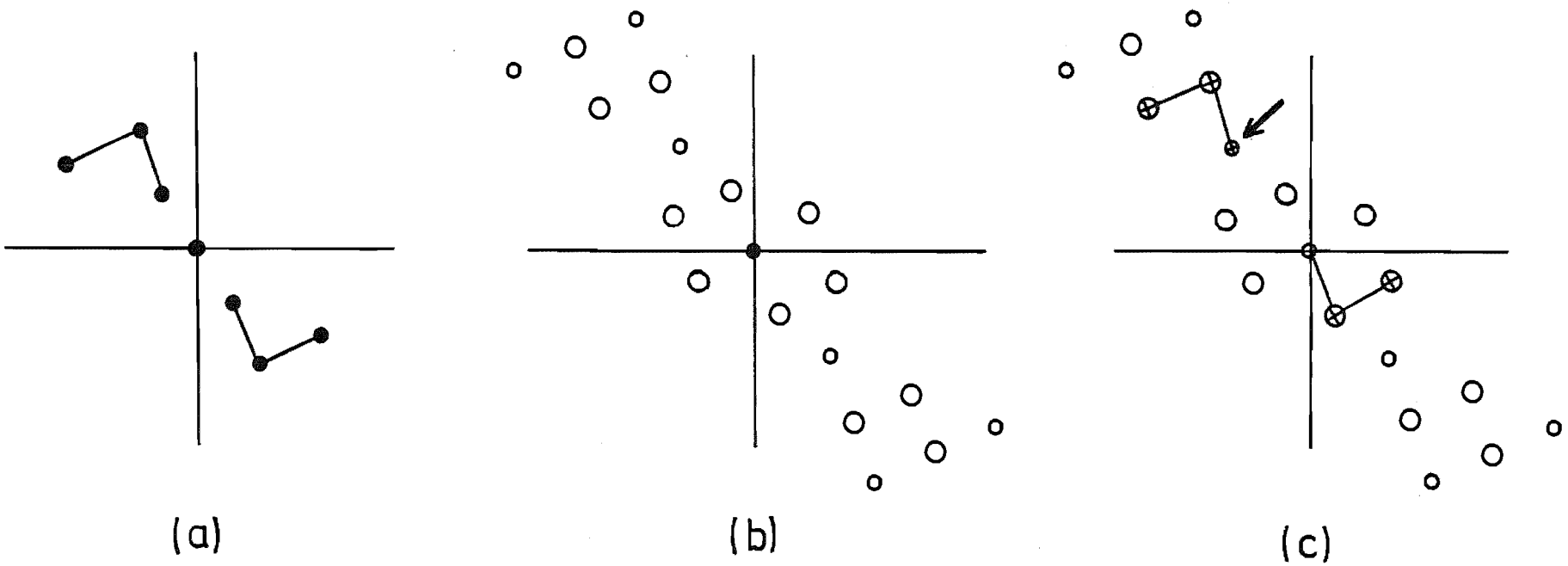

Vector Superposition Technique. FIGURE 5.1

(a) Actual atom positions in a centrosymmetric case.

(b) Patterson map obtained for these atomic positions.

(c) Superimposing a duplicate Patterson map but with its origin shifted to the position indicated by an arrow. Coincidences between the two overlapping maps are indicated by X and are identical with the set shown in (a). The true origin becomes the midpoint of the shift of one map relative to the other.

The positions of the ruthenium and three bromine atoms as well as the nitrosyl N atom, and the sulphur and oxygen atoms of the sulphoxide ligand were determined using the superposition method. At this point it became clear that the complex was probably a centrosymmetric dimer.

To evaluate whether the atomic positions found were correct or not a full-matrix least-square refinement[145] was begun. The least-squares method involved the minimizing of the weighted sum of the squares of the differences between the observed (F_o) and calculated (F_c) structure factor amplitudes,

$$\Sigma w(|F_o|-|F_c|)^2,$$

where the weights w were taken as

$$4F_o^2/\sigma^2(F_o^2).$$

The conventional R factors which measure the agreement between the observed structure factors and those calculated for a particular set of atomic positions are defined as

$$R_1 = \Sigma||F_o|-|F_c||/\Sigma|F_o|$$

and $$R_2 = [\Sigma w(|F_o|-|F_c|)^2/\Sigma wF_o^2]^{\frac{1}{2}}.$$

Using those data for which $F_o^2 \geqslant 3\sigma(F_o^2)$ the agreement factors, after 2 cycles of least-squares refinement, were 0.243 and 0.325, respectively, when including only the ruthenium and bromine atom positions and isotropic thermal parameters. The rest of the atoms in the structure were located from a difference Fourier synthesis. In this method the residual electron density is found using the differences between the observed and calculated structure

factors as well as the phase angle computed for the current model. This may be expressed as

$$\Delta\rho(x,y,z) = \frac{1}{v}\sum_{h}\sum_{k}\sum_{l}(|F_o|-|F_c|)\exp(i\alpha_c)\exp(-2\pi i(hx + ky + lz)),$$

where v is the unit cell volume, α_c is the phase angle computed from the trial structure and $\Delta\rho(x,y,z)$ is the electron density at point x,y,z. The electron density peak positions and heights are calculated in three dimensions over a unique asymmetric unit of the unit cell, using program FOURIER.[145] The peak positions may yield possible coordinates for atoms which are then added to the trial model, and further least-squares refinement will determine their correctness.

In order to calculate the structure factor for the assumed arrangement of atoms, the X-ray scattering power for each kind of atom involved must be known. The atomic scattering factors used here were those reported by Cromer and Mann[146] for neutral atoms. The anomalous dispersion parts of the scattering factor were included for the Ru, Br and S atoms using the $\Delta f'$ and $\Delta f''$ values reported by Cromer.[147]

Using the positions of all the non-hydrogen atoms obtained from the difference Fourier synthesis and after 2 cycles of refinement, the agreement factors reduced to 0.097 and 0.128 respectively, with isotropic temperature factors describing the thermal motion of the atoms. The difference Fourier map of this atomic arrangement showed regions of high electron density (up to 5 $e/\text{Å}^3$) around the heavy atoms. Accordingly all atoms were assigned anisotropic thermal vibration parameters in the final cycles of least-squares refinement. These refinements, using the 1337

reflections for which $F_o^2 \geq 3\sigma(F_o^2)$, converged to give agreement factors of $R_1 = 0.047$ and $R_2 = 0.058$. No attempt was made to locate the hydrogen atoms.

The estimated standard deviation of an observation of unit weight was 1.34 electrons and the highest peak in a final difference Fourier synthesis was one-fourth of the height of a typical carbon atom found during this analysis. Structure factor calculations for the 828 reflections having $F_o^2 < 3\sigma(F_o^2)$ showed no large discrepancies between $|F_c|$ and $|F_o|$. There was no evidence of secondary extinction amongst the intense low angle reflections. Analyses of average values of the minimised function showed little dependence on $|F_o|$ and $\sin\theta/\lambda$ after the 'p' factor was increased to 0.065. Thus the weighting scheme used was judged satisfactory.

The final positional and vibrational parameters are presented in Table 5.2 along with their estimated standard deviations as obtained from the inverse matrix in the course of the least-squares calculations. Table 5.3 contains the root-mean-square amplitudes of vibration along the principal axes of the thermal ellipsoids for those atoms refined with anisotropic thermal parameters. Listings of the final values of $|F_o|$ and $|F_c|$ (in electrons) for the 1337 reflections used in the refinements are given in Appendix C.

5.3 DISCUSSION

5.3.1 Description of the Crystal Structure

The dimeric complex $[RuBr_3(NO)(Et_2SO)]_2$ crystallises as well separated molecules, one of them is illustrated in

TABLE 5.2

Final Positional[a] and Thermal[b] Parameters for $[RuBr_3(NO)(Et_2SO)]_2$

	x	y	z	U_{11}	U_{22}	U_{33}	U_{12}	U_{13}	U_{23}
Ru	0.1382(1)	0.1387(1)	0.0407(1)	0.0314(6)	0.0277(5)	0.0437(6)	0.0032(4)	0.0082(5)	0.0107(4)
Br(1)	-0.0306(2)	0.0510(1)	0.2366(2)	0.0605(9)	0.0338(7)	0.0435(8)	0.0022(6)	0.0195(7)	0.0079(6)
Br(2)	0.2147(2)	0.3310(1)	0.3083(2)	0.064(1)	0.0411(8)	0.0621(9)	-0.0049(7)	-0.0038(8)	0.0031(7)
Br(3)	0.2711(2)	0.2242(1)	-0.1774(2)	0.0496(9)	0.0572(9)	0.090(2)	0.0049(7)	0.0342(8)	0.0324(8)
S	-0.1012(4)	0.3465(2)	-0.0977(4)	0.037(2)	0.031(2)	0.044(2)	0.001(2)	0.011(2)	0.012(2)
O(1)	-0.0874(9)	0.2155(6)	-0.058(1)	0.025(5)	0.032(4)	0.047(5)	0.002(4)	0.003(4)	0.011(4)
O(2)	0.434(1)	0.014(1)	0.188(2)	0.057(8)	0.094(8)	0.104(9)	0.028(7)	0.001(7)	0.034(7)
N	0.316(1)	0.0661(9)	0.127(2)	0.038(7)	0.053(7)	0.058(7)	0.007(6)	0.003(6)	0.020(6)
C(11)	-0.177(2)	0.315(1)	-0.359(2)	0.061(9)	0.053(8)	0.047(8)	0.009(7)	0.009(7)	0.019(7)
C(12)	-0.320(2)	0.211(1)	-0.442(2)	0.045(9)	0.10(2)	0.044(9)	-0.011(8)	0.005(7)	-0.001(8)
C(21)	-0.292(2)	0.405(1)	-0.010(2)	0.045(8)	0.043(7)	0.052(8)	0.015(6)	0.021(7)	0.011(6)
C(22)	-0.267(2)	0.422(1)	0.203(2)	0.057(9)	0.09(2)	0.042(9)	0.018(8)	0.024(8)	0.011(8)

[a] x,y, and z are in fractional coordinates. [b] The form of the thermal ellipsoid expression is $\exp[-(\beta_{11}h^2 + \beta_{22}k^2 + \beta_{33}l^2 + 2\beta_{12}hk + 2\beta_{13}hl + 2\beta_{23}kl)]$; $U_{ij} = (\beta_{ij}/2\pi^2)a_i^*a_j^*(\mathring{A})^2$. [c] Numbers in parentheses here and in succeeding tables are the estimated standard deviations in the least significant figure.

TABLE 5.3

Root-Mean-Square Amplitudes of Vibration (Å) for $[RuBr_3(NO)(Et_2SO)]_2$

Atom	Min	Intermed	Max
Ru	0.162(1)	0.178(2)	0.210(1)
Br(1)	0.183(2)	0.197(2)	0.250(2)
Br(2)	0.191(2)	0.239(2)	0.295(2)
Br(3)	0.181(2)	0.228(2)	0.310(2)
S	0.173(4)	0.190(5)	0.212(4)
O(1)	0.15(1)	0.18(1)	0.22(1)
O(2)	0.19(2)	0.33(1)	0.34(1)
N	0.18(2)	0.23(1)	0.25(1)
C(11)	0.20(2)	0.23(2)	0.26(2)
C(21)	0.17(2)	0.23(2)	0.24(2)
C(12)	0.19(2)	0.22(2)	0.33(2)
C(22)	0.17(2)	0.24(2)	0.31(2)

Figure 5.2, which also defines the atom labelling scheme used throughout this chapter. The shortest non-bonding intermolecular contact not involving hydrogen atoms is 3.1 Å between the O(2) atom of one dimeric unit and the same atom of another unit. Selected interatomic distances and bond angles are listed in Tables 5.4 and 5.5, respectively.

The dimeric molecules consist of two octahedrally coordinated ruthenium atoms which are bridged through two bromine atoms. A crystallographic centre of symmetry imposed on the molecule occurs at the centroid of the

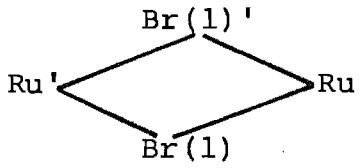

ring. The diethyl sulphoxide and nitrosyl ligands which are coordinated <u>trans</u> to each other on each ruthenium atom, are bonded above and below the Ru_2Br_2 plane, (see Figure 5.2). Although the coordination about the ruthenium atoms is approximately octahedral, the plane containing the terminal bromine atoms Br(2) and Br(3) and the Ru atom makes an angle of 7.8° with the plane Ru, Br(1), Ru', Br(1)'. The terminal bromine atoms are displaced towards the diethyl sulphoxide ligand as is shown in the side-on view of the structure in Figure 5.3.

The Ru-Ru' (3.496(2) Å) and Br(1)-Br(1)' (3.673(2) Å) distances preclude metal-metal bonding between the ruthenium atoms. The nitrosyl group is coordinated in a linear manner to the ruthenium atom. The diethyl sulphoxide ligand is coordinated to ruthenium through the oxygen atom.

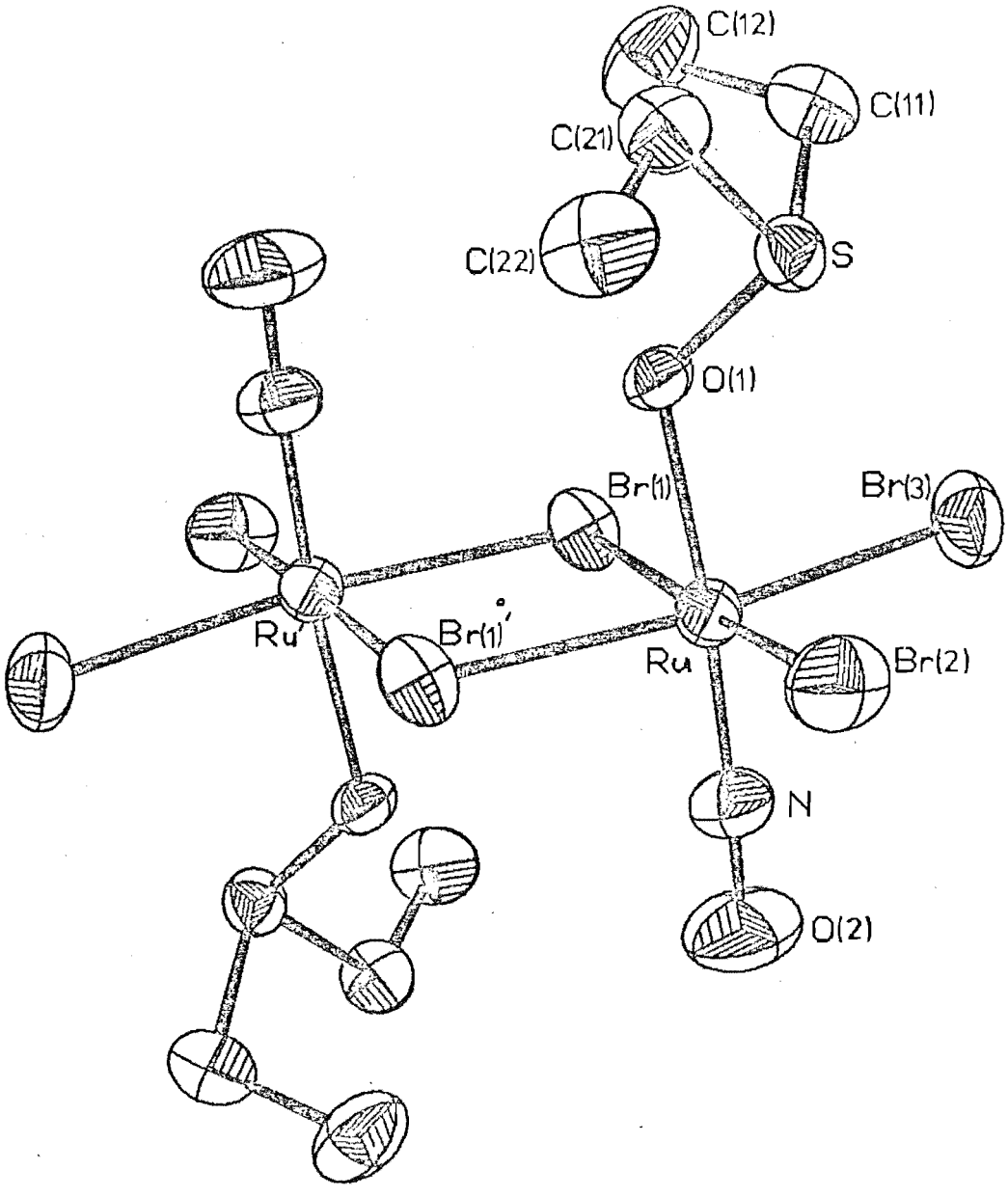

FIGURE 5.2

Diagram of the $[RuBr_3(NO)(Et_2SO)]_2$ molecule. The atom labelling system is illustrated. Thermal ellipsoids are drawn at the 50% probability level. The molecule has an imposed centre of symmetry.

TABLE 5.4

Intramolecular Distances (Å) for $[RuBr_3(NO)(Et_2SO)]_2^-$

Bonded distances

Ru-N	1.71(1)
Ru-O(1)	2.050(7)
Ru-Br(3)	2.476(2)
Ru-Br(2)	2.477(2)
Ru-Br(1)	2.539(2)
S-O(1)	1.541(7)
S-C(11)	1.82(1)
S-C(21)	1.83(1)
N-O(2)	1.16(1)
C(11)-C(12)	1.55(2)
C(21)-C(22)	1.49(2)
Ru-Br(1)'	2.533(2)

Non-bonded distances

Ru-Ru'	3.673(2)
Br(1)-Br(1)'	3.496(2)

TABLE 5.5

Intramolecular angles (deg) for $[RuBr_3(NO)(Et_2SO)]_2$

N-Ru-O(1)	175.3(4)
N-Ru-Br(3)	94.9(4)
N-Ru-Br(2)	91.8(3)
N-Ru-Br(1)	93.4(3)
O(1)-Ru-Br(3)	89.4(2)
O(1)-Ru-Br(2)	90.0(2)
O(1)-Ru-Br(1)	84.7(2)
Br(3)-Ru-Br(2)	92.32(6)
Br(3)-Ru-Br(1)	89.30(6)
Br(2)-Ru-Br(1)	174.46(6)
Br(1)-Ru-Br(1)'	87.18(5)
Ru-Br(1)-Ru'	92.82(5)
O(1)-S-C(11)	104.3(5)
O(1)-S-C(21)	101.9(5)
C(11)-S-C(21)	101.8(6)
S-O(1)-Ru	123.9(4)
O(2)-N-Ru	177.8(11)
C(12)-C(11)-S	113.6(9)
C(22)-C(21)-S	111.6(9)

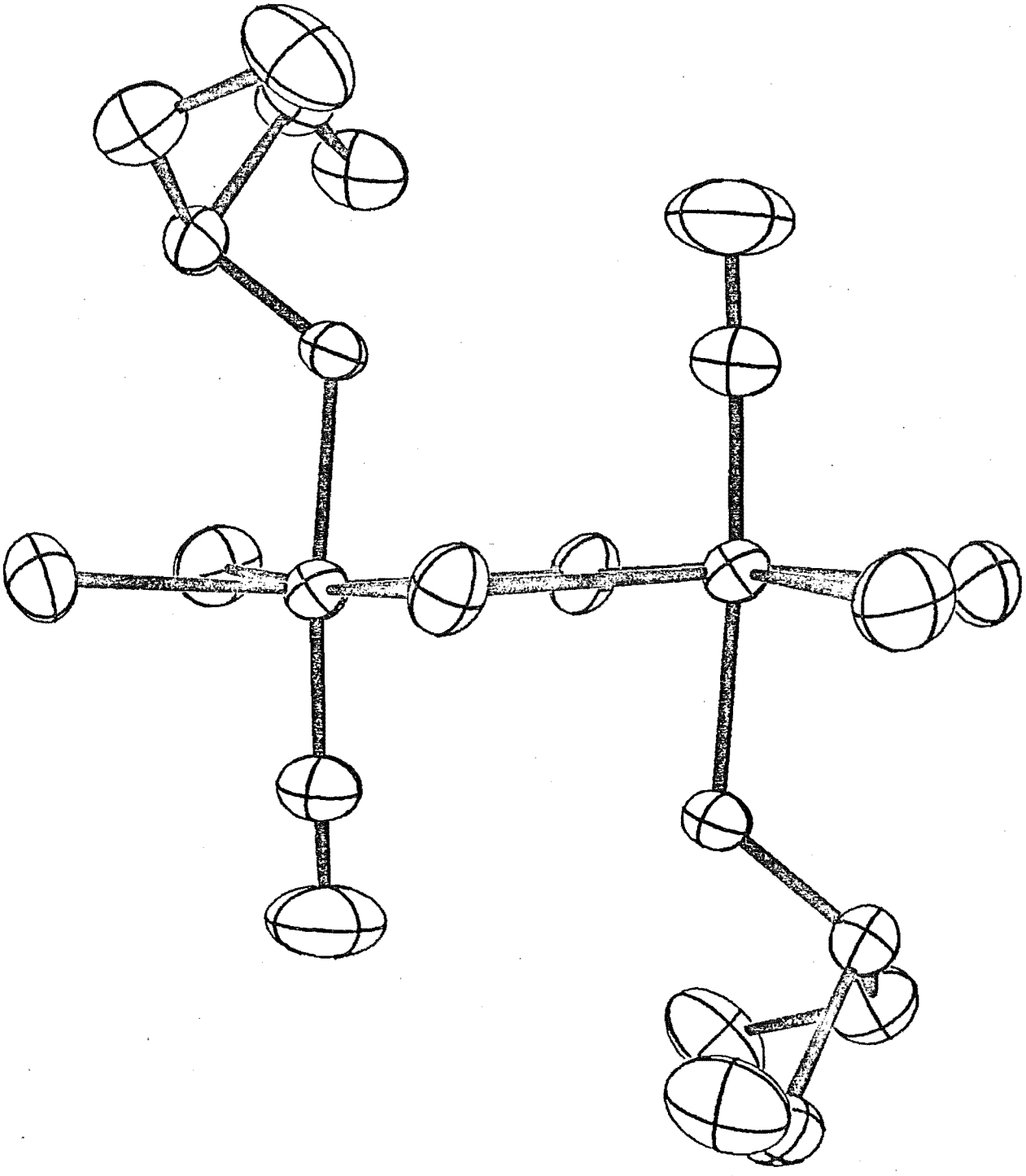

FIGURE 5.3

Side-on view of the $[RuBr_3(NO)(Et_2SO)]_2$ molecule.

5.3.2 Comparison with other Sulphoxide Structures

The bond lengths and angles obtained for the diethyl sulphoxide ligand agree well with those of other sulphoxide structures reported.[67,148-150] The orientation of the sulphoxide ligand is similar to that reported[67,148] and appears to be that expected from a consideration of intramolecular forces. Also the C-C and C-S bond lengths and angles agree with those reported for thioether structures with ethyl sulphide groups.[47,51] The Ru-O(1) bond length of 2.050(7) Å was found to be similar to those in other structures reported with oxygen bonded sulphoxides. For example, the Rh(III)-O[148] and Ru(II)-O[67] bond lengths are 1.999(13) and 2.142(3) Å, respectively.

When a transition metal atom acts as a σ electron acceptor and a π electron donor, as the low spin d^6 Ru(II) atom is able to do, then the possibility of sulphoxide coordination through the sulphur atom is expected to be enhanced.[151] However, in this structure the sulphoxide ligand is coordinated to the Ru(II) atom through the oxygen atom. The mode of coordination in this case may be a consequence of the nitrosyl group <u>trans</u> to the sulphoxide coordination site reducing some of the ruthenium atom's electron density through π back-bonding (see Section 2.1.2).

Steric interactions with neighbouring groups will also prevent the sulphoxide ligand binding through the sulphur atom. From a comparison with other ruthenium sulphoxide complexes it appears that the steric factors are probably the principal reason for bonding through the oxygen atom (see Table 2.4).

The shift in frequency of the strong ν(S-O) absorption in the infrared spectrum is consistent with oxygen being the donor atom of the sulphoxide. The absorption at 921 cm^{-1} is shifted to a lower frequency with respect to that observed[152] for free diethyl sulphoxide at 1030 cm^{-1}. The position of the ν(S-O) vibration has been used as an indicator of the mode of coordination of the sulphoxide ligand in transition metal complexes.[153] Three resonance forms can be thought of as contributors to the electron density distribution within the sulphoxide molecule as shown below.

$R_2S^+ - O^-$ (I) $\qquad$ $R_2S = O$ (II) $\qquad$ $R_2S^- \equiv O^+$ (III)

Configuration (II) is representative of the situation in the free ligand, but when oxygen coordination occurs the electron distribution tends towards configuration (I), and hence a slight weakening of the S-O bond is expected. The weakening in bond strength should be able to be detected as a shift of ν(S-O) to lower energy. Crystal structures of the sulphoxide complexes have confirmed that there is a lengthening of the S-O bond in this situation, although it is still somewhat short of the estimated S-O single bond length of 1.70 Å.[154] For sulphoxide ligands coordinated through oxygen the reported average S-O bond lengths and ν(S-O) frequencies are listed in Table 5.6.

On the other hand, when coordination takes place through the sulphur atom the electron distribution tends slightly towards that indicated by configuration (III). Therefore the S-O bond length is shortened with respect to free sulphoxide (as listed in Table 5.6), representing an

TABLE 5.6

Mean S-O bond lengths ($\AA$) and ν(S-O) frequencies (cm^{-1})

Compound	S-O	ν(S-O)	Reference
	Oxygen coordinated sulphoxides		
$RuCl_2(DMSO)_4$	1.557(4)	915	67
$[RuBr_3(NO)(Et_2SO)]_2$	1.541(7)	921	This work
$RuBr_3(NO)(Et_2SO)(Et_2S)$	1.543(8)	924	This work
$[FeCl_2(DMSO)_4]FeCl_4$	1.541(6)	933	150
$RhCl_3(DMSO)_3$	1.56(2)	935	148
$Me_2SnCl_2(DMSO)_2$	1.56(4)	942	156
$[UCl_2(DMSO)_6]UCl_6$	1.52(5)	960	157
$[Sn(Ph)_2NO_3(DMSO)_3]NO_3$	1.55(1)	980	158
trans-$CuCl_2(DMSO)_2$	1.531(4)	987	149
$Nd(NO_3)_3(DMSO)_4$	1.51(2)	1010	159
$La(NO_3)_3(DMSO)_4$	1.51(3)	1010	160
$Yb(NO_3)_3(DMSO)_3$	1.48(3)	1010	161
$[Ag(DMSO)_2ClO_4]_n$	1.509(8)	1020	162
	Free dimethyl sulphoxide		
DMSO (at 5°C)	1.513(5)	1045	163
	Sulphur coordinated sulphoxides		
$[Ru(NH_3)_5(DMSO)](PF_6)_2$	1.527(8)	1049	62
$RuCl_3(DMSO)_3$	1.49(1)	1100	66
$RuCl_2(DMSO)_4$	1.485(5)	1105	67
$Na[Rh(DMSO)_2Cl_4]$	1.47(2)	1113	164
$PdCl_2(DMSO)_2$	1.476(5)	1116	165
$RhCl_3(DMSO)(py)_2$	1.47(1)	1118	166
$RhCl_3(DMSO)_3$	1.43(2)	1138	148
cis-$PtCl_2(DMSO)_2$	1.461(8)	1146	167
cis-$Pd(NO_3)_2(DMSO)_2$	1.463(7)	1147	168

increase in the multiple-bond character of the S-O linkage, but still considerably longer than the 1.39 Å bond length predicted by the covalent radii[155] for a S-O triple bond.

The crystal structure analysis of dimethyl sulphoxide,[163] at 5°C, gave a S-O bond length which was intermediate between the sulphur coordinated and oxygen coordinated bond lengths. Figure 5.4 shows that the ν(S-O) frequency decreases as the S-O bond length increases with the position for the free sulphoxide occurring in the middle of the respective regions.

Hence from the knowledge of the ν(S-O) absorption an indication of the mode of coordination of the sulphoxide to the metal atom and even an estimate of the S-O bond distance can be obtained.

5.3.3 Coordination of the Nitrosyl Group

The nitrosyl ligand is coordinated in a linear manner to ruthenium, the Ru-N-O bond angle being 178(1)°. The bond lengths are close to those reported for other linear nitrosyl ligands in reviews on metal nitrosyl complexes.[56,56,61] The nitrosyl stretching frequency of 1878 cm^{-1} is consistent with the NO^+ type of ligand and the linear grouping found.[10] A detailed explanation of the modes of coordination of the nitrosyl is given in section 2.1.2. The Ru-N distance of 1.71(1) is slightly but not significantly shorter than the corresponding distance in other ruthenium-nitrosyl complexes, such as 1.744(6) Å in $[RuCl_3(NO)(PMePh_2)_2]$,[9] 1.737(7) Å in $[RuCl_3(NO)(PPh_3)_2]$[10] and 1.747(6) Å in $[Ru(NO)Cl_5]^{2-}$.[169] When the Ru-N-O moiety is bent, the Ru-N length is found to be significantly longer,

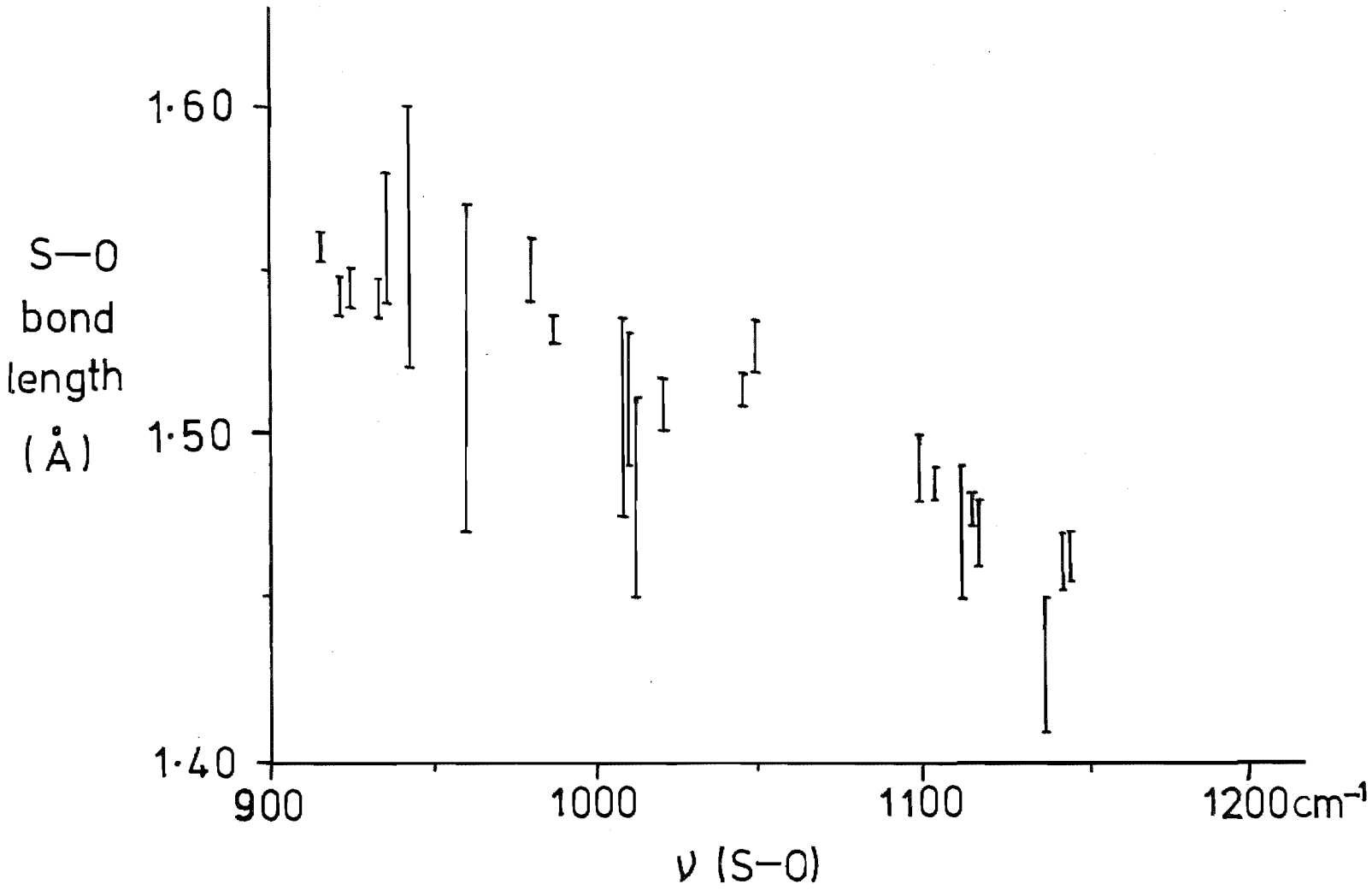

FIGURE 5.4 S-O bond length versus ν(S-O) stretching frequency for the sulphoxide complexes in Table 5.6.

such as 1.85(2) Å for $[RuCl(NO)(PPh_3)_2]^+$.[170]

The short Ru-N distance observed, together with the linear Ru-N-O arrangement, is explained in terms of strong π back-bonding between the nitrosyl ligand the the ruthenium atom, see section 2.1.2. The N-O bond length of 1.16(1) Å is similar to those reported in references 9, 10 and 169 mentioned above, with values of 1.132(6), 1.142(8) and 1.112(7) Å respectively.

CHAPTER 6

THE CRYSTAL AND MOLECULAR STRUCTURE OF TRIBROMO(DIETHYL SULPHOXIDE)(DIETHYL SULPHIDE)-NITROSYLRUTHENIUM(II)

The work described in this Chapter is concerned with the X-ray structure determination of the $[RuBr_3(NO)(Et_2SO)(Et_2S)]$ complex. This complex was obtained from reacting the '$RuBr_3(NO)$' entity with diethyl sulphoxide contaminated with diethyl sulphide. It is believed that the complex is identical to an intermediate product obtained in the photochemical reaction of $[RuBr_3(NO)(Et_2S)_2]$. The evidence for this is outlined in section 4.2.3.

6.1 EXPERIMENTAL DETAILS

6.1.1 Preparation

An ethanolic solution containing the entity '$RuBr_3(NO)$' in the presence of a small excess of diethyl sulphoxide (prepared by the oxidation of diethyl sulphide), was heated under reflux for one hour, as mentioned in section 4.4.2(b). A dark red crystalline product separated, upon cooling, over a period of several days.

6.1.2 Crystal Data

From precession and Weissenberg photographs, it was determined that the crystal belonged to the monoclinic system with extinctions for $h0\ell$, $\ell = 2n+1$, and $0k0$, $k = 2n+1$, which uniquely determine the space group as $P2_1/c$. In a

similar manner to that mentioned in Chapter 5, twelve reflections were used to obtain accurate unit cell dimensions for this crystal. See Table 6.1 for pertinent crystal information and details of the crystal data collection.

The experimental density obtained by the flotation method using an aqueous solution of zinc bromide is in good agreement with the calculated density for four molecules per unit cell.

The crystal displayed acceptable mosaicities for the θ-2θ scan technique and the intensities of all the independent reflections in the h and k positive quadrant of reciprocal space for $0 < 2\theta < 50^{o}$ were collected. Background counts were measured at both ends of the scan range with both the crystal and counter stationary. The intensities of the standard reflections were measured every 50 reflections, and all three remained statistically constant during the entire data collection.

The data set was processed as outlined in Chapter 5, with $\sigma(F_o^2)$ calculated using a value of 0.05 for 'p'. Of the 3197 unique reflections collected only the 1585 reflections with $F_o^2 \geqslant 3\sigma(F_o^2)$ were used in subsequent solution and refinement of the structure. An absorption correction using an analytical method[171] was applied to the data set.

6.2 STRUCTURE REFINEMENT

Interpretation of the Patterson synthesis for this compound resulted in considerable confusion concerning the location of that fragment of the molecule containing the four heavy atoms. Accordingly direct methods were used in

TABLE 6.1

Summary of Crystal, Intensity Collection and Refinement Data.

Compound	$RuBr_3(NO)(Et_2SO)(Et_2S)$
Formula	$C_8H_{20}Br_3NO_2S_2Ru$
Formula weight	567.18
a, Å	13.633(1)
b, Å	8.514(2)
c, Å	16.340(5)
β, deg	106.56(3)
V, $Å^3$	1818
Z	4
Density, g/cm^3	2.07 (calcd);
	2.06(3) (exptl)
Space group	$P2_1/c$
Crystal dimensions, mm^3	0.37 x 0.32 x 0.20
Crystal volume, mm^3	0.0190
Radiation wavelength, Å	λ(Mo K$\bar{\alpha}$) = 0.7107
Crystal mosaicity, deg	0.15
Temperature, °C	25
μ, cm^{-1}	80.44
Transmission factors	0.19 - 0.28
Receiving aperture	5.0 mm diameter,
	230 mm from crystal
Take-off angle, deg	3.0
Scan speed	2.0° in 2θ/min
Scan range	1.60°
Background counting	20 sec
2θ limit, deg	50

Table 6.1 continued.

Final no. of variables	155
Unique data used $(F_o^2 \geqslant 3\sigma(F_o^2))$	1585
Error in observation of unit weight, electrons	1.60
R_1	0.049
R_2	0.058

an attempt to obtain a correct starting model for this moiety.

In the direct methods computer program,[172] the phases of the structure factors are derived directly by means of mathematical relationships.[173] A set of phases for the data are determined and given a figure of merit, which measures the reliability of the phases assigned. An E-map calculated using these phase angles as coefficients for a Fourier synthesis, indicated a model with the atomic positions of a

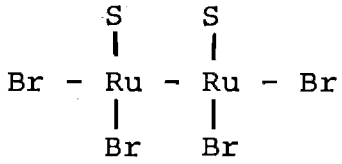

unit. This arrangement did not refine satisfactorily. However, a model taking the mid-point of the Ru-Ru positions and similarly with the other positions, corresponded with 2x,2y,2z peaks in the Patterson map. This doubling effect with a pseudo mirror plane occurring when using direct methods has been observed previously.[174]

The atomic positions of the

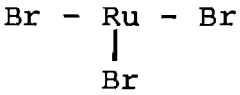

arrangement were refined using least-squares methods to give agreement factors of $R_1 = 0.236$ and $R_2 = 0.332$. A difference Fourier synthesis revealed the positions of all of the rest of the non-hydrogen atoms. Using isotropic temperature factors the $[RuBr_3(NO)(Et_2SO)(Et_2S)]$ model converged with R_1 and R_2 at 0.080 and 0.104 respectively.

In the final refinements, anisotropic thermal parameters were used for all the atoms located. No attempt was made to locate or refine the hydrogen atoms. On the final cycle of least-squares refinement, the agreement factors converged to values of 0.048 and 0.058 for R_1 and R_2, respectively.

The highest peak in a final difference Fourier synthesis was approximately 30% of the height of a carbon atom located earlier during this structure analysis. The source of scattering factors has been detailed in Chapter 5. Observed intensities for reflections at low θ angles were systematically less than their calculated values, hence the data were corrected for secondary extinction[175] using the expression

$$F_o = F_o(W + (1 + W^2)^{\frac{1}{2}})^{\frac{1}{2}}$$

where $W = g.\beta.I_o$, g is the extinction coefficient, β is Zachariasen's angularly dependent function and I_o is the observed intensity.

The parameters obtained from the final cycle of refinement are presented in Table 6.2 along with their estimated standard deviations obtained from the inverse matrix. In Table 6.3 the root-mean-square amplitudes of vibration along the principal axes of the thermal ellipsoids for those atoms refined with anisotropic thermal parameters are presented. A list of the final values of F_o and $|F_c|$ for the 1585 reflections included in the refinement is given in Appendix D.

A structure factor calculation on all 3197 independent reflections collected showed no large discrepancies between the $|F_c|$ and $|F_o|$ values.

TABLE 6.2

Final Positional and Thermal Parameters for $[RuBr_3(NO)(Et_2SO)(Et_2S)]$

	x	y	z	U_{11}	U_{22}	U_{33}	U_{12}	U_{13}	U_{23}
Ru	0.2355(1)	0.1893(1)	0.0849(1)	0.0491(6)	0.0522(7)	0.0495(6)	-0.0089(6)	0.0114(5)	-0.0076(6)
Br(1)	0.0854(1)	0.2061(2)	0.1445(1)	0.060(1)	0.084(1)	0.078(1)	-0.0020(8)	0.0241(8)	0.0062(9)
Br(2)	0.3913(1)	0.1917(2)	0.0331(1)	0.068(1)	0.104(1)	0.084(1)	-0.001(1)	0.0328(9)	-0.006(1)
Br(3)	0.3369(1)	0.0503(2)	0.2167(1)	0.077(1)	0.0587(9)	0.080(1)	0.0065(9)	0.0136(8)	0.0097(9)
S(1)	0.3869(3)	0.4438(4)	0.1987(2)	0.054(2)	0.047(2)	0.073(2)	-0.000(2)	-0.001(2)	-0.005(2)
S(2)	0.1329(3)	0.3560(6)	-0.0262(2)	0.069(3)	0.117(4)	0.062(3)	0.004(3)	0.012(2)	0.010(2)
O(1)	0.2785(6)	0.4033(9)	0.1421(5)	0.053(5)	0.041(5)	0.057(5)	-0.001(4)	-0.000(4)	-0.003(4)
O(2)	0.179(1)	-0.102(1)	0.0043(9)	0.10(1)	0.075(9)	0.15(1)	-0.023(7)	0.027(8)	-0.044(9)
N	0.1981(9)	0.012(2)	0.0350(9)	0.060(8)	0.069(9)	0.10(1)	-0.019(7)	0.023(7)	-0.018(8)
C(111)	0.372(1)	0.462(2)	0.3086(9)	0.11(1)	0.09(1)	0.06(1)	0.01(1)	0.024(9)	-0.02(1)
C(112)	0.285(2)	0.558(2)	0.312(1)	0.19(2)	0.14(2)	0.09(1)	0.08(2)	0.06(1)	0.00(1)
C(121)	0.397(1)	0.647(2)	0.169(1)	0.08(1)	0.038(9)	0.14(2)	-0.010(8)	-0.01(1)	0.01(1)
C(122)	0.419(2)	0.655(2)	0.085(1)	0.16(2)	0.11(1)	0.08(1)	-0.03(1)	0.05(1)	0.01(1)
C(211)	0.029(2)	0.214(3)	-0.089(1)	0.10(2)	0.17(2)	0.10(2)	-0.03(2)	-0.02(1)	0.03(1)
C(212)	-0.050(2)	0.291(3)	-0.144(1)	0.17(2)	0.18(3)	0.10(2)	-0.04(2)	-0.01(2)	0.02(2)
C(221)	0.194(1)	0.403(2)	-0.1090(9)	0.12(1)	0.09(1)	0.06(1)	0.03(1)	0.04(1)	0.025(9)
C(222)	0.163(2)	0.565(2)	-0.143(1)	0.18(2)	0.09(1)	0.12(2)	0.03(1)	0.10(2)	0.04(1)

TABLE 6.3

Root-Mean-Square Amplitudes of Vibration (Å) for $[RuBr_3(NO)(Et_2SO)(Et_2S)]$

Atom	Min.	Intermed.	Max.
Ru	0.198(2)	0.230(2)	0.246(2)
Br(1)	0.236(2)	0.274(2)	0.297(2)
Br(2)	0.240(2)	0.293(2)	0.325(2)
Br(3)	0.231(2)	0.277(2)	0.302(2)
S(1)	0.211(5)	0.221(5)	0.305(4)
S(2)	0.241(5)	0.277(5)	0.346(5)
O(1)	0.20(1)	0.21(1)	0.28(1)
O(2)	0.22(2)	0.33(2)	0.42(2)
N	0.21(2)	0.28(2)	0.33(2)
C(111)	0.21(2)	0.32(2)	0.35(2)
C(112)	0.24(3)	0.32(3)	0.50(3)
C(121)	0.19(2)	0.26(2)	0.42(2)
C(122)	0.24(2)	0.32(2)	0.42(2)
C(211)	0.25(2)	0.35(3)	0.46(3)
C(212)	0.30(3)	0.37(3)	0.50(3)
C(221)	0.21(2)	0.27(2)	0.38(2)
C(222)	0.24(2)	0.30(2)	0.46(2)

6.3 DESCRIPTION OF THE STRUCTURE AND DISCUSSION

The crystal structure described by the unit cell constants, the symmetry of the space group, and the parameters of Table 6.2 is made up from the packing of well separated molecules of $[RuBr_3(NO)(Et_2SO)(Et_2S)]$. There were no intermolecular contacts (excluding hydrogen atoms) within 3.5 Å.

The coordination about the ruthenium atom is essentially octahedral with the three bromine ligands situated in a meridional configuration, and the sulphide and sulphoxide ligands placed in a *cis* arrangement. The linear nitrosyl ligand is *trans* to the diethyl sulphoxide group which is coordinated through its oxygen atom. Figure 6.1 is a perspective drawing of a molecule of the complex, which also defines the atom numbering scheme used throughout this thesis. All important intramolecular distances and angles are tabulated in Tables 6.4 and 6.5, respectively. A stereoscopic drawing showing the packing of molecules with respect to one unit cell, is shown in Figure 6.2.

6.3.1 Nitrosyl Ligand

The nitrosyl ligand of the $[RuBr_3(NO)(Et_2SO)(Et_2S)]$ complex is coordinated in an essentially linear manner to the ruthenium atom with a bond angle at nitrogen of 176.5(14)°. The Ru-N bond length of 1.72(1) Å agrees well that found for the dimeric $[RuBr_3(NO)(Et_2SO)]_2$ complex reported in Chapter 5. The N-O distance of 1.09(1) Å is somewhat shorter than the 1.16(1) Å value obtained for the

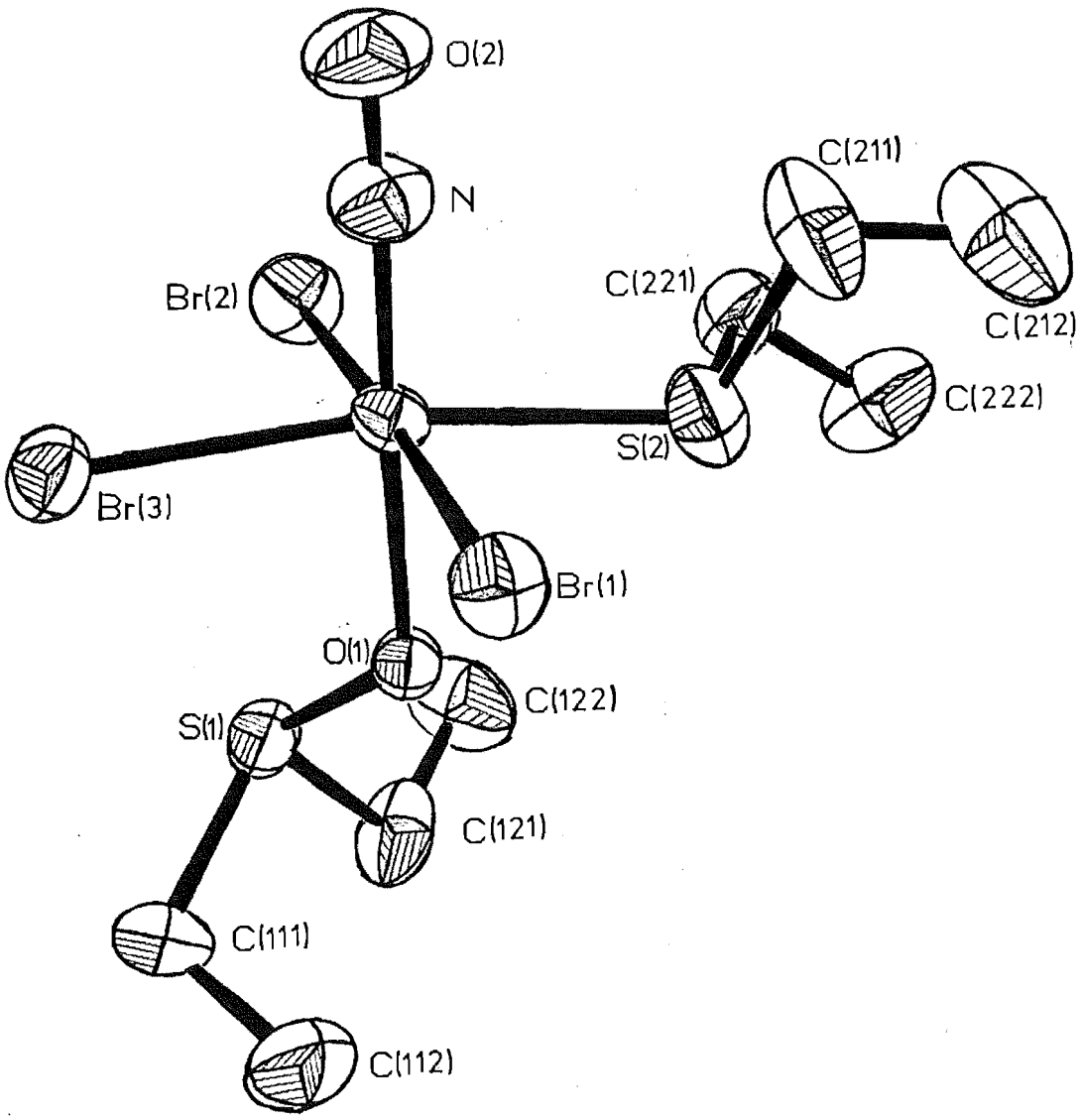

FIGURE 6.1

A perspective view of the $[RuBr_3(NO)(Et_2SO)(Et_2S)]$ molecule. The atom labelling scheme is also shown. Vibrational ellipsoids are drawn at the 40% probability level.

TABLE 6.4

Intramolecular Distances (Å) for $[RuBr_3(NO)(Et_2SO)(Et_2S)]$

Ru-N	1.72(1)
Ru-O(1)	2.055(8)
Ru-S(2)	2.412(4)
Ru-Br(1)	2.509(2)
Ru-Br(2)	2.501(2)
Ru-Br(3)	2.500(2)
S(1)-O(1)	1.543(8)
S(1)-C(111)	1.87(1)
S(1)-C(121)	1.81(1)
S(2)-C(211)	1.93(2)
S(2)-C(221)	1.83(2)
N-O(2)	1.09(1)
C(111)-C(112)	1.45(2)
C(121)-C(122)	1.49(2)
C(211)-C(212)	1.36(3)
C(221)-C(222)	1.50(2)

TABLE 6.5

Intramolecular Angles (deg) for $[RuBr_3(NO)(Et_2SO)(Et_2S)]$

N-Ru-O(1)	178.8(5)
N-Ru-S(2)	97.5(5)
N-Ru-Br(3)	90.5(5)
N-Ru-Br(2)	90.7(4)
N-Ru-Br(1)	94.0(4)
O(1)-Ru-S(2)	81.4(2)
O(1)-Ru-Br(3)	90.7(2)
O(1)-Ru-Br(2)	89.3(2)
O(1)-Ru-Br(1)	86.0(2)
S(2)-Ru-Br(3)	170.5(1)
S(2)-Ru-Br(2)	96.1(1)
S(2)-Ru-Br(1)	84.0(1)
Br(3)-Ru-Br(2)	88.90(7)
Br(3)-Ru-Br(1)	90.25(6)
Br(2)-Ru-Br(1)	175.23(7)
O(1)-S(1)-C(111)	100.8(6)
O(1)-S(1)-C(121)	104.2(7)
C(111)-S(1)-C(121)	102.3(9)
C(211)-S(2)-C(221)	99.3(9)
Ru-S(2)-C(211)	102.3(7)
Ru-S(2)-C(221)	113.3(5)
Ru-N-O(2)	176.5(14)
Ru-S(1)-O(1)	124.8(5)
S(1)-C(111)-C(112)	113.6(13)
S(1)-C(121)-C(122)	109.8(13)
S(2)-C(211)-C(212)	111.7(18)
S(2)-C(221)-C(222)	109.1(12)

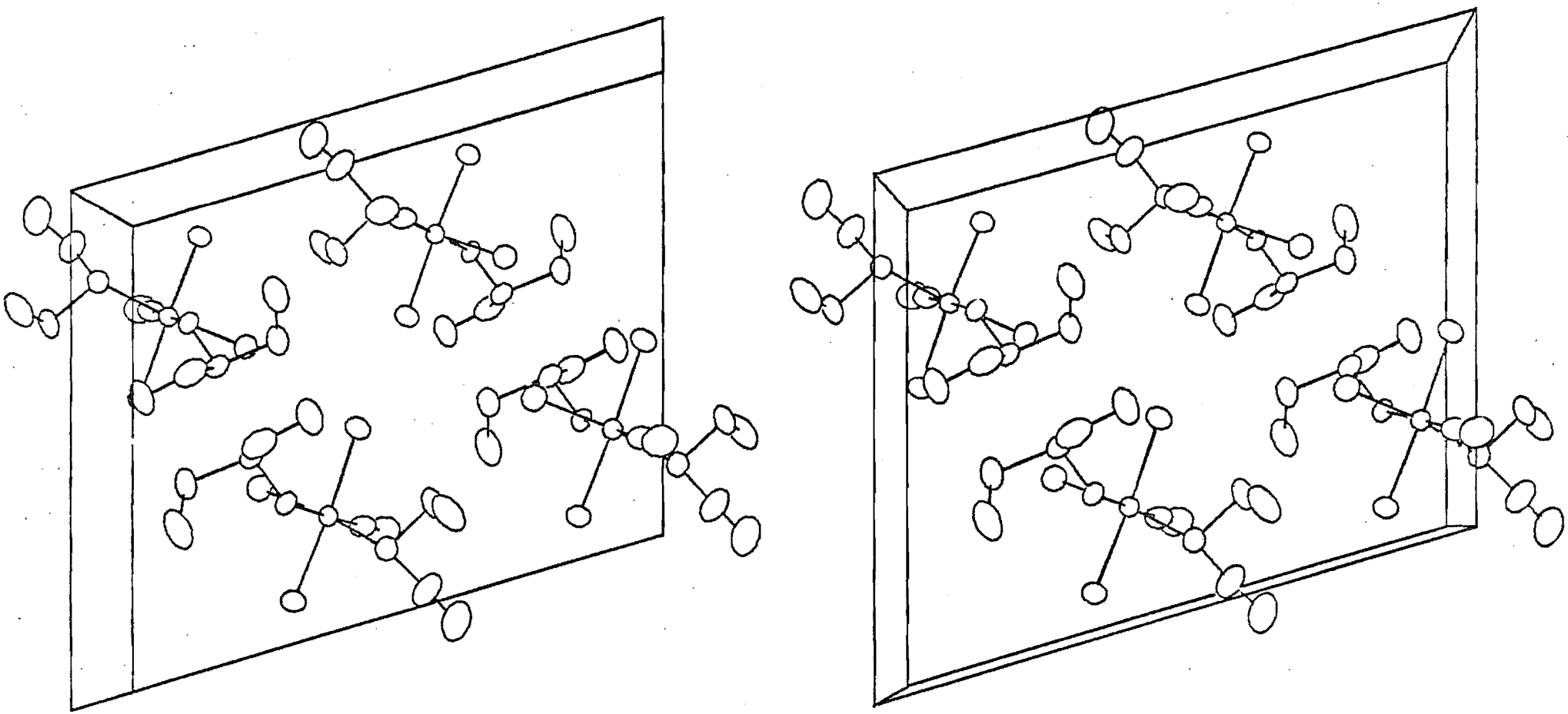

FIGURE 6.2

Stereoscopic diagram of the packing of the $[RuBr_3(NO)(Et_2SO)(Et_2S)]$ species with respect to the unit cell.

dimer. From the infrared spectrum of $[RuBr_3(NO)(Et_2SO)(Et_2S)]$ the ν(N-O) absorption was observed at 1866 cm^{-1}, compared with 1878 cm^{-1} obtained for the dimeric complex. Therefore it appears, in this case at least, that there exists little correlation between the bond length and ν(N-O) absorption position[176] whereas a reasonable correlation was observed for the S-O bond length and ν(S-O) parameters as described in section 5.3.2.

6.3.2 Sulphoxide Ligand

The diethyl sulphoxide ligand is coordinated in a similar manner to that observed for the dimeric species previously described. This is shown in Figure 6.3 where the perspective view looking down the O-Ru bond is presented for both the $[RuBr_3(NO)(Et_2SO)(Et_2S)]$ and $[RuBr_3(NO)(Et_2SO)]_2$ complexes.

The bond lengths and angles for the diethyl sulphoxide ligand are similar to the values obtained for the dimeric species.

6.3.3 Sulphide Ligand

The diethyl sulphide ligand has bond lengths and angles which agree with those obtained in other reports[47-54] on crystal structure analyses of complexes with thioether ligands, as listed in Table 6.6. Here the Ru-S bond distance of 2.412(4) $\mathring{A}$ is longer than the sum of the covalent radii (2.37 $\mathring{A}$),[155] hence there is unlikely to be any significant π type interaction between the ruthenium and sulphur atoms. In contrast the metal-sulphur bond lengths listed in Table 6.6 are generally shorter than the value expected from the sum

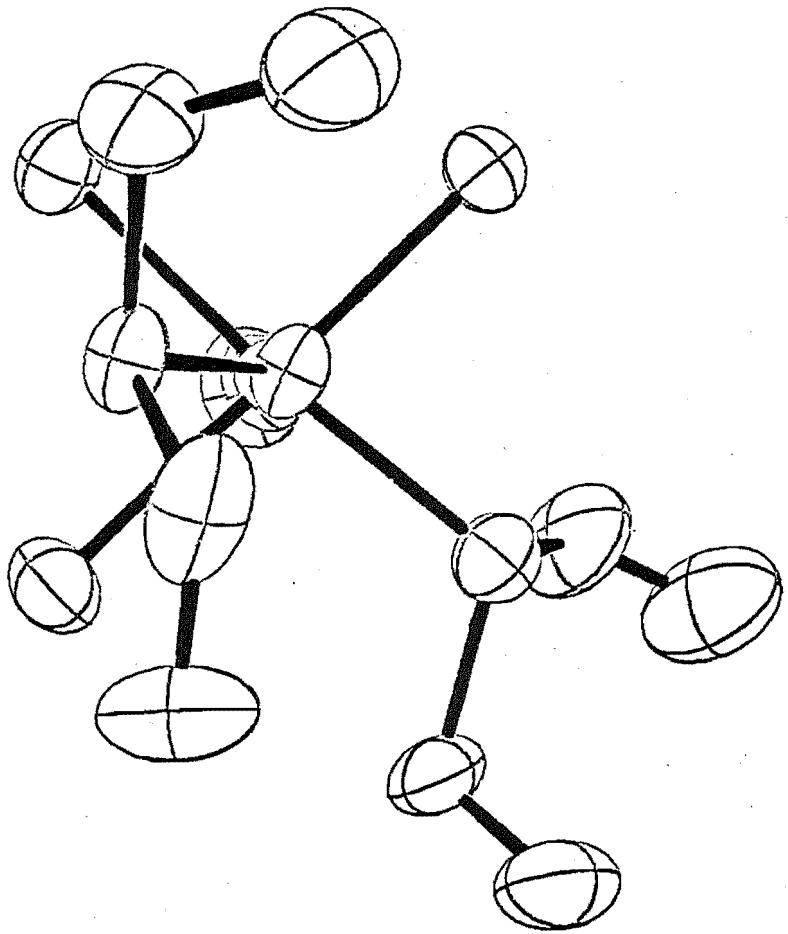

$[RuBr_3(NO)(Et_2SO)(Et_2S)]$

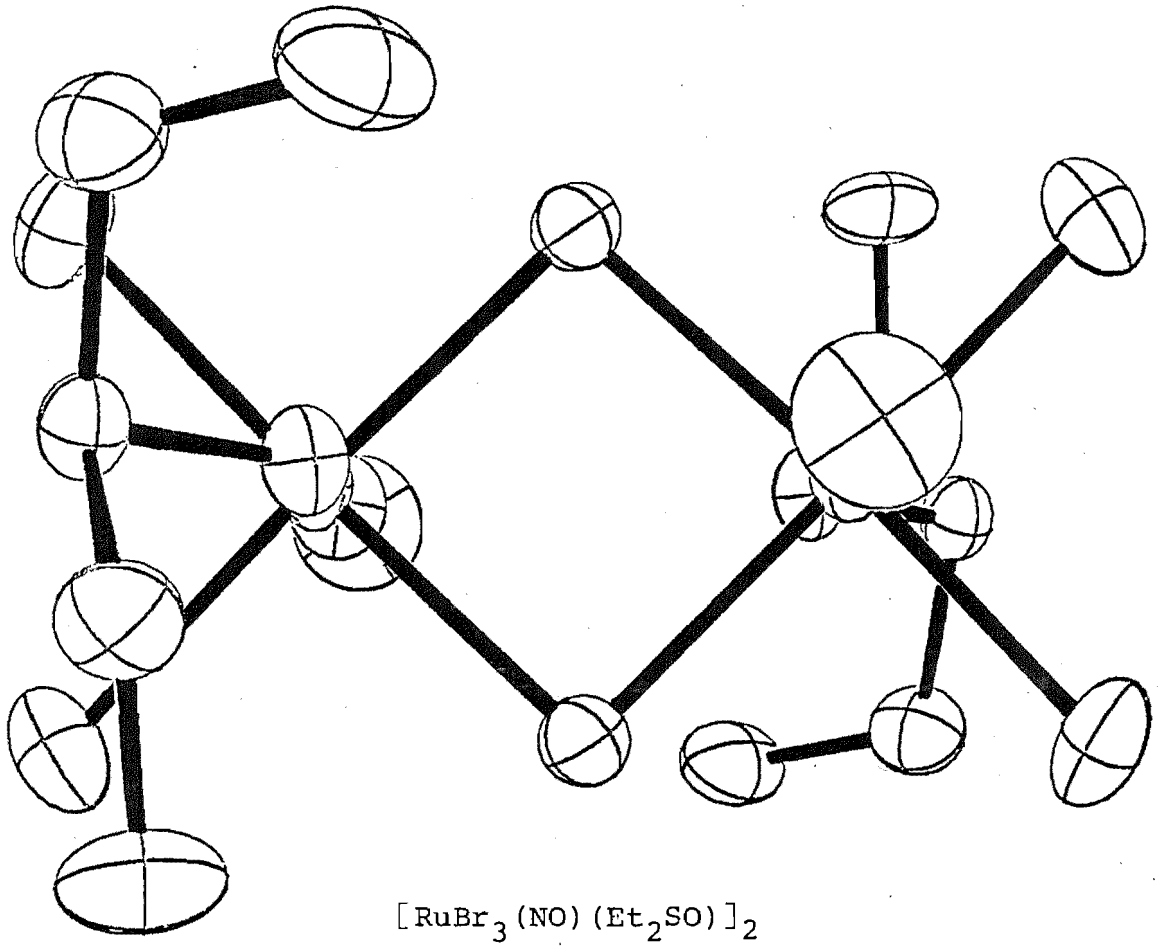

$[RuBr_3(NO)(Et_2SO)]_2$

FIGURE 6.3

Perspective view looking down the O-Ru bonds of the $[RuBr_3(NO)(Et_2SO)(Et_2S)]$ and $[RuBr_3(NO)(Et_2SO)]_2$ molecules.

TABLE 6.6

Bond Lengths and Angles for Thioether Complexes

Compound	M-S, Å	S-C, Å	M-S-C, deg	C-S-C, deg	Reference
$RuBr_3(NO)(Et_2SO)(Et_2S)$	2.412(4)	1.83(2), 1.93(2)	113.3(5), 102.3(7)	99.3(9)	This work
$RuBr_3(NO)(PhSEt)_2$	2.43(2), 2.40(2)	1.68-1.90(7)	105-113(1)	95-107(2)	This work
$Cr(CO)_5(BzSEt)$	2.458(2)	1.872(8), 1.810(8)	112.0(3), 106.0(2)	100.6(4)	47
$Pd_2Br_4(Me_2S)_2$	2.30(2)	1.85(6), 1.73(4)	113(3), 96(2)	107(3)	48
$Pt_2Br_4(Et_2S)_2$	2.21(1), 2.25(1)[a]	1.87(8), 1.79(4)	113-120(2)	93(3)	48
$AuCl_2(C_6H_5)(n\text{-}Pr_2S)$	2.31(1)	1.83(6), 1.80(5)	108(2), 107(2)	91(3)	49
trans $PdCl_2(Et_2Se)_2$[b]	2.424(7)	1.96(3), 1.94(4)	110,101	99	50
$HgCl_2.(Et_2S)$	2.41(2)	1.86(7), 1.77(7)	106(2), 100(2)	104(3)	51
$Rh_2I_2(Me_2S)_3(Me)_4$	2.284-2.328(9)	1.73-1.86(3)	106-116(1)	102(2), 98(1)	52
$RhCl_3.3Me_2S$	2.32-2.39(2)	1.80-1.95(6)	107-112(3)	93(3)	53
cis $Pt((p\text{-}ClC_6H_5)_2S)_2Cl_2$	2.292(6), 2.278(7)	1.80(2)	106.2-110.7(7)	103(1), 105(1)	54

[a] Bridging sulphide groups.

[b] Results are M-Se, Se-C, M-Se-C and C-Se-C values.

of the covalent radii. In these cases the results suggest some tendency for the dialkyl sulphide ligands to act as π acceptors. Further evidence for the absence of a Ru-S π interaction in $[RuBr_3(NO)(Et_2SO)(Et_2S)]$ is that the Ru-Br bond length for the bromo ligand which is <u>trans</u> to the diethyl sulphide ligand is not significantly different from that obtained for the mutually <u>trans</u> bromo ligands.

The sulphur atom of the coordinated diethyl sulphide group is bonded in pyramidal fashion with the lone pair of electrons occupying the vacant region above the apex. The M-S-C and C-S-C bond angles listed in Table 6.6 confirm the distorted tetrahedral arrangement of the groups about the sulphur atom. The small deviations from octahedral geometry about the ruthenium atom in $[RuBr_3(NO)(Et_2SO)(Et_2S)]$ can be rationalised in terms of non-bonded repulsions between the electron pair of the sulphide sulphur atom and the neighbouring ligands.

CHAPTER 7

THE CRYSTAL AND MOLECULAR STRUCTURE OF TRIBROMONITROSYLBIS(PHENYL ETHYL SULPHIDE)RUTHENIUM(II)

The X-ray crystal structure analysis of $[RuBr_3(NO)(PhSEt)_2]$ was undertaken in order to confirm the postulated arrangement of ligands about the ruthenium atom in the $[RuX_3(NO)L_2]$ complexes. The ^1H n.m.r. results could be interpreted in terms of a trans-meridional configuration.

7.1 EXPERIMENTAL DETAILS

7.1.1 Preparation

Nitric oxide was bubbled through an ethanolic solution of hydrated $RuBr_3$ for several hours and phenyl ethyl sulphide was then added in slight excess. The solution was heated under reflux for one hour. $[RuBr_3(NO)(PhSEt)_2]$ precipitates as the solvent, ethanol, is removed in vacuo. Crystals were also obtained by slowly evaporating, in the dark, a chloroform solution of $[RuBr_3(NO)(PhSEt)_2]$. These were intimately twinned, so the same method of slow crystallisation, but using ethanol as solvent, was used to obtain single crystals suitable for analysis.

7.1.2 Data Collection

Preliminary precession photographs, using CuKα X-radiation, yielded approximate cell dimensions, indicated 2/m Laue symmetry, and revealed the only condition limiting possible reflections to be 0k0; k = 2n. This is consistent with the monoclinic space groups $P2_1$ and $P2_1/m$. The subsequent

structure solution and refinements have confirmed the correct space group is $P2_1$.

The crystal used for data collection was transferred to the Hilger and Watts 4-circle diffractometer and accurately centred in the X-ray beam. The unit cell parameters were determined from a least-squares fit to the setting angles of the peak intensities of twelve reflections with $18^{o}<2\theta<24^{o}$. The cell dimensions and other crystal data are listed in Table 7.1. The experimental density was measured by neutral buoyancy in an aqueous zinc bromide solution and was consistent with four $[RuBr_3(NO)(PhSEt)_2]$ chemical units occupying the unit cell.

The crystal displayed acceptable mosaicity, with peak widths at half-height not exceeding 0.25^{o} for strong, low angle reflections. The θ-2θ scan technique was used to collect the 3591 independent reflections in that positive k and ℓ quadrant of reciprocal space for which $0<2\theta<48^{o}$. Two strong reflections required attenuation in order to bring the intensity within the linear response range of the scintillation counter. The intensities of three standard reflections, measured every 50 reflections, dropped slowly during the course of the data collection to 95% of their original values. These standard reflection intensities were used to place all the collected intensities on the same relative scale.

The data set was processed in the manner described in Chapter 5, with the details presented in Table 7.1. An absorption correction was applied to the data using the program ABSORB.[171] Only those 1529 reflections with $F_o^2 \geq 3\sigma(F_o^2)$ were included in least-squares refinement calculations.

TABLE 7.1

Summary of Crystal, Intensity Collection and Refinement Data

Compound	$RuBr_3(NO)(PhSEt)_2$
Formula	$C_{16}H_{20}Br_3NOS_2Ru$
Formula weight	647.25
a, Å	15.352 (3)
b, Å	16.712 (4)
c, Å	8.584 (2)
β, deg	90.36 (1)
V, $Å^3$	2202
Z	4
Density, g/cm^3	1.95 (calcd); 1.94 (3) (exptl)
Space group	$P2_1$
Crystal dimensions, mm^3	0.38 x 0.19 x 0.19
Crystal volume, mm^3	0.00501
Radiation	Mo $K\bar{\alpha}$ (λ = 0.7107 Å)
Crystal mosaicity, deg	0.10 - 0.20
Temperature, ^oC	21
μ, cm^{-1}	66.52
Transmission factors	0.36 - 0.61
Receiving aperture	5.0 mm diameter, 230 mm from crystal
Take off angle, deg	3.0
Scan speed	2.0^o in 2θ/min
Scan range, deg	1.60
Background counting, sec	20
2θ limit, deg	48
Final no. of variable parameters	205

Table 7.1 continued.

Unique data used ($F_o^2 \geq 3\sigma(F_o^2)$)	1529
Error in observation of unit weight, electrons	1.81
R_1	0.091
R_2	0.118

7.2 STRUCTURE SOLUTION AND REFINEMENT

Initial attempts to solve the structure in the space group $P2_1/m$ failed. There were no maxima of type 0,2y,0 in the Patterson function[177] and thus no mirror plane of symmetry in real space.

An attempt was then made to solve the structure in the noncentrosymmetric space group $P2_1$. Since this space group has only two equivalent positions, there must be two crystallographically nonequivalent molecules in the asymmetric unit. A number of maxima in the Patterson function, of the type $2x,\frac{1}{2},2z$,[140,177] were chosen such that they yielded reasonable positional coordinates for two Ru-Br heavy atom fragments. Since, in the space group $P2_1$, the origin may be fixed anywhere on the two fold axis, one ruthenium atom (Ru(1)) was arbitrarily assigned an invariant y coordinate of zero.

As the four heavy atoms Ru(1), Ru(2), Br(13) and Br(23), located from the Patterson maps, all lay on, or very close to, the x,o,z plane, the structure factors calculated using these positions will all have phase angles of 0 or π.[140] Thus, resulting electron-density maps contain a correct set of atom positions and a mirror image set.

After a detailed analysis of the interatomic vectors obtained from the Patterson synthesis, four further bromine and four sulphur atom positions, not on the x,o,z plane, were established. Two cycles of least-squares refinement of the positions of two ruthenium, six bromine and four sulphur atoms yielded $R_1 = 0.169$ and $R_2 = 0.211$. The phase angles calculated from this refinement were used to generate an F_{obs} Fourier electron-density map. This enabled the positions

of the four phenyl and four ethyl group carbon atoms to be extracted. In subsequent refinements the phenyl rings were treated as rigid hexagonal groups located by defining three positional parameters for the group centroid and three angles for its orientation. These parameters, together with a single overall temperature factor, were refined for each ring. The phenyl ring C-C bond length was kept fixed at 1.392 Å and the C-C-C bond angle at 120°.

Although the electron density map revealed peaks corresponding with a linear Ru-N-O linkage for both ruthenium atoms, attempts to refine these nitrogen and oxygen atoms positions resulted in large shifts in their assigned coordinates. A difference Fourier synthesis, calculated using the results of a least-squares refinement including all atoms, except those of the two nitrosyl groups, again revealed peaks consistent with linear coordination of these groups, (Figure 7.1). A detailed study of electron density in the region of these nitrosyl groups does not support disorder of the type

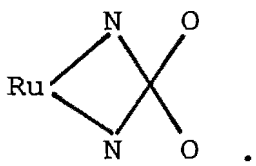

178

If there is any disorder involving the nitrosyl positions it could not be detected crystallographically.

Using those positions obtained from the difference Fourier synthesis for the nitrosyl groups, and including the other atoms, least-squares refinements were continued. All the atoms were assigned isotropic temperature factors and rigorous corrections for anomalous dispersion were made for the Ru, Br and S atoms, these least-squares refinements

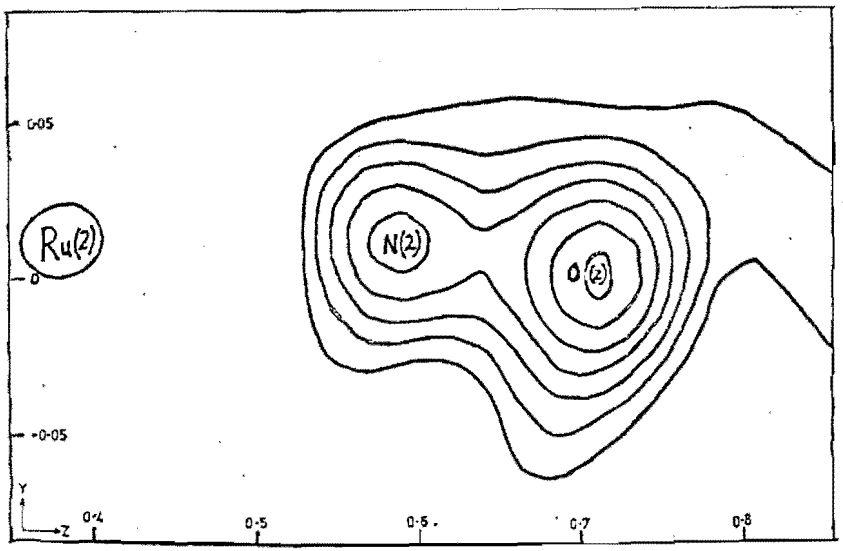

(a)

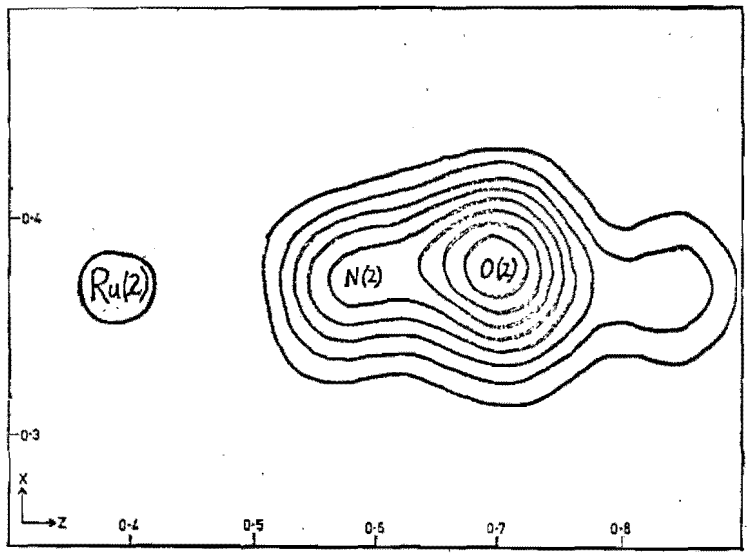

(b)

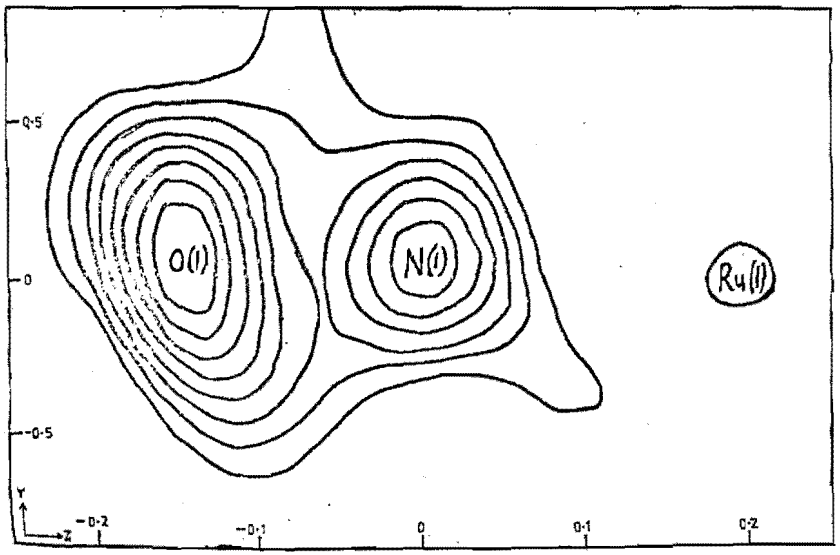

(c)

FIGURE 7.1

Contour plots from a ΔF synthesis in the region of the two independent nitrosyl groups. Contours are approximately 1 eA^{-3} apart.

(a) A yx section at z = 0.363

(b) An xz section at y = 0.009

(c) A yz section at z = 0.875

converged with $R_1 = 0.122$ and $R_2 = 0.142$. To determine the polarity in the noncentrosymmetric space group, refinements with the y axis direction reversed yielded $R_1 = 0.126$ and $R_2 = 0.147$. Since the former model gave the better agreement factors it was used in all subsequent calculations.

An examination of the structure factor magnitudes indicated that $\Sigma w(|F_o|-|F_c|)^2$ increased systematically with increasing magnitude of the structure factors. The intensity data were reprocessed using a 'p' value of 0.088 (the original 'p' factor was 0.050) in order to obtain a better weighting scheme.

In the final stages of refinement all atoms, except carbon atoms, were assigned anisotropic thermal vibration parameters. These full-matrix least-squares refinements, using the 1529 reflections for which $F_o^2 \geq 3\sigma(F_o^2)$, converged to give agreement factors $R_1 = 0.091$ and $R_2 = 0.118$. No attempt was made to locate the hydrogen atoms.

The estimated standard deviation of an observation of unit weight was 1.81 electrons and the highest peak in a final difference Fourier synthesis was one-third of the height of a typical carbon atom found during this analysis. The scattering factors used were those detailed in Chapter 5. There was evidence for secondary extinction amongst intense low angle reflections and $a^{correction}_{A}$ was applied in the manner outlined in Chapter 6.

The positional and thermal vibrational parameters obtained from the final cycle of refinement are presented in Table 7.2 along with their estimated standard deviations obtained from the inverse matrix. Table 7.3 contains the root-mean-square amplitudes of vibration, along the principal

TABLE 7.2

Final Positional and Thermal Parameters for $[RuBr_3(NO)(PhSEt)_2]$

	x	y	z	U_{11}	U_{22}	U_{33}	U_{12}	U_{13}	U_{23}
Ru(1)	0.8776 (4)	0.0000	0.2075 (8)	0.035 (3)	0.047 (4)	0.037 (3)	-0.004 (3)	0.006 (2)	-0.014 (3)
Ru(2)	0.3742 (3)	0.0135 (5)	0.3743 (6)	0.024 (3)	0.046 (4)	0.036 (3)	-0.013 (3)	-0.001 (2)	0.024 (3)
Br(11)	0.9825 (5)	0.1131 (9)	0.208 (1)	0.047 (5)	0.045 (6)	0.075 (6)	-0.018 (4)	0.012 (4)	0.005 (5)
Br(12)	0.7706 (5)	0.1163 (9)	0.202 (1)	0.033 (5)	0.064 (7)	0.104 (8)	-0.023 (5)	-0.002 (4)	-0.017 (6)
Br(13)	0.8793 (5)	-0.0008 (8)	0.5025 (7)	0.061 (4)	0.096 (7)	0.030 (4)	-0.012 (5)	0.023 (3)	0.021 (5)
Br(21)	0.4802 (5)	0.1277 (7)	0.3881 (8)	0.060 (5)	0.046 (6)	0.065 (5)	-0.010 (4)	-0.003 (4)	-0.009 (4)
Br(22)	0.2688 (4)	-0.1029 (8)	0.3702 (9)	0.047 (4)	0.054 (6)	0.064 (5)	-0.014 (4)	-0.011 (4)	0.011 (4)
Br(23)	0.3714 (5)	0.0203 (7)	0.084 (1)	0.063 (5)	0.075 (8)	0.082 (6)	-0.006 (5)	-0.022 (4)	0.015 (6)
S(11)	0.750 (1)	0.081 (1)	0.236 (2)	0.04 (1)	0.06 (2)	0.08 (2)	-0.00 (1)	-0.00 (1)	-0.04 (1)
S(12)	1.006 (1)	-0.083 (1)	0.241 (2)	0.04 (1)	0.05 (1)	0.08 (1)	-0.01 (1)	-0.034 (9)	-0.02 (1)
S(21)	0.502 (1)	-0.066 (1)	0.340 (2)	0.04 (1)	0.04 (1)	0.05 (1)	-0.014 (9)	0.020 (8)	0.010 (9)
S(22)	0.244 (1)	0.095 (1)	0.359 (2)	0.04 (1)	0.06 (1)	0.08 (1)	-0.01 (1)	0.037 (9)	0.03 (1)
O(1)	0.886 (2)	0.019 (3)	-0.136 (4)	0.04 (1)	0.08 (2)	0.03 (1)	0.00 (1)	0.02 (1)	0.01 (1)
O(2)	0.391 (2)	0.015 (3)	0.686 (4)	0.06 (1)	0.08 (2)	0.04 (1)	0.00 (1)	0.00 (1)	0.00 (1)
N(1)	0.873 (3)	0.002 (3)	0.027 (5)	0.05 (1)	0.06 (1)	0.06 (1)	0.00 (1)	0.02 (1)	-0.01 (1)
N(2)	0.370 (3)	0.001 (3)	0.005 (5)	0.04 (1)	0.06 (1)	0.06 (1)	-0.01 (1)	0.01 (1)	0.00 (1)

TABLE 7.2 continued

	x	y	z	U
C(1111)	0.774 (4)	0.180 (4)	0.332 (6)	0.07 (1)
C(1112)	0.703 (3)	0.227 (4)	0.328 (5)	0.05 (1)
C(1211)	0.975 (4)	-0.189 (4)	0.297 (6)	0.07 (1)
C(1212)	1.044 (5)	-0.230 (5)	0.380 (7)	0.12 (2)
C(2111)	0.464 (4)	-0.160 (4)	0.275 (6)	0.07 (1)
C(2112)	0.545 (4)	-0.219 (4)	0.222 (6)	0.07 (1)
C(2211)	0.264 (4)	0.183 (4)	0.272 (6)	0.08 (2)
C(2212)	0.190 (4)	0.258 (4)	0.289 (6)	0.06 (1)
C(1121)	0.706	0.111	0.063	0.063
C(1122)	0.625	0.078	0.022	0.062
C(1123)	0.591	0.091	-0.127	0.062
C(1124)	0.638	0.137	-0.234	0.062
C(1125)	0.719	0.169	-0.192	0.062
C(1126)	0.752	0.156	-0.044	0.062
C(1221)	1.054	-0.111	0.060	0.086
C(1222)	1.008	-0.156	-0.049	0.086
C(1223)	1.040	-0.166	-0.198	0.086
C(1224)	1.119	-0.132	-0.0240	0.086
C(1225)	1.166	-0.086	-0.131	0.086
C(1226)	1.133	-0.076	0.018	0.086
C(2121)	0.544	-0.099	0.533	0.087
C(2122)	0.626	-0.069	0.567	0.087
C(2123)	0.665	-0.083	0.711	0.087
C(2124)	0.621	-0.129	0.822	0.087
C(2125)	0.539	-0.160	0.788	0.087
C(2126)	0.500	-0.145	0.644	0.087
C(2221)	0.204	0.117	0.544	0.055
C(2222)	0.252	0.152	0.663	0.055
C(2223)	0.219	0.155	0.814	0.055
C(2224)	0.138	0.122	0.845	0.055
C(2225)	0.089	0.086	0.725	0.055
C(2226)	0.122	0.084	0.575	0.055

TABLE 7.3

Root-Mean-Square Amplitudes of Vibration (Å)

for $[RuBr_3(NO)(PhSEt)_2]$

Atom	Min.	Intermed.	Max.
Ru(1)	0.163 (9)	0.18 (1)	0.24 (1)
Ru(2)	0.11 (2)	0.16 (1)	0.26 (1)
Br(11)	0.16 (2)	0.25 (1)	0.28 (1)
Br(12)	0.14 (2)	0.27 (1)	0.33 (2)
Br(13)	0.11 (2)	0.27 (1)	0.32 (1)
Br(21)	0.19 (1)	0.26 (1)	0.26 (1)
Br(22)	0.19 (1)	0.22 (1)	0.28 (1)
Br(23)	0.22 (1)	0.26 (1)	0.32 (1)
S(11)	0.17 (4)	0.20 (3)	0.34 (3)
S(12)	0.11 (4)	0.23 (3)	0.32 (3)
S(21)	0.11 (4)	0.23 (3)	0.25 (3)
S(22)	0.08 (6)	0.24 (3)	0.33 (3)
O(1)	0.13 (7)	0.22 (6)	0.29 (6)
O(2)	0.19 (7)	0.24 (6)	0.29 (6)
N(1)	0.18 (8)	0.25 (7)	0.28 (7)
N(2)	0.17 (8)	0.23 (7)	0.26 (7)

axes of the thermal ellipsoids, for the sixteen atoms refined with anisotropic thermal parameters. Listings of the final values of $|F_o|$ and $|F_c|$ (in electrons) for the 1529 reflections used in the refinements are given in Appendix E.

A structure factor calculation on all 3591 independent reflections collected showed only two reflections, $\bar{1}$ 0 1 and $\bar{1}$ 0 3, had large discrepancies between the $|F_c|$ and $|F_o|$ values.

7.3 DISCUSSION

7.3.1 Description of the Crystal Structure

The crystal structure consists of an assemblage of discrete molecules of $[RuBr_3(NO)(PhSEt)_2]$. The geometry of the two crystallographically independent molecules in the asymmetric unit is illustrated in Figure 7.2, which also defines the atom labelling scheme used throughout this chapter. The shortest nonbonding intermolecular contact not involving hydrogen atoms is 3.13 Å between the Br(13) atom of one molecule and the O(1) atom of a neighbouring molecule. All the important intramolecular distances and bond angles are listed in Tables 7.4 and 7.5, respectively. A stereoscopic drawing illustrating the packing of molecules with respect to one unit cell, is shown in Figure 7.3.

The coordination about the ruthenium atoms is approximately octahedral with the bromine ligands in a meridional configuration and the phenyl ethyl sulphide ligands in a trans arrangement. The nitrosyl ligand in each case is trans to a bromine ligand.

It is evident from the large shifts in position in the final cycle of refinement (up to 1.5σ) that the nitrosyl

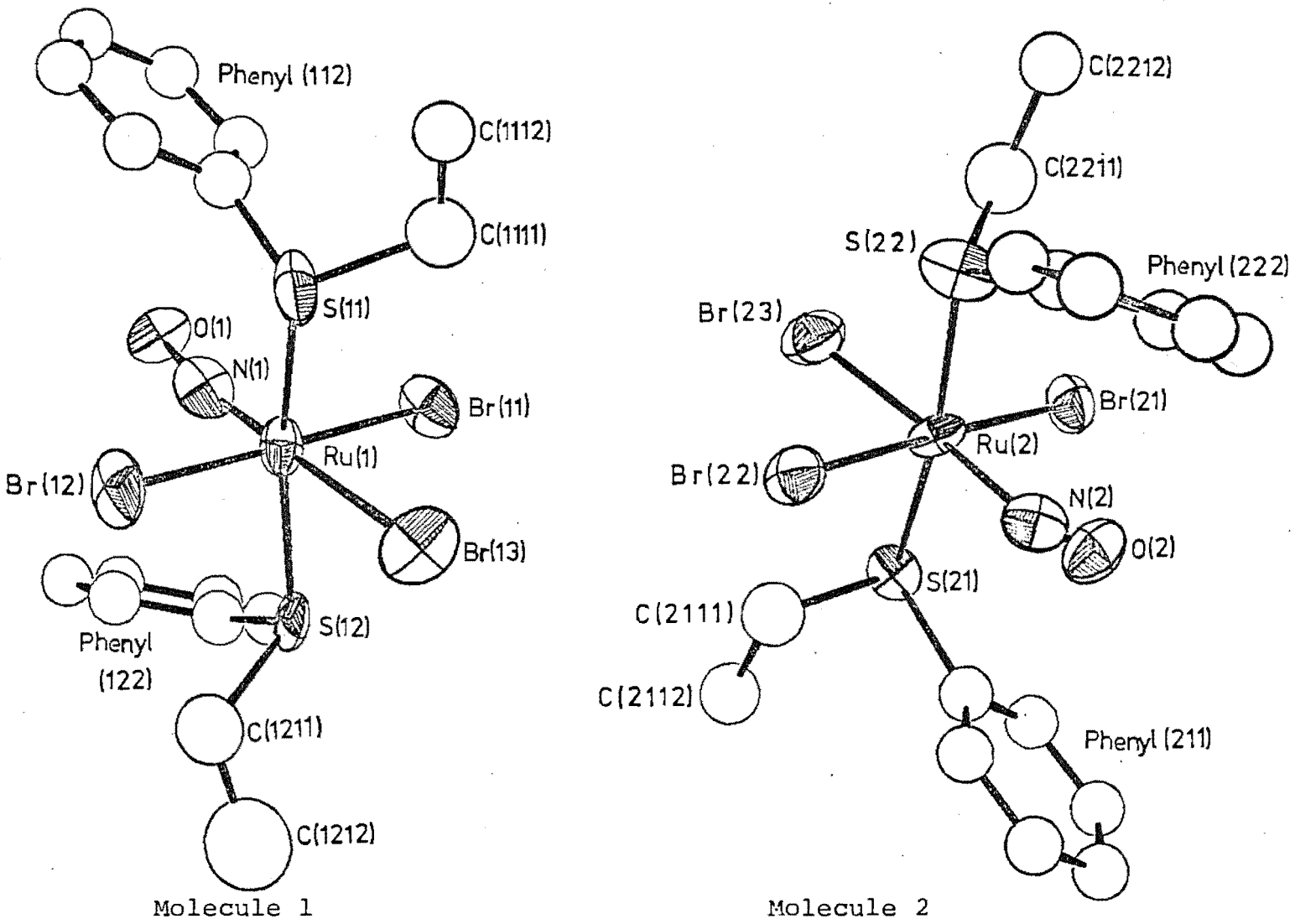

FIGURE 7.2

Perspective views of the two crystallographically independent $[RuBr_3(NO)(PhSEt)_2]$ molecules. The atom labelling scheme is also shown. Vibrational ellipsoids are drawn at the 50% probability level.

TABLE 7.4

Intramolecular Distances (Å) for $[RuBr_3(NO)(PhSEt)_2]$

Molecule 1		Molecule 2	
Ru(1)-Br(11)	2.48 (1)	Ru(2)-Br(21)	2.51 (1)
Ru(1)-Br(12)	2.55 (1)	Ru(2)-Br(22)	2.53 (1)
Ru(1)-Br(13)	2.532 (9)	Ru(2)-Br(23)	2.49 (1)
Ru(1)-S(11)	2.40 (2)	Ru(2)-S(21)	2.39 (2)
Ru(1)-S(12)	2.43 (2)	Ru(2)-S(22)	2.43 (2)
Ru(1)-N(1)	1.56 (4)	Ru(2)-N(2)	1.99 (4)
N(1)-O(1)	1.44 (6)	N(2)-O(2)	0.80 (6)
S(11)-C(1111)	1.89 (7)	S(21)-C(2111)	1.77 (7)
C(1111)-C(1112)	1.33 (8)	C(2111)-C(2112)	1.66 (8)
S(12)-C(1211)	1.90 (7)	S(22)-C(2211)	1.68 (7)
C(1211)-C(1212)	1.44 (9)	C(2211)-C(2212)	1.69 (9)
S(11)-C(1121)	1.70	S(21)-C(2121)	1.86
S(12)-C(1221)	1.79	S(22)-C(2221)	1.74

TABLE 7.5

Intramolecular Angles (deg)

for $[RuBr_3(NO)(PhSEt)_2]$

N(1)-Ru(1)-S(11)	93 (1)
N(1)-Ru(1)-S(12)	99 (1)
N(1)-Ru(1)-Br(11)	91 (1)
N(1)-Ru(1)-Br(12)	88 (1)
N(1)-Ru(1)-Br(13)	178 (1)
S(11)-Ru(1)-S(12)	167.4 (6)
S(11)-Ru(1)-Br(11)	95.9 (5)
S(11)-Ru(1)-Br(12)	84.5 (5)
S(11)-Ru(1)-Br(13)	84.6 (5)
S(12)-Ru(1)-Br(11)	84.8 (5)
S(12)-Ru(1)-Br(12)	95.1 (5)
S(12)-Ru(1)-Br(13)	82.9 (5)
Br(11)-Ru(1)-Br(12)	178.9 (5)
Br(11)-Ru(1)-Br(13)	90.0 (4)
Br(12)-Ru(1)-Br(13)	91.1 (4)
Ru(1)-N(1)-O(1)	165 (5)
Ru(1)-S(11)-C(1111)	112 (1)
Ru(1)-S(11)-C(1121)	113 (1)
Ru(1)-S(12)-C(1211)	111 (1)
Ru(1)-S(12)-C(1221)	113 (1)
S(11)-C(1111)-C(1112)	111 (3)
S(12)-C(1211)-C(1212)	113 (3)
C(1111)-S(11)-C(1121)	101 (2)
C(1211)-S(12)-C(1221)	95 (2)

Table 7.5 continued.

N(2)-Ru(2)-S(21)	96 (1)
N(2)-Ru(2)-S(22)	95 (1)
N(2)-Ru(2)-Br(21)	93 (1)
N(2)-Ru(2)-Br(22)	85 (1)
N(2)-Ru(2)-Br(23)	176 (1)
S(21)-Ru(2)-S(22)	169.8 (6)
S(21)-Ru(2)-Br(21)	83.9 (5)
S(21)-Ru(2)-Br(22)	95.7 (5)
S(21)-Ru(2)-Br(23)	84.8 (5)
S(22)-Ru(2)-Br(21)	96.2 (5)
S(22)-Ru(2)-Br(22)	84.6 (5)
S(22)-Ru(2)-Br(23)	85.0 (5)
Br(21)-Ru(2)-Br(22)	178.0 (4)
Br(21)-Ru(2)-Br(23)	91.1 (4)
Br(22)-Ru(2)-Br(23)	90.8 (4)
Ru(2)-N(2)-O(2)	145 (5)
Ru(2)-S(21)-C(2111)	105 (1)
Ru(2)-S(21)-C(2121)	109 (1)
Ru(2)-S(22)-C(2211)	111 (1)
Ru(2)-S(22)-C(2221)	112 (1)
S(21)-C(2111)-C(2112)	111 (3)
S(22)-C(2211)-C(2212)	119 (3)
C(2111)-S(21)-C(2121)	97 (2)
C(2211)-S(22)-C(2221)	107 (2)

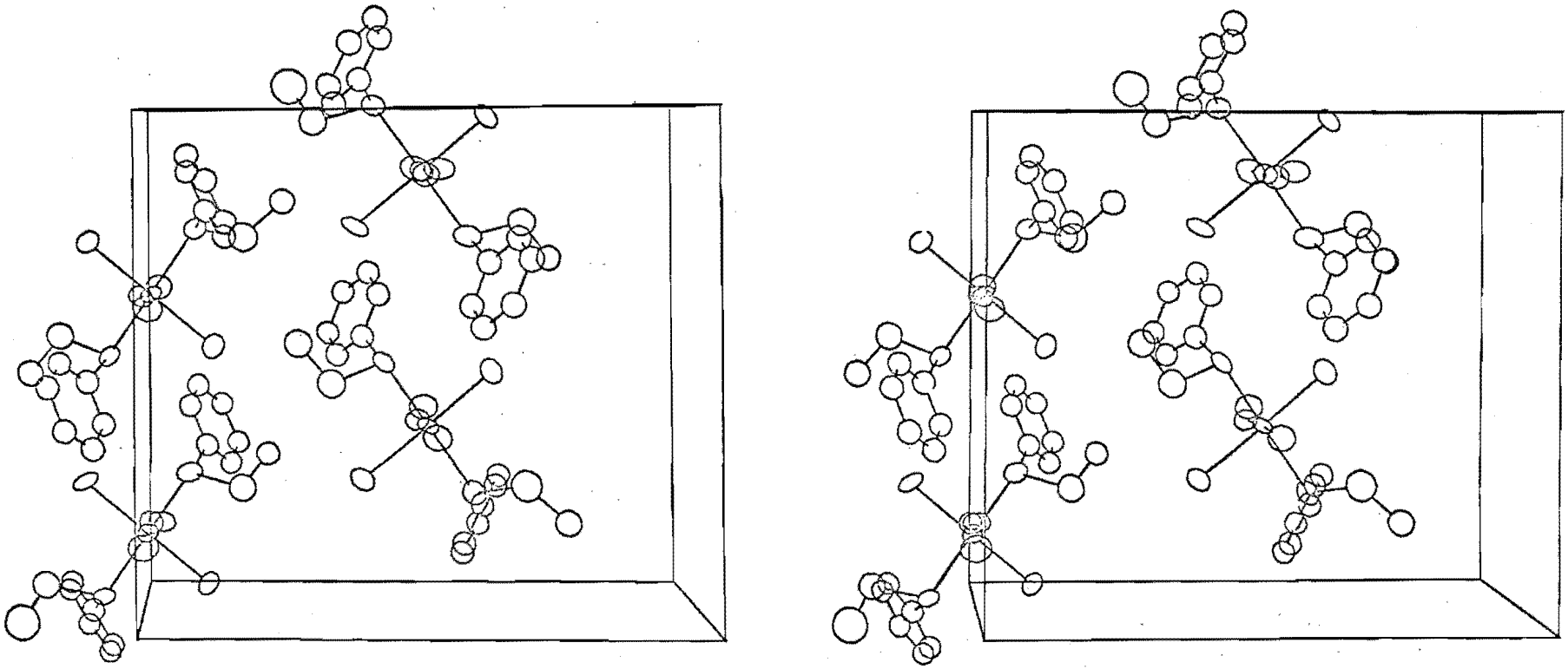

FIGURE 7.3

Stereoscopic diagram of the packing of the $[RuBr_3(NO)(PhSEt)_2]$ species with respect to the unit cell.

groups in these $[RuBr_3(NO)(PhSEt)_2]$ molecules, are not well characterised structurally. The low precision of the bond distances and angles calculated, restricts the useful discussion of the results obtained. However, the geometry of the ligands about the ruthenium atom has been established unequivocally and is in agreement with the interpretation of the spectroscopic results given in Chapter 2.

The two crystallographically independent $[RuBr_3(NO)(PhSEt)_2]$ molecules are mirror images of each other, as is shown in Figure 7.4. Also each molecule apparently belongs to point group C_2, (i.e. contains a two-fold rotation axis along Br(13)-Ru(1)-N(1) and Br(23)-Ru(2)-N(2)). Most of the corresponding bond lengths and angles between the two independent molecules are not significantly different (Tables 7.4 and 7.5).

7.3.2 Comparison of Results with Other Crystal Structures

The four Ru-S bond lengths, which range from 2.39(2) to 2.43(2) Å, are significantly longer than for most transition metal - sulphur bond lengths for thioether ligands, see Table 6.6. Whereas by comparison the sulphur bonded sulphoxide ligands are found to give shorter Ru-S bond lengths, for example $[Ru(NH_3)_5(Me_2SO)][PF_6]_2$,[62] $[RuCl_3(Me_2SO)][NH_2Me]$[66] and $[RuCl_2(Me_2SO)_4]$[67] gave mean bond lengths of 2.188(3), 2.261(8) and 2.277(1) Å respectively. The sum of the Ru and S covalent radii is 2.37 Å,[155] therefore in this case the competition from the other ligands, especially the nitrosyl, for the available π-donor orbitals results in an essentially σ dative Ru-S bond.

The variable temperature ^1H n.m.r. results (Chapter 3) indicated there was no high energy barrier to rotation about

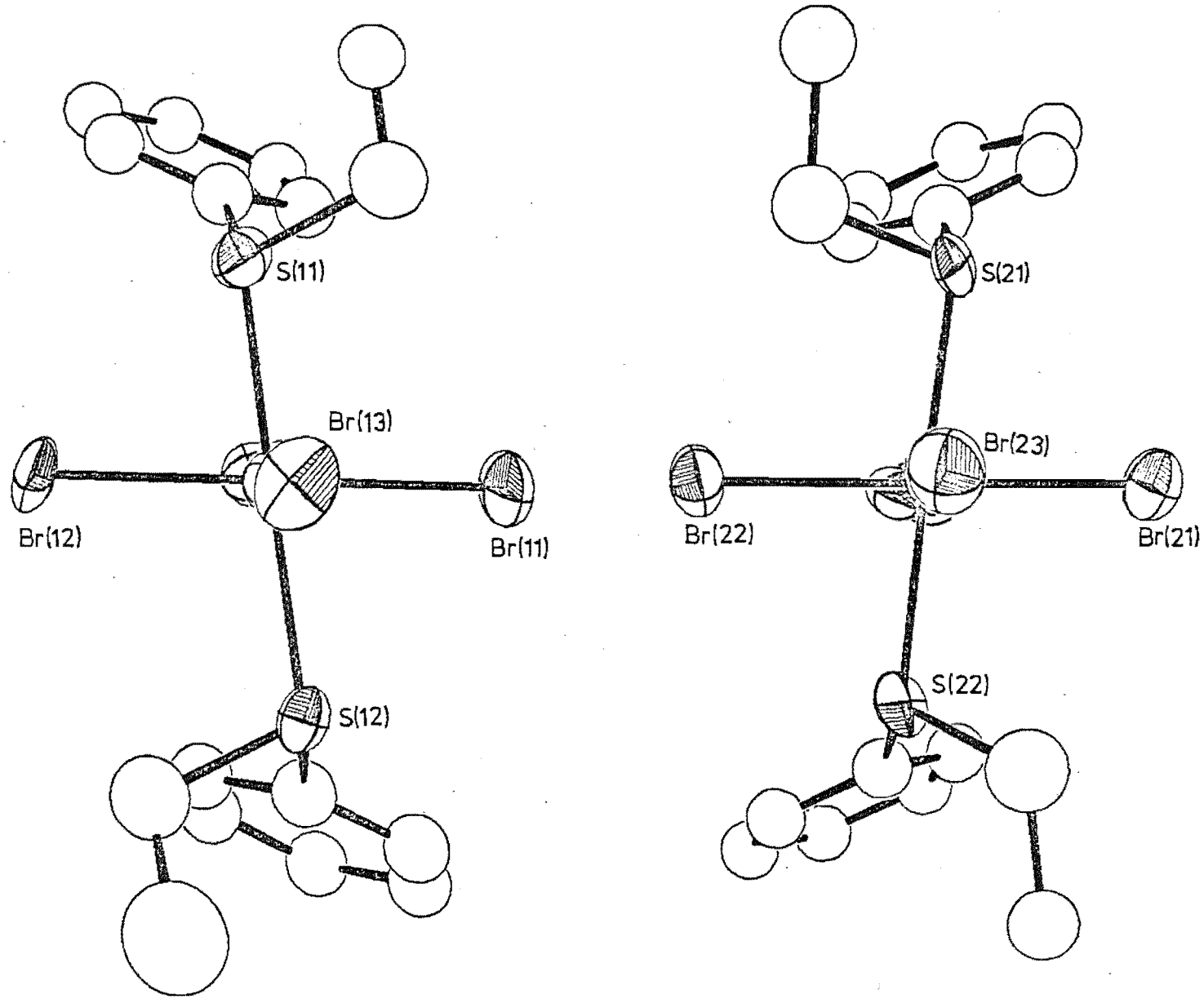

Molecule 1

Molecule 2

FIGURE 7.4

Perspective view down the Br-Ru bond, showing the apparent 2 fold axis in each molecule.

Molecule 1

Molecule 2

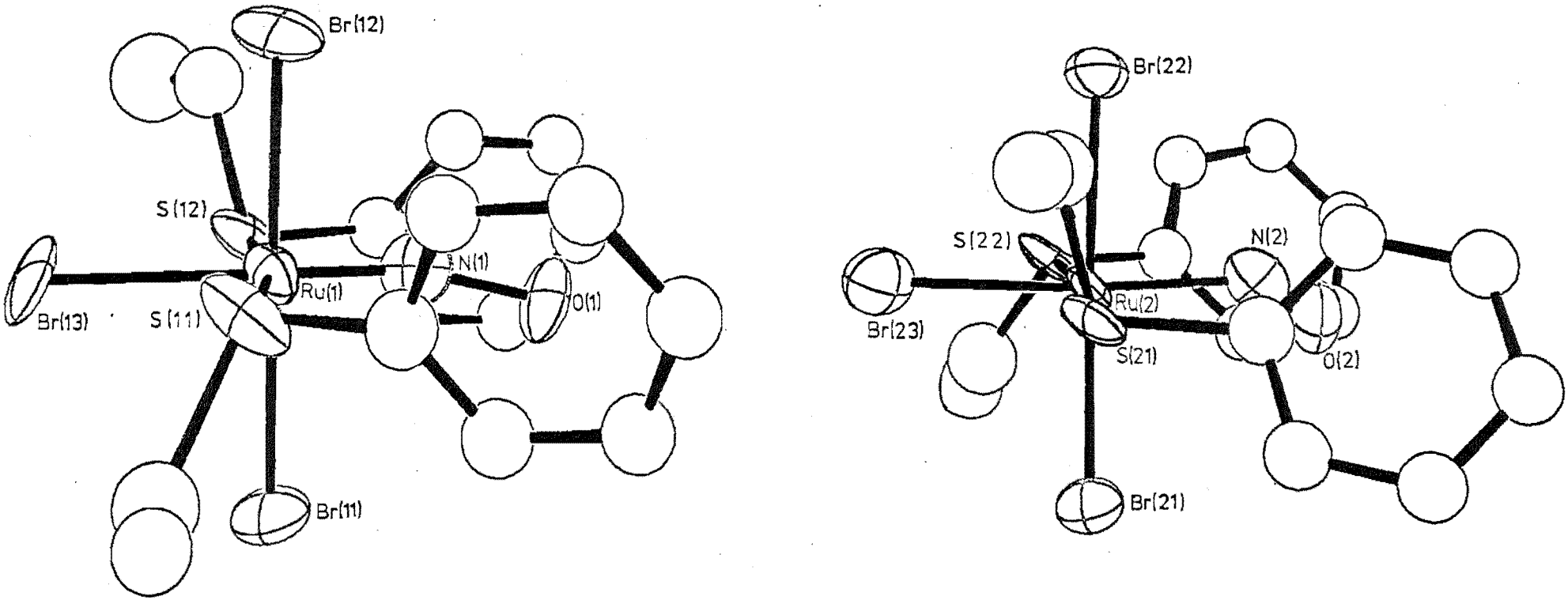

FIGURE 7.5

Perspective view down the S-Ru bond of the two independent $[RuBr_3(NO)(PhSEt)]_2$ molecules.

the R-S bond, as would have been expected if there was some Ru-S π interaction. The chemical environment of each of the ethyl groups is equivalent (as was observed by n.m.r.) in solution and also in the crystalline state since each molecule contains a two-fold rotation axis, see Figures 7.4 and 7.5.

The stereochemical arrangement of atoms coordinated to the sulphur atom is trigonal pyramidal. The Ru-S-C, S-C-C and C-S-C bond angles, as well as the S-C and C-C bond lengths, are similar to those found for other thioether complexes, see Table 6.6 and references therein.

The phenyl rings of the phenyl ethyl sulphide ligand are orientated such that they minimise the nonbonded repulsions between the electron density of the phenyl rings and the bulky bromine ligands, see Figure 7.5. The nitrosyl ligand is not as well characterised structurally as desirable because even when the structure refinement converged the shifts in positions of the nitrosyl atoms were still large. The nitrosyl groups refined to positions somewhat inconsistent with the results obtained from a Fourier synthesis and the ν(N-O) absorption in the infrared spectrum. The Ru-N-O angles obtained, 165(5)^{o} and 145(5)^{o}, cannot be considered to be linear, however, a difference Fourier calculation (using the 2516 reflections with $F_o^2 \geqslant 1\sigma(F_o^2)$) over the region where the nitrosyl groups lie, indicated Ru-N-O angles of 174^{o} and 172^{o} respectively, (Figure 7.1). The single ν(N-O) absorption for $[RuBr_3(NO)(PhSEt)_2]$ occurs at 1870 cm^{-1} which is a value well within the range expected for a linearly coordinated nitrosyl group.[9,10]

In molecule 2 the Ru-Br bond <u>trans</u> to the nitrosyl entity is shorter than the other two Ru-Br bond lengths,

(2.49(1) Å compared with 2.51(1) and 2.53(1) Å). This effect has been observed previously but only with linearly coordinated nitrosyl groups,[9,10,19] whereas the metal-ligand bond trans to nitrosyl groups is often lengthened for bent M-N-O entities. However, in molecule 1 the Ru-Br bond lengths do not show a similar trend.

The small distortion from octahedral coordination about the ruthenium atom is caused by the phenyl ethyl sulphide ligands, in each molecule, being displaced towards Br(13) or Br(23) and therefore away from the nitrosyl group. For example the N-Ru-S bond angles are 93(1)-99(1)° compared with the Br(13) (or Br(23))-Ru-S bond angles of 82.9(5)-85.0(5)°. This effect has been observed previously[9,10] and may be rationalized in terms of electron repulsion between the ruthenium-nitrosyl and ruthenium-sulphur bonds. Whether the displacement of the sulphide ligand is due to the nearness of the nitrosyl ligand to the ruthenium atom or is a result of the π-bonding interaction of the nitrosyl group with the ruthenium atom, is difficult to say.

The nitrosyl group positions were not sufficiently well resolved to enable the Ru-N bond lengths to the correlated with the observed magnitude of the Ru-N-O bond angle as described in Section 2.1.2.

CHAPTER 8

SUMMARY OF SOME OF THE PRINCIPAL RESULTS AND CONCLUSIONS

This spectroscopic and crystallographic study of the series of $[RuX_3(NO)L_2]$ complexes has enabled

(i) the changes in electron density distribution within the $[RuX_3(NO)L_2]$ complexes,

and (ii) the stereochemistry of the complexes, to be determined.

8.1 MODIFICATION OF ELECTRON DENSITY DISTRIBUTION

8.1.1 Influence of Nitrosyl Ligand

The results of the crystal structure analyses of $[RuBr_3(NO)(Et_2SO)]_2$ and $[RuBr_3(NO)(Et_2SO)(Et_2S)]$ indicate that the Ru-N bond distances are short, which supports the suggestion of a strong π back-bonding interaction between the ruthenium atom and nitrosyl group. In the structural analysis of $[RuBr_3(NO)(PhSEt)_2]$ it appears that the nitrosyl group is also linearly coordinated to the ruthenium atom and therefore the electron acceptor properties of the nitrosyl ligand confer a slight electropositive character on the ruthenium atom. This results in a drift of electron density away from the other ligands, especially the Ru-X bond *trans* to the nitrosyl group in the case of the $[RuX_3(NO)L_2]$ complexes. Therefore this halogeno ligand is more strongly bonded than the others. Spectroscopic evidence which supports these suggestions comes from the following observations:

(i) the ν(Ru-Cl) stretching mode absorption for the Ru-Cl bond *trans* to the nitrosyl group occurs at a

higher frequency (by approximately 20 cm^{-1}) than was observed for the ν(Ru-Cl) stretching modes for other ruthenium chloro chalcogen $[RuX_3L_3]$ complexes, (Section 2.2.2(a));

(ii) additional deshielding in the proton n.m.r. spectra of the methylene protons is observed, as compared with other transition metal organic chalcogen complexes which do not contain a nitrosyl ligand, (Section 2.2.3(b)).

8.1.2 Influence of the Halogeno Ligand

Changes in the electron density distribution within the $[RuX_3(NO)L_2]$ complexes when the halogeno ligand is varied from chloro to bromo were explained in terms of:

(i) the greater π electron acceptor properties of the bromo ligands,

and (ii) the greater electronegativity of the chloro ligand. Hence, the change in position of the ν(N-O) stretching.absorption (Section 2.2.1), the greater deshielding of the methylene atoms for the bromo complexes (Section 2.2.3(b)) and the difference in the rate of inversion of configuration about the sulphur atom (Br > Cl), (Section 3.2.6), may be rationalised in terms of the above two properties.

8.1.3 Ruthenium-Sulphur Bond

From the results of the crystallographic analyses reported in Chapters 6 and 7, the Ru-S bond lengths are found to be significantly longer than the sum of the covalent radii of these two atoms, which suggests that the Ru-S bond does not contain a π bonding component. However, in order to

interpret the trends observed in the activation energies of the inversion of configuration process about the sulphur (or selenium) atom, it is necessary to postulate a $S_{p_\pi} \rightarrow Ru_{d_\pi}$ type overlap for the planar transition state (Section 3.2.6). The activation energy reflects the degree of stabilisation of the transition state that occurred through the π overlap. For example, the phenyl alkyl sulphide ligands were found to destabilize the transition state (i.e. have less π overlap) due to the electron withdrawing influence of the phenyl group with respect to the ethyl group.

8.1.4 Photo-oxidation of $[RuBr_3(NO)(Et_2S)_2]$

In the presence of visible radiation the $[RuBr_3(NO)(Et_2S)_2]$ complex undergoes a photo-oxidation reaction of the sulphide ligands. The conversion of the sulphide ligand to a sulphoxide ligand may involve a free radical mechanism, where the source of the oxygen atoms is atmospheric oxygen. Both the complexes, $[RuBr_3(NO)(Et_2SO)(Et_2S)]$ and $[RuBr_3(NO)(Et_2SO)]_2$, contain oxygen coordinated sulphoxide ligands, this appears to be due to steric interactions which hinders coordination through the sulphur atom.

The ν(S-O) stretching frequency was found to correlate with the S-O bond length for both oxygen and sulphur atom coordinated sulphoxide ligands (Section 5.3.2). Therefore the S-O bond length and ν(S-O) stretching frequency are good indicators of the mode of coordination of the sulphoxide ligand, i.e. whether bonded through the oxygen or sulphur atom or is non bonded.

8.2 STEREOCHEMISTRY OF THE COMPLEXES

The trans-meridional stereochemistry of the $[RuX_3(NO)L_2]$

complexes was deduced from the n.m.r. results. The spectra obtained indicated only a single environment for all the alkyl groups within each complex, hence the other two possible isomers could be discounted. Assuming the stereochemistry of the complex remains unaltered from the solution to the solid, the single crystal X-ray structure analysis of $[RuBr_3(NO)(PhSEt)_2]$ confirmed the trans-meridional stereochemistry and indicated that the alkyl groups are equivalent due to a 2 fold rotation axis within each molecule. Since there is essentially a tetrahedral arrangement about each of the sulphur atoms in the $[RuBr_3(NO)(PhSEt)_2]$ complex (if the lone pair of electrons is considered), then it is possible to obtain complexes with the sulphide ligands in different orientations with respect to the '$RuBr_3(NO)$' unit. The crystal structure analysis revealed that in the solid state the two observed stereoisomers are mirror images of each other, (Section 7.3.1).

In solution there would appear to be little if any Ru-S π interaction to inhibit rotation about the Ru-S bond. Also the sulphur atom readily undergoes an inversion of configuration process, (Chapter 3). Hence the two different stereochemical arrangements isolated in the crystal structure were not able to be identified separately in solution.

The crystal structures of $[RuBr_3(NO)(Et_2SO)]_2$ and $[RuBr_3(NO)(Et_2SO)(Et_2S)]$ revealed the composition as well as the stereochemical arrangement of the products isolated in the photo-oxidation of $[RuBr_3(NO)(Et_2S)_2]$. These results facilitated in the postulation of a reaction scheme for the photochemical reaction.

APPENDIX A

ATTEMPTED SOLUTIONS FOR CRYSTAL STRUCTURES OF COBALT AND ZINC DITHIOCACODYLATO COMPLEXES

The compound [(dimethyl arsino)thio]dimethyl arsine sulphide,[179]

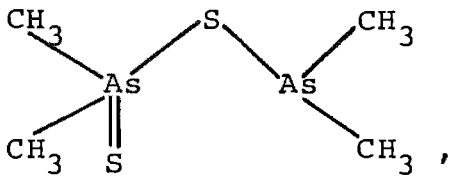

when reacted with cobalt and zinc salts forms complexes involving the dithiocacodylato anionic ligand,

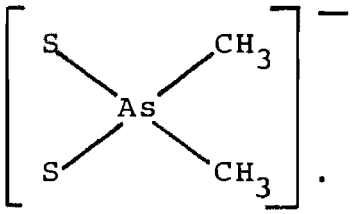

By varying the physical and chemical conditions of crystallisation, several products were obtained.[2]

The crystal structure of the zinc type (III) complex (see table below) has been determined,[2,3] therefore in an attempt to extend the work already carried out in this field the crystal structure analyses of the type I and type II complexes were attempted.

	Transition Metal Used	Crystal Type	Space Group
Type I	Co	hexagonal	$P6_3$ or $P6_3/m$
II	Co, Zn	monoclinic	$P2_1/n$
III	Zn	monoclinic	$P2_1/c$
IV	Zn	trigonal	-

The cobalt type I (hexagonal) crystal structure had been studied previously,[2] in this department, but needed to be reinvestigated since the calculated and observed densities did not agree. Also weak reflections on several X-ray photographs had been overlooked, so that the unit cell used in these earlier calculations was only $\frac{1}{3}$ of the true unit cell volume.

The methods used to prepare these crystalline products are presented in detail elsewhere.[2] However, in order to obtain a large type I crystal of the cobalt dithiocacodylato complex use was made of a specialised crystallisation apparatus[180] with dichloromethane as solvent and acetone as the precipitating agent. This isopiestic method of growing crystals was used at around $0^{o}C$ and well formed, dark green hexagonal discs resulted after three weeks.

Long, thin, transparent needle-like crystals of the zinc dithiocacodylato complex (type II) were prepared as before.[2]

The Crystal Structure of the Cobalt Complex

Weak reflections in the X-ray photographs were considered in redefining a new unit cell for the type I crystalline material and the hexagonal (6/m) symmetry was confirmed. The one condition limiting possible reflection (00ℓ, $\ell = 2n$) was consistent with either of the space groups $P6_3$ (noncentrosymmetric) or $P6_3/m$ (centrosymmetric). The methods detailed in Chapter 5 were used to refine the unit cell dimensions and to collect and process the intensity data. The unit cell constants were a = b = 18.623(3),

$c = 10.304(2)$ Å; $\alpha = \beta = 90^{\circ}$ and $\gamma = 120^{\circ}$. The crystal dimensions were 0.19 x 0.19 x 0.15 mm^3 and, using the four circle computer controlled Hilger and Watts diffractometer, 1033 independent reflections in the h, k, ℓ positive region of reciprocal space were collected for $0<2\theta<40^{\circ}$. With 319 reflections where $F_o^2 \geq 3\sigma(F_o^2)$ this data set contained about twice the number of strong reflections that the previous data set had.[2]

A three-dimensional Patterson synthesis revealed most peaks coincided with the Z = 0.0 and 0.5 sections. Therefore initial attempts used projection data (i.e. hk0 data only) to position the heavy atoms in two dimensions.

Assuming the space group to be noncentrosymmetric ($P6_3$), and using the least-squares and difference Fourier procedures detailed in Chapter 5, the best agreement factor obtained was $R_1 = 0.115$ for the 399 reflections where $F_o^2 \geq 2\sigma(F_o^2)$. However, impossible bond lengths and negative temperature factors for some atoms indicated this structure was incorrect.

By restarting and fixing the atoms in the positions located from successive structure factor calculations and difference Fourier syntheses, an agreement factor of $R_1 = 0.112$ was achieved when the constraints on the variables were released. Assigning anisotropic thermal parameters to all the atoms improved the agreement factor to $R_1 = 0.095$. This corresponded to $R_1 = 0.075$ for the 319 reflections where $F_o^2 \geq 3\sigma(F_o^2)$. However the structure was not chemically sensible and approximately ½ of the atoms had negative temperature factors.

The possibility of a simple disordered structure was then investigated using the centrosymmetric $P6_3/m$ space group, since this imposes a mirror plane at $Z = \frac{1}{4}$. The best agreement factor obtained from models in this space group was 0.127. The structure was chemically sensible and refined satisfactorily until the carbon atoms were added to the refinements. This was the same problem as had occurred in refinements of earlier models.

The basic structural unit that appeared in all the models was the type shown in the diagram below. A further methyl group should be bonded to each arsenic atom, however, considerable difficulty was encountered in locating the methyl carbon atoms.

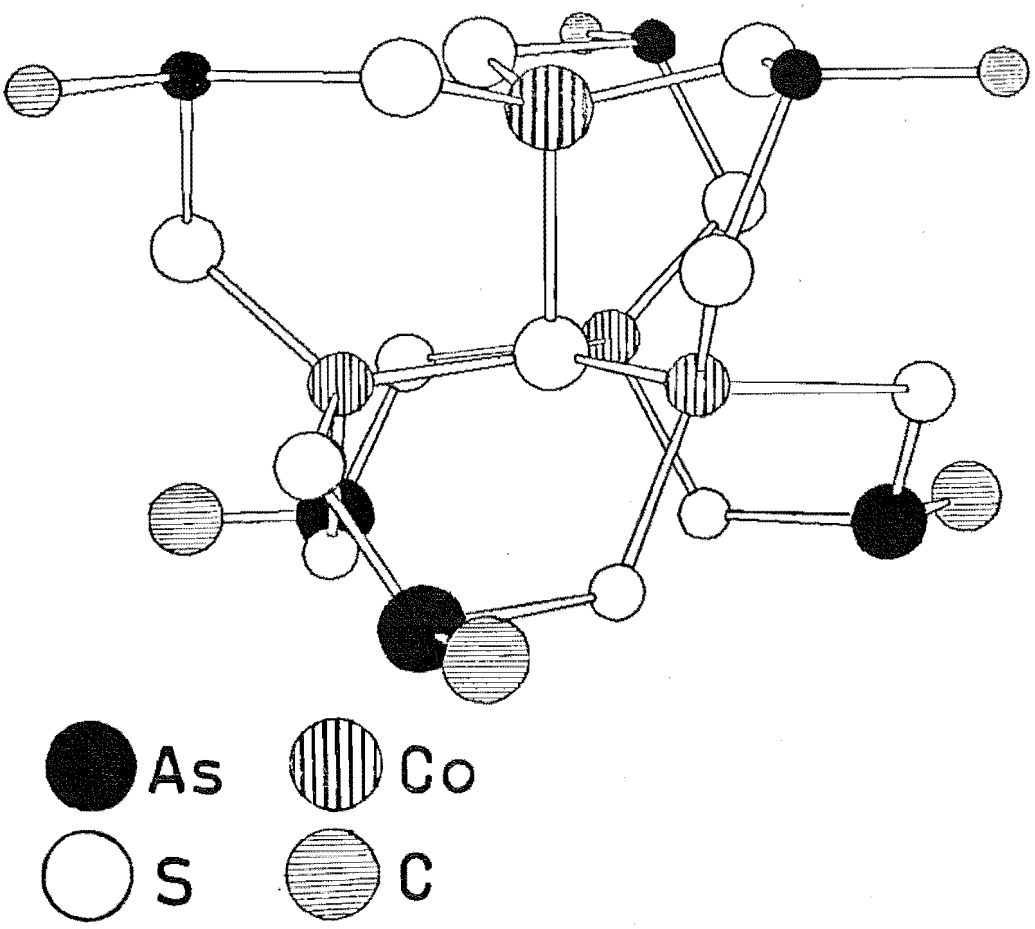

The actual crystal structure probably consists of the units shown but there is some unresolvable disorder of the methyl groups or of the units themselves. The above $Co_4As_6S_{13}C_{12}H_{36}$ formula unit gives reasonable agreement with the chemical analyses (Found: Co, 17.5%, S, 30.9%; C, 12.2%; H, 2.9%; Calculated: Co, 18.4%, S, 32.5%; C, 11.2%; H, 2.8%), similarly for 3 formula units in the unit cell the calculated (2.06 $g.cm^{-3}$) and the experimental (2.05(2) $g.cm^{-3}$) densities agree.

A larger crystal or else a more accurate data set may be needed if the solution to this structure is to be obtained.

The Crystal Structure of the Zinc Complex

The type II zinc dithiocacodylato complex crystallises in the space group $P2_1/n$, with a large unit cell, a = 32.508(12), b = 18.489(7), c = 30.589(12) and $\beta = 95.70(2)^{o}$. Of the 7389 independent reflections collected in the positive k and ℓ region of reciprocal space for $0<2\theta\leqslant 30^{o}$, only 735 reflections had $(F_o^2)\leqslant 3\sigma(F_o^2)$. From density measurements it appears that four of the $Zn_4As_6S_{13}C_{12}H_{36}$ formula units are in the asymmetric unit. Thus, with a total of 40 heavy atoms to be located, this appeared a suitable problem for modern direct methods computer programs and the problem was taken over by a fellow crystallographer experienced in these procedures. The crystal structure was eventually solved[181] and found to contain four of the $Zn_4As_6S_{13}C_{12}H_{36}$ units in the asymmetric unit. Three of the independent molecules had the same conformation as had been observed in type III crystals. The fourth independent molecule is another conformational isomer and appears to be the only known example of a chemical species belonging to symmetry point group T(23).

APPENDIX B

PHYSICAL METHODS

Throughout the work presented in this thesis several physical methods have been used to study the complexes prepared. The instrumental methods and techniques employed are outlined below.

Infrared Spectra

In the high frequency region (4000-400 cm^{-1}) a Shimadzu IR-27G spectrophotometer was used, with samples as nujol mulls between KBr plates or as KBr pellets. In the low frequency region (400-40 cm^{-1}) a R.I.I.C. Fourier FS720 spectrophotometer was used and samples were studied as nujol mulls on polythene discs.

N.m.r. Spectra

N.m.r. spectra were obtained using a Varian T-60 spectrometer at 60MHz and 32^{o}C with Me_4Si as internal standard. The spectra were recorded using deuterochloroform as the solvent. Details of the low temperature n.m.r. measurements are given in Section 3.3.

^{13}C n.m.r. spectra were recorded on a Varian CFT-20 instrument using deuterochloroform as solvent and as a field frequency lock signal, with Me_4Si as internal standard.

Ultra-violet and visible spectra

Ultra-violet and visible spectra were recorded over the range 240-800 nm using a Varian Techtron 635 spectrophotometer. The solvent used was chloroform.

Molar extinction coefficients (ε) were determined according to the expression

$$\varepsilon = {}^{A}/_{c.l}$$

where A is the absorbance,

c is the concentration in moles litre^{-1} and

l is the pathlength in cm.

X-ray powder photographs

X-ray powder photographs were collected using a Philips Debye Scherrer powder camera and Cu$K\alpha$ radiation.

Analyses

Carbon and hydrogen analyses were determined at the Microanalytical Laboratory, University of Otago, Dunedin.

Melting Points

Melting points were obtained using a Kofler hot-stage apparatus.

Crystallographic Computing Programs[145,171,172]

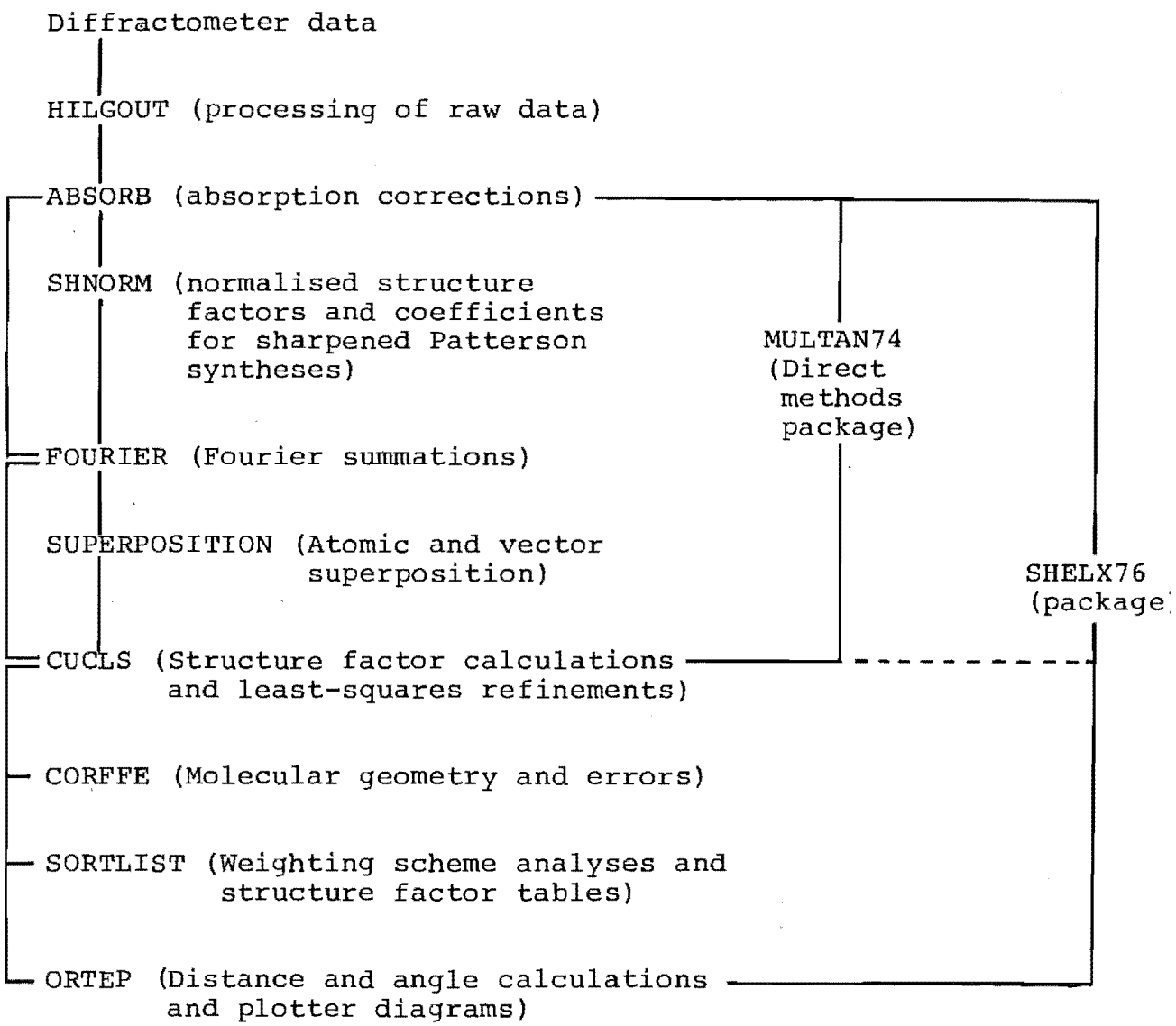

APPENDIX C

F_{obs} and F_{calc} values for $[RuBr_3(NO)(Et_2SO)]_2$

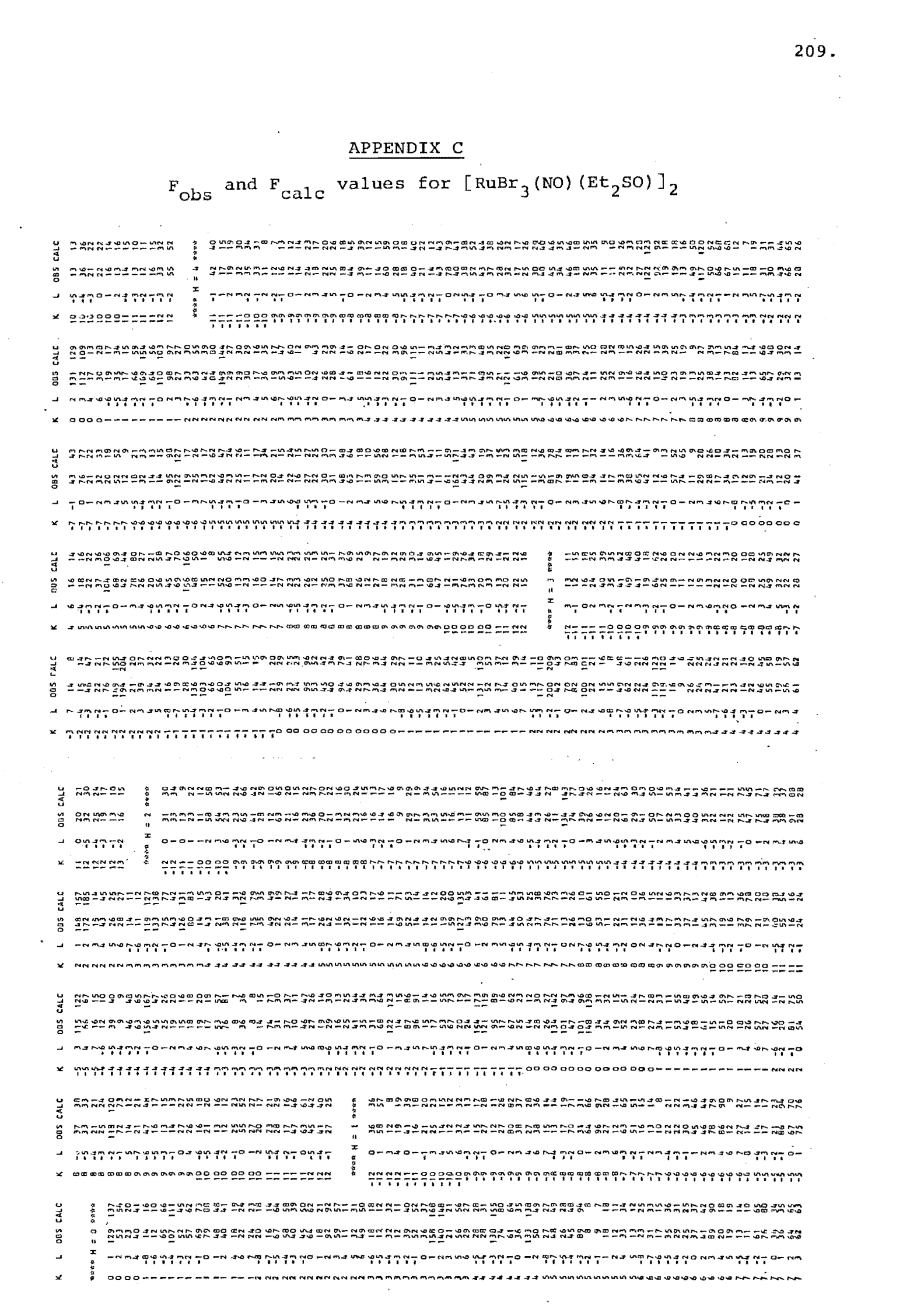

K	L	OBS	CALC
-2	-1	36	34
-2	1	36	34
-2	2	10	17
-2	3	24	24
-2	4	46	43
-1	-8	29	29
-1	-7	24	24
-1	-4	21	22
-1	-3	43	42
-1	-2	43	37
-1	-1	50	46
-1	0	56	54
-1	2	54	52
-1	3	83	81
-1	4	16	14
-1	5	22	19
-1	6	17	14
0	-4	13	12
0	-2	119	111
0	-1	131	123
0	0	19	20
0	1	14	18
0	2	99	96
0	3	63	61
1	-7	22	23
1	-6	74	71
1	-5	47	43
1	-4	49	44
1	-2	109	103
1	-1	41	37
1	0	33	30
1	2	23	22
1	6	16	14
2	-7	25	27
2	-6	64	59
2	-5	24	22
2	-3	10	10
2	-1	13	14
2	1	43	43
2	2	50	51
2	3	24	25
2	4	45	46
2	5	38	39
3	-7	17	15
3	-3	33	33
3	-2	41	42
3	-1	47	48
3	0	83	86
3	1	26	25
3	2	45	45
3	3	30	32
3	4	56	57
4	-5	44	42
4	-4	56	57
4	-3	19	19
4	-2	32	35
4	-1	98	99
4	0	92	95
4	2	12	13
4	4	12	10
5	-6	25	24
5	-5	94	97
5	-4	66	67
5	-3	21	20
5	-2	22	23
5	3	25	25
6	-7	13	13
6	-5	29	28
6	-4	24	23
6	-3	29	30
6	-1	41	42
6	0	22	22
6	1	40	38
6	2	48	49
7	-5	26	29
7	-4	30	32
7	-3	40	51
7	-2	25	26
7	-1	22	21
7	0	18	17
7	1	63	64
7	2	15	14
7	3	18	17
8	-7	14	9
-8	-6	12	13
-8	-4	58	58
-8	-3	85	87
-8	-2	16	17
-8	-1	13	12
-8	0	32	33
-8	1	17	19
-7	-7	30	31
-7	-4	26	26
-7	-3	19	18
-7	0	12	13
-6	-6	12	7
-6	-1	31	30
-6	0	18	19
-6	1	44	44
-6	2	30	20
-6	3	41	40
-6	5	13	12
-5	-7	15	10
-5	-6	41	40
-5	-5	40	40
-5	-4	30	30
-5	-3	24	22
-5	-2	104	97
-5	-1	104	104
-5	0	19	19
-5	3	23	25
-5	6	24	21
-4	-7	14	14
-4	-6	60	56
-4	-5	33	32
-4	-4	19	17
-4	-3	16	16
-4	-2	28	26
-4	-1	44	44
-4	1	22	19
-4	2	68	66
-4	3	31	30
-4	4	19	21
-4	5	30	29
-4	6	21	20
-3	-6	21	19
-3	-5	52	50
-3	-4	69	65
-3	-3	14	11
-3	-2	41	41
-3	-1	37	36
-3	0	100	103
-3	2	23	24
-3	4	16	16
-3	5	56	54
-3	6	19	19
-2	-7	77	76
-2	-4	13	13
-2	-1	24	25
-2	4	27	25
-2	5	27	27
-2	6	15	15
-1	-8	38	40
-1	0	33	33
-1	1	16	15
-1	2	38	37
-1	3	16	16
-1	4	19	19
-1	5	22	21
-1	6	13	16
0	-7	15	10
0	-6	41	40
0	-5	40	40
0	-4	30	30
0	-3	24	22
0	-2	104	97
0	-1	104	104
0	0	19	19
0	3	23	25
0	6	24	21
1	-7	14	14
1	-6	60	56
1	-5	33	32
1	-4	19	17
1	-3	16	16
1	-2	28	26
1	-1	44	44
1	1	22	19
1	2	33	30
1	4	19	21
1	5	30	29
2	-4	21	20
2	-2	28	27
2	-1	43	42
2	0	83	80
2	1	64	63
2	4	48	47
2	5	15	11
3	-6	21	19
3	-5	52	50
3	-4	69	65
3	-3	14	11
3	-2	41	41
3	-1	37	36
3	0	100	103
3	2	23	24
4	-8	16	16
4	-5	56	54
4	-4	77	76
4	-2	13	13
4	-1	24	25
4	3	27	25
4	4	23	22
5	-8	27	27
5	-5	15	15
5	-2	14	15
5	-1	38	40
5	0	33	33
5	1	16	15
5	2	38	37
5	3	16	16
6	-4	19	19
6	-3	22	21
6	-2	28	27
6	1	68	68
6	2	44	44
7	-7	22	22
7	-6	13	16
7	-4	43	43
7	-3	84	83
7	-2	18	19
7	-1	39	39
7	1	23	20
8	-7	29	30
8	-5	17	14
8	-4	28	26
8	-3	44	44
8	-2	17	17
8	1	25	23
8	2	14	11
9	-4	14	17
9	-3	24	24
9	-1	15	16
9	0	14	14
9	1	13	7
10	-2	49	47
10	-1	46	45
11	-4	14	13
11	-2	29	30

**** H = 6 ****

K	L	OBS	CALC
-9	0	40	40
-9	1	39	40
-9	3	14	13
-8	-3	19	18
-8	-2	16	17
-8	0	21	21
-8	4	20	18
-7	-4	17	21
-7	-3	12	1
-7	-1	15	16
-7	0	29	29
-7	1	25	25
-7	2	22	23
-7	3	21	23
-6	-4	13	12
-6	-3	16	17
-6	-2	14	15
-6	1	29	30
-6	2	68	66
-6	3	31	31
-5	-3	50	50
-5	-2	70	71
-5	0	37	38
-5	1	15	12
-5	2	21	22
-4	-6	22	21
-4	-5	17	17
-4	-3	39	39
-4	-2	31	32
-4	1	20	18
-4	2	20	23
-4	4	25	24
-4	5	23	25
-3	-6	21	22
-3	-3	17	16
-3	-2	29	29
-3	-1	15	15
-3	0	29	26
-3	1	22	23
-3	3	29	27
-3	4	31	32
-2	-6	15	14
-2	-2	33	32
-2	-1	85	81
-2	0	50	40
-2	1	27	27
-2	3	46	45
-1	-6	36	37
-1	-5	56	55
-1	-4	15	13
-1	-3	20	21
-1	-2	48	47
-1	-1	75	74
-1	1	29	30
-1	2	18	19
-1	3	17	16
0	-6	32	31
0	-5	48	44
0	2	37	38
0	3	28	29
0	5	28	28
1	-3	16	15
1	-2	44	45
1	-1	36	35
1	0	44	44
1	1	51	52
1	3	20	19
1	4	21	17
1	5	18	18
2	-5	22	23
2	-4	44	44
2	-3	27	28
2	-2	19	19
2	-1	25	26
2	0	96	93
2	1	57	57
3	-6	15	11
3	-5	38	36
3	-4	83	79
3	-3	29	26
3	-2	40	40
4	-6	21	19
4	-5	14	10
4	-4	18	18
4	-3	15	15
4	-2	16	15
4	-1	20	21
4	0	33	31
4	1	18	21
4	2	32	33
4	3	32	32
5	-5	26	25
5	-4	35	34
5	-3	35	35
5	-2	33	33
5	-1	14	15
5	1	34	34
5	2	41	42
6	-7	16	15
6	-3	63	63
6	-2	54	53
6	-1	14	13
6	1	30	30
7	-7	45	44
7	-6	22	22
7	-5	21	18
7	-3	20	22
7	-1	13	11
7	1	19	21
8	-6	14	15
8	0	24	24
8	1	13	14
9	-5	14	14
9	-4	15	14
9	-2	27	26
9	-1	37	36
10	-2	32	32
10	-1	24	23

**** H = 7 ****

K	L	OBS	CALC
-8	1	19	16
-8	2	13	11
-7	-3	16	17
-7	-2	24	23
-7	-1	26	28
-7	0	17	17
-7	1	13	18
-7	2	34	33
-7	3	21	19
-6	-3	19	17
-6	-2	39	39
-6	-1	18	16
-6	0	13	14
-6	2	31	30
-5	-2	28	28
-5	1	15	14
-5	2	24	25
-5	3	14	13
-4	-5	12	7
-4	-2	16	17
-4	1	17	23
-4	2	19	19
-4	3	29	30
-4	4	33	33
-3	-3	23	22
-3	-2	33	33
-3	-1	53	54
-3	0	40	38
-3	2	13	12
-3	3	25	26
-3	4	14	17
-2	-6	14	17
-2	-5	35	36
-2	-4	15	15
-2	-3	41	42
-2	0	18	21
-2	1	54	53
-2	2	10	20
-2	4	15	16
-1	-8	29	30
-1	-6	29	30
-1	-5	54	54
-1	-4	22	20
-1	-3	15	13
-1	-1	23	22
-1	0	17	18
-1	2	10	19
-1	3	17	18
0	-2	14	12
0	-1	32	32
0	0	30	31
0	1	39	40
0	2	23	24
1	-5	28	28
1	-4	43	44
1	-3	45	44
1	0	41	43
1	1	31	33
1	2	18	17
2	-4	62	64
2	-3	41	42
2	0	18	21
3	-6	15	15
3	-4	15	16
3	-1	15	15
3	0	33	36
3	1	19	17
3	2	16	12
4	-4	23	23
4	-3	18	17
4	-2	25	24
4	-1	20	22
4	1	23	23
4	2	41	45
4	3	17	13
4	4	23	22
5	-3	50	51
5	-2	53	56
5	0	21	23
6	-6	22	21
6	-3	26	28
6	-2	25	27
7	-4	18	15
7	-3	25	26
7	-2	21	23
7	0	18	20
8	-3	14	5
8	-2	19	19
8	-1	40	40
8	0	25	24
9	-3	19	16

**** H = 8 ****

K	L	OBS	CALC
-6	-2	23	25
-5	-2	15	18
-5	-1	17	19
-5	1	22	21
-4	-1	24	24
-4	0	37	37
-3	-5	31	33
-3	-4	27	30
-3	-1	36	35
-3	0	32	32
-2	-5	27	25
-2	-2	15	14
-2	3	19	22
-1	-2	26	26
-1	-1	30	34
-1	0	24	26
-1	1	27	27
-1	2	18	21
0	-4	25	24
0	-3	22	22
0	0	16	18
0	1	41	45
0	2	14	12
1	-4	42	45
1	-3	50	53
1	-1	24	24
1	2	15	9
2	-3	16	14
2	0	22	23
2	1	19	22
3	-4	21	24
3	-3	30	30
3	-2	19	21
3	-1	19	21
3	2	16	18
4	-3	23	24
4	-2	50	49

**** H = 9 ****

K	L	OBS	CALC
-4	-1	16	17
-2	0	17	16
-1	-4	23	24
-1	-3	25	29
-1	-2	21	21
-1	1	28	27
0	-3	28	30
1	0	18	21
2	-4	15	15
2	-3	19	19
2	-2	32	37
3	-2	16	18
4	-1	17	23
5	-4	16	12
5	-2	17	21
0	0	0	0
0	0	0	0
0	0	0	0

APPENDIX D

F_{obs} and F_{calc} values for $[RuBr_3(NO)(Et_2SO)(Et_2S)]$

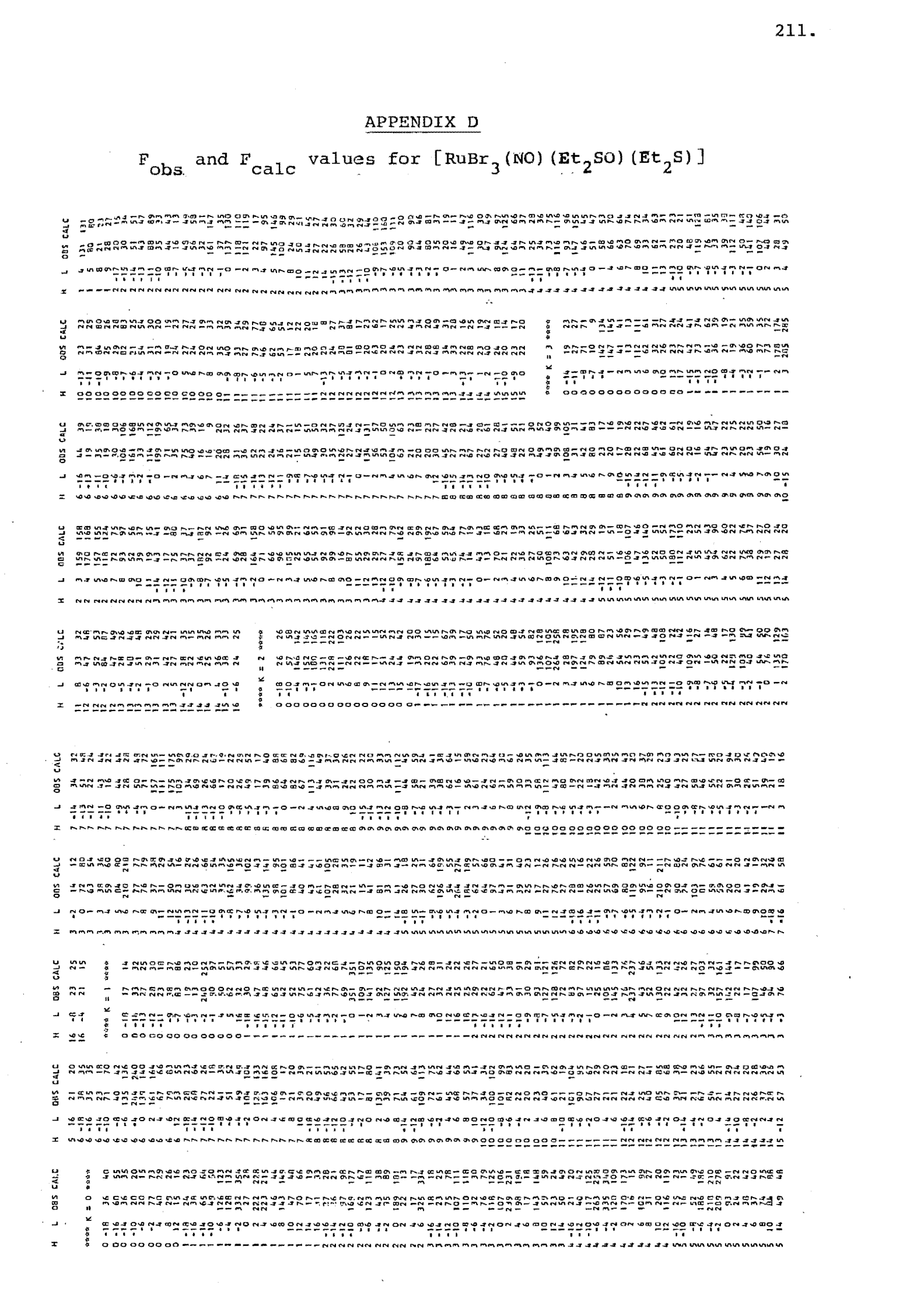

H	L	OBS	CALC
5	5	17	19
5	8	32	35
5	9	58	60
5	10	23	21
5	11	30	30
5	14	20	22
5	15	28	28
6	-18	23	15
6	-17	40	34
6	-15	20	13
6	-12	19	22
6	-9	32	35
6	-7	38	39
6	-5	48	49
6	-3	71	74
6	-2	151	154
6	-1	94	95
6	0	25	21
6	1	143	141
6	6	20	24
6	7	37	34
6	8	24	24
6	10	24	19
6	12	33	29
6	13	23	18
7	-17	21	18
7	-16	31	31
7	-15	35	31
7	-13	31	30
7	-11	30	32
7	-8	18	23
7	-7	43	46
7	-6	35	35
7	-4	16	19
7	-3	57	61
7	-2	44	44
7	-1	155	159
7	0	65	65
7	1	25	24
7	2	47	47
7	3	66	65
7	5	75	75
7	6	55	57
7	8	24	20
7	10	26	25
8	-17	28	27
8	-15	36	32
8	-14	31	28
8	-12	34	34
8	-11	70	71
8	-9	27	30
8	-6	39	40
8	-5	39	39
8	-4	33	35
8	-3	42	42
8	-2	18	17
8	-1	36	36
8	1	63	62
8	3	53	55
8	4	79	80
8	5	56	54
8	7	70	71
9	-13	64	63
9	-11	50	49
9	-10	59	58
9	-9	52	53
9	-5	27	24
9	-1	17	11
9	0	28	31
9	2	32	33
9	3	43	41
9	5	90	88
9	6	43	41
10	-16	20	10
10	-12	31	31
10	-11	57	58
10	-9	40	42
10	-8	42	40
10	-6	34	34
10	-5	71	72
10	-3	31	34
10	1	26	27
10	2	19	17
10	3	34	33
10	4	20	23
10	5	22	19
10	7	31	29
11	-9	23	22
11	-7	77	77
11	-6	18	9
11	-5	53	52
11	-4	59	61
11	-3	46	47
11	1	19	17
12	-6	42	41
12	-5	64	65
12	-3	44	45
12	-2	25	30
12	0	22	19
12	1	41	39
12	3	25	25
12	4	19	2
13	-4	20	20
13	-3	19	19
13	-1	51	51
13	1	29	32
13	2	29	30
13	3	22	23
14	0	27	28
14	1	45	40
15	-8	23	15
15	-4	20	13

**** K = 4 ****

H	L	OBS	CALC
0	-17	18	18
0	-15	24	25
0	-14	17	16
0	-7	33	34
0	-4	13	6
0	-3	205	203
0	-1	98	93
0	0	29	29
0	2	45	45
0	5	13	14
0	8	20	21
0	11	19	22
0	13	28	26
1	-15	22	20
1	-13	34	39
1	-11	72	72
1	-9	45	46
1	-7	42	44
1	-6	35	32
1	-5	40	39
1	-4	45	46
1	-3	25	24
1	-1	103	101
1	1	195	192
1	2	41	37
1	4	56	56
1	5	150	148
1	6	24	26
1	7	42	42
1	10	35	36
1	11	23	24
2	-15	31	31
2	-13	81	79
2	-11	42	43
2	-9	27	30
2	-8	59	60
2	-7	60	62
2	-4	16	15
2	-2	48	48
2	-1	34	36
2	0	18	18
2	2	30	35
2	3	196	197
2	4	40	39
2	5	57	56
2	6	37	40
2	7	37	37
2	9	88	91
3	-15	29	27
3	-13	44	46
3	-11	75	75
3	-10	37	38
3	-9	50	52
3	-8	39	38
3	-7	46	49
3	-5	108	113
3	-4	14	10
3	-3	52	54
3	-2	29	29
3	-1	71	71
3	0	41	44
3	1	49	46
3	2	28	27
3	4	42	43
3	5	62	60
3	6	21	20
3	7	104	105
3	8	19	23
3	11	52	52
3	13	20	19
4	-11	19	15
4	-9	49	51
4	-7	196	205
4	-5	67	68
4	-4	20	10
4	-3	55	54
4	-2	52	51
4	-1	31	34
4	1	20	21
4	2	16	17
4	4	55	49
4	9	92	91
4	11	35	36
4	15	31	27
5	-17	22	22
5	-13	26	24
5	-11	29	25
5	-9	75	77
5	-7	91	94
5	-6	31	32
5	-5	129	138
5	-4	25	21
5	-3	68	71
5	-2	19	17
5	-1	48	48
5	1	115	118
5	2	31	33
5	3	53	53
5	5	45	43
5	6	16	10
5	7	31	30
5	9	21	20
5	11	29	26
5	13	35	36
6	-15	35	31
6	-11	18	16
6	-8	17	19
6	-7	38	38
6	-6	27	31
6	-5	24	24
6	-4	18	17
6	-3	85	88
6	-1	207	211
6	1	54	54
6	2	28	27
6	3	26	23
6	5	29	26
7	-17	47	43
7	-15	22	19
7	-9	18	22
7	-8	23	24
7	-7	40	40
7	-5	35	38
7	-3	92	93
7	-1	84	87
7	0	52	53
7	1	114	117
7	3	29	23
7	6	17	14
7	7	45	49
8	-15	31	25
8	-13	56	55
8	-12	22	21
8	-11	50	45
8	-9	56	54
8	-7	46	46
8	-5	24	26
8	-4	19	14
8	-2	32	33
8	-1	53	57
8	0	17	16
8	1	26	31
8	2	25	28
8	3	38	38
8	5	108	106
9	-11	83	81
9	-9	40	44
9	-3	20	24
9	-2	26	25
9	-1	35	34
9	1	31	30
9	3	66	65
9	5	36	33
9	7	57	56
10	-13	35	34
10	-11	28	27
10	-9	46	45
10	-7	66	67
10	-6	23	23
10	-5	57	57
10	-3	50	50
10	-1	39	35
10	1	19	21
10	5	46	47
11	-11	23	22
11	-9	20	25
11	-6	22	22
11	-5	94	96
11	-3	30	32
11	3	32	31
12	-7	48	50
12	-5	28	29
12	-3	40	41
12	-1	38	37
12	1	37	36
12	3	27	25
13	-5	29	25
13	-3	24	19
13	-1	22	17
13	1	57	54
13	3	24	19
14	-1	31	34
14	1	24	21

**** K = 5 ****

H	L	OBS	CALC
0	-10	38	38
0	-5	51	50
0	-2	45	42
0	1	164	159
0	3	33	31
0	4	89	89
0	6	68	66
0	12	16	11
1	-15	31	35
1	-13	34	30
1	-12	30	27
1	-11	19	19
1	-8	57	50
1	-7	23	24
1	-6	31	35
1	-3	39	39
1	-2	72	73
1	-1	71	71
1	0	41	39
1	1	74	71
1	2	100	102
1	3	155	153
1	4	84	79
1	5	58	55
1	6	17	14
1	7	19	20
1	8	36	34
1	9	17	17
1	14	24	19
1	15	20	21
2	-14	24	21
2	-13	28	39
2	-11	68	71
2	-8	20	23
2	-7	20	22
2	-6	35	34
2	-4	71	70
2	-2	56	56
2	-1	24	26
2	0	93	94
2	1	71	71
2	2	83	79
2	5	103	102
2	6	24	26
2	8	81	82
2	10	54	53
2	12	18	26
3	-13	33	33
3	-12	33	28
3	-10	17	13
3	-9	81	83
3	-8	40	40
3	-7	70	72
3	-6	49	49
3	-4	29	30
3	-3	19	17
3	-2	59	58
3	0	49	50
3	3	44	45
3	4	80	82
3	5	60	63
3	7	31	32
3	8	66	67
3	9	67	60
3	10	33	31
3	11	26	24
4	-14	24	26
4	-11	42	43
4	-9	41	42
4	-8	32	31
4	-7	61	63
4	-6	21	20
4	-5	138	139
4	-3	29	25
4	-2	16	24
4	-1	28	29
4	0	47	47
4	2	79	82
4	4	41	37
4	6	39	38
4	7	43	48
4	8	33	34
4	11	38	34
4	13	30	34
5	-10	22	20
5	-9	23	22
5	-8	19	20
5	-7	86	90
5	-6	40	41
5	-3	114	117
5	-2	53	63
5	-1	78	79
5	0	56	55
5	2	38	39
5	4	23	24
5	6	26	23
5	10	36	34
6	-8	29	27
6	-6	17	17
6	-5	78	78
6	-4	11	11
6	-3	58	62
6	-2	41	41
6	-1	75	76
6	0	31	32
6	1	89	87
6	4	21	21
6	6	40	39
6	8	35	38
6	10	24	22
7	-15	27	24
7	-13	20	26
7	-12	18	19
7	-10	21	19
7	-3	47	48
7	-1	87	89
7	0	35	33
7	3	68	69
7	4	42	39
7	5	38	37
7	6	37	36
8	-15	29	28
8	-11	45	46
8	-9	23	22
8	-8	17	19
8	-2	30	33
8	0	22	27
8	1	58	60
8	3	50	50
8	4	32	32
8	5	24	21
8	7	33	35
9	-13	42	41
9	-11	31	29
9	-10	24	21
9	-9	38	38
9	-7	44	45
9	-6	17	19
9	1	18	18
9	2	24	21
9	3	21	21
9	5	45	45
9	9	22	24
10	-11	37	38
10	-10	20	19
10	-9	57	55
10	-5	48	48
10	-2	23	22
10	7	27	28
11	-10	23	15
11	-7	64	62
11	-5	23	27
11	-4	20	22
11	-3	37	34
12	-5	40	40
12	-4	22	17
12	-3	45	45
12	1	20	22
13	-1	43	39

**** K = 6 ****

H	L	OBS	CALC
0	-16	33	30
0	-4	18	17
0	-3	45	45
0	-2	63	64
0	-1	82	82
0	0	39	35
0	5	24	25
0	6	27	28
1	-14	26	18
1	-13	30	28
1	-12	19	10
1	-9	23	19
1	-7	21	23
1	-6	17	16
1	-5	45	48
1	-4	54	55
1	-3	26	27
1	-2	17	14
1	-1	74	72
1	1	99	105
1	2	57	58
1	4	49	51
1	5	54	55
1	7	30	31
1	10	24	27
1	11	24	21
2	-15	27	25
2	-12	26	30
2	-10	18	15
2	-9	67	69
2	-7	21	22
2	-6	27	27
2	-1	50	53
2	0	19	18
2	1	21	18
2	2	31	31
2	3	49	47
2	4	42	40
2	5	68	67
2	6	38	36
2	7	50	52
2	8	44	44
2	9	22	24
3	-11	58	60
3	-9	28	26
3	-8	44	47
3	-7	52	55
3	-4	22	21
3	-3	31	30
3	-1	24	27
3	0	24	24
3	1	30	31
3	2	39	41
3	3	35	32
3	5	42	42
3	7	54	57
3	8	33	33
3	10	20	19
3	11	21	18
4	-11	18	14
4	-10	20	23
4	-9	59	62
4	-6	45	46
4	-5	20	24
4	-4	25	26
4	-3	88	93
4	-2	36	37
4	0	23	23
4	3	32	30
4	5	29	32
4	6	30	29
4	8	20	16
4	9	26	28
4	10	26	26
4	11	26	20
4	12	20	13
5	-11	20	19
5	-8	42	44
5	-5	113	114
5	-4	21	19
5	-3	43	46
5	-2	47	47
5	-1	61	61
5	0	19	23
5	1	21	23
5	3	26	29
5	6	21	17
5	8	23	26
5	11	20	15
6	-11	20	18
6	-7	21	20
6	-6	26	30
6	-5	37	37
6	-4	41	40
6	-3	95	95
6	-1	34	31
6	0	49	49
6	1	23	23
6	2	29	31
6	3	49	47
6	4	21	20
6	6	25	26
6	11	21	23
7	-15	33	28
7	-9	21	23
7	-7	31	26
7	-5	43	45
7	-2	34	37
7	1	69	68
7	3	38	41
7	4	43	40
7	5	30	30
8	-13	34	35
8	-7	36	35
8	-5	19	18
8	-4	20	14
8	0	26	28
8	1	40	37
8	2	30	32
8	3	65	65
8	6	28	23
9	-11	23	24
9	-9	49	43
9	-0	21	18
9	-6	19	16
9	-3	22	22
9	-1	33	35
9	1	37	30
9	4	23	24
9	7	26	27
10	-12	20	12
10	-10	31	29
10	-9	20	19
10	-7	58	58
10	-3	20	13
10	-1	21	19
11	-9	37	36
11	-8	22	18
11	-5	21	21
11	-3	35	35
11	0	19	19
12	-5	23	20
12	-4	28	24
12	-1	40	39
13	-3	34	33

**** K = 7 ****

H	L	OBS	CALC
0	-8	36	36
0	-2	67	66
0	1	48	49
0	6	33	34
1	-10	35	35
1	-8	22	24
1	-1	39	40
1	0	87	87
1	1	21	22
1	3	33	32
1	5	18	15
1	6	64	61
1	7	27	28
2	-12	23	24
2	-11	21	25
2	-10	25	27
2	-8	26	27
2	-7	24	26
2	-5	37	37
2	-2	56	55
2	0	33	33
2	4	55	55
2	5	35	39
2	7	33	35
2	8	56	52
3	-12	28	27
3	-10	40	38
3	-9	45	46
3	-8	20	19
3	-5	19	12
3	-4	45	43
3	5	31	36
3	6	70	69
3	7	18	14
3	9	19	23
4	-12	19	18
4	-11	29	25
4	-10	33	35
4	-8	35	33
4	-7	20	22
4	-6	25	25
4	-5	29	29
4	-4	31	32
4	-3	23	20
4	-2	42	42
4	1	28	30
4	2	19	22
4	4	40	42
4	7	25	26
4	8	27	19
4	10	24	24
5	-7	19	8
5	-6	39	39
5	-5	20	21
5	-4	60	61
5	-3	54	57
5	-2	17	17
5	2	40	45
6	-9	22	21
6	-7	21	21
6	-6	19	19
6	-5	38	38
6	-4	40	38
6	-3	22	22
6	-2	33	35
6	-1	19	16
6	0	37	38
6	1	26	26
6	2	20	14
6	4	33	32
7	-6	18	18
7	-4	25	24
7	0	33	27
7	2	50	48
7	3	42	43
7	8	20	20
8	-12	23	15
8	-5	18	3
8	-1	19	22
8	0	27	28
8	1	41	38
8	2	26	26
8	3	19	20
8	4	29	28
8	6	21	13
9	-10	24	21
9	-8	21	17
9	-7	24	24
9	-6	20	16
9	-3	22	20
9	2	23	20
10	-9	33	31
10	-8	34	29
10	0	22	15
11	-6	22	21
11	-1	27	22

**** K = 8 ****

H	L	OBS	CALC
0	-6	27	28
0	0	90	87
1	-8	21	25
1	-4	18	15
1	-2	52	52
1	0	19	19
1	2	40	39
1	4	37	39
1	5	20	21
1	8	41	40
2	-10	33	32
2	-8	25	23
2	-5	18	14
2	-4	21	25
2	0	30	33
2	1	22	24
2	3	26	26
2	6	72	68
3	-10	33	31
3	-8	25	20
3	-2	24	26
3	-1	29	27
3	0	24	26
3	2	19	11
3	4	51	53
3	8	29	26
4	-10	28	25
4	-6	30	28
4	-5	25	22
4	-4	46	46
4	-2	25	27
4	2	20	25
4	6	27	29
4	7	21	17
5	-10	20	14
5	-8	22	20
5	-6	30	32
5	-4	34	35
5	-2	29	31
5	4	30	27
6	-6	24	24
6	-4	29	29
6	-1	20	20
6	0	28	25
6	2	43	44
6	4	21	17
7	-5	26	20
7	-4	21	16
7	-3	23	18
7	-2	23	23
7	0	35	32
7	1	20	16
7	4	24	23
8	0	22	23
8	2	21	27

**** K = 9 ****

H	L	OBS	CALC
0	-2	32	35
0	4	23	23
1	0	30	29
1	2	22	21
1	4	20	23
1	5	19	10
1	6	22	24
2	-3	20	18
2	-1	21	20
2	2	22	26
2	4	28	32
3	-6	26	27
3	-5	25	19
3	1	23	22
3	6	21	19
4	-8	35	33
4	-4	24	24
4	-2	27	27
4	0	25	25
4	2	29	28
4	4	30	28
4	6	26	22
4	8	23	24
5	-8	22	20
5	-6	20	20
5	-4	23	23
5	-2	43	44
5	0	28	25
5	2	32	32
5	4	21	20
5	6	24	23
6	-4	30	27
6	-2	24	24
6	0	29	29
6	2	20	20
6	4	17	17
6	6	24	23
7	-2	23	23
7	0	35	32
7	2	28	28
7	4	23	23
8	0	23	23
8	2	27	27

**** K =10 ****

H	L	OBS	CALC
0	2	28	27
1	0	19	18
1	2	23	23
0	0	0	0

APPENDIX E

F_{obs} and F_{calc} values for $[RuBr_3(NO)(PhSEt)_2]$

**** L = 0 ****

H	K	OBS	CALC
-16	0	72	70
-16	2	75	77
-16	3	59	52
-16	4	63	70
-16	7	34	34
-14	1	30	35
-14	2	27	24
-14	3	127	125
-14	5	121	122
-14	11	50	52
-13	3	29	31
-12	0	87	84
-12	1	59	59
-12	2	90	82
-12	3	85	84
-12	4	128	128
-12	5	55	55
-12	6	134	137
-12	7	90	85
-12	10	29	36
-11	1	121	119
-11	2	23	21
-11	5	33	30
-11	10	32	34
-10	1	232	218
-10	3	61	64
-10	5	61	61
-10	6	42	35
-10	7	150	141
-10	8	41	33
-10	9	151	149
-10	11	44	48
-9	8	46	50
-9	9	43	42
-8	0	387	366
-8	1	123	115
-8	2	273	250
-8	3	159	132
-8	4	61	50
-8	5	37	40
-8	6	72	72
-8	7	106	96
-8	8	133	133
-8	9	25	27
-8	10	132	130
-8	11	73	65
-8	14	34	35
-7	0	22	20
-7	6	41	44
-7	7	82	81
-7	8	34	35
-7	13	30	37
-7	14	37	37
-7	15	37	31
-6	1	157	148
-6	2	43	45
-6	3	333	290
-6	5	301	265
-6	10	114	110
-6	11	110	104
-6	12	62	60
-6	13	103	104
-6	14	36	35
-5	2	32	32
-5	3	59	59
-5	4	68	68
-5	6	47	48
-5	7	35	39
-5	12	41	49
-4	0	31	19
-4	1	136	121
-4	2	305	277
-4	3	64	66
-4	4	452	457
-4	5	59	60
-4	7	123	93
-4	10	31	51
-4	11	37	43
-4	12	94	100
-4	14	84	91
-4	15	34	28
-3	3	37	40
-3	5	61	67
-3	7	58	54
-3	8	41	44
-3	10	51	51
-3	12	43	37
-3	13	41	36
-2	1	273	263
-2	2	84	95
-2	3	329	329
-2	4	84	89
-2	5	324	267
-2	8	68	49
-2	10	143	124
-2	13	42	45
-2	14	68	62
-2	16	39	48
-1	1	25	17
-1	5	35	34
-1	6	46	39
-1	8	76	69
-1	9	88	80
-1	11	55	52
-1	12	36	39
-1	14	34	26
-1	16	33	42
-1	17	37	39
0	2	331	392
0	4	113	103
0	6	83	77
0	8	296	290
0	10	213	215
0	12	80	74
0	14	44	50
1	10	85	84
1	15	30	37
2	6	197	167
2	7	280	243
2	9	181	162
2	11	96	94
2	12	63	66
2	15	49	48
2	17	37	40
3	4	52	49
3	6	68	65
3	9	36	38
3	11	55	51
4	6	307	277
4	8	97	86
4	9	34	35
5	11	34	32
5	13	54	58
5	15	31	31
6	6	96	97
6	7	122	117
6	9	76	72
6	16	33	41
7	5	31	28
7	10	46	55
7	11	82	87

**** L = 1 ****

H	K	OBS	CALC
-16	1	43	47
-16	3	57	57
-16	4	57	57
-14	2	58	50
-14	4	90	87
-14	6	90	97
-13	2	41	44
-13	3	41	44
-13	5	40	37
-12	1	30	27
-12	2	74	72
-12	3	57	57
-12	5	94	96
-12	6	83	80
-12	7	100	97
-11	1	50	53
-11	3	35	30
-11	4	36	31
-11	5	41	44
-11	10	36	39
-10	0	201	187
-10	1	76	77
-10	2	74	70
-10	3	74	76
-10	6	72	65
-10	7	87	85
-10	8	110	114
-10	10	44	51
-9	0	30	42
-9	1	54	58
-9	2	32	35
-9	3	33	35
-9	5	43	39
-9	7	48	52
-9	8	40	52
-9	9	51	60
-8	0	52	55
-8	1	194	185
-8	2	96	96
-8	3	86	87
-8	4	87	83
-8	6	82	89
-8	7	92	89
-8	8	205	188
-8	9	92	85
-8	11	101	97
-7	0	36	43
-7	1	45	48
-7	3	54	39
-7	5	53	62
-7	6	63	56
-7	7	68	73
-7	8	31	32
-7	11	41	40
-7	14	42	36
-6	0	32	25
-6	1	69	59
-6	2	125	117
-6	3	67	71
-6	4	205	188
-6	5	59	65
-6	6	52	49
-6	7	51	53
-6	9	46	46
-6	10	61	60
-6	11	76	73
-6	12	67	67
-6	13	36	33
-5	1	61	61
-5	3	68	74
-5	4	66	72
-5	5	99	103
-5	6	43	53
-5	7	47	39
-5	12	47	41
-5	13	41	47
-5	14	40	43
-4	0	37	36
-4	1	104	101
-4	2	90	82
-4	3	210	194
-4	4	90	82
-4	5	312	291
-4	6	97	98
-4	7	142	130
-4	8	42	39
-4	9	34	26
-4	10	72	62
-4	13	58	70
-4	15	43	41
-3	0	75	79
-3	1	67	78
-3	2	55	77
-3	3	111	119
-3	4	100	99
-3	5	46	43
-3	7	28	24
-3	10	54	60
-3	11	52	65
-3	12	42	48
-2	0	224	268
-2	1	86	104
-2	2	176	149
-2	3	114	95
-2	5	128	145
-2	6	155	125
-2	7	97	90
-2	8	125	116
-2	9	67	67
-2	10	54	50
-2	11	95	101
-2	14	44	49
-2	15	51	58
-2	16	69	67
-1	0	82	90
-1	1	104	107
-1	2	34	28
-1	3	73	58
-1	4	120	110
-1	6	44	31
-1	7	31	24
-1	8	65	54
-1	9	104	98
-1	10	94	102
-1	11	65	63
0	0	90	106
0	1	264	316
0	2	40	47
0	3	44	54
0	4	54	47
0	5	30	43
0	6	40	36
0	7	32	29
0	8	32	25
0	9	43	41
0	10	32	34
0	11	32	37
0	12	32	41
0	13	32	30
0	14	32	26
0	15	32	32
0	16	32	32
0	17	32	32
1	0	32	32
1	1	32	32
1	2	32	32
1	3	32	32
1	4	32	32
1	5	32	32
1	6	32	32
1	7	32	32
1	8	32	32
1	9	32	32
1	10	32	32
1	11	32	32
1	12	32	32
1	13	32	32
1	14	32	32
1	15	32	32
1	16	32	32
1	17	32	32
2	0	32	32
2	1	32	32
2	2	32	32
2	3	32	32
2	4	32	32
2	5	32	32
2	6	32	32
2	7	32	32
2	8	32	32
2	9	32	32
2	10	32	32
2	11	32	32
2	12	32	32
2	13	32	32
2	14	32	32
2	15	32	32
2	16	32	32
2	17	32	32
3	0	32	32
3	1	32	32
3	2	32	32
3	3	32	32
3	4	32	32
3	5	32	32
3	6	32	32
3	7	32	32
3	8	32	32
3	9	32	32
3	10	32	32
3	11	32	32
4	0	32	32
4	1	32	32
4	2	32	32
4	3	32	32
4	4	32	32
4	5	32	32
4	6	32	32
4	7	32	32
4	8	32	32
4	9	32	32
4	10	32	32
4	11	32	32
5	0	32	32
5	1	32	32
5	2	32	32
5	3	32	32
5	4	32	32
5	5	32	32
5	6	32	32
5	7	32	32
5	8	32	32
5	9	32	32
5	10	32	32
5	11	32	32
6	0	32	32
6	1	32	32
6	2	32	32
6	3	32	32
6	4	32	32
6	5	32	32
6	6	32	32
6	7	32	32
6	8	32	32
6	9	32	32
6	10	32	32
6	11	32	32
7	0	32	32
7	1	32	32
7	2	32	32
7	3	32	32
7	4	32	32
7	5	32	32
7	6	32	32
7	7	32	32
7	8	32	32
7	9	32	32
7	10	32	32
7	11	32	32
7	12	32	32

**** L = 2 ****

H	K	OBS	CALC
-17	1	38	33
-17	3	44	48
-15	3	51	51
-15	5	48	45
-13	0	32	29
-13	1	44	41
-13	3	52	56
-13	4	71	67
-13	6	46	50
-13	7	47	48
-12	0	43	37
-12	5	35	29
-12	6	56	57
-12	10	35	25
-11	1	44	44
-11	2	59	59
-11	4	65	65
-11	7	55	56
-11	9	55	56
-10	0	152	157
-9	1	40	53
-9	2	50	55
-9	3	63	66
-9	4	73	73
-9	8	79	84
-9	10	75	75
-8	0	39	47
-8	2	91	99
-8	4	55	56
-8	5	44	46
-8	6	51	55
-8	7	32	38
-8	10	40	32
-8	11	36	34
-7	1	37	37
-7	2	126	123
-7	3	59	57
-7	4	31	31
-7	5	31	31
-7	7	79	77
-7	10	66	64
-7	12	34	46
-6	0	32	29
-6	1	34	34
-6	3	43	43
-6	4	31	25
-6	6	37	41
-6	7	50	51
-6	10	34	42
-6	11	34	36
-5	0	31	32
-5	1	46	46
-5	3	40	44
-5	4	169	161
-5	5	62	63
-5	6	112	108
-5	8	66	61
-5	9	56	55
-5	10	43	37
-5	12	54	58
-5	13	33	27
-4	0	126	147
-4	1	71	65
-4	2	59	61
-4	4	42	50
-4	5	41	51
-4	6	64	65
-4	7	34	41
-4	9	34	29
-4	10	42	45
-3	1	73	71
-3	2	152	138
-3	3	50	46
-3	4	44	43
-3	5	137	123
-3	6	160	139
-3	7	46	50
-3	9	31	21
-3	10	72	68
-3	11	41	33
-3	12	31	24
-3	14	45	45
-2	0	151	186
-2	1	50	59
-2	2	56	60
-2	4	104	118
-2	5	63	62
-2	6	48	55
-2	8	38	26
-2	9	55	49
-2	10	52	54
-1	1	172	170
-1	2	145	143
-1	3	38	38
-1	5	63	62
-1	6	54	49
-1	7	58	53
-1	8	124	111
-1	9	43	40
-1	10	131	120
-1	11	45	40
0	0	151	166
0	1	50	59
0	2	56	60
0	4	104	118
0	5	63	62
0	6	48	55
0	8	38	26
0	9	55	49
0	10	38	37
1	0	46	61
1	1	172	170
1	2	145	143
1	3	38	38
1	5	63	62
1	6	54	49
1	7	58	53
1	8	124	111
1	9	43	40
1	10	131	120
1	11	45	40
2	0	151	166
2	1	50	59
2	2	56	60
2	4	104	118
2	5	63	62
2	6	48	55
2	8	38	26
2	9	55	49
2	10	38	37
3	0	46	61
3	1	172	170
3	2	145	143
3	3	38	38
3	5	63	62
3	6	54	49
3	7	58	53
3	8	124	111
3	9	43	40
3	10	131	120
3	11	45	40
4	0	151	166
4	1	50	59
4	2	56	60
4	4	104	118
4	5	63	62
4	6	48	55
4	8	38	26
4	9	55	49
4	10	38	37
5	0	46	61
5	1	172	170
5	2	145	143
5	3	38	38
5	5	63	62
5	6	54	49
5	7	58	53
5	8	124	111
5	9	43	40
5	10	131	120
5	11	45	40
6	0	151	166
6	1	50	59
6	2	56	60
6	4	104	118
6	5	63	62
6	6	48	55
6	8	38	26
6	9	55	49
6	10	38	37
7	0	46	61
7	1	172	170
7	2	145	143
7	3	38	38
7	5	63	62
7	6	54	49
7	7	58	53
7	8	124	111
7	9	43	40
7	10	131	120
7	11	45	40
8	0	151	166
8	1	50	59
8	2	56	60
8	4	104	118
8	5	63	62
8	6	48	55
8	8	38	26
8	9	55	49
8	10	38	37
9	0	46	61
9	1	172	170
9	2	145	143
9	3	38	38
9	5	63	62
9	6	54	49
9	7	58	53
9	8	124	111
9	9	43	40
9	10	131	120
9	11	45	40
10	0	151	166
10	1	50	59
10	2	56	60
10	4	104	118
10	5	63	62
10	6	48	55
10	8	38	26
10	9	55	49
10	10	38	37
11	0	46	61
11	1	172	170
11	2	145	143
11	3	38	38
11	5	63	62
11	6	54	49
11	7	58	53
11	8	124	111
11	9	43	40
11	10	131	120
11	11	45	40
12	0	151	166
12	1	50	59
12	2	56	60
12	4	104	118
12	5	63	62
12	6	48	55
12	8	38	26
12	9	55	49
12	10	38	37
13	0	46	61
13	1	172	170
13	2	145	143
13	3	38	38
13	5	63	62
13	6	54	49
13	7	58	53
13	8	124	111
13	9	43	40
13	10	131	120
13	11	45	40
14	0	151	166
14	1	50	59
14	2	56	60
14	4	104	118
14	5	63	62
14	6	48	55
14	8	38	26
14	9	55	49
14	10	38	37
15	0	46	61
15	1	172	170
15	2	145	143
15	3	38	38
15	5	63	62
15	6	54	49
15	7	58	53
15	8	124	111
15	9	43	40
15	10	131	120
15	11	45	40
16	0	151	166
16	1	50	59
16	2	56	60
16	4	104	118
16	5	63	62
16	6	48	55
16	8	38	26
16	9	55	49
16	10	38	37
17	0	46	61
17	1	172	170
17	2	145	143
17	3	38	38
17	5	63	62
17	6	54	49
17	7	58	53
17	8	124	111
17	9	43	40
17	10	131	120
17	11	45	40

**** L = 3 ****

H	K	OBS	CALC
-15	0	37	37
-15	2	60	59
-15	4	67	77
-14	3	33	36
-14	5	35	27
-13	1	81	84
-13	3	81	84
-13	4	37	30
-13	5	107	105
-13	6	56	54
-13	7	51	54
-13	8	48	50
-12	1	34	36
-12	2	38	37
-12	3	57	58
-11	3	87	73
-11	4	54	49
-11	5	58	53
-11	8	96	93
-11	7	65	65
-11	8	109	114
-11	10	52	54
-10	1	39	46
-10	2	31	39
-10	3	33	33
-10	5	82	82
-10	6	48	43
-10	7	217	203
-9	2	85	82
-9	3	47	52
-9	4	45	46
-9	7	86	89
-9	9	139	135
-9	11	58	63
-8	0	30	25
-8	2	29	30
-8	4	31	35
-8	5	39	36
-8	6	40	44
-8	7	36	36
-8	8	41	39
-8	9	41	37
-8	10	33	29
-7	0	166	174
-7	1	87	82
-7	2	178	167
-7	3	109	109
-7	4	125	120
-7	5	35	42
-7	7	66	66
-7	8	46	48
-7	9	64	52
-7	10	74	78
-7	11	79	84
-7	12	89	99

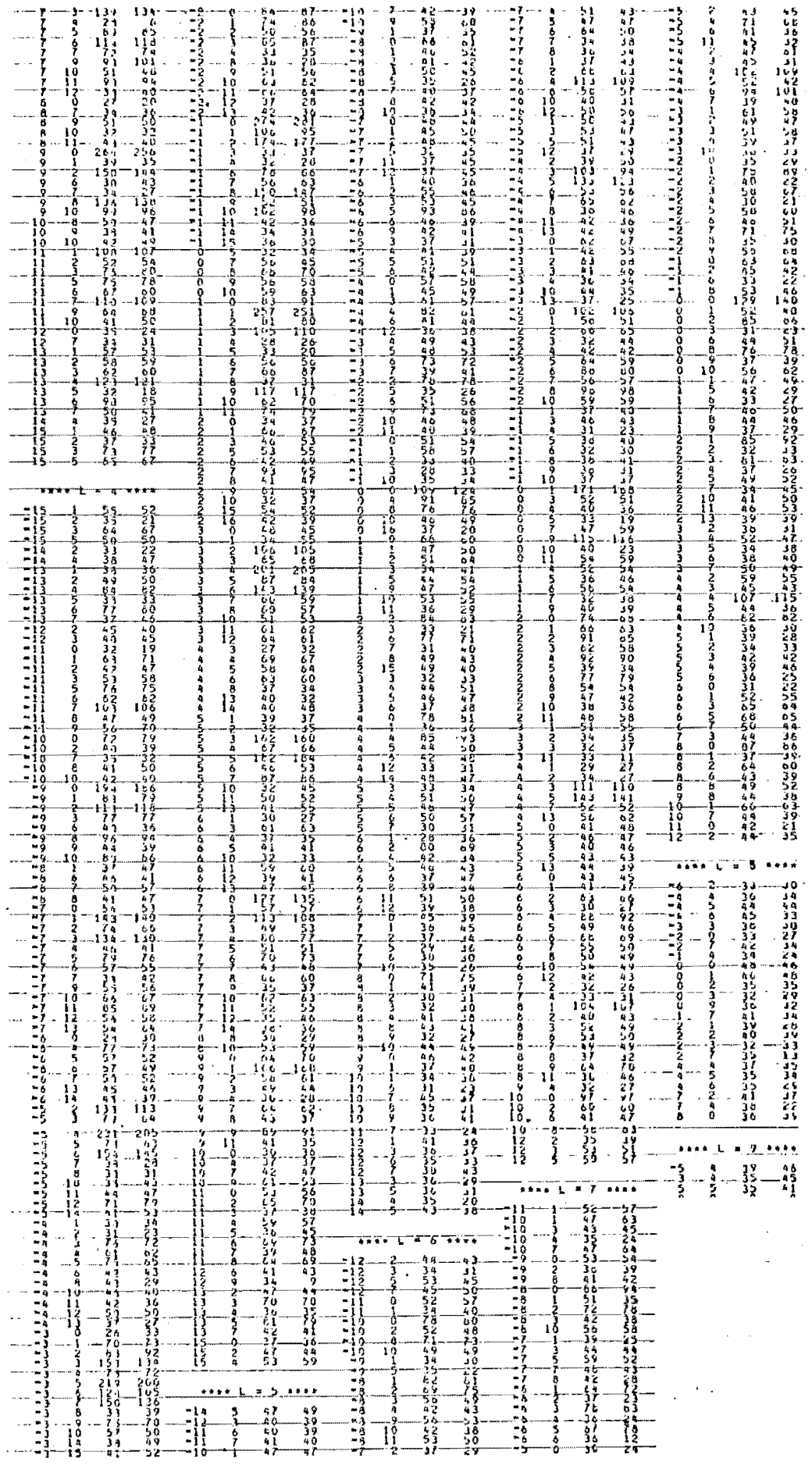

REFERENCES

1. C. T. Page, B.Sc.(Hons) Project, University of Canterbury, 1973.
2. D. E. Johnstone, M.Sc. Thesis, University of Canterbury, 1972.
3. D. Johnstone, J. E. Fergusson and W. T. Robinson, Bull. Chem. Soc. Japan, 45, 3721 (1972).
4. M. B. Fairy and R. J. Irving, J. Chem. Soc. A, 475 (1966).
5. J. Chatt and B. L. Shaw, J. Chem. Soc. A, 1811 (1966).
6. K. R. Laing and W. R. Roper, J. Chem. Soc. A, 2149 (1970).
7. R. E. Townsend and K. J. Coskran, Inorg. Chem., 10, 1661 (1971).
8. S. D. Robinson and M. F. Uttley, J. Chem. Soc., Dalton Trans., 1 (1972).
9. A. J. Schultz, R. L. Henry, J. Reed and R. Eisenberg, Inorg. Chem., 13, 732 (1974).
10. B. L. Haymore and J. A. Ibers, Inorg. Chem., 14, 3060 (1975).
11. P. F. Heveldt, Ph.D. Thesis, University of Canterbury, 1975.
12. J. T. Mague and J. P. Mitchener, Inorg. Chem., 11, 2714 (1972).
13. J. E. Fergusson and P. F. Heveldt, J. Inorg. Nucl. Chem., 39, 825 (1977).
14. M. C. Baird, Inorg. Chim. Acta, 5, 46 (1971).
15. L. Malatesta, M. Angoletta and G. Caglio, Angew. Chem., Int. Ed. Engl., 2, 739 (1963).

16. A. Araneo, V. Valenti and F. Cariati, J. Inorg. Nucl. Chem., 32, 1877 (1970).

17. R. W. Adams, J. Chatt, N. E. Hooper and G. J. Leigh, J. Chem. Soc., Dalton Trans., 1075 (1974).

18. J. E. Fergusson and P. F. Heveldt, J. Inorg. Nucl. Chem., 38, 2231 (1976).

19. a) K. W. Muir and R. Walker, Acta Crystallogr., 31A, S132 (1975).

    b) Personal communication to J. E. Fergusson from K. W. Muir.

20. K. Natarajan, R. K. Poddar and U. Agarwala, Inorg. Nucl. Chem. Lett., 12, 749 (1976).

21. R. Taube and K. Seyferth, Z. Chem., 14, 284 (1974).

22. J. Chatt and B. L. Shaw, J. Chem. Soc. A, 1437 (1966).

23. M. A. Bennett, R.J.H. Clark and D. L. Milner, Inorg. Chem., 6, 1647 (1967).

24. J. Chatt, N. P. Johnson and B. L. Shaw, J. Chem. Soc., 1625 (1964).

25. B. L. Shaw and A. C. Smithies, J. Chem. Soc. A, 2784 (1968).

26. L. Vallarino, J. Inorg. Nucl. Chem., 8, 288 (1958).

27. L. Ruiz-Ramirez, T. A. Stephenson and E. S. Switkes, J. Chem. Soc., Dalton Trans., 1770 (1973).

28. J. Chatt, G. J. Leigh and A. P. Storace, J. Chem. Soc. A, 1380 (1971).

29. K. A. Jensen, Z. Anorg. Chem., 225, 97 (1935).

30. P. C. Ray and N. Adhikari, J. Indian Chem. Soc., 9, 251 (1932) and references therein.

31. F. G. Angell, H.D.K. Drew and W. Wardlaw, J. Chem. Soc., 349 (1930).

32. F. P. Dwyer and R. S. Nyholm, J. Proc. Roy. Soc. N.S.W., 78, 67 (1944).

33. J. E. Fergusson and K. S. Loh, Aust. J. Chem., 26, 2615 (1973).

34. J. R. Allkins and P. J. Hendra, J. Chem. Soc. A, 1325, (1967).

35. J. R. Allkins and P. J. Hendra, Spectrochim. Acta, 24A, 1305 (1968).

36. R. J. Cross, T. H. Green and R. Keat, J. Chem. Soc., Dalton Trans., 382 (1976).

37. D. M. Adams, J. Chatt, J. Gerratt and A. D. Westland, J. Chem. Soc., 734 (1964).

38. R.J.H. Clark, G. Natile, U. Belluco, L. Cattalini and C. Filippin, J. Chem. Soc. A, 659 (1970).

39. E. A. Allen and W. Wilkinson, Spectrochim. Acta, 28A, 725 (1972).

40. B. E. Aires, J. E. Fergusson, D. T. Howarth and J. E. Miller, J. Chem. Soc. A, 1144 (1971).

41. B. Singh and R. K. Mehra, Indian J. Chem., 13, 1194 (1975).

42. J. E. Fergusson, J. D. Karran and S. Seevaratnam, J. Chem. Soc., 2627 (1965).

43. E. A. Allen and W. Wilkinson, J. Chem. Soc., Dalton Trans., 613 (1972).

44. G. B. Kauffman, J. H. Tsai, R. C. Fay and C. K. Jorgensen, Inorg. Chem., 2, 1233 (1963).

45. A. P. Kochetkova, L. B. Sveshnikova, V. I. Sokol and A. A. Gribenyuk, Russ. J. Inorg. Chem., 18, 1290 (1973) and references therein.

46. P. Biscarini and G. D. Nivellini, J. Chem. Soc. A, 2206 (1969).

47. H. G. Raubenheimer, J.C.A. Boeyens and S. Lotz, J. Organomet. Chem., 112, 145 (1976).

48. D. L. Sales, J. Stokes and P. Woodward, J. Chem. Soc. A, 1852 (1968).

49. a) M. McPartlin and A. J. Markwell, J. Organomet. Chem., 57, C25 (1973).

b) A. J. Markwell, Ph.D. Thesis, University of London, 1973.

50. P. E. Skakke and S. E. Rasmussen, Acta Chem. Scand., 24, 2634 (1970).

51. C. I. Branden, Ark. Kemi, 22, 83 (1964).

52. a) E. F. Paulus, H. P. Fritz and K. E. Schwarzhans, J. Organomet. Chem., 11, 647 (1968).

b) Personal communication to J. E. Fergusson from E. F. Paulus.

53. V. I. Sokol, V. N. Nikolaev, M. A. Porai-Koshits and L. P. Kochetkova, Koord. Khim., 1, 675 (1973).

54. W. A. Spofford, Inorg. Chem., 10, 2309 (1971).

55. D. J. Hodgson and J. A. Ibers, Inorg. Chem., 7, 2345 (1968).

56. R. Eisenberg and C. D. Meyer, Acc. Chem. Res., 8, 26 (1975).

57. J. H. Enemark and R. D. Feltham, Coord. Chem. Rev., 13, 339 (1974).

58. M. A. Porai-Koshits, V. S. Sergienko and T. S. Khodashova, Russ. J. Inorg. Chem., 18, 1751 (1973).

59. K. G. Caulton, Coord. Chem. Rev., 14, 317 (1975).

60. a) J. E. Fergusson and G. A. Rodley, M.T.P. Int. Rev. Sci., Inorg. Chem., Ser. Two, 6, 37 (1975).

b) J. A. McGinnety, M.T.P. Int. Rev. Sci., Inorg. Chem., Ser. One, 5, 229 (1972).

61. B. A. Frenz and J. A. Ibers, M.T.P. Int. Rev. Sci., Phys. Chem., Ser. One, 11, 33 (1972).

62. F. C. March and G. Fergusson, Can. J. Chem., 49, 3590 (1971).

63. M. Ghedini, G. Dolcetti, O. Gandolf, and B. Giovannitti, Inorg. Chem., 15, 2385 (1976).

64. M. J. Cleare and W. P. Griffith, J. Chem. Soc. A, 372 (1969).

65. I. P. Evans, A. Spencer and W. Wilkinson, J. Chem. Soc., Dalton Trans., 204 (1973).

66. R. S. McMillan, A. Mercer, B. R. James and J. Trotter, J. Chem. Soc., Dalton Trans., 1006 (1975).

67. A. Mercer and J. Trotter, J. Chem. Soc., Dalton Trans., 2480 (1975).

68. J. Chatt, G. J. Leigh and D.P.M. Mingos, J. Chem. Soc. A, 1674 (1969).

69. C.W.N. Crumper, J. F. Read and A. I. Vogel, J. Chem. Soc. A, 239 (1966).

70. E. Hoyer, W. Dietzsch and H. Heber, 3rd Proc. Symp. Coord. Chem., 1, 259 (1970).

71. D. W. Allen, P. N. Braunton, I. T. Millar and J. C. Tebby, J. Chem. Soc. C, 3462 (1971).

72. 'Chelating Agents and Metal Chelates', by F. P. Dwyer and D. P. Mellor, Academic Press, New York, (1964), p120.

73. F. G. Mann and D. Purdie, J. Chem. Soc., 1549 (1935).

74. D. S. Tarbell and C. Weaver, J. Am. Chem. Soc., 63, 2939 (1941).

75. 'Inorganic Syntheses', edited by H. F. Holtzlaw, McGraw-Hill, U.S.A., 8, 192 (1966).

76. J. Chatt and G. A. Rowe, J. Chem. Soc., 4019 (1962).

77. D. Giusto and G. Cova, Gazz. Chim. Ital., 102, 265 (1972).

78. N. M. Sergeev, Russ. Chem. Rev., 42, 339 (1973).

79. 'Dynamic Nuclear Magnetic Resonance', edited by L. M. Jackson and F. A. Cotton, Academic Press, New York, (1975).

80. G. Binsch, Topics in Stereochemistry, 3, 97 (1968).

81. W. B. Jennings, Chem. Rev., 75, 307 (1975).

82. A. Rauk, L. C. Allen and K. Mislow, Angew. Chem., Int. Ed. Engl., 9, 400 (1970).

83. G. Binsch and D. A. Kleier, Program 165, Quantum Chemistry Program Exchange, Indiana University.

84. G. Binsch, J. Magn. Reson., 3, 146 (1970).

85. H. J. Whitfield, J. Chem. Soc. A, 113 (1970).

86. J. B. Lambert, Topics in Stereochemistry, 6, 19 (1971).

87. T. D. Coyle and F.G.A. Stone, J. Am. Chem. Soc., 83, 4138 (1961).

88. S. Brownstein, J. Am. Chem. Soc., 98, 2663 (1976).

89. E. W. Abel, R. P. Bush, F. J. Hopton and C. R. Jenkins, J. Chem. Soc., Chem. Commun., 58 (1966).

90. P. Haake and P. C. Turley, J. Am. Chem. Soc., 89, 4611 (1967).

91. P. C. Turley and P. Haake, J. Am. Chem. Soc., 89, 4617 (1967).

92. R. J. Cross, I. G. Dalgleish, G. J. Smith and R. Wardle, J. Chem. Soc., Dalton Trans., 992 (1972).

93. F. Coletta, R. Ettorre, and A. Gambaro, Inorg. Nucl. Chem. Lett., 8, 667 (1972).

94. H. Schmidbaur and K. C. Dash, Chem. Ber., 105, 3662 (1972).

95. R. J. Cross, T. H. Green and R. Keat, J. Chem. Soc., Chem. Commun., 207 (1974).

96. R. J. Cross, T. H. Green and R. Keat, J. Chem. Soc., Dalton Trans., 1150 (1976).

97. R. J. Cross, T. H. Green, R. Keat and J. F. Paterson, J. Chem. Soc., Dalton Trans., 1486 (1976).

98. E. W. Abel, G. W. Farrow and K. G. Orrell, J. Chem. Soc., Dalton Trans., 1160 (1976).

99. E. W. Abel, G. W. Farrow, K. G. Orrell and V. Sik, J. Chem. Soc., Dalton Trans., 42 (1977).

100. E. W. Abel, A.K.S. Ahmed, G. W. Farrow, K. G. Orrell and V. Sik, J. Chem. Soc., Dalton Trans., 47 (1977).

101. D. W. Scott, H. L. Finke, W. N. Hubbard, J. P. McCullough G. D. Oliver, M. E. Gross, C. Katz, K. D. Williamson, G. Waddington and H. M. Huffman, J. Am. Chem. Soc., 74, 4656 (1952).

102. R. Donaldson, G. Hunter and R. C. Massey, J. Chem. Soc., Dalton Trans., 288 (1974).

103. G. Hunter and R. C. Massey, J. Chem. Soc., Dalton Trans., 209 (1975).

104. G. Hunter and R. C. Massey, J. Chem. Soc., Dalton Trans, 2007 (1976).

105. R. J. Cross, G. Hunter and R. C. Massey, J. Chem. Soc., Dalton Trans., 2015 (1976).

106. R. M. Silverstein and R. G. Silberman, J. Chem. Ed., 50, 484 (1973).

107. R. Roulet and C. Barbey, Helv. Chim. Acta, 56, 2179 (1973).

108. 'Organic Spectroscopy', by S. F. Dyke, A. J. Floyd, M. Sainsbury and R. S. Theobald, Penguin Books, London, 1971.

109. D. R. Rayner, A. J. Gordon and K. J. Mislow, J. Am. Chem. Soc., 90, 4854 (1968).

110. Reference 79, Chapter 3.

111. J. E. Fergusson and C. T. Page, Aust. J. Chem., 29, 2159 (1976).

112. H. Kessler, Angew. Chem., Int. Ed. Engl., 9, 219 (1970).

113. a) A. L. Van Geet, Anal. Chem., 40, 2227 (1968).
b) A. L. Van Geet, Anal. Chem., 42, 679 (1970).

114. J. E. Fergusson, C. T. Page, and W. T. Robinson, Inorg. Chem., 15, 2270 (1976).

115. J. E. Fergusson, C. T. Page and W. T. Robinson, Abstract T18, 7th C.O.M.O. Conference, La Trobe University, Melbourne, 1977.

116. R. B. Bucat and D. W. Watts, M.T.P. Int. Rev. Sci., Inorg. Chem., Ser. One, 9, 159 (1972).

117. W. L. Waltz and R. G. Sutherland, Chem. Soc. Rev., 1, 241 (1972).

118. P. C. Ford, J. D. Peterson and R. E. Hintze, Coord. Chem. Rev., 14, 67 (1974).

119. L. Vaska, Science , 140, 809 (1963).

120. S. Cenini, A. Mantovani, A. Fusi and M. Keubler, Gazz. Chim. Ital., 105, 255 (1975).

121. G. L. Geoffroy, D. A. Denton, M. E. Keeney and R. R. Bucks, Inorg. Chem., 15, 2382 (1976).

122. G. L. Geoffroy, D. A. Denton and C. W. Eigenbrot, Inorg. Chem., 15, 2310 (1976).

123. 'Organic Sulphur Compounds' edited by N. Kharasch, Pergamon Press, London, 1961, Volume 1, Chapter 21.

124. P. Haake and T. A. Hylton, J. Am. Chem. Soc., 84, 3774 (1962).

125. P. R. Brookes and B. L. Shaw, J. Chem. Soc., Chem. Commun., 919 (1968).

126. J. Jeffrey and R. J. Mawby, J. Organomet. Chem., 40, C42 (1972).

127. C. E. Betts, R. N. Haszeldine and R. V. Parish, J. Chem. Soc., Dalton Trans., 2215 (1975).

128. F. Scandola, O. Traverso, V. Balzani, G. L. Zucchini, and V. Carassiti, Inorg. Chim. Acta, 1, 76 (1967).

129. 'Solubilities of Inorganic and Organic Compounds', edited by H. Stephen and T. Stephen, Volume 1, Part 1, p575.

130. P. Biscarini, L. Fusina and G. D. Nivellini, J. Chem. Soc. A, 1128 (1971).

131. R. Harville and S. F. Reed, J. Org. Chem., 33, 3976 (1968).

132. Y. N. Kukushkin and V. V. Golosov, Russ. J. Inorg. Chem., 18, 248 (1973).

133. W. Kitching, C. J. Moore and D. Doddrell, Inorg. Chem., 9, 541 (1970).

134. W. Kitching, C. J. Moore and D. Doddrell, Aust. J. Chem., 22, 1149 (1969).

135. R. Bravo, M. Durand and J. P. Laurent, Org. Magn. Reson., 5, 357 (1973).

136. R. V. Est-Stammer and J.B.F.N. Engberts, Can. J. Chem., 51, 1187 (1973).

137. G. O. Schenck and C. H. Krauch, Chem. Ber., 96, 517, (1963)

138. 'Organic Syntheses', edited by E. J. Corey, J. Wiley and Sons, New York, 46, 78 (1966).

139. 'Handbook of Chemistry and Physics', edited by R. C. Weast, The Chemical Rubber Co., Ohio, 52, C500 (1971).

140. 'X-ray Structure Determination', by G. H. Stout and L. H. Jensen, MacMillan Co., New York, 1968.

141. 'Single Crystal Orienter Instruction Manual', by T. C. Furnas, General Electric Co., Milwaukee, 1966.

142. P.W.R. Corfield, R. J. Doedens and J. A. Ibers, Inorg. Chem., 6, 197 (1967).

143. D. F. Grant, R.C.G. Killean and J. L. Lawerence, Acta Crystallogr., 25B, 374 (1969).

144. Program DABS was used, a modified version of DATAPH by P. Coppens.

145. All calculations were carried out at the University of Canterbury using a Burroughs B6718 computer. The data processing program HILGOUT is based on the programs DRED (J. Blount) and PICKOUT (R. J. Doedens). Structure factor calculations and least-squares refinements were carried out using program CUCLS and Fourier summations using program FOURIER. These are highly modified versions of the well-known programs ORFLS (W. A. Busing, K. O. Martin, and H. A. Levy) and FORDAP (A. Zalkin), respectively. Other programs used include local modifications of Busing and Levy's ORFFE function and error program, and C. K. Johnson's ORTEP thermal ellipsoid plotting program.

146. D. T. Cromer and J. B. Mann, Acta Crystallogr., 24A, 321 (1968).

147. D. T. Cromer, Acta Crystallogr., 18, 17 (1965).

148. V. I. Sokol and M. A. Porai-Koshits, Koord. Khim., 1, 577 (1975).

149. R. D. Willet and K. Chang, Inorg. Chim. Acta, 4, 447 (1970).

150. M. J. Bennett, F. A. Cotton and D. L. Weaver, Acta Crystallogr., 23, 581 (1967).

151. V. I. Baranovskii, Y. N. Kukushkin, N. S. Panina and A. I. Panin, Russ. J. Inorg. Chem., 18, 844 (1973).

152. W. Kitching and C. J. Moore, Inorg. Nucl. Chem. Lett., 4, 691 (1968).

153. F. A. Cotton, R. Francis and W. D. Horrocks, J. Phys. Chem., 64, 1534 (1960).

154. M. J. Bennett, F. A. Cotton and D. L. Weaver, Nature (London), 212, 287 (1966).

155. 'Physical Data for Inorganic Chemists', by M. C. Ball and A. H. Norburg, Longman, London, 1974.

156. N. W. Isaacs and C.H.L. Kennard, J. Chem. Soc. A, 1257 (1970).

157. G. Bombieri and K. W. Bagnall, J. Chem. Soc., Chem. Commun., 188 (1975).

158. L. Coghi, C. Pelizzi and G. Pelizzi, J. Organomet. Chem., 114, 52 (1976).

159. L. A. Aslanov, L. I. Soleva, M. A. Porai-Koshits and S. S. Goukhberg, J. Struct. Chem. USSR, 13, 610 (1972).

160. K. K. Bandary and H. Manohar, Acta Crystallogr., 29B, 1093 (1973).

161. K. K. Bandary, H. Manohar and K. Venatesan, J. Chem. Soc., Dalton Trans., 288 (1975).

162. N. O. Bjork and A. Cassel. Acta Chem. Scand., 30A, 235 (1976).

163. R. Thomas, C. B. Shoemaker and K. Eriks, Acta Crystallogr., 21, 12 (1966).

164. V. I. Sokol, N. D. Rubtsova and A. Y. Gribenyuk, J. Struct. Chem. USSR, 15, 296 (1974).

165. M. J. Bennett, F. A. Cotton, D. L. Weaver, R. J. Williams and W. H. Watson, Acta Crystallogr., 23, 788 (1967).

166. P. Colamarino and P. Orioli, J. Chem. Soc., Dalton Trans., 845 (1976).

167. R. Melanson and F. D. Rochon, Can. J. Chem., 53, 2371 (1975).

168. D. A. Langs, C. R. Hare and R. G. Little, J. Chem. Soc., Chem. Commun., 1080 (1967).

169. J. T. Veal and D. J. Hodgson, Acta Crystallogr., 28B, 3525 (1972).

170. C. G. Piepont and R. Eisenberg, Inorg. Chem., 11, 1088 (1972).

171. Program ABSORB was used, this is a locally adapted version of the program by L. Templeton and D. Templeton described in Abstract E10, Amer. Cryst. Assoc., Storrs, Conn., 1973, using the analytical method of J. De Meulenaer and H. Tompa, Acta Crystallogr., 19, 1014 (1965).

172. Program SHELX-76, a group of X-ray crystallographic programs developed by G. M. Sheldrick, University of Cambridge, 1976.

173. 'Direct Methods in Crystallography', by M. M. Woolfson, Clarendon Press, Oxford, 1961.

174. R. G. Hazell and A. C. Hazell, Acta Crystallogr., 31A, S19 (1975).

175. W. H. Zachariasen, Acta Crystallogr., 23, 558 (1967).

176. J. Reed, A. J. Schultz, C. G. Pierpont and R. Eisenberg, Inorg. Chem., 12, 2949 (1973).

177. 'Vector Space', by M. J. Buerger, Wiley, New York, 1959.

178. D.M.P. Mingos and J. A. Ibers, Inorg. Chem., 10, 1035 (1971).

179. N. Camerman and J. Trotter, J. Chem. Soc., 219 (1964).

180. H. Hope, J. Appl. Crystallogr., 4, 333 (1971).

181. D. L. Evans, Ph.D. Thesis, University of Canterbury, to be presented.

Abstract T18, 7th C.O.M.O. Conference, La Trobe Univ., Melbourne, 1977.

REACTION OF A RUTHENIUM THIOETHER COMPLEX EXPOSED TO SUNLIGHT

T18

J. E. Fergusson, C. T. Page and Ward T. Robinson*
Department of Chemistry, University of Canterbury, Christchurch, New Zealand

As part of a study of the bonding of thioether ligands to the platinum metals, a series of complexes of the type $[RuX_3(NO)L_2]$, (where X = Cl, Br and L = thioether, R_2S), were prepared (1). When a dilute chloroform solution of one of the complexes, $[RuBr_3NO(Et_2S)_2]$, was exposed to sunlight it rapidly changed colour from light yellow to dark red, from which a crystalline product was obtained in low yield. A single crystal X-ray study of the product was undertaken, and it was found to have the formulation di-μ-bromo-bis[dibromo(diethylsulphoxide)-nitrosyl ruthenium II], $[RuBr_3NO(Et_2SO)]_2$. The compound crystallised in the triclinic space group $P\bar{1}$ (2). The unit cell dimensions were a = 8.042, b = 11.020, c = 7.324 Å, α = 104.83°, β = 102.31°, γ = 88.54°, R = 0.047 for 1337 reflections having $F^2 \geq 3\sigma(F^2)$.

In forming the dimeric molecule the sulphide ligand has been oxidised under mild conditions (i.e. sunlight) to a sulphoxide ligand which is then bound to ruthenium through the oxygen atom. The source of oxygen is dioxygen dissolved in the chloroform and the oxidation is assisted by the presence of a small amount of ethanol.

The yield of the dimeric complex is low and other product(s) are formed which may be intermediates in the reaction,

$$[RuBr_3NO(Et_2S)_2] \xrightarrow{O,h\nu} [RuBr_3NO(Et_2SO)]_2.$$

One such product was obtained which crystallised in the monoclinic space group $P2_1/c$ with a = 13.633, b = 8.514, c = 16.340 Å, and β = 106.56°. The structure of trisbromo (diethylsulphide)-(diethylsulphoxide)nitrosyl ruthenium (II), $[RuBr_3(NO)(Et_2SO)(Et_2S)]$, was determined and refined to R = 0.048 for 1585 reflections with $F^2 \geq 3\sigma(F^2)$.

This intermediate containing both Et_2S and Et_2SO has the sulphoxide ligand bonded through oxygen to the ruthenium. The Ru-S bond at 2.412Å is long, and compared with the $[RuBr_3NO(Et_2S)_2]$ starting material there has been a rearrangement of the thio-ligands around the metal ion.

1. J. E. Fergusson and C. T. Page, Aust. J. Chem., 29, 2159 (1976).

2. J. E. Fergusson, C. T. Page and W. T. Robinson, Inorg. Chem., 15, 2270 (1976).

(2) J. A. Bertrand and C. E. Kirkwood, *Inorg. Chim. Acta*, **6**, 248 (1972).
(3) E. D. Estes, W. E. Estes, R. P. Scaringe, W. E. Hatfield, and D. J. Hodgson, *Inorg. Chem.*, **14**, 2564 (1975).
(4) R. M. Countryman, W. T. Robinson, and E. Sinn, *Inorg. Chem.*, **13**, 2013 (1974).
(5) R. D. Willett and C. Chow, *Acta Crystallogr., Sect. B*, **30**, 207 (1974).
(6) M. Texter, E. Dubler, and H. R. Oswald, *Inorg. Chem.*, **13**, 1361 (1974).
(7) D. J. Hodgson, P. K. Hale, and W. E. Hatfield, *Inorg. Chem.*, **10**, 1061 (1971).
(8) M. Sundaralingam and J. A. Carrabine, *J. Mol. Biol.*, **60**, 287 (1971); J. P. DeClerq, M. Debbaudt, and M. van Meersche, *Bull. Soc. Chim. Belg.*, **80**, 527 (1971).
(9) R. B. Wilson, W. E. Hatfield, and D. J. Hodgson, *Inorg. Chem.*, **15**, 1712 (1976).
(10) E. Sletten and A. Apeland, *Acta Crystallogr., Sect. B*, **31**, 2019 (1975).
(11) D. H. Svedung, *Acta Chem. Scand.*, **23**, 2865 (1969).
(12) V. F. Duckworth and N. C. Stephenson, *Acta Crystallogr., Sect. B*, **25**, 1795 (1969).
(13) E. D. Estes, W. E. Estes, W. E. Hatfield, and D. J. Hodgson, *Inorg. Chem.* **14**, 106 (1975).
(14) P. Singh, D. Y. Jeter, W. E. Hatfield, and D. J. Hodgson, *Inorg. Chem.*, **11**, 1657 (1972).
(15) E. Luukkonen and A. Pajunen, *Suom. Kemistil. B*, **46**, 292 (1973).
(16) A. R. Hendrickson, R. L. Martin, and D. Taylor, *J. Chem. Soc., Chem. Commun.*, 843 (1975).
(17) R. A. Bream, E. D. Estes, and D. J. Hodgson, *Inorg. Chem.*, **14**, 1672 (1975).
(18) V. C. Copeland, P. Singh, W. E. Hatfield, and D. J. Hodgson, *Inorg. Chem.*, **11**, 1826 (1972).
(19) V. C. Copeland, W. E. Hatfield, and D. J. Hodgson, *Inorg. Chem.*, **12**, 1340 (1973).
(20) J. D. Dunitz, *Acta Crystallogr.*, **10**, 307 (1957).
(21) V. Kupcik and S. Durovic, *Czech. J. Phys.*, **10**, 182 (1960).
(22) B. Morosin, *Acta Crystallogr., Sect. B*, **31**, 632 (1975).
(23) R. D. Willett and K. Chang, *Inorg. Chim. Acta*, **4**, 447 (1970).
(24) M. Laing and E. Horsfield, *Chem. Commun.*, 735 (1968).
(25) M. Laing and G. Carr, *J. Chem. Soc. A*, 1141 (1971).
(26) E. D. Estes and D. J. Hodgson, *J. Chem. Soc., Dalton Trans.*, 1168 (1975).
(27) R. Näsänen, E. Luukkonen, H. Palonen, and M. Sivonen, *Suom. Kemistil. B*, 44, 93 (1971).
(28) W. R. Busing and H. A. Levy, *Acta Crystallogr.*, **22**, 457 (1967).
(29) D. J. Hodgson and J. A. Ibers, *Inorg. Chem.*, **8**, 326 (1969).
(30) P. W. R. Corfield, R. J. Doedens, and J. A. Ibers, *Inorg. Chem.*, **6**, 197 (1967).
(31) W. R. Busing and H. A. Levy, *J. Chem. Phys.*, **26**, 563 (1957).
(32) For a description of the programs used, see D. L. Lewis and D. J. Hodgson, *Inorg. Chem.*, **13**, 143 (1974).
(33) "International Tables for X-Ray Crystallography", Vol. IV, Kynoch Press, Birmingham, England: (a) Table 2.2A; (b) Table 2.1C.
(34) R. F. Stewart, E. R. Davidson, and W. T. Simpson, *J. Chem. Phys.*, **42**, 3175 (1965).
(35) J. A. Ibers and W. C. Hamilton, *Acta Crystallogr.*, **17**, 781 (1964).
(36) W. H. Zachariasen, *Acta Crystallogr.*, **16**, 1139 (1963); *Acta Crystallogr., Sect A*, **24**, 212 (1968); D. J. Hodgson and J. A. Ibers, *Acta Crystallogr., Sect. B*, **25**, 469 (1969).
(37) Supplementary data.
(38) W. E. Estes and W. E. Hatfield, private communication.
(39) D. J. Hodgson, *Prog. Inorg. Chem.*, in press, and references therein.
(40) D. S. Brown, F. W. B. Einstein, and D. G. Tuck, *Inorg. Chem.*, **8**, 14 (1969).
(41) D. J. Hodgson and J. A. Ibers, *Inorg. Chem.*, **8**, 1282 (1969).
(42) T. P. Mitchell, W. H. Bernard, and J. R. Wasson, *Acta Crystallogr., Sect. B*, **26**, 2096 (1970).
(43) L. Pauling, "The Nature of the Chemical Bond", 3d ed, Cornell University Press, Ithaca, N.Y. 1960, p 225.
(44) N. T. Watkins, E. E. Dixon, V. H. Crawford, K. T. McGregor, and W. E. Hatfield, *J. Chem. Soc., Chem. Commun.*, 133 (1973).
(45) H. H. Jaffe, *Chem. Rev.*, **53**, 191 (1953).

Contribution from the Department of Chemistry, The University of Canterbury, Christchurch, New Zealand

Crystal and Molecular Structure of Di-μ-bromo-bis[dibromo(diethyl sulfoxide)nitrosylruthenium(II)]

J. E. FERGUSSON,* C. T. PAGE, and WARD T. ROBINSON

Received February 6, 1976 AIC601028

The crystal and molecular structures of di-μ-bromo-bis[dibromo(diethyl sulfoxide)nitrosylruthenium(II)], $[RuBr_3(NO)(Et_2SO)]_2$, have been determined from three-dimensional x-ray data obtained by counter methods. The compound crystallizes in the centrosymmetric space group $P\bar{1}$ of the triclinic system, with 1 formula unit in a unit cell of dimensions $a = 8.042$ (1) Å, $b = 11.020$ (2) Å, $c = 7.324$ (1) Å, $\alpha = 104.83$ (1)°, $\beta = 102.31$ (1)°, and $\gamma = 88.54$ (1)°. Full-matrix least-squares refinement of the structure has led to a final R value of 0.047 for the 1337 independent reflections having $F_o^2 > 3\sigma(F_o^2)$. The dimeric molecules consist of octahedrally coordinated ruthenium atoms sharing one edge through the two bridging bromine atoms, two coordinated to each ruthenium atom. Above and below this plane are nitrosyl and diethyl sulfoxide groups trans to each other on each ruthenium atom with a crystallographic center of symmetry imposed on the whole molecule. The nitrosyl ligand is linearly coordinated as expected for NO^+ complexes of Ru(II). This sulfoxide complex was formed from the $RuBr_3(NO)(Et_2S)_2$ complex dissolved in chloroform and exposed to sunlight. The oxidation was achieved by dioxygen dissolved in the chloroform assisted by the presence of ethanol. The diethyl sulfoxide ligand is coordinated to the Ru(II) atom through the oxygen atom.

Introduction

During the study of a series of complexes $RuX_3(NO)L_2$ (X = Cl, Br, I; L = Me_2S, PhMeS, Et_2S, PhEtS, Et_2Se, PhEtSe, $(n\text{-Pr})_2S$, Ph-n-PrS)[1] it was observed that a chloroform solution of $RuBr_3(NO)(Et_2S)_2$ changed color from light yellow to dark red in sunlight. After a period of a few weeks a small quantity of dark red-brown crystals was separated from the solution. The infrared spectrum of these crystals contained a strong absorption at 920 cm^{-1} absent in the parent compound. This suggested the existence of a sulfoxide group bonded to the metal atom through its oxygen atom. The product of this ready conversion seemed best characterized by a crystal structure analysis. This analysis has confirmed the existence of sulfoxide ligands coordinated to ruthenium atoms. The source of the oxygen has also been investigated.

Experimental Section

Preparations. Nitric oxide was bubbled through an ethanol solution of $RuBr_3 \cdot 3H_2O$ for several hours, and then diethyl sulfide was added in slight excess. The solution was heated under reflux for 1 h. Crystals of $RuBr_3(NO)(Et_2S)_2$ formed as ethanol was removed in vacuo. A chloroform solution of $RuBr_3(NO)(Et_2S)_2$ was allowed to evaporate slowly over a period of a few weeks, while exposing the solution to sunlight. The mother liquor was poured off and the crystals obtained in low yield were dried in vacuo. Dark red-brown crystals, of empirical formula $RuBr_3(NO)(Et_2SO)$, formed.

Study of the Reaction. Exposure of chloroform solutions of $RuBr_3(NO)(Et_2S)_2$ to sunlight which first passed through color filters (Ilford) indicated that radiation within the wavelength range 380–480 nm was necessary.

The color change which was observed also corresponded to changes in the ^1H NMR and electronic spectra of the solution. The form of

the ^1H NMR spectrum suggested that at least two other products were formed during the course of the reaction. Whether one of these corresponds to the dimeric crystalline compound is not known as the low solubility of the material prevents the running of its ^1H NMR spectrum. One product may correspond to a diethyl sulfone (Et_2SO_2) complex, but work on this is currently in progress. There is no evidence to suggest that free diethyl sulfide is present in the solution.

The compound $RuBr_3(NO)(Et_2S)_2$ was dissolved in chloroform under the following conditions: (a) chloroform free of ethanol (still containing dissolved oxygen); (b) chloroform free of dissolved oxygen (still containing ethanol); (c) chloroform free of ethanol and dissolved oxygen; (d) reagent grade chloroform.

When the solutions were exposed to sunlight, the color change occurred within 2 min in (d), occurred only faintly in (a), and occurred not at all in (b) and (c). However, addition of ethanol to (a) and oxygen to (b) brought about a color change within a few minutes. No color change was observed in (c) until both oxygen and ethanol had been added. This indicates that both dissolved oxygen and ethanol are necessary before the oxidation of the sulfide will occur. The color change was also observed when acetic acid was added instead of ethanol to (a); also, in the case of acetaldehyde addition the change was observed but was slower.

Collection and Reduction of the X-Ray Data. On the basis of precession photography using Cu Kα x radiation it was established that the crystals belong to the triclinic system. The success of this analysis has confirmed that the correct space group is $P\bar{1}$.

Unit cell dimensions of $a = 8.042$ (1) Å, $b = 11.020$ (2) Å, $c = 7.324$ (1) Å, $\alpha = 104.83$ (1)°, $\beta = 102.31$ (1)°, and $\gamma = 88.54$ (1)° [30] were obtained from a least-squares refinement of the setting angles of 12 reflections accurately centered in a 5-mm diameter, circular receiving aperture set 23 cm from the crystal mounted on a Hilger and Watts four-circle, computer-controlled diffractometer [λ(Mo K$\bar{\alpha}$) 0.7107 Å; 23 °C]. All numbers in this paper refer to this unit cell which can be related to the reduced cell of dimensions $a = 8.04$ Å, $b = 11.02$ Å, $c = 11.57$ Å, $\alpha = 142.26°$, $\beta = 96.36°$, and $\gamma = 91.46°$, by the matrix

$$\begin{matrix} 1 & 0 & 0 \\ 0 & -i & 0 \\ 0 & 1 & 1 \end{matrix}$$

An experimental density of 2.56 (±0.03) g cm^{-3} obtained by the flotation method, using aqueous zinc bromide solution, is in good agreement with the calculated density of 2.59 g cm^{-3} for 2 empirical formula units in the unit cell. Thus the one dimeric molecule found has a crystallographic center of symmetry imposed on it in space group $P\bar{1}$.

The crystal used for data collection was of dimensions 0.13 × 0.33 × 0.09 mm. Its suitability for intensity measurement was examined by means of open-counter ω scans at a takeoff angle of 3°. Under these conditions typical scan widths, at half-height, for intense low-angle reflections were 0.12° and peak profiles were symmetric. Zirconium-filtered Mo Kα radiation and the θ–2θ scan technique were used to collect the intensities of all of the independent reflections in the positive h hemisphere of reciprocal space for which $0 < 2\theta \leq 50°$. The scintillation counter had a circular receiving aperture 5 mm in diameter. A symmetric scan range of 1.20° in 2θ, centered on the calculated peak position [λ(Mo Kα) 0.7107 Å], was composed of 60 steps each of 1-s duration. Stationary-crystal, stationary-counter background counts of 15 s were measured at each end of the scan range. Attenuation was necessary for nine reflections when the count rate exceeded 8000 counts/s during the scan. By the end of the data collection, the intensities of three standard reflections, monitored at intervals of every 50 reflections, were found to have dropped to 83% of their original values. These observations were used to place all of the intensities on the same relative scale.

Data processing included the application of Lorentz and polarization corrections and the calculations of $\sigma(I) = [c + 0.25(t_c/t_b)^2(B_1 + B_2) + (PI)^2]^{1/2}$ where $I = c - (t_c/2t_b)(B_1 + B_2)$ and c is the total integrated peak count obtained in scan time t_c; B_1 and B_2 are the background counts, each obtained in time t_b. P was initially given the value of 0.05 (this was changed to 0.065 to render $\sum w|F_o - F_c|^2$ independent of $|F_o|$ and $(\sin\theta)/\lambda$ at the end of the structure refinement) and is the factor included to avoid overweighting the more intense reflections. The data set consisted of 2165 unique reflections of which 1337 had $F_o^2 > 3\sigma(F_o^2)$. An absorption correction was applied [μ(Mo Kα) = 117.49 cm^{-1}], using Gaussian integration (4^3 grid points) with transmission factors ranging from 0.18 to 0.40.

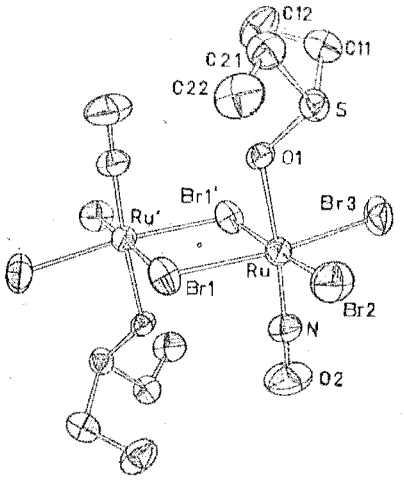

Figure 1.

Solution and Refinement of Structure.[2] A three-dimensional Patterson synthesis was carefully analyzed since the exact composition of the compound was not known. It indicated a triangular arrangement of one ruthenium and two terminal bromine atoms. By carrying out a three-dimensional vector superposition of two Patterson maps the positions of the ruthenium and three bromine atoms as well as the nitrosyl N atom and the sulfur and oxygen atoms of the sulfoxide ligand were determined. Full-matrix least-squares refinement was begun using the ruthenium and bromine atom positions and isotropic thermal parameters using those data for which $F_o^2 > 3\sigma(F_o^2)$. The function $\sum w(|F_o| - |F_c|)^2$ was minimized where the weights w were taken as $4F_o^2/\sigma^2(F_o^2)$; $|F_o|$ and $|F_c|$ are the observed and calculated structure factor amplitudes. The agreement factors are defined as

$$R_1 = \Sigma||F_o| - |F_c||/\Sigma F_o$$

$$R_2 = [\Sigma[w(|F_o| - |F_c|)^2]/\Sigma(wF_o^2)]^{1/2}$$

these reduced to 0.243 and 0.325, respectively. Difference Fourier syntheses and full-matrix least-squares refinements were used to determine the positions of all of the nonhydrogen atoms. Atomic scattering factors were those reported by Cromer and Mann[3] for neutral atoms. Anomalous dispersion effects for the Ru, Br, and S atoms were included using the $\Delta f'$ and $\Delta f''$ values reported by Cromer.[4]

Using isotropic temperature factors, refinement of this model converged with R_1 and R_2 at 0.097 and 0.128, respectively. The difference Fourier maps had shown regions of high electron density (up to 5 e/Å^3) around the heavy atoms. Accordingly final least-squares refinements were carried out with all atoms assigned anisotropic thermal vibrational parameters. These refinements, using 1337 reflections for which $F_o^2 > 3\sigma(F_o^2)$, converged to give agreement factors $R_1 = 0.047$ and $R_2 = 0.058$.

The estimated standard deviation of an observation of unit weight was 1.34 electrons and the highest peak in a final difference Fourier synthesis was approximately one-fourth of the height of a typical carbon atom found during this analysis. Structure factor calculations for the 828 reflections having $F_o^2 < 3\sigma(F_o^2)$ showed no large discrepancies between $|F_c|$ and $|F_o|$. There was no evidence for secondary extinction.

The final positional and vibrational parameters are presented in Table I along with their estimated standard deviations as obtained from the inverse matrix in the course of the least-squares calculations. Table II contains root-mean-square amplitudes of thermal motion for those atoms refined with anisotropic thermal parameters. A table of the final values of $|F_o|$ and $|F_c|$ for the 1337 reflections included in the refinement is available.[5]

Description and Discussion

The dimeric complex $[RuBr_3(NO)(Et_2SO)]_2$ exists as discrete molecules, one of which is illustrated in Figure 1. Selected interatomic distances and bond angles are listed in Tables III and IV. The shortest nonbonding intermolecular contact not involving hydrogen atoms is 3.1 Å. The coor-

Table I. Final Positional[a] and Thermal[b] Parameters for $[RuBr_3(NO)(Et_2SO)]_2$

	x	y	z	U_{11}	U_{22}	U_{33}	U_{12}	U_{13}	U_{23}
Ru	0.1382 (1)	0.1387 (1)	0.0407 (1)	0.0314 (6)	0.0277 (5)	0.0437 (6)	0.0032 (4)	0.0082 (5)	0.0107 (4)
Br(1)	−0.0306 (2)	0.0510 (1)	0.2366 (2)	0.0605 (9)	0.0338 (7)	0.0435 (8)	0.0022 (6)	0.0195 (7)	0.0079 (6)
Br(2)	0.2147 (2)	0.3310 (1)	0.3083 (2)	0.064 (1)	0.0411 (8)	0.0621 (9)	−0.0049 (7)	−0.0038 (8)	0.0031 (7)
Br(3)	0.2711 (2)	0.2242 (1)	−0.1774 (2)	0.0496 (9)	0.0572 (9)	0.090 (2)	0.0049 (7)	0.0342 (8)	0.0324 (8)
S	−0.1012 (4)	0.3465 (2)	−0.0977 (4)	0.037 (2)	0.031 (2)	0.044 (2)	0.001 (2)	0.011 (2)	0.012 (2)
O(1)	−0.0874 (9)	0.2155 (6)	−0.058 (1)	0.025 (5)	0.032 (4)	0.047 (5)	0.002 (4)	0.003 (4)	0.011 (4)
O(2)	0.434 (1)	0.014 (1)	0.188 (2)	0.057 (8)	0.094 (8)	0.104 (9)	0.028 (7)	0.001 (7)	0.034 (7)
N	0.316 (1)	0.0661 (9)	0.127 (2)	0.038 (7)	0.053 (7)	0.058 (7)	0.007 (6)	0.003 (6)	0.020 (6)
C(11)	−0.177 (2)	0.315 (1)	−0.359 (2)	0.061 (9)	0.053 (8)	0.047 (8)	0.009 (7)	0.009 (7)	0.019 (7)
C(12)	−0.320 (2)	0.211 (1)	−0.442 (2)	0.045 (9)	0.10 (2)	0.044 (9)	−0.011 (8)	0.005 (7)	−0.001 (8)
C(21)	−0.292 (2)	0.405 (1)	−0.010 (2)	0.045 (8)	0.043 (7)	0.052 (8)	0.015 (6)	0.021 (7)	0.011 (6)
C(22)	−0.267 (2)	0.422 (1)	0.203 (2)	0.057 (9)	0.09 (2)	0.042 (9)	0.018 (8)	0.024 (8)	0.011 (8)

[a] x, y, and z are in fractional coordinates. [b] The form of the thermal ellipsoid expression is $\exp[-(\beta_{11}h^2 + \beta_{22}k^2 + \beta_{33}l^2 + 2\beta_{12}hk + 2\beta_{13}hl + 2\beta_{23}kl)]$; $U_{ij} = (\beta_{ij}/2\pi^2)a_i^*a_j^*$ (Å^2).

Table II. Root-Mean-Square Amplitudes of Vibration (Å)

Atom	Min	Intermed	Max
Ru	0.162 (1)	0.178 (2)	0.210 (1)
Br(1)	0.183 (2)	0.197 (2)	0.250 (2)
Br(2)	0.191 (2)	0.239 (2)	0.295 (2)
Br(3)	0.181 (2)	0.228 (2)	0.310 (2)
S	0.173 (4)	0.190 (5)	0.212 (4)
O(1)	0.15 (1)	0.18 (1)	0.22 (1)
O(2)	0.19 (2)	0.33 (1)	0.34 (1)
N	0.18 (2)	0.23 (1)	0.25 (1)
C(11)	0.20 (2)	0.23 (2)	0.26 (2)
C(21)	0.17 (2)	0.23 (2)	0.24 (2)
C(12)	0.19 (2)	0.22 (2)	0.33 (2)
C(22)	0.17 (2)	0.24 (2)	0.31 (2)

Table III. Intramolecular Distances (Å) for $[RuBr_3(NO)(Et_2SO)]_2$

Ru-N	1.71 (1)	S-C(21)	1.83 (1)
Ru-O(1)	2.050 (7)	N-O(2)	1.16 (1)
Ru-Br(3)	2.476 (2)	C(11)-C(12)	1.55 (2)
Ru-Br(2)	2.477 (2)	C(21)-C(22)	1.49 (2)
Ru-Br(1)	2.535 (2)	Ru-Ru′	3.673 (2)
S-O(1)	1.541 (7)	Br(1)-Br(1)′	3.496 (2)
S-C(11)	1.82 (1)		

Table IV. Intramolecular Angles (deg) for $[RuBr_3(NO)(Et_2SO)]_2$

N-Ru-O(1)	175.3 (4)	Br(1)-Ru-Br(1)′	87.18 (5)
N-Ru-Br(3)	94.9 (4)	Ru-Br(1)-Ru′	92.82 (5)
N-Ru-Br(2)	91.8 (3)	O(1)-S-C(11)	104.3 (5)
N-Ru-Br(1)	93.4 (3)	O(1)-S-C(21)	101.9 (5)
O(1)-Ru-Br(3)	89.4 (2)	C(11)-S-C(21)	101.8 (6)
O(1)-Ru-Br(2)	90.0 (2)	S-O(1)-Ru	123.9 (4)
O(1)-Ru-Br(1)	84.7 (2)	O(2)-N-Ru	177.8 (11)
Br(3)-Ru-Br(2)	92.32 (6)	C(12)-C(11)-S	113.6 (9)
Br(3)-Ru-Br(1)	89.30 (6)	C(22)-C(21)-S	111.6 (9)
Br(2)-Ru-Br(1)	174.46 (6)		

dination about the ruthenium atoms is approximately octahedral, but the plane containing the terminal bromine atoms Br(2) and Br(3) and Ru makes an angle of 7.8° with the plane Ru, Br(1), Ru′, and Br(1)′. The terminal bromine atoms are displaced toward the diethyl sulfoxide group. The Ru_2Br_2 ring geometry is nearly square with diagonals of 3.496 (2) and 3.673 (2) Å.

The bond lengths and angles for the diethyl sulfoxide ligand agree well with those of other sulfoxide structures reported.[6-17] The orientation of the sulfoxide ligand is similar to that reported[11] and appears (Figure 1) to be that expected from a consideration of intramolecular forces. Also C–C and C–S bond lengths and angles agree with those reported for a diethyl sulfide structure.[18] In this structure the oxygen atom of the sulfoxide ligand acts as the donor atom to Ru(II). It may be that steric effects of neighboring groups inhibit the sulfoxide ligand bonding through the sulfur atom. That oxygen is the donor atom is consistent with the infrared spectrum, where the shift is to a lower position for the ν(S–O) absorption (920 cm^{-1}) than that observed for the free sulfoxide (1030 cm^{-1}).[19] When oxygen is the donor atom, a slight weakening of the S–O bond is expected and hence there is a shift of the ν(S–O) absorption to lower energy. This effect has been confirmed by crystal structures of sulfoxide complexes. For sulfoxide ligands coordinated through oxygen the following average S–O bond lengths (in Å) have been reported: $CuCl_2(DMSO)_2$, 1.531 (4);[6] $[FeCl_2(DMSO)_4]FeCl_4$, 1.541 (6);[7] $Me_2SnCl_2(DMSO)_2$, 1.56 (4);[8] $Lu(NO_3)_3(DMSO)_3$, 1.54 (4);[9] $[RuBr_3(NO)(Et_2SO)]_2$, 1.541 (7);[10] $RuCl_2(DMSO)_4$, 1.557 (4).[11] On the other hand, for the sulfur-coordinated sulfoxides the reported average S–O bond lengths (Å) are as follows: $RuCl_2(DMSO)_4$, 1.485 (5);[11] $PdCl_2(DMSO)_2$, 1.476 (5);[12] $[Ru(NH_3)_5(DMSO)](PF_6)_2$, 1.527 (8);[13] $Pd(NO_3)_2(DMSO)_2$, 1.463 (7);[14] $Ir(C_{15}H_{13}O)Cl_2(DMSO)_2$, 1.45 (2);[15] $Na[Rh(DMSO)_2Cl_4]$, 1.47;[16] $(NH_2Me_2)[RuCl_3(DMSO)_3]$, 1.48 (1) Å.[17] The crystal structure analysis of dimethyl sulfoxide[20] (DMSO), at 5 °C, gave an S–O bond length of 1.513 (5) Å which is intermediate between the sulfur-coordinated and oxygen-coordinated S–O bond lengths. Hence, for sulfoxide complexes the ν(S–O) absorption can be used as an indicator of the mode of coordination of the sulfoxide to the metal atom, especially when the S–O bond length differs from that of the free sulfoxide.

The nitrosyl ligand is nearly linear, the Ru–N–O bond angle being 178 (1)°, and the bond lengths correspond to those reported for other linear nitrosyl ligands in reviews on metal nitrosyl complexes.[21,22] The nitrosyl stretching frequency of 1874 cm^{-1} is also consistent with the NO^+ ligand and linear M–N–O grouping found. The Ru–N bond distance of 1.71 (1) Å agrees well with those of other ruthenium–nitrosyl complexes such as 1.74 (2) Å in $[RuCl(NO)_2PPh_3]_2^+$,[23] 1.744 (6) Å in $RuCl_3(NO)(PMePh_2)_2$,[24] and 1.738 (2) Å in $[Ru(NO)Cl_5]^{2-}$.[25] When the Ru–N–O group is bent, the Ru–N length is found to be significantly longer, such as 1.85 (2) Å for $[RuCl(NO)_2(PPh_3)_2]^+$.[23]

The short Ru–N distance observed together with the linear Ru–N–O arrangement confirms that strong π back-bonding exists when the nitrosyl ligand is coordinated as NO^+.

The initial complex $RuBr_3NO(Et_2S)_2$ has a trans arrangement of sulfide ligands as shown by its ^{1}H NMR spectrum and supported by crystal structure determinations of related phosphine complexes.[24,26] Hence, considerable steric rearrangement of the ligands is necessary in forming the dimeric structure. Studies of the ^{1}H NMR spectra of the sulfide complexes RuX_3NOL_2 indicate that the sulfide ligands undergo a reasonably facile interconversion

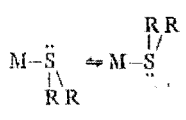

either by inversion at the S atom or rotation about the M–S

bond or by complete bond breaking and re-forming.[1] The interchange is rapid at room temperature (i.e., only one methylene quartet is observed). At low temperatures the ^1H NMR spectrum shows two methylene quartets indicating two sulfide arrangements in the complex. The frequency of the process in $RuBr_3(NO)(Et_2S)_2$ has been found to be 32/s at the temperature of multiplet collapse. The interconversion does not necessarily mean the M–S bond is broken, but it is possible[27] and suggests that considerable ligand rearrangement is quite feasible.

The oxygen responsible for the formation of the sulfoxide appears to be dissolved dioxygen in the chloroform, and the ethanol is probably a source of protons since the replacement of ethanol with other protic sources also gives the same red solution. It is known that sulfides oxidize to sulfoxides under more forcing conditions than those encountered in the present work and in acid-catalyzed conditions and also in the presence of H-bonding reagents.[28]

This appears to be the first report of the mild oxidation of a sulfide, and the metal ion may have an influence similar to that found in the oxidation of phosphines in metal complexes.[29] Attempts to isolate a dioxygen complex have so far been unsuccessful, but a detailed investigation of this possibility is currently under study as well as an investigation of the general occurrence of the reaction in other systems.

Acknowledgment. We wish to thank the New Zealand Universities Grants Committee for equipment grants and for a UGC scholarship to C.T.P.

Registry No. $[RuBr_3(NO)(Et_2SO)]_2$, 59492-73-8.

Supplementary Material Available: Listing of observed and calculated structure factor amplitudes (5 pages). Ordering information is given on any current masthead page.

References and Notes

(1) C. T. Page and J. E. Fergusson, *Aust. J. Chem.*, in press.
(2) Calculations were carried out at the University of Canterbury using a Burroughs B6718 computer. The data processing program HILGOUT is based on programs DRED (J. F. Blount) and PICKOUT (R. J. Doedens). Numerical absorption corrections were applied using program DABS which is a modification of DATAPH (P. Coppens). Structure factor calculations and least-square refinements were carried out using program CUCLS and Fourier summations using program FOURIER. These are highly modified versions of the well-known programs ORFLS (W. A. Busing, K. O. Martin, and H. A. Levy) and FORDAP (A. Zalkin), respectively. Other programs include local modifications of Busing and Levy's ORFFE function and error program and C. K. Johnson's ORTEP thermal ellipsoid plotting program.
(3) D. T. Cromer and J. B. Mann, *Acta Crystallogr., Sect. A*, 24, 321 (1968).
(4) D. T. Cromer, *Acta Crystallogr.*, 18, 17 (1965).
(5) Supplementary material.
(6) R. D. Willett and K. Chang, *Inorg. Chim. Acta*, 4, 447 (1970).
(7) M. J. Bennett, F. A. Cotton, and D. L. Weaver, *Acta Crystallogr.*, 23, 581 (1967).
(8) N. W. Isaacs and C. H. L. Kennard, *J. Chem. Soc. A*, 1257 (1970).
(9) L. A. Aslanov, L. I. Soleva, and M. A. Porai-Koshits, *Zh. Strukt. Khim.*, 14, 1064 (1973), and references therein.
(10) This work.
(11) A. Mercer and J. Trotter, *J. Chem. Soc., Dalton Trans.*, 2480 (1975).
(12) M. J. Bennett, F. A. Cotton, D. L. Weaver, R. J. Williams, and W. H. Watson, *Acta Crystallogr.*, 23, 788 (1967).
(13) F. C. March and G. Ferguson, *Can. J. Chem.*, 49, 3590 (1971).
(14) D. A. Langs, C. R. Hare, and R. G. Little, *Chem. Commun.*, 1080 (1967).
(15) M. McPartlin and R. Mason, *J. Chem. Soc. A*, 2206 (1970).
(16) V. I. Sokol, N. D. Rubtsova, and A. Yu. Gribenyuk, *Zh. Strukt. Khim.*, 15, 318 (1974).
(17) R. S. McMillan, A. Mercer, B. R. James, and J. Trotter, *J. Chem. Soc., Dalton Trans.*, 1006 (1975).
(18) C. I. Branden, *Ark. Kemi.*, 22, 83 (1964).
(19) W. Kitching and C. J. Moore, *Inorg. Nucl. Chem. Lett.*, 4, 691 (1968).
(20) R. Thomas, C. B. Shoemaker, and K. Eriks, *Acta Crystallogr.*, 21, 12 (1966).
(21) J. H. Enemark and R. D. Feltham, *Coord. Chem. Rev.*, 13, 339 (1974).
(22) R. Eisenberg and C. D. Meyer, *Acc. Chem. Res.*, 8, 26 (1975).
(23) C. G. Pierpont and R. Eisenberg, *Inorg. Chem.*, 11, 1088 (1972).
(24) A. J. Schultz, R. L. Henry, J. Reed, and R. Eisenberg, *Inorg. Chem.*, 13, 732 (1974).
(25) J. T. Veal and D. J. Hodgson, *Inorg. Chem.*, 11, 1420 (1972).
(26) B. L. Haymore and J. A. Ibers, *Inorg. Chem.*, 14, 3060 (1975).
(27) R. J. Cross, I. G. Dalgleish, G. J. Smith, and R. Wardle, *J. Chem. Soc., Dalton Trans.*, 992 (1972).
(28) N. Kharasch, "Organic Sulfur Compounds", Vol. 1, D. Barnard, L. Bateman, and J. I. Cunneen, Ed., Pergamon Press, New York, N.Y., 1961, Chapter 21.
(29) L. Vaska, *Science*, 140, 809 (1963).
(30) Numbers in parentheses here and in succeeding tables are estimated standard deviations in the least significant figure.

Aust. J. Chem., 1976, **29**, 2159–65

Sulphide and Selenide Nitrosyl Complexes of Ruthenium

Jack E. Fergusson and Campbell T. Page

Chemistry Department, University of Canterbury, Christchurch, New Zealand.

Abstract

Complexes of the type $[Ru(NO)X_3L_2]$ have been isolated where X = Cl, Br and L = R_2S and PhRS (R = Me, Et, Pr) and Et_2Se and PhEtSe. The complexes, which have the ligands L *trans* to each other, have been studied by ^1H, ^{13}C n.m.r., low-frequency infrared and electronic spectroscopy. Low-temperature ^1H n.m.r. investigations were of assistance in determining the structure of the complexes.

Introduction

The entity RuX_3NO (X = halogen) forms a number of complexes of the type $[RuX_3(NO)L_2]$. Numerous studies have been carried out where L is a tertiary phosphine,[1–5] but only two compounds have been reported where L is a sulphide R_2S or RR'S.[5] To extend previous work carried out with other platinum metal sulphide complexes[6,7] a range of complexes of the type $[RuX_3(NO)L_2]$, containing the sulphides R_2S and PhRS where R = Me, Et and Pr, as well as the selenides Et_2Se and PhEtSe, has been studied.

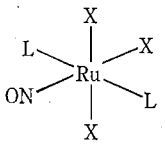

(1)

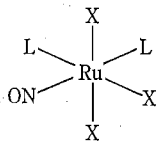

(2)

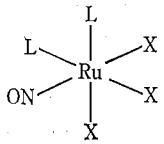

(3)

The possible isomeric forms of the complexes are given by (1)–(3). Evidence from dipole moments[1] and single crystal X-ray studies[3,4] indicate that configuration (1) occurs for the phosphine complexes, where the ligands L are *trans* to each other. The results obtained in the present work suggest a similar configuration for the sulphide complexes.

[1] Chatt, J., and Shaw, B. L., *J. Chem. Soc. A*, 1966, 1811.
[2] Townsend, R. E., and Coskran, K. J., *Inorg. Chem.*, 1971, **10**, 1661.
[3] Schultz, A. J., Henry, R. L., Reed, J., and Eisenberg, R., *Inorg. Chem.*, 1974, **13**, 732.
[4] Haymore, B. L., and Ibers, J. A., *Inorg. Chem.*, 1975, **14**, 3060.
[5] Fairy, M. B., and Irving, R. J., *J. Chem. Soc. A*, 1966, 475.
[6] Fergusson, J. E., and Loh, K. S., *Aust. J. Chem.*, 1973, **26**, 2615.
[7] Aires, B. E., Fergusson, J. E., Howarth, D. T., and Miller, J. M., *J. Chem. Soc. A*, 1971, 1144.

Results and Discussion

Nuclear Magnetic Resonance Spectra

^1H n.m.r. spectra.—The ^1H n.m.r. spectra of the complexes were recorded in deuterochloroform solutions (Table 1). The influence of the metal ion is to deshield the protons on the sulphide ligands. The α-protons of the alkyl groups, in the R_2S complexes, shift downfield by approximately 40 Hz and in the case of PhRS ligands by a further 8–17 Hz. The downfield shift is greater for the bromo complexes (compared with chloro) by 3–9 Hz. This has been found previously and discussed.[6,7] The β-protons, as would be expected, shift much less (3–15 Hz) on coordination, and the order with respect to halogen is variable.

A number of the ^1H n.m.r. spectra have rather broad peaks at room temperature with some evidence of splitting. As the temperature was lowered from 25° to −60°C it was found that the methylene band collapses into a broad peak and reforms into two distinct methylene resonances of equal intensity at lower temperatures (Table 2). This effect has been observed before[6,8–12] and corresponds to the non-equivalence of the methylene groups due to inversion about the sulphur atom. Evidence has also been given previously[12] that the process does not involve breaking of the metal–sulphur bond.

The results rule out isomer (2) as a possible structure as the sulphide ligand would be in different environments at all temperatures. Provided the process being observed[6,8–12] at the temperature of multiplet collapse is inversion about the sulphur atom, and not free rotation about the metal–sulphur bond, the single methylene resonance at room temperature for both $[RuX_3(NO)(R_2S)_2]$ and $[RuX_3(NO)(PhRS)_2]$ complexes is consistent with isomer (1). The position of the square planar group 'RuX_3NO', which is presumably freely rotating with respect to the sulphide or selenide ligands, will not affect the spectra as the magnetic influence of the NO group will be averaged out over all the methylene groups. For isomer (3) the two R groups for the complexes of R_2S are in different magnetic environment with respect to the NO, and provided the phenyl groups of the PhRS ligands are *trans* to each other, which is the arrangement giving least steric interactions, the same applies for these R groups. One therefore expects two methylene multiplets of equal intensity at room temperature, or at a temperature above the inversion temperature. Free rotation about the metal–sulphur bond would be difficult for isomer (3) because of the very close interactions of the groups bonded to the donor atom sulphur. Since the observed spectrum at room temperature is that of a single methylene resonance this suggests that the most likely isomer is (1). The two multiplets occurring at lower temperature correspond to the 'frozen-out' inversion forms. At −2°C the inversion rate for $[RuBr_3NO(Et_2S)_2]$ is found to be 32 times per second.

The temperature at which the single spectrum collapses before splitting out into two separate spectra varies from complex to complex as shown in Table 2. The lower the temperature of the collapse the more readily does the inversion occur. For

[8] Haake, P., and Turley, P. C., *J. Am. Chem. Soc.*, 1967, **89**, 4611.
[9] Turley, P. C., and Haake, P., *J. Am. Chem. Soc.*, 1967, **89**, 4617.
[10] Cross, R. J., Dalgleish, I. C., Smith, C. J., and Wardle, R., *J. Chem. Soc., Dalton Trans.*, 1972, 992.
[11] Cross, R. J., Green, T. H., and Keat, R., *J. Chem. Soc., Chem. Commun.*, 1974, 207.
[12] Cross, R. J., Green, T. H., Keat, R., and Paterson, J. F., *Inorg. Nucl. Chem. Lett.*, 1975, **11**, 145.

Table 1. ^{1}H n.m.r. spectra

Chemical shift δ (ppm) from Me_4Si. Coupling constants for alkyl protons are 7–8 Hz and 2–3 Hz for phenyl protons

Compound	α	β	γ	Phenyl
Me_2S	2·12 (s)			
$RuCl_3(NO)(Me_2S)_2$	2·66 (s)			
$RuBr_3(NO)(Me_2S)_2$	2·76 (s)			
PhSMe	2·25 (s)			7·11
$RuCl_3(NO)(PhSMe)_2$	2·97 (s)			7·35 (*p*+*m*), 7·70 (*o*)
$RuBr_3(NO)(PhSMe)_2$	3·12 (s)			7·35 (*p*+*m*), 7·75 (*o*)
Et_2S	2·53 (q)	1·23 (t)		
$RuCl_3(NO)(Et_2S)_2$	3·19 (q)	1·46 (t)		
$RuBr_3(NO)(Et_2S)_2$	3·28 (q)	1·47 (t)		
PhSEt	2·87 (q)	1·23 (t)		7·21
$RuCl_3(NO)(PhSEt)_2$	3·70 (q)	1·30 (t)		7·41 (*p*+*m*), 7·76 (*o*)
$RuBr_3(NO)(PhSEt)_2$	3·79 (q)	1·27 (t)		7·38 (*p*+*m*), 7·77 (*o*)
Pr_2S	2·48 (t)	1·61 (sx)[A]	0·97 (t)	
$RuCl_3(NO)(Pr_2S)_2$	3·13 (t)	1·84 (sx)[A]	1·07 (t)	
$RuBr_3(NO)(Pr_2S)_2$	3·18 (t)	1·84 (sx)[A]	1·08 (t)	
PhSPr	2·82 (t)	1·61 (sx)[A]	0·96 (t)	7·20
$RuCl_3(NO)(PhSPr)_2$	3·60 (t)	1·65 (sx)[A]	1·00 (t)	7·36 (*p*+*m*), 7·72 (*o*)
$RuBr_3(NO)(PhSPr)_2$	3·71 (t)	*c.* 1·6	*c.* 1·0	7·37 (*p*+*m*), 7·77 (*o*)
Et_2Se	2·58 (q)	1·39 (t)		
$RuCl_3(NO)(Et_2Se)_2$	[B,C]	[B,C]		
$RuBr_3(NO)(Et_2Se)_2$	3·42, 3·13[C]	1·54 (t)		
$RuI_3(NO)(Et_2Se)_2$	3·38 (q)	1·55 (t)		
PhSeEt	2·83 (q)	1·35 (t)		7·14, 7·20, 7·45
$RuCl_3(NO)(PhSeEt)_2$	3·67 (q)	1·44 (t)		7·36 (*p*), 7·44 (*m*), 7·78 (*o*)
$RuBr_3(NO)(PhSeEt)_2$	3·75 (q)	1·42 (t)		7·39 (*p*+*m*), 7·78 (*o*)

[A] Sextet. [B] For this complex, α: 3·38, 3·08, 3·02; β: 1·55, 1·52, 1·50. [C] Overlapping quartets or triplets of equal intensity.

Table 2. ^{1}H n.m.r. spectra of α-protons over a temperature range (°C)

Chemical shift δ (ppm) from Me_4Si

Compound	25°	−35°	Temp. of coalescence
$RuCl_3(NO)(Et_2S)_2$	3·19 (q)	3·36, 3·15[A]	11°
$RuCl_3(NO)(PhSEt)_2$	3·70 (q)	3·86, 3·62	8°
$RuBr_3(NO)(Et_2S)_2$	3·28 (q)	3·41, 3·22	−2°
$RuBr_3(NO)(PhSEt)_2$	3·79 (q)	3·99, 3·67	3°
$RuCl_3(NO)(Pr_2S)_2$	3·13 (t)	3·30, 2·98	10° to 0°
$RuBr_3(NO)(Pr_2S)_2$	3·18 (t)	3·34, 3·03	0° to −10°
$RuCl_3(NO)(Et_2Se)_2$	3·38, 3·08, 3·02 (q)	3·28, 3·15	not observed from +40° to −60°
$RuCl_3(NO)(PhSeEt)_2$	3·67 (q)	3·78, 3·64	−25 to −30°
$RuBr_3(NO)(Et_2Se)_2$	3·42, 3·13 (q)	3·43, 3·21	not observed from +25° to −60°
$RuBr_3(NO)(PhSeEt)_2$	3·75 (q)	coalescence	−40°

[A] Overlapping quartets or triplets.

analogous compounds (i.e. same sulphide ligand) the temperature of collapse is lower for the bromo compounds, as observed by others,[8–11] perhaps indicating a weaker Ru–S bonding system for the bromo compounds. The selenide complexes are unusual in that the Et_2Se complexes show two methylene multiplets, even at room temperature and still at 40°C, while the EtPhSe complexes display the usual splitting of the single room temperature spectra at lower temperatures. The results could suggest that the Et_2Se complexes may have a different structure, or more likely that the coalescence temperature is above 40°C as reported for $[PtX_2(Et_2Se)_2]$.[11]

Table 3. ^{13}C **n.m.r. spectra**
In ppm downfield from Me_4Si

Compound	α	β	γ	Phenyl
$RuCl_3(NO)(Me_2S)_2$	22·7			
$RuCl_3(NO)(PhSMe)_2$	20·8			129·3 (*p*), 129·6 (*m*), 130·9 (*o*)
$RuCl_3(NO)(Et_2S)_2$	30·7	13·2		
$RuCl_3(NO)(PhSEt)_2$	32·0	12·2		129·7 (*p*), 130·7 (*m*), 131·1 (*o*)
$RuCl_3(NO)(Pr_2S)_2$	39·3	21·7	13·2	
$RuCl_3(NO)(PhSPr)_2$	39·7	20·7	13·1	129·7 (*p*), 130·6 (*m*), 131·0 (*o*)
$RuCl_3(NO)(Et_2Se)_2$	26·4	13·7		
$RuCl_3(NO)(PhSeEt)_2$	29·5, 29·2	12·8		129·9 (*p*), 130·7 (*m*), 131·3 (*o*)
$RuBr_3(NO)(Me_2S)_2$	25·2			
$RuBr_3(NO)(PhSMe)_2$	23·7			129·5 (*p*), 129·7 (*m*), 131·0 (*o*)
$RuBr_3(NO)(Et_2S)_2$	32·8	13·6		
$RuBr_3(NO)(PhSEt)_2$	35·2	12·9		129·7 (*p*), 130·6 (*m*), 131·0 (*o*)
$RuBr_3(NO)(Pr_2S)_2$	41·3	22·1	13·1	
$RuBr_3(NO)(Et_2Se)_2$	27·9	14·0		
$RuBr_3(NO)(PhSeEt)_2$	31·0, 31·6	13·3		129·9 (*p*), 130·7 (*m*), 131·3 (*o*)

^{13}C n.m.r. spectra.—The ^{13}C n.m.r. spectra of the complexes (Table 3) are comparable to those of the ^1H n.m.r. spectra in trends and presumably for the same reasons.[6] The spectra of the chloro and bromo complexes of the ligand PhEtSe are different from the rest in showing a doublet for the α carbon (CH_2 carbon). This splitting was not evident in the ^1H n.m.r. spectra and likewise the splitting of the ^1H n.m.r. spectra of the Et_2Se complexes is not evident in the ^{13}C n.m.r. spectra. This may suggest that both the Et_2Se and PhEtSe complexes are differently constituted from the others.

Infrared Spectra

All of the $[RuX_3(NO)L_2]$ complexes have a strong band in the 1835–1880 cm^{-1} region due to activating the ν(NO) stretching mode.

The point group symmetry of complexes with the configuration (1) is C_{2v}, and one expects three infrared-active Ru–X stretching modes ($2a_1+b_1$). Most of the chloro complexes display three bands in the 304–356 cm^{-1} region, which are assigned to the three stretching modes (Table 4). The other two configurations [(2) and (3)] are also expected to give rise to three ν(Ru–Cl) stretching bands, hence the infrared spectra are not helpful for distinguishing the three isomers. The bromo compounds have one or two intense bands in the region 249–270 cm^{-1} rather than three. Again the spectra cannot be used for structural investigations.

The ν(Ru–Cl) stretching band of highest energy occurs within the region 336–356 cm^{-1} which is around 20 cm^{-1} higher than for $[RuCl_3L_3]$ complexes.[7,13] Taking into account the difference in the ruthenium oxidation levels the values at 336–356 cm^{-1} are high. These may correspond to the ν(Ru–Cl) stretch for the chlorine *trans* to the NO as this Ru–Cl bond is significantly shorter than the others.[3,4] The highest energy absorptions assigned to the ν(Ru–Br) stretch may also be a consequence of the nitrosyl influence on the Ru–Br bond.

Table 4. Infrared spectra (cm^{-1})

Compound	ν(N–O)	ν(Ru–X)	ν(Ru–S(Se))	δ(RuS(Se)C)	Other bands
$RuCl_3(NO)(Me_2S)_2$	1872	348s, 332s, 316m	290m, 271m	224m	163m, 121mw
$RuCl_3(NO)(PhSMe)_2$	1878	352m, 343sh, 332s	301m	218m	128mw
$RuCl_3(NO)(Et_2S)_2$	1868	356sh, 342s, 334s	289m, 282m		252w, 179w, 162w
$RuCl_3(NO)(PhSEt)_2$	1845	347s, 335s, 327sh	296m	211s	252m, 171w
$RuCl_3(NO)(Pr_2S)_2$	1870	342s, 331sh, 319sh	292m	222w	210w, 135m
$RuCl_3(NO)(PhSPr)_2$	1867	350sh, 335sh, 327s	295w	220m	165w, 145w, 108w
$RuCl_3(NO)(Et_2Se)_2$	1867	336s, 325sh, 304sh	226m	146w	292m
$RuCl_3(NO)(PhSeEt)_2$	1835	340s, 331sh, 320sh	233m, 205s?	146w	302m, 295m, 277w
$RuBr_3(NO)(Me_2S)_2$	1872	275s, 236m	293w, 315s?	208s	124s, 180w
$RuBr_3(NO)(PhSMe)_2$	1872	264s	293m, 298m, 307m	235s	212m, 121w
$RuBr_3(NO)(Et_2S)_2$	1857	249s, 229s	280sh	212w	353w, 162m, 122m
$RuBr_3(NO)(PhSEt)_2$	1870	268s, 250m		230s	213m, 117mw
$RuBr_3(NO)(Pr_2S)_2$	1849	270s	322m?	228s	132–125m(br)
$RuBr_3(NO)(PhSPr)_2$	1867	264s, 235mw		220m	183w, 145w, 125w
$RuBr_3(NO)(Et_2Se)_2$	1850	263s	228s	112w	
$RuBr_3(NO)(PhSeEt)_2$	1862	260s	221w, 209m	110m	303w

The ν(Ru–S) stretch is assigned to the absorptions in the vicinity of 290 cm^{-1} and the ν(Ru–Se) stretch to bands around 220 cm^{-1}. The bending mode δ(RuSC) occurs as a strong band around 220 cm^{-1}. In assigning the ν(Ru–Cl) and ν(Ru–S) stretching modes it is possible that since they overlap that some bands are incorrectly assigned, especially the lowest energy absorption assigned to ν(RuCl).

Electronic Spectra

The electronic spectra of the complexes consist of a four-band system, one which is almost invariant for the chloro compounds at 43000 cm^{-1} and at 41000–43000 for the bromo compounds with extinction coefficients around 20000. This band may be a halogen → ruthenium charge transfer. A band in the vicinity of 39000 cm^{-1} with extinction coefficient of 13000 is probably an intraligand band. An intense band occurs around 30000–35000 cm^{-1} with an extinction coefficient of around 15000. This band has lowest energy for the phenylalkyl sulphide complexes and also for the selenide

[13] Chatt, J., Leigh, G. J., and Storace, A. P., *J. Chem. Soc. A*, 1971, 1380.

complexes and is assigned to a S(Se) → Ru metal reduction charge transfer. A weaker band around 20000–23000 cm^{-1}, with an extinction coefficient of about 100–250, is assigned to the $^1A_1 \rightarrow {}^1T_1$ ligand field band. This latter band is at lower energy for the bromo compounds as would be expected.

Experimental

Preparations

The entity $RuCl_3NO$ was obtained by adding nitric oxide to an ethanol solution of $RuCl_3,3H_2O$.[2] The bromo analogue was obtained in a similar manner after $RuCl_3,3H_2O$ was converted into $RuBr_3,3H_2O$ by treatment with hydrobromic acid and evaporation to dryness three times.

The sulphides were obtained commercially, or by procedures outlined previously.[7]

The complexes were obtained by the following general method. The sulphide (0·5 ml) was added to an ethanol solution (30 ml) containing 'RuX_3NO' and heated under reflux for 1 h. On reduction of the volume of the solution crystals formed, and if difficulty was encountered cooling in an ice bath was necessary. The crystalline product was filtered and washed with ice-cold light petroleum (50–70°). Ethanol was used for recrystallization. For the complex $[RuBr_3(NO)(PhPrS)_2]$ it was necessary to stand the solution for 3–4 weeks to obtain good crystals, but the yield was low, and no C and H analysis was carried out.

The complex $[RuBr_3(NO)(Et_2Se)_2]$ was also prepared by adding NaBr to the corresponding chloro complex in ethanol and heating under reflux for 2 h. The iodide $[RuI_3(NO)(Et_2Se)_2]$ was prepared in a similar manner.

Chloroform solutions of all the bromo complexes changed colour from yellow to dark red when left to stand in sunlight. The chloro complexes undergo the change less rapidly. In the case of the complex $[RuBr_3(NO)(Et_2S)_2]$ crystals were obtained which were found subsequently to be $[RuBr_3(NO)(Et_2SO)]_2$ by single crystal X-ray analyses.[14]

Table 5. Analytical data

Compound	Found (%) C	Found (%) H	Calc. (%) C	Calc. (%) H	Colour
$RuCl_3(NO)(Me_2S)_2$	13·9	3·6	13·3	3·3	red
$RuCl_3(NO)(PhSMe)_2$	34·7	3·6	34·6	3·3	red
$RuCl_3(NO)(Et_2S)_2$	21·4	4·7	23·0	4·8	red-brown
$RuCl_3(NO)(PhSEt)_2$	37·0	3·9	37·4	3·9	brown
$RuCl_3(NO)(Pr_2S)_2$	30·0	6·0	30·4	6·0	light brown
$RuCl_3(NO)(PhSPr)_2$	38·8	4·6	39·9	4·5	brown
$RuCl_3(NO)(Et_2Se)_2$	18·4	4·0	18·8	3·9	red-brown
$RuCl_3(NO)(PhSeEt)_2$	31·6	3·3	31·6	3·3	red
$RuBr_3(NO)(Me_2S)_2$	9·9	2·5	9·7	2·4	red-brown
$RuBr_3(NO)(PhSMe)_2$	26·6	2·9	27·1	2·6	red-brown
$RuBr_3(NO)(Et_2S)_2$	17·6	3·6	17·4	3·7	red
$RuBr_3(NO)(PhSEt)_2$	29·8	3·2	29·7	3·1	brown
$RuBr_3(NO)(Pr_2S)_2$	24·4	4·8	23·7	4·7	red
$RuBr_3(NO)(Et_2Se)_2$	15·2	3·2	14·9	3·1	brown
$RuBr_3(NO)(PhSeEt)_2$	26·7	2·8	25·9	2·7	brown
$RuI_3(NO)(Et_2Se)_2$	12·6	2·8	12·2	2·6	very dark red

Physical Measurements

Infrared spectra were obtained on a RIIC Fourier FS 720 interferometer over the range 400–40 cm^{-1}. High frequency spectra (4000–400 cm^{-1}) were obtained using a Shimadzu IR 27G spectrophotometer.

[14] Fergusson, J. E., Page, C. T., and Robinson, W. T., *Inorg. Chem.*, in press.

N.m.r. spectra were obtained on a Varian T-60 spectrometer at 60 MHz and 25°C (for ^{1}H n.m.r.). Proton-noise-decoupled 20-MHz ^{13}C n.m.r. spectra were obtained by means of a Varian CFT20 spectrometer. The solvent was deuterochloroform and the spectra were recorded at 32°C. δ values relative to tetramethylsilane are given in Table 3 and have an uncertainty of $\pm 0{\cdot}05$.

Electronic spectra were obtained on a Varian Techtron 635 u.v.–visible spectrophotometer with chloroform as solvent.

Carbon and hydrogen analyses (Table 5) were determined at the Microanalytical Laboratory, University of Otago, New Zealand.

Acknowledgments

The authors acknowledge support, by way of grants for equipment, from the New Zealand Universities Grants Committee and one of us (C.T.P.) for a UGC Scholarship.

Manuscript received 24 February 1976